

Synthesis of Amino Acids from Chiral Ni^{II} Schiff Base Complexes for Novel Stapled Peptides

Thesis submitted for the degree of

Doctor of Philosophy

at University of Leicester

by

Emad Khelil Mohammed Zangana

MSc (University of Baghdad)

Department of Chemistry

University of Leicester

November 2018



UNIVERSITY OF
LEICESTER

Synthesis of Amino Acids from Chiral Ni^{II} Schiff Base Complexes for Novel Stapled Peptides

Emad Khelil Mohammed Zanagana

Abstract

Protein–protein interactions (PPIs) are key elements of several important biological processes. Several types of stapled peptides have been reported to increase the binding affinity and the stability of the peptides in the biological area. Work on a new generation of hydrocarbon staple, that avoids the weaknesses of olefins stapled peptides, has involved asymmetric synthesis of alkyne functionalised amino acids for novel 1,3-diyne bridged peptides will be described by C-alkylation of a series of Ni^{II} Schiff base complexes using ligand (*S*) or (*R*)-*N*-(2-benzoylphenyl)-1-(2-fluorobenzyl)-pyrrolidine-2-carboxamide (2-FBPB) from L-proline.

This thesis describes, in chapter two, the design, synthesis and characterisation of a series of Ni^{II} Schiff base 2-FBPB complexes with glycine, alanine, valine, leucine or phenylalanine: (*S,S*) **55** and (*S,R*) **97**; (*S,S*) **101** and (*S,R*) **102**; (*S,S*) **56** and (*S,R*) **98** complexes with high yields and with excellent diastereoselectivities. In chapter three, new Ni^{II} Schiff base complexes **134-142** have been synthesised by alkylation reactions. The methodology for alkylation has been modified. Decomposition of these complexes has led to novel amino acids in good yields and high diastereoselectivities **137, 143-148**. Fmoc protection of these amino acids have been achieved successfully **149-152**. In chapter four, the same strategies have been adopted to generate a number of novel fluorinated amino acids via either alkylation or aldol reactions. Amino acids **202-207** have been generated in good yields and high diastereoselectivities (>99 % de). Chapter five describes the design, synthesis and evaluation of stapled peptides. Four model peptide pairs (linear and 1,3-diyne bridged) have been prepared and their helicity established by CD spectroscopy. The greatest helicity was shown for a 1,3-diyne bridge peptide incorporating a C7-alkynyl-alanine amino acid. This was then applied to a new model of the Bim peptide and the helicity of the resulting 1,3-diyne bridged peptide compared to the linear (unbridged) peptide: 67 % for ring closure and 51 % for ring opening. Chapter six outlines the experimental work and characterisation data for the products prepared in this work. Complexes **95-97, 99-101, 134, 136, 137, 140, 141, 190, 192** and **198** have been structurally characterised by single crystal X-ray diffraction.

Acknowledgments

I would like to express my gratitude and appreciation to my first supervisor, Prof Eric Hope, for his support, guidance and encouragement to me throughout my PhD. I would never have reached this point without your encouragement when you always say “this is your thesis”. I could not have imagined having a better adviser and mentor for my studies, so many thanks for being my supervisor. Also I would like to thanks my supervisors: Dr Andrew Jamieson and and Dr Sandeep Handa for their guidance and support during the project.

I would like to thank all the people who have been involved in this project, Dr Gerry Griffith and Dr Vanessa Timmermann for NMR spectral analysis, Mr Kuldip Singh for the X-ray structure determination and Mr Mick Lee for mass spectra. To all the members of the Chemistry Department, thank you for your respectfulness and friendship.

I would also like to acknowledge support of the Human Capacity Development Program (HCDP) in the Iraqi Kurdistan Regional Government for a scholarship and funding this research.

I am thankful to all my colleagues in the Inorganic Lab Group and Organic Lab Group for their help and support during my studies, particularly when I ran into difficulties. A special thank to my close friends: Ahmed, Rusul, Meshari, Martyna, William, Simran, Jinting and Alice for being really helpful and friendly to me throughout my PhD study.

My immeasurable appreciation for my parents, who made me what I am today. Unlimited thanks for all your prayers, sacrifices and love is unmatched and priceless for you. I am very grateful to all my brothers (Nihad, Abdulqader and Fouad) and my lovely sister Media A. Alhaideri, who have helped and supported me throughout all my life. Also I would like to thank Mr Maher F. Chalabi and his family for their special support and the encouragement. Thank you for everything.

Special thanks and deeply express my gratitude to my dear and lovely wife Ronak A. Alhaideri, for here encouragement, support and patience to me throughout my PhD study and also she being a lovely mother to her children. A good wife makes a good husband, many thanks to a wonderful wife like you. Finally, thank you so much to my dear sons (Mohammed and Moustafa) for listening to me, you are so special to me and I am so proud and so blessed that I have sons like you.

Dedication to
My dearest parent and brothers
My lovely wife Ronak Alhaideri
My sons
Mohammed and Moustafa

Emad Zangana

Leicester 2018

Statement

The work explained in this thesis for the degree of Ph.D. entitled "Synthesis of Amino Acids from Chiral Ni^{II} Schiff Base Complexes for Novel Stapled Peptides" was carried out by the author in the Department of Chemistry at the University of Leicester between July 2014 and November 2018. In this thesis, the work recorded was original except where acknowledged or referenced. None of the work has been submitted for another degree at this or any other university.

Signed Date

Thesis contents

Abstract.....	i
Acknowledgements.....	ii
Dedication.....	iii
Statement.....	iv
Thesis contents.....	v
Abbreviations	xiv
1 Chapter 1	1
1.1 Introduction	2
1.2 Peptidomimetics	3
1.3 Helix stabilisation	3
1.3.1 Hydrogen-bonding surrogates	5
1.3.2 Hydrophobic interactions	6
1.3.3 Salt bridges	8
1.3.4 Photocontrollable macrocycles.....	10
1.3.5 Disulfide bridges	10
1.4 Metal ligation.....	11
1.4.1 Lactams	12
1.5 Hydrocarbon stapling	13
1.6 Design of alkene-stapled peptides	13
1.7 Catalysts for ring closing metathesis RCM (Hoveyda-Grubbs) reaction	14
1.8 Fluorinated amino acid in peptides and proteins.	16
1.9 Synthesis of α,α -disubstituted amino acids via a Ni ^{II} Schiff base complex	19
1.9.1 Synthesis of Ni ^{II} Schiff base complexes.....	19

1.9.2 Application of Ni ^{II} Schiff base complexes in amino acids synthesis	21
1.9.3 Synthesis of Fluorinated α -Amino Acids	26
1.10 Application of alkynyl derivatives of amino acids in peptide synthesis	28
1.10.1 Synthesis of triazoles.....	28
1.10.2 Preparation of 1,3-diyne group.	30
1.11 Peptide synthesis.....	34
1.11.1 Solid phase peptide synthesis	34
1.12 Project aims	37
2 Chapter 2	40
2.1 Introduction	41
2.2 Synthesis of Ni ^{II} complexes of Schiff base derivatives	43
2.3 The aims of this chapter are:.....	45
2.4 Synthesis of a chiral Ni ^{II} Schiff base complexes	45
2.4.1 Alkylation reaction	45
2.4.2 Synthesis of (<i>S</i>)- <i>N</i> -(2-benzoylphenyl)-1-(2-fluorobenzyl)pyrrolidine-2-carboxamide (pre-ligand (FBPB)) 95	47
2.4.3 Synthesis of (<i>R</i>)- <i>N</i> -(2-benzoylphenyl)-1-(2-fluorobenzyl)pyrrolidine-2-carboxamide 96	50
2.5 Synthesis of Ni ^{II} Schiff base complexes	54
2.6 Conclusions	60
3 Chapter 3	61
3.1 Introduction	62
3.2 Synthesis of alkynyl derivatives of amino acids.....	62

3.3 Aims of Chapter three.....	66
3.4 Synthesis of the iodoalkyne electrophiles	67
3.4.1 Method A.....	68
3.4.2 Method B	70
3.4.3 Synthesis of 5-iodopent-1-yne 133	72
3.5 Alkylation reaction	72
3.5.1 Alkylation of alanine Ni ^{II} Schiff base complex.....	74
3.5.2 Alkylation of glycine Ni ^{II} Schiff base complex	76
3.5.3 Alkylation of leucine Ni ^{II} Schiff base complex.....	81
3.5.4 Alkylation of phenylalanine Ni ^{II} Schiff base complex.....	86
3.5.5 Alkylation of valine Ni ^{II} Schiff base complex	90
3.6 Hydrolysis or decomplexation of Ni ^{II} Schiff base complexes	92
3.6.1 Acidification hydrolysis	92
3.6.2 Hydrolysis of the complexes under neutral conditions (chelation)	95
3.7 Protection of Amino acids	97
3.8 Conclusions	100
4 Chapter 4.....	103
4.1 Introduction	104
4.2 Fluorination in peptide and protein	107
4.2.1 Conformational pre-organization (gauche effects).....	109
4.2.2 Substituted aromatic amino acids interaction (π - π stacked).....	109
4.2.3 Effect of hydrogen bond between H \cdots F	111

4.3 The aims of the work in this chapter are:	114
4.4 New methodology for the synthesis of fluorinated aromatic amino acids	114
4.4.1 Alkylation with 1-(bromomethyl)-4-trifluoromethyl)benzene.....	115
4.4.2 Alkylation by using 1-(bromomethyl)-2-fluorobenzene	121
4.5 Aldol reaction with glycine Ni ^{II} Schiff base complex	124
4.5.1 Aldol reaction with alanine Ni ^{II} Schiff base complex	130
4.5.2 Hydrolysis of the complexes under mild conditions	132
4.5.3 Fmoc-protection of a fluorinated amino acid	134
4.5.4 Conclusions	135
5 Chapter 5	137
5.1 Introduction	138
5.2 Alkyne bonds	141
5.3 1,3-diyne bonds	142
5.4 Analysis of the conformation of peptides	144
5.5 Apoptosis of peptides	146
5.6 Synthesis of peptide models using the SPPS method	147
5.7 Deprotection of the Fmoc group	148
5.8 Coupling reaction in peptide synthesis	148
5.9 Synthesis of the peptide models	151
5.10 Oxidative coupling	153
5.11 Conformation analysis of the peptides models	154
5.12 Application of the 1,3-diyne helices in peptides	155

5.13 Conclusions.....	158
6 Chapter 6	160
6.1 General information.....	161
6.2 General methods:	162
6.2.1 Synthesis of 1-(2-fluorobenzyl)pyrrolidine-2-carboxylic acids (A)	162
6.2.2 Synthesis of <i>N</i> -(2-benzoylphenyl)-1-(2-fluorobenzyl)pyrrolidine-2-carboxamides (B).....	163
6.2.3 Synthesis of ({2-[1-(2-fluorobenzyl)benzyl]pyrrolidine-2-carboxamide}-phenyl}phenylmethylene)-(amino acid)ato- <i>N,N',N'',O</i> } nickel ^{II} (C)	163
6.2.4 Alkylation of chiral Ni ^{II} complexes Schiff bases using alkyl iodide (D)	164
6.2.5 Alkylation of chiral glycine Schiff bases Ni ^{II} complexes using alkyl iodide (E)	164
6.2.6 Alkylation of chiral Schiff bases Ni ^{II} complexes using alkyl bromide (F)	165
6.2.7 Generation of amino acids by hydrolysis of the complexes (G)	165
6.2.8 Generation of amino acids by using 8-hydroxyquinoline (H).....	166
6.2.9 Synthesis of Fmoc protected amino acids (I)	166
6.3 Synthesis of Starting materials	167
6.3.1 Synthesis of 7-iodohept-1-yne:	167
6.4 Experimental for Chapter 2	171
6.4.1 Synthesis of (S)-1-(2-fluorobenzyl)pyrrolidine-2-carboxylic acid 93	171
6.4.2 Synthesis of (R)-1-(2-fluorobenzyl)pyrrolidine-2-carboxylic acid 94	171
6.4.3 Synthesis of (<i>S</i>)- <i>N</i> -(2-benzoylphenyl)-1-(2-fluorobenzyl)pyrrolidine-2-carboxamide 95	172
6.4.4 Synthesis of (<i>R</i>)- <i>N</i> -(2-benzoylphenyl)-1-(2-fluorobenzyl)pyrrolidine-2-carboxamide 96	173

6.4.5 Synthesis of (S)-({2-[1-(2-fluorobenzyl)benzyl]pyrrolidine-2-carboxamide}-phenyl}phenylmethylene)-alaninato- <i>N,N',N'',O</i> nickel ^(II) 56	174
6.4.6 Synthesis of (R)-({2-[1-(2-fluorobenzyl)benzyl]pyrrolidine-2-carboxamide}-phenyl}phenylmethylene)- <i>R</i> -alaninato- <i>N,N',N'',O</i> nickel ^{II} 98	175
6.4.7 Synthesis of (S)-({2-[1-(2-fluorobenzyl)benzyl]pyrrolidine-2-carboxamide}-phenyl}phenylmethylene)-glycinato- <i>N,N',N'',O</i> nickel ^{II} 55	176
6.4.8 Synthesis of (R)-({2-[1-(2-fluorobenzyl)benzyl]pyrrolidine-2-carboxamide}-phenyl}phenylmethylene)-glycinato- <i>N,N',N'',O</i> nickel ^{II} 97	177
6.4.9 Synthesis of (S)-({2-[1-(2-fluorobenzyl)benzyl]pyrrolidine-2-carboxamide}-phenyl}phenylmethylene)-phenylalaninato- <i>N,N',N'',O</i> nickel ^(II) 99	178
6.4.10 Synthesis of (S)-({2-[1-(2-fluorobenzyl)benzyl]pyrrolidine-2-carboxamide}-phenyl}phenylmethylene)-(S)-leucinato- <i>N,N',N'',O</i> nickel ^{II} 100	179
6.4.11 Synthesis of (S)-({2-[1-(2-fluorobenzyl)benzyl]pyrrolidine-2-carboxamide}-phenyl}phenylmethylene)- <i>S</i> -valinato- <i>N,N',N'',O</i> nickel ^{II} 101	180
6.4.12 Synthesis of (R)-({2-[1-(2-fluorobenzyl)benzyl]pyrrolidine-2-carboxamide}-phenyl}phenylmethylene)- <i>R</i> -valinato- <i>N,N',N'',O</i> nickel ^{II} 102	181
6.5 Experimental for Chapter 3	181
6.5.1 Synthesis of (S)-({2-[1-(2-fluorobenzyl)benzyl]pyrrolidine-2-carboxamide}-phenyl}phenylmethylene)-(S)-hexynylalaninato- <i>N,N',N'',O</i> nickel ^(II) 134	181
6.5.2 Synthesis of (S)-({2-[1-(2-fluorobenzyl)benzyl]pyrrolidine-2-carboxamide}-phenyl}phenylmethylene)-(S)-heptynylalaninato- <i>N,N',N'',O</i> nickel ^{II} 135	182
6.5.3 Synthesis of (S)-({2-[1-(2-fluorobenzyl)benzyl]pyrrolidine-2-carboxamide}-phenyl}phenylmethylene)-(S)-hexynylglycinato- <i>N,N',N'',O</i> nickel ^(II) 136	183
6.5.4 Synthesis of (S)-({2-[1-(2-fluorobenzyl)benzyl]pyrrolidine-2-carboxamide}-phenyl}phenyl methylene)-(S)-heptynylglycinato- <i>N,N',N'',O</i> nickel ^(II) 137	184
6.5.5 Synthesis of (S)-({2-[1-(2-fluorobenzyl)benzyl]pyrrolidine-2-carboxamide}-phenyl}phenyl methylene)-1-pentyl-leucinato- <i>N,N',N'',O</i> nickel ^{II} 138	185

6.5.6 Synthesis of (S)-({2-[1-(2-fluorobenzyl)benzyl]pyrrolidine-2-carboxamide}phenyl}phenyl methylene)-(S)-1-hexyl-leucinato- <i>N,N',N'',O</i> }nickel ^{II} 139	186
6.5.7 Synthesis of (S)-({2-[1-(2-fluorobenzyl)benzyl]pyrrolidine-2-carboxamide}phenyl}phenylmethylene)-(S)-1-pentyl-phenylalaninato- <i>N,N',N'',O</i> }nickel ^{II} 140	187
6.5.8 Synthesis of (S)-({2-[1-(2-fluorobenzyl)benzyl]pyrrolidine-2-carboxamide}phenyl}phenylmethylene)-(S)-pentenylalaninato- <i>N,N',N'',O</i> }nickel ^{II} 142	188
6.5.9 (S)-2-amino-2-methyloct-7-ynoic acid 143	189
6.5.10 Synthesis of (S)-2-amino-2-methylhept-6-enoic acid 144	189
6.5.11 Synthesis of (S)-2-aminooct-7-ynoic acid 145	189
6.5.12 Synthesis of (S)-2-amino-2-methylnon-8-ynoic acid 146	190
6.5.13 Synthesis of (S)-2-aminonon-8-ynoic acid 147	190
6.5.14 Synthesis of (S)-2-amino-2-benzylhept-6-ynoic acid 148	191
6.5.15 Synthesis of (S)-2-(((9H-fluoren-9-yl)methoxy)carbonyl)amino)-2-methyloct-7-ynoic acid 149	191
6.5.16 Synthesis of (S)-2-(((9H-fluoren-9-yl)methoxy)carbonyl)amino)-2-methylnon-8-ynoic acid 150	192
6.5.17 Synthesis of (S)-2-(((9H-fluoren-9-yl)methoxy)carbonyl)amino)oct-7-ynoic acid. 151	192
6.5.18 Synthesis of (S)-2-(((9H-fluoren-9-yl)methoxy)carbonyl)amino)non-8-ynoic acid. 152	193
6.6 Experimental for Chapter 4	194
6.6.1 Synthesis of (S)-({2-[1-(2-fluorobenzyl)benzyl]pyrrolidine-2-carboxamide}phenyl}phenylmethylene)-(S)-4-(trifluoromethyl)benzenyl-alaninato- <i>N,N',N'',O</i> }nickel ^(II) . 186	194

6.6.2 Synthesis of (S)-({2-[1-(2-fluorobenzyl)benzyl]pyrrolidine-2-carboxamide}phenyl}phenylmethylene)-(S and R)-4-(trifluoromethyl)benzenyl-glycinato-N,N',N'',O}nickel ^(II) (187 and 188)	195
6.6.3 Synthesis of (S)-({2-[1-(2-fluorobenzyl)benzyl]pyrrolidine-2-carboxamide}phenyl}phenylmethylene)-(S and R)-4-(trifluoromethyl)benzenyl-leucinato-N,N',N'',O}nickel ^(II) (190 and 191)	196
6.6.4 Synthesis of (S)-({2-[1-(2-fluorobenzyl)benzyl]pyrrolidine-2-carboxamide}phenyl}phenylmethylene)-(S)-2-fluorobenzenyl-glycinato-N,N',N'',O}nickel ^(II) 191	199
6.6.5 Synthesis of (S)-({2-[1-(2-fluorobenzyl)benzyl]pyrrolidine-2-carboxamide}phenyl}phenylmethylene)-(S)-2-fluorobenzenyl-alaninato-N,N',N'',O}nickel ^(II) 192	200
6.6.6 Synthesis of (S)-({2-[1-(2-fluorobenzyl)benzyl]pyrrolidine-2-carboxamide}phenyl}phenylmethylene)-(S)-2-hydroxy-4-fluorobenzenyl-glycinato-N,N',N'',O}nickel ^(II) 198	201
6.6.7 Synthesis of (S)-2-amino-3-(2-fluorophenyl)-2-methylpropanoic acid 202	202
6.6.8 Synthesis of (S)-2-amino-3-(2-fluorophenyl)propanoic acid 203	202
6.6.9 Synthesis of (S)-2-amino-3-(4-(trifluoromethyl)phenyl)propanoic acid 204	203
6.6.10 Synthesis of (S)-2-amino-2-methyl-3-(4-(trifluoromethyl)phenyl)propanoic acid 205	203
6.6.11 Synthesis of 2-amino-3-(4-fluorophenyl)-3-hydroxypropanoic acid 206	204
6.6.12 Synthesis of (S)-2-(((9H-fluoren-9-yl)methoxy)carbonyl)amino)-3-(4-(trifluoromethyl)phenyl)propanoic acid 207	204
6.7 Experimental for Chapter 5	205
6.7.1 Peptide syntheses	205
6.7.2 General procedure	205

6.7.3 Glaser-Hay Coupling ring closing metathesis:	208
6.7.4 Peptide purification:	210
6.7.5 Circular Dichroism	210
6.8 Synthesis of peptides modules (1-8).....	211
6.8.1 Synthesis a modification of BIM peptide and purification.	214
6.8.2 BIM stapled helix pepide	214
7 References	Error! Bookmark not defined.
8 Appendix	Error! Bookmark not defined.

Abbreviations

AA	Amino Acid
2-FBPB	(<i>R</i>) or (<i>S</i>)- <i>N</i> -(2-benzoylphenyl)-1-(2-fluorobenzyl)-pyrrolidine-2-carboxamide
Å	Angstrom
Abs	Absorbance
Acm	Acetamidomethyl
AcOH	Acetic Acid
Ala	Alanine
ALR1	Aldehyde reductase
ALR2	Aldose reductase
AM	Aminomethyl
Arg	Arginine
Asn	Asparagine
Asp	Aspartic acid
b.p.	Boiling point
Bcl-2	B cell leukemia/lymphoma 2
BH3	Bcl-2 homology 3 domain
Bim	BCL-2–interacting mediator of cell death
BPB	(<i>R</i>) or (<i>S</i>)- <i>N</i> -(2-benzoylphenyl)-pyrrolidine-2-carboxamide
Bax	Bcl-2 Associated X protein
Bad	Bcl-2 Associated death promoter
Bid	BH3 interacting-domain death agonist
Bok	Bcl-2 related ovarian killer
Bik	Bcl-2 Interacting killer
Bak	Bcl-2 homologous antagonist killer
CD	Circular dichroism
CuAAC	Copper(I)-catalysed azide-alkyne Cycloaddition
CuOAc	Copper(I) acetate
Cys	Cysteine
Dab	diaminobutyric acid
Dap	diaminopropionic acid
DCM	Dichloromethane

dd	Doublet of doublets
ddt	Doublet of doublets of triplets
DMF	N,N-Dimethylformamide
de	Diastereomeric excess
dt	Doublet of triplets
ee	Enantiomeric excess
equiv.	Equivalents
ESI	Electrospray Ionisation
EtOAc	Ethyl acetate
Fmoc	9-Fluorenylmethyl
FPB	1-(2-fluorobenzyl)pyrrolidine-2-carboxylic acid
GC-Mass	Gas Chromatography and mass spectrometry
GCN4	General Control Nondepressible
GCN4-p1	General Control Nondepressible -single polar Asn residue
Glu	Glutamic acid
Gly	Glycine
h	Hours
HBS	hydrogen bond surrogates
HPLC	High Performance Liquid Chromatography
HRMS	High Resolution Mass Spectrometry
<i>in vitro</i>	In an artificial environment outside a living organism
<i>in vivo</i>	Within a living organism
IR	Infra-red
J	Coupling constant
<i>K</i>	Stability constant
KAPA	7-keto-8-aminopelargonic Acid
LC MS	Liquid Chromatography Mass Spectrometry
Leu	Leucine
Lys	Lysine
M	Molar(mol dm ⁻³)
m	Multiplet (NMR Spectroscopy)
m.p.	Melting point
<i>m/z</i>	Mass-to-charge Ratio

MALDI	Matrix Assisted Laser Desorption Ionisation
MBHA	4-methylbenzhydramine
MeCN	Acetonitrile
MeOH	Methanol
mg	Milligram
min	Minutes
mL	Milliliter
mM	Millimolar (mmol dm^{-3})
mmol	Millimoles
mol	Moles
MS Mass	Mass Spectrometry
MsCl	Methanesulfonyl chloride
MW	Microwave
Nle	butyl-derivative amino acid
NMR	Nuclear Magnetic Resonance
NPra	<i>N</i> -propargylated amino acids (<i>NPro</i>)
°C	Degrees Celsius
Orn	ornithine
PABA	<i>p</i> -alkoxybenzyl alcohol
PG	Protecting Group
pH	negative logarithm of the hydronium ions
Phe	phenylalanine
PPIs	protein–protein interactions
ppm	Parts per million
Pra	Propargylglycine amino acids
Pro	Proline
PTC	phase-transfer conditions
PTS	phase-transfer system
q	quartet
RCM	Ring closing metathesis
RP-HPLC	Reverse-Phase High Performance Liquid Chromatography
rt	Room temperature
SPPS	Solid phase peptide synthesis
t	triplet

TBAB	tetra-n-butylammonium bromide
TBAF	tetrabutylammonium bromide
^t Bu	tert-butyl group
THF	Tetrahydrofuran
Trp	Tryptophan
UV	Ultraviolet

Chapter 1

Introduction



UNIVERSITY OF
LEICESTER

1.1 Introduction

Classic drugs in some fields have been unsuccessful in treating diseases such as cancer because certain diseases are genetic.¹ Peptides have come to represent an alternative drug over the course of the last decade, and more than twenty percent of newly developed drugs are peptides. Therefore, the synthesis of new peptides and amino acids is of particular importance in order to follow the rapidly changing requirements for new peptide drugs.² In addition, newly designed and synthesised synthetic amino acids are required to design and modify these peptides.³ Protein sequences are the key to finding the biologically active part of the protein.

Proteins and peptides are the central components of cells that achieve important biological functions. Structurally both are very similar, consisting of amino acid chains that are interconnected with each other by peptide bonds (also called amide bonds). The number of amino acids in a chain is the fundamental means of distinguishing between a peptide and a protein, where there should be between 2-50 amino acids in a peptide, and more than 50 amino acids in a protein; simply put, peptides are smaller than proteins. However, peptides can be divided into oligopeptides, which have 2-20 amino acids, and polypeptides, which have more than 20 amino acids.⁴ Protein structures can be classified according to four types with respect to their structure: primary, secondary, tertiary and quaternary. α -Helixes and β -sheets are the main common conformations of secondary structures (Figure 1.1).

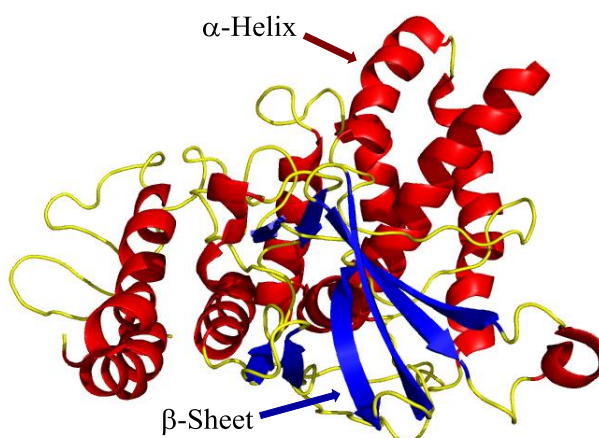


Figure 1.1: α -Helix and the β -sheet

Large physical or chemical interactions, specifically between two or more proteins, are called protein–protein interactions (PPIs). This category of interaction is significant in terms of the overall stability of the resultant proteins.^{5, 6} PPIs have been studied in fields including biochemistry, molecular dynamics and signal transduction.⁷ One of the most significant efforts has been invested in improved methods to identify and analyse PPIs as a part of drug targets analysis. Drugs should have sufficient specificity to compete and interact with their intended targets, minimizing probable interactions with thousands of other intracellular proteins. Nevertheless, most proteins that have been synthesised are still at the biochemical *in vitro* assay stage, and have not progressed to drug discovery.

1.2 Peptidomimetics

Peptidomimetics, which are small molecules designed to imitate peptides, can be classified in three ways: as functional mimetics, as structural peptides and as native active peptides. The design of peptidomimetics with high bioactivity can be achieved via numerous routes, such as conformation restriction, modification and non-peptide design. This thesis will focus on the first and second types.⁸

Peptides Bim-BH3 and BAK-BH3, which are members of the anti-apoptotic Bcl-2 family, have been modified by substituting β -amino acids instead of various α -amino acids in different positions in the peptide sequence to form $\alpha\alpha\beta$ and $\alpha\alpha\alpha\beta$ peptide patterns. The new peptides have been shown to bind with BH3-recognition sites and support an α -helix. Also, the new peptides represent good inhibitors for both BAK and Bim-peptide proteins in comparison to the native peptides (Figure 1.2).⁹

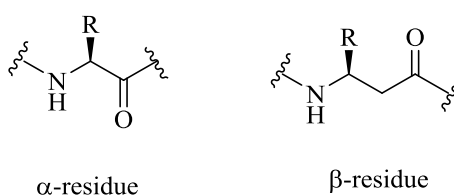


Figure 1.2: α -amino acid and β -amino acid.

1.3 Helix stabilisation

Helices are a major class of secondary protein structures and play an active role in mediating PPIs.¹⁰ Protein and peptide architectures can be categorised into four common groups: α -helices, 3^{10} helices, β -sheets and residues (random).^{11, 12} Helices are

represented in approximately one-third of natural proteins,¹⁰ of which α -helices are the most common secondary structure in proteins. They can increase stability by introducing constraints into the forms of the helix. As an example, hydrogen bonding between the carbonyl and amine proton provides the thermodynamic driver for peptide folding into the helix. The fundamental design of the α -helix is that of a periodicity of 3.6 residues per turn, where the constraint bond should be at positions $i, i+3$,¹³ or $i, i+4$ or $i, i+7$ or $i, i+11$;¹⁴ the $i, i+3$ combination is extremely rare compared to the other combinations (Figure 1.3). The α -helix is very important compared to other secondary structures because 62 % of the secondary structure in proteins is α -helical, whereas this conformation is rarely adopted in isolated small peptides. As an example, hydrogen-bonding between the carbonyl and the amide proton provides the thermodynamic driving force both for bridges within the same peptide strand and also between strands in dimers (Figure 1.3).¹⁵

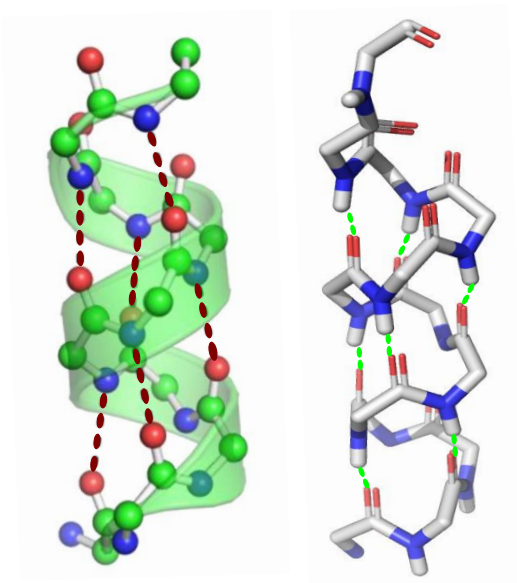


Figure 1.3: Diagram of α -Helix peptide showing hydrogen bonds between NH and CO groups to form the helix.¹⁶

Many forms of constraint within α -helix structures have been discovered and developed over the last few years; for instance salt bridges,¹⁷ hydrophobic interactions,¹⁸ hydrogen-bonding surrogates¹⁹, lactams,²⁰ photo-controllable macrocycles,²¹ disulphide bridges,²² metal ligation^{23, 24} and hydrocarbon stapling.²⁵ Proteins are a major component of the biochemistry field, and indeed human health. Therefore, a lot of research has focussed on studying proteins' α -helices so as to study their three-dimensional shapes or to design

novel constrained helices. There are many advanced approaches that can stabilize a given conformation. The main strategies include side-chain cross-linked helices, α -peptide helices, mini-proteins, terphenyl helix mimetics, and peptoid helices (Figure 1.4).²⁶⁻²⁹ For side-chain cross –linked helix there are six different categories.

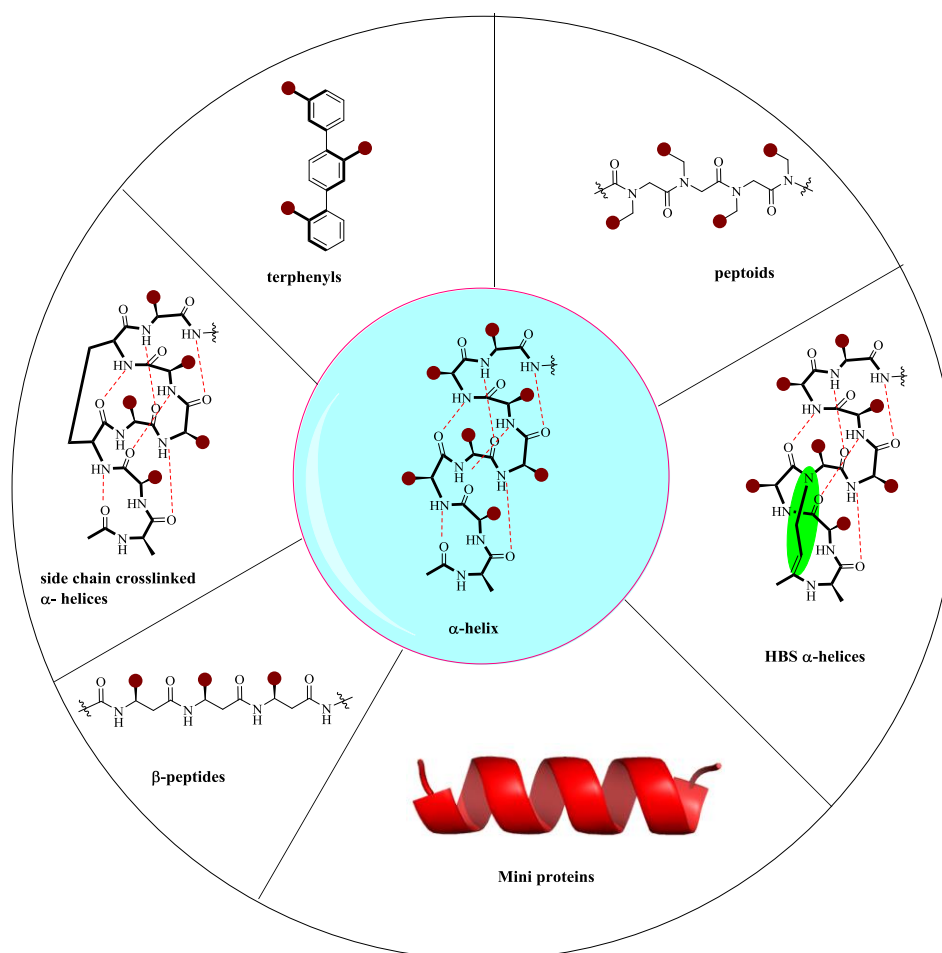


Figure 1.4: Stabilized helices and non-natural helix mimetics¹⁰

1.3.1 Hydrogen-bonding surrogates

Hydrogen bonds are common in helical peptides. However, there is another type of hydrogen bond in peptides, known as hydrogen bond surrogates (HBS), where one or more regular hydrogen bonds are replaced with a covalent bond that affects the helix conformation at that position. These hydrogen-bonding linkages can be a motif with specific groups such as hydrazones¹⁹ or alkenes.¹⁰ The conformation is generally established by 2D NMR and CD spectroscopy.^{19, 30, 31} Chapman *et al.*¹⁹ utilised the ring-closing metathesis reaction to create an alkene linkage between the *i* and *i*+4 residues in the Bcl-2-antagonist/killer Bcl-2 homology3 Bak-BH3 peptide type (Figure 1.5). In

addition, much shorter peptides with a helical conformation have been synthesised using the HBS strategy. However, the maximum number of the amino acids confirmed for the use of the HBS strategy in α -helices is ten residues, because of the low probability of nucleation beyond this.^{32, 33} Nevertheless, the HBS has been used in the short peptides, where it is more possible to constrain them within helical conformations.

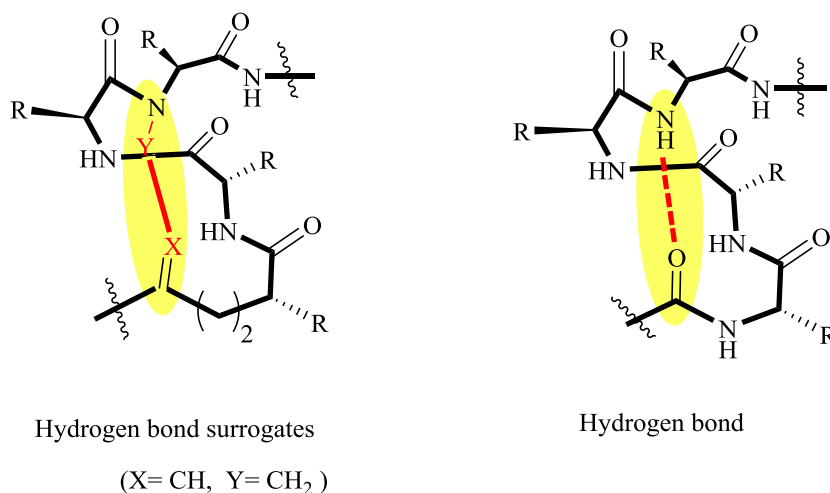


Figure 1.5: Stabilizing α -helices via hydrogen bond surrogates and hydrogen bonding.¹⁹

1.3.2 Hydrophobic interactions

Tyrosine, phenylalanine, histidine and tryptophan are all good examples of amino acids with aromatic side chains. These contribute to stabilising peptides by forming α -helices through π - π stacking^{18, 34} with free energies between -0.6 and -1.3 kcal/mol.^{35, 36} Hamilton and co-workers supported this hypothesis by designing sequences of short α -helix peptides (14-20 amino acid residues) at the i and $i+4$, $i+7$ and $i+13$ positions including ϵ -(3,5-dinitrobenzoyl)Lys (Figure 1.6). Their results showed that the ϵ -(3,5-dinitrobenzoyl)Lys $i+4$, $i+13$ and the ϵ -(3,5-dinitrobenzoyl)Lys i , $i+7$ peptides, and the ϵ -(3,5-dinitrobenzoyl)Lys $i+4$ peptide, have the best α -helical characters, where ~ 6 Å is the distance between the two aromatic rings that interact in the peptide.¹⁸

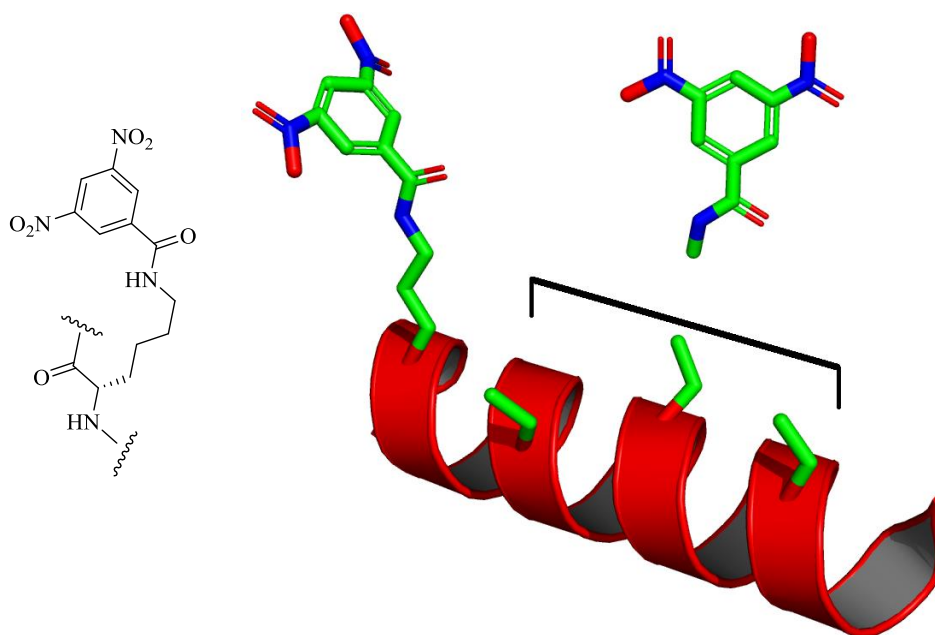


Figure 1.6: Example of a hydrophobic interactions in peptides.¹⁸

A recent study on hydrophobic interactions, as reported by by Tatko and Waters, made an extensive comparison of different pairings in a β -hairpin peptide. Lys formed a better polarization interaction with Phe or Trp, however, the unnatural butyl-derivative amino acid (Nle) Lys did not, in general, interact indicating that a number of factors affect this type of hydrophobic interaction (Figure 1.7).³⁷

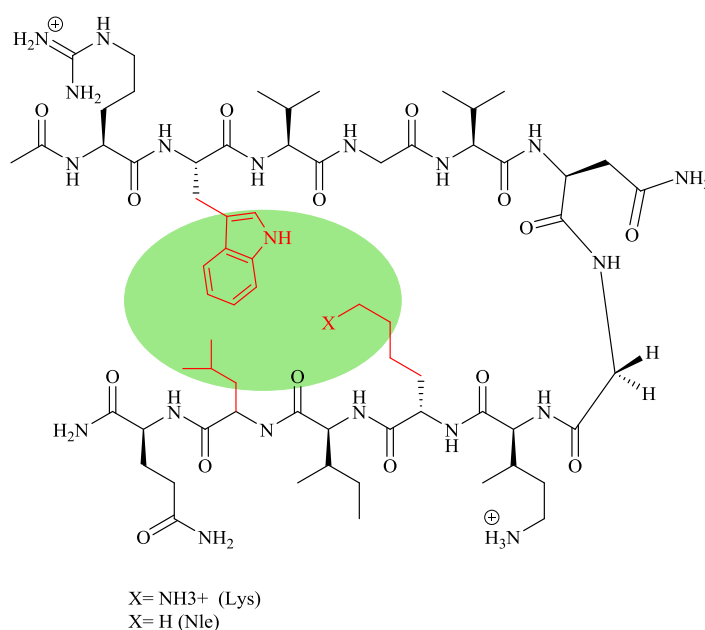


Figure 1.7: Interaction of the Lys and Nle with Trp.³⁷

1.3.3 Salt bridges

It is well known that electrostatic interactions can affect helical conformations in solution,³⁸ and a salt bridge was one of the first methods of constraint to be examined and involves the interactions between i and $i+4$ residues of an α -helix. The amino acid residues involved in this type of constraint include lysine, arginine, aspartic acid and glutamic acid (Figure 1.8).¹⁷ These amino acids have either positively or negatively charged side chains that facilitate an electrostatic interaction. In some cases, residues such as histidine, serine and tyrosine can also be ionized. Therefore, the major types of amino acids that participate in the salt bridge-type constraints depend on the environment within which the amino acids are located in order to form an electrostatic or hydrogen-bonding interaction. There are both advantages and disadvantages to this type of helix constraint. The main factors that affect the nature of a salt bridge are:

- 1) The distance between the amino acids in the peptide as well as their stereochemistry. The distance required to form a salt bridge is believed to be less than 4 Å.³⁸
- 2) The positioning of the amino acids within the peptide α -helix sequence. For instance, the difference in helicity is more obvious when a glutamic acid residue is located at the i position and a lysine at the $i+3$ or $i+4$ position.³⁹
- 3) The peptide environment also has an influence on the stabilization of the α -helix induced by the formation of a salt bridge. The degree of helicity of the peptides can be influenced by the pH of the solution and the salt concentration.³⁹

The main, highly specific interaction can be seen between these amino acids: Asp-Arg, Asp-Cys, Glu-Arg, Glu-Cys.⁴⁰ Walther and Ulrich found that the most helical peptide conformation occurred at pH 7 in 0.01 M NaCl at 1°C in a pH titration. In addition, either side of this pH value (that is an increased or a decreased pH) made the peptide helicity significantly lower.⁴¹ On the other hand, changing the concentration of NaCl to 1.0 M also had an impact on the helical structure of the peptide.³⁹

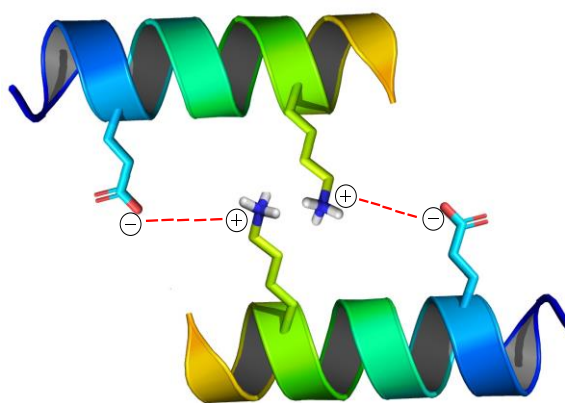


Figure 1.8: Salt bridging motifs found between glutamic acid and lysine residues showing electrostatic interactions.³⁹

Ibarra-Molero *et al.* showed how a dimeric coiled-coil peptide has two types of interactions; intra- and inter-chain salt bridges in the folded state that increase stability. The compound GCN4-p1 is a 33-residue peptide in which the leucine has an electrostatic field to the glutamine which had been substituted at the GCN4 component. At neutral pH, the interactions were located at the N-terminal to give a helical structure as determined by circular dichroism. Circular dichroism studies of urea-induced unfolding at neutral pH revealed that both types of ionic interactions, localised primarily in the N-terminal of the molecule, showed better helicity relative to the native coiled-coil. In a different compound, E22/R25, the amino acids were shown to form an intramolecular salt bridge with an increased helicity of the peptides. GCN4-p1 is stabilised by dimerization through intramolecular helical salt bridges between parallel-stranded coiled-coil, with the bridges formed between Lys and Glu in the peptide (Figure 1.9).⁴²⁻⁴⁴

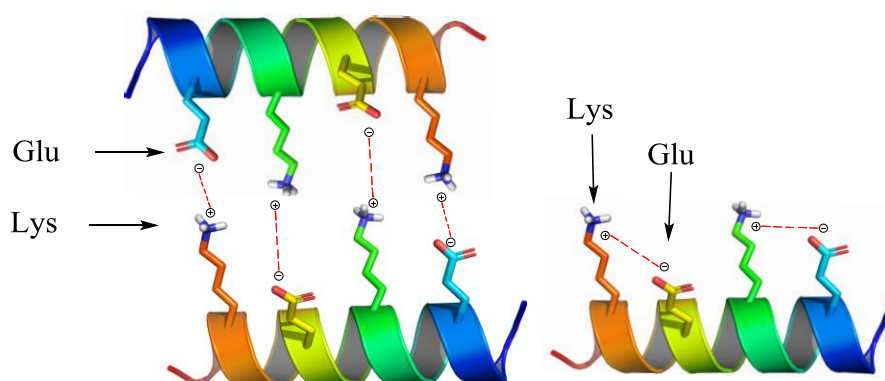


Figure 1.9: Inter- and intra-molecular helical-salt bridges in peptides.⁴²

1.3.4 Photocontrollable macrocycles

External stimulus is one of the main factors affecting α -helix stability. Alleman and co-workers reported a new method which restricted the helix through using light of different wavelengths.²¹ An azobenzene cross-linker was reacted with cysteine residues to make the peptide bridge at i , $i+4$, $i+7$ or $i+11$. The peptides with azobenzene crosslinks positioned at the i and $i+4$ residues adopt a *cis* configuration; however, with the crosslink positioned at i and $i+7$ residues, a *trans* configuration is adopted. Furthermore, both the *cis* and *trans* species depend on the wavelength of light used for excitation (Figure 1.10).²¹

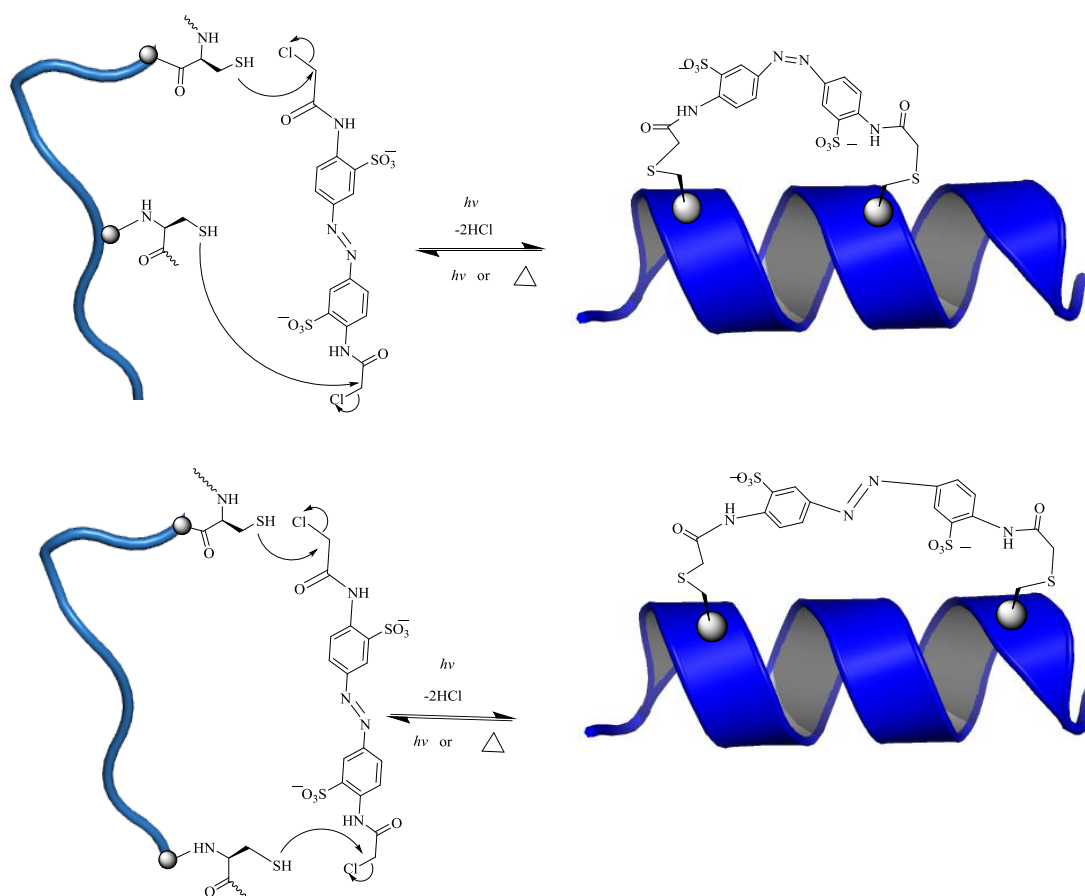


Figure 1.10: The structure of the azobenzene crosslinker changed on irradiation with light or application of heat.²¹

1.3.5 Disulfide bridges

Disulfide bridges have been exploited by numerous researchers to increase the stability of α -helices during peptide synthesis.²⁰ Short peptides containing a two-turn α -helix were created by Jackson *et al.*²² A single intramolecular disulfide bond was

synthesised as a bridge between the i and $i+7$ residue positions (Figure 1.11). These peptides dissolved in water at temperatures of 0 °C and 60 °C. The new peptides showed higher helicity in comparison to their native peptides.

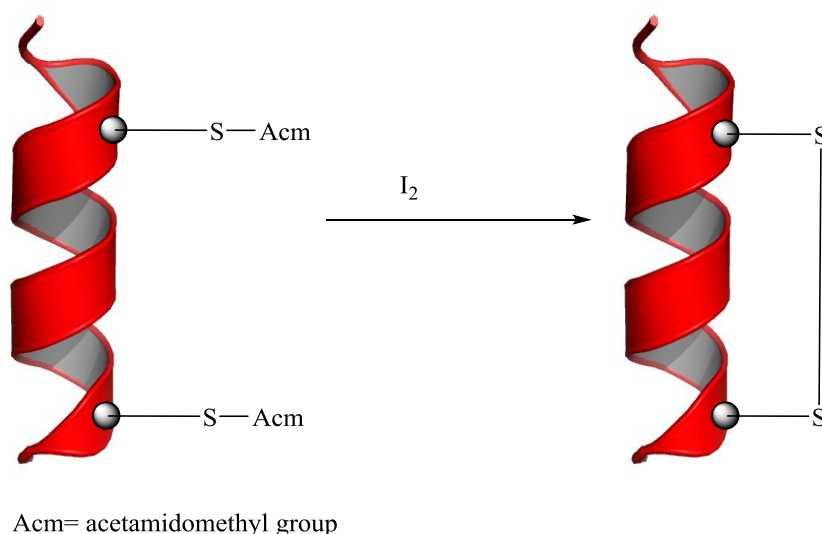


Figure 1.11: Synthesis of a disulfide-bridged α -helical peptide.²²

1.4 Metal ligation

One more significant type of α -helix stabilisation is the metal ligation technique in which a metal ion coordinates to ligands in the peptide sequence. The entropy should decrease on formation of the helix in the peptide on coordination between the metal ion and the ligands that form the bridge. Ruan and co-workers found the position $i, i+4$ ligand preferred metal ligation. Twenty types of the peptides were synthesised, of which only fifteen peptide-metal complexes enhanced the helical structure with increased stabilization (Figure 1.12).²³

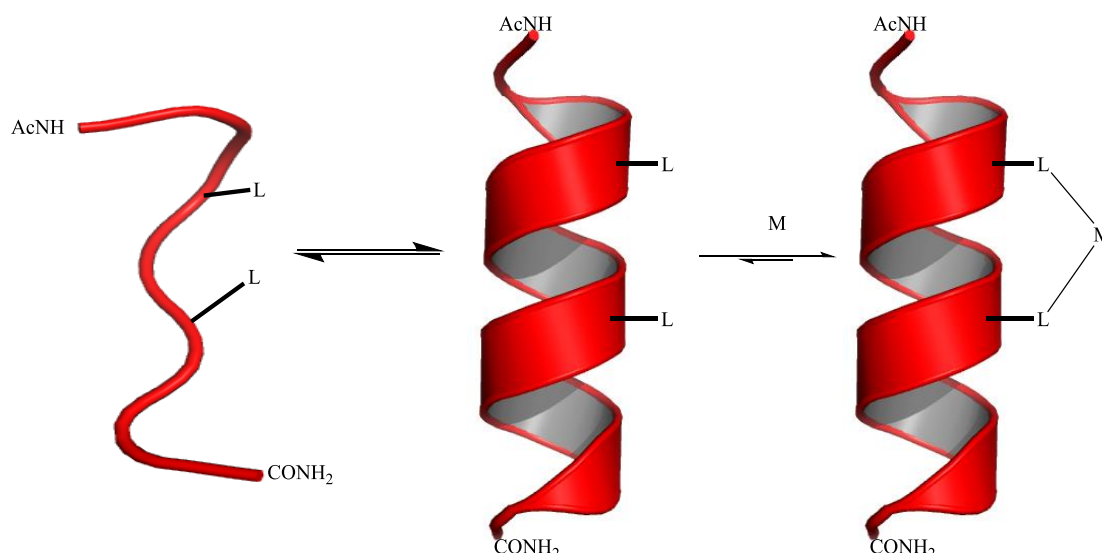


Figure 1.12: Metal ligation as a means of stabilizing an α -helix.²³

1.4.1 Lactams

A lactam is a cyclic di-amide. In 1987, Rosenblatt and co-workers demonstrated the first lactam bridge used to link a lysine and an aspartic acid residue at the i , $i+4$ positions on a peptide.⁴⁵ Luyt and co-workers (2018)⁴⁶ have also used the lactam bridge on Ghrelin peptides (20-residue amino acids). The lactam was designed using glutamic acid and lysine in the $i+4$ and $i+7$ positions in the peptides. Palladium(0) was used to catalyse the formation of the bridge because it has highly selectivity without affecting protecting groups on the amino acids during the peptide-resin ring closure reaction. Lactam-bridged peptides showed greater helicity in comparison with those of the native linear peptides, as well as greater fluorescence and good receptor binding with ovarian cancer cells (Figure 1.13).⁴⁷

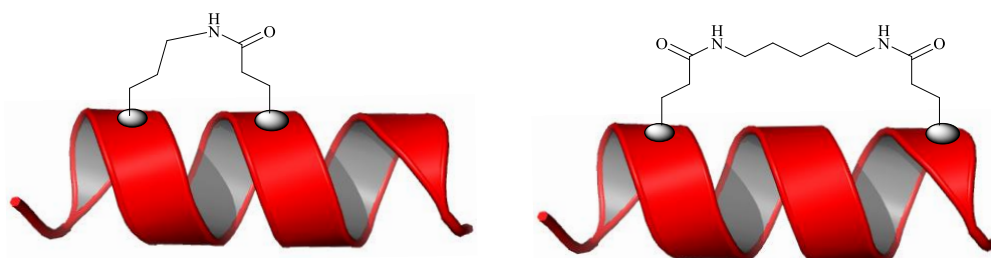


Figure 1.13: Lactam bridge to stabilize an α -helix peptide.⁴⁶

1.5 Hydrocarbon stapling

One of the more recent categories for stabilising the helical conformation of peptides is hydrocarbon stapling. This uses alkenes in the design of unnatural amino acids, which form a bridge in the peptide through metathesis catalysis (Figure 1.14). The bridge between the positions i , $i+4$ is the most common type in α -helix hydrocarbon stapling related to the other positions at i , $i+3$, i , $i+7$ and i , $i+11$.⁴⁸ A large number of research groups have used the same strategy to synthesise a large variety of hydrocarbon staples and have examined the stability of the associated peptides, as can be seen in the research of Grossmann,⁴⁹ Belokon,⁵⁰ Chapman,¹⁹ Verdine,^{13, 51-54} Grubbs^{55, 56} and Walensky.⁵⁷

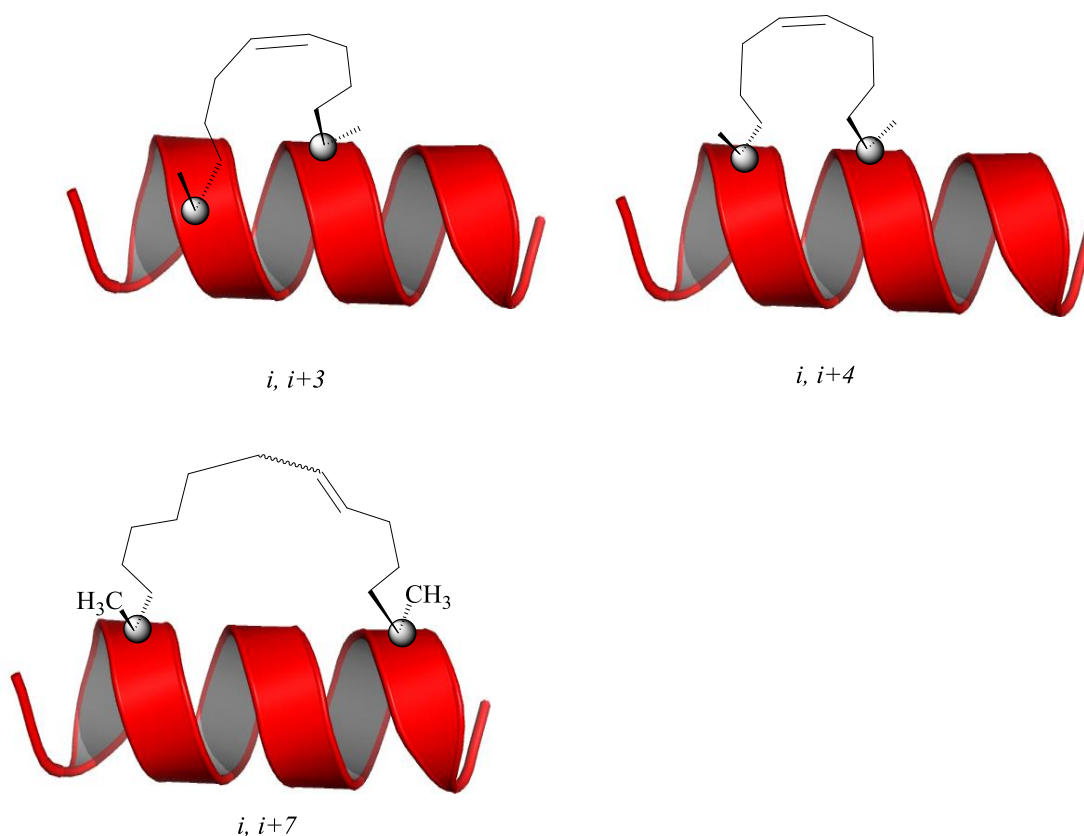


Figure 1.14: Categories of hydrocarbon staple.

1.6 Design of alkene-stapled peptides

Ring closing metathesis (RCM) bridges strongly affect the stabilization of peptides. In RCM synthesis, there are several factors that need to be taken into account to increase the stabilization in peptides. For example, the length of the bridge that forms the macrocycle, heteroatoms in the bridge, multiple bonds and side chains in the bridging

peptide, the primary structure of the original amino acids in peptide, the stereochemistry (*D* or *L*), the location of and the distance between the bridgehead amino acids (Figure 1.14) and the type of ruthenium (pre)catalysts the used in RCM reaction (Figure 1.15).⁵⁸ However, there can be weaknesses in this strategy from the conformation of the closed RCM bridge. Both *cis* and *trans* conformations, in different ratios, can arise depending on the ruthenium derivatives that were used as catalysts or from the length of the bridges, especially when distant positions, such as *i, i+7* or *i, i+11*, are used because these show less conformational constraint. In addition, when these mixed conformations are present they can be too difficult to isolate from each other because both have the same molecular weight and the same active groups.⁵⁹

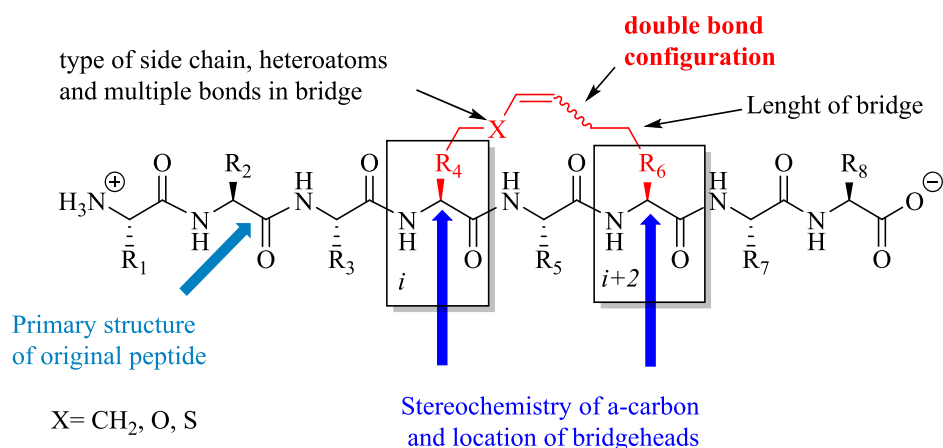
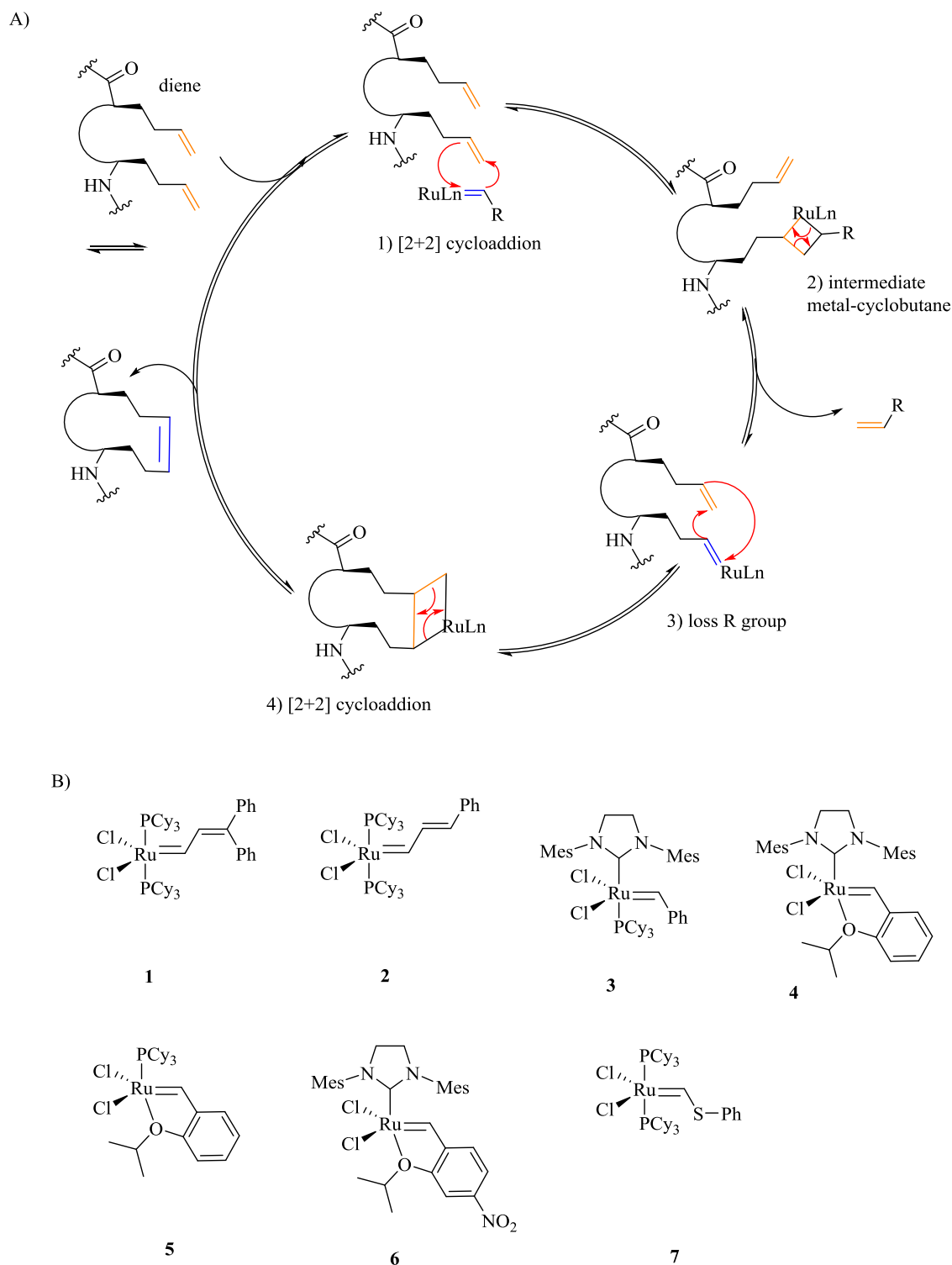


Figure 1.15: Considerations needed in installing a constraint.

1.7 Catalysts for ring closing metathesis RCM (Hoveyda-Grubbs) reaction

The general mechanism for RCM using ruthenium catalysts, which is known as the Grubbs reaction, is shown in (Scheme 1.1 A). Moreover, there are many types of ruthenium catalyst, which have been used in this reaction, as shown in (Scheme 1.1 B). The first generation of such are exemplified by compounds 1-3 that were utilised (at 5-40 mol %) to give selective products (*E*/*Z*) (4:1) in CH_2Cl_2 .^{55, 60} The second generation of ruthenium catalysts were developed by Hoveyda and Grubbs, who used catalyst 4 under microwave reaction, at 100 °C in CH_2Cl_2 : DMF (9:1) to give nearly complete (*E*)-selectivity.⁶¹ Catalysts 1, 2 and 7 failed to deliver good results under the same reaction conditions.⁶²



Scheme 1.1: A) The Grubbs mechanism reaction of ring closing. B) The most commonly used metathesis pre-catalysts for RCM in peptide.

In 2000, Verdine and co-workers demonstrated the hydrocarbon staple using both unnatural *R* and *S* alkyne amino acids. They synthesised an enormous series of new α,α -disubstituted amino acid olefin moieties, where the stability of the folded peptides was

shown to depend upon the stereochemistry of the amino acid. The group investigated RCM staples of between 8 and 11 carbon atoms, and showed a difference in stability dependent on the staple length. Overall, they found an increased helical structure stability of more than 15 % in the alkene RCM stapled peptides as compared to the native peptides. $Ri,i+7S(11)$ showed the best helicity, with 44 % helix stability from CD data. (Figure 1.16).⁶³

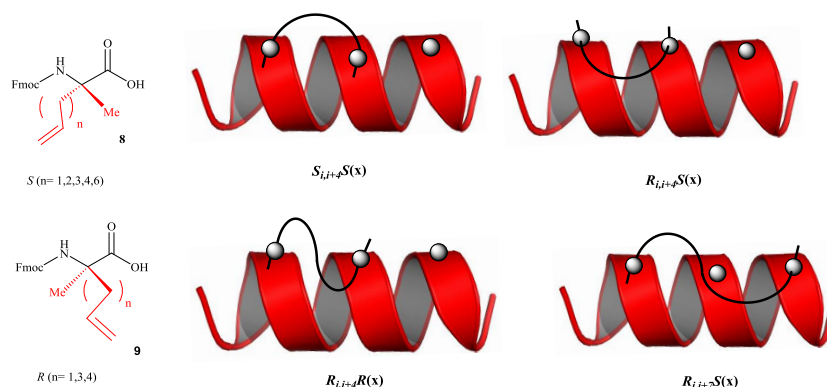


Figure 1.16: Stabilizing α -helices into peptides at i , $i+4$ or i , $i+7$ positions.⁶³

1.8 Fluorinated amino acid in peptides and proteins.

Fluorine has two significant factors which make it an important element. Firstly, it has a small van der Waals radius (1.47 Å).⁶⁴ Secondly, it has the highest electronegativity (3.98).⁶⁵ These factors have led to a significant growth of fluorinated organic compounds in many research fields, such as materials chemistry,^{66, 67} synthesis of fluorinated organic molecules including amino acids,⁶⁸⁻⁷¹ and fluorinated proteins.⁷²⁻⁷⁵ Fluorination is now considered a common strategy for modification of the features of small organic molecules, peptides and amino acids. This design has been so effective that, today, around one-quarter of all pharmaceuticals include at least one fluorine atom, in spite of the fact that fluorinated organic compounds are very rare in nature (Figure 1.17).^{72, 76, 77} Many peptides have been examined as potentially promising, extremely active, pharmaceutical compounds.

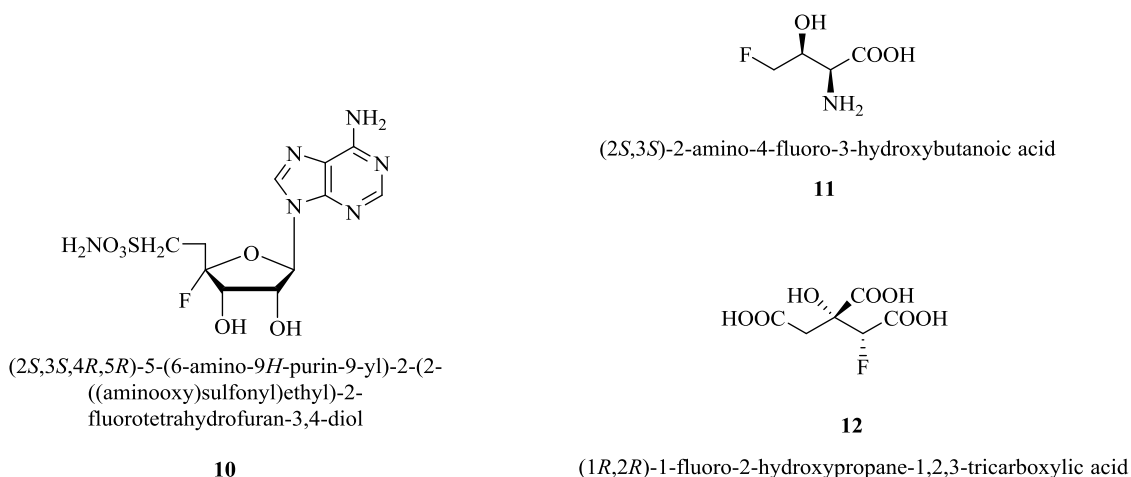


Figure 1.17: Natural products containing fluorine

^{19}F NMR is a beneficial tool for examining both interactions and dynamics of fluorine-labelled biomolecules such as proteins, peptides and nucleic acids. Moreover, fluorinated substrates have been used to investigate the mechanisms of many enzymes.⁷⁸ Synthetic strategies have developed rapidly for the synthesis of many fluorinated analogues of amino acids.^{79, 80} Most recently, research has focussed on the synthesis of amino acid derivatives with fluorine containing aliphatic and aromatic side chains.^{72, 81} Fluorine substituents on the aromatic side chain in an amino acid leads to structural rearrangement and increased hydrophobicity of the aryl side chain. Recently, the C-F polar bond has been used to affect protein interactions, in particular protein stabilization due to the formation of polar bonds (H-bond) between with protein side-chains with carbonyl and guanidine ions.⁸²

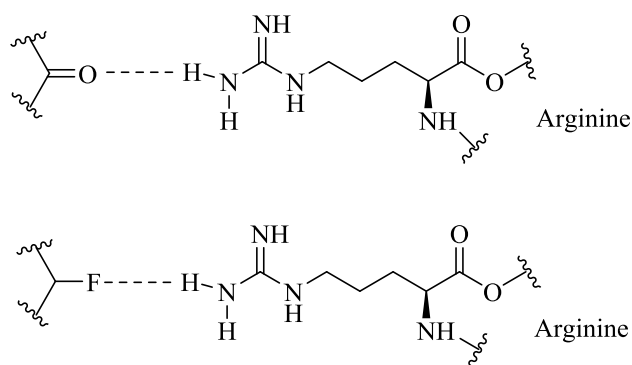


Figure 1.18: Use of fluorine as an isosteric analogue instead of the carbonyl group

Wipf *et al.* reported the synthesis of an isosteric analogue of the gramicidin peptide, (similar shape with different atoms) incorporating a CF_3 -(*E*-alkene), which functions as

an antibiotic cyclic peptide. Here, NH (Val) and C=O (Leu), in two positions, make interstrand hydrogen bonds in the structure.⁸³

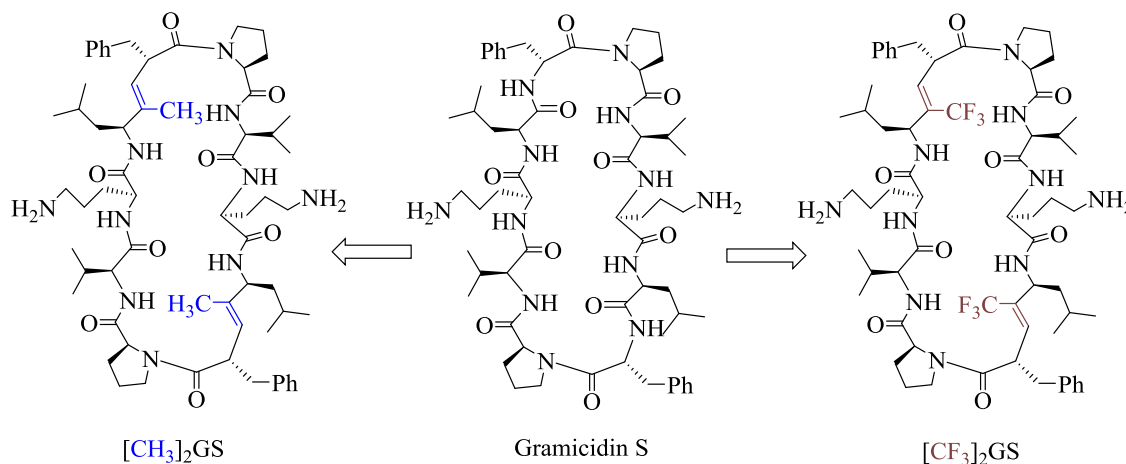
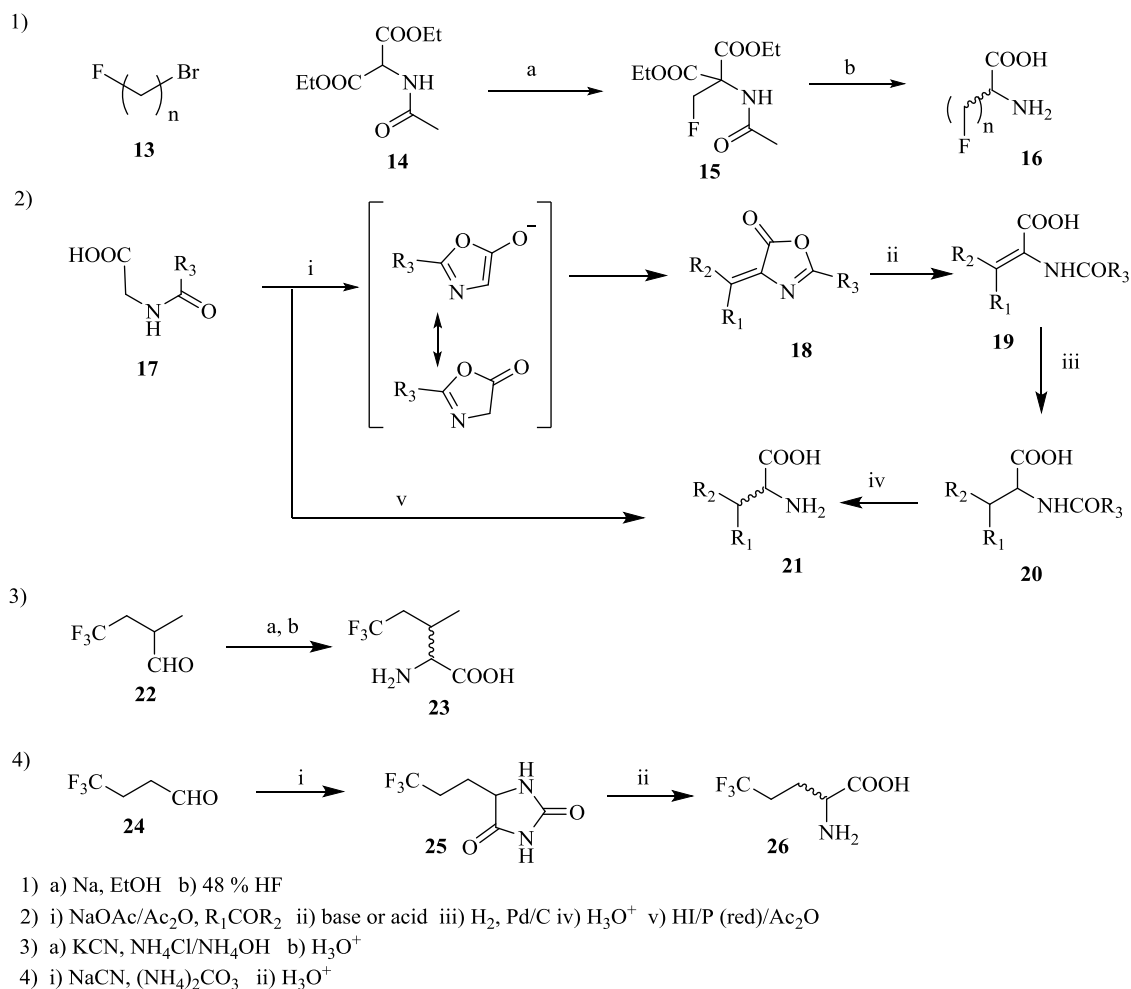


Figure 1.19: Synthesis of Gramicidin S and include two (*E*)-alkene isosteric analogues.

Synthesis of fluorinated amino acids can be divided into two methods: the classical and the modern method. Classical syntheses include (Scheme 1.2) alkylation of amino carboxylic,^{84, 85} azalactone synthesis (Erlenmeyer synthesis),⁸¹ the Bucherer-Bergs approach (hydantoin intermediates)⁸⁶ and the Strecker reaction (cyanohydrin synthesis).⁸⁷



Scheme 1.2: 1) Alkylation of amino carboxylates 2) Erlenmeyer Synthesis 3) Bucherer-Bergs Approach 4) Strecker reaction.

1.9 Synthesis of α,α -disubstituted amino acids via a Ni^{II} Schiff base complex

1.9.1 Synthesis of Ni^{II} Schiff base complexes

α -Amino acids (*S*) are uncommon in nature compared to their corresponding (*R*) enantiomers. α -Amino acids (*S*) show significant activity in peptide mechanisms (cell wall, venoms) in both microorganisms and plants. Enantiomer (*S*) has also been found in a type of peptide synthesized by animal cells and as well as in a few enzymes producing or metabolizing amino acids (*S*).⁸⁸ The synthesis of chiral α -amino acids has become one of the major areas in chemical industries because their associated utility in food production and health care. For these reasons α -amino acids (*S*) have been the subject of strong synthetic activity. The asymmetric synthesis of enantiomerically pure α -amino acids (unnatural) can be achieved using different chiral auxiliaries and catalysts. These methods have become a major modern method in the field of bioorganic chemistry,¹ and

have been seen in several syntheses of amino acids during the last century. Several types of Ni^{II} Schiff base complexes have been created to generate chiral α -amino acids.⁸⁹ Their design can be divided into four major components as related to structure: phenone, amine, acid, amino acid (Figure 1.20).⁹⁰

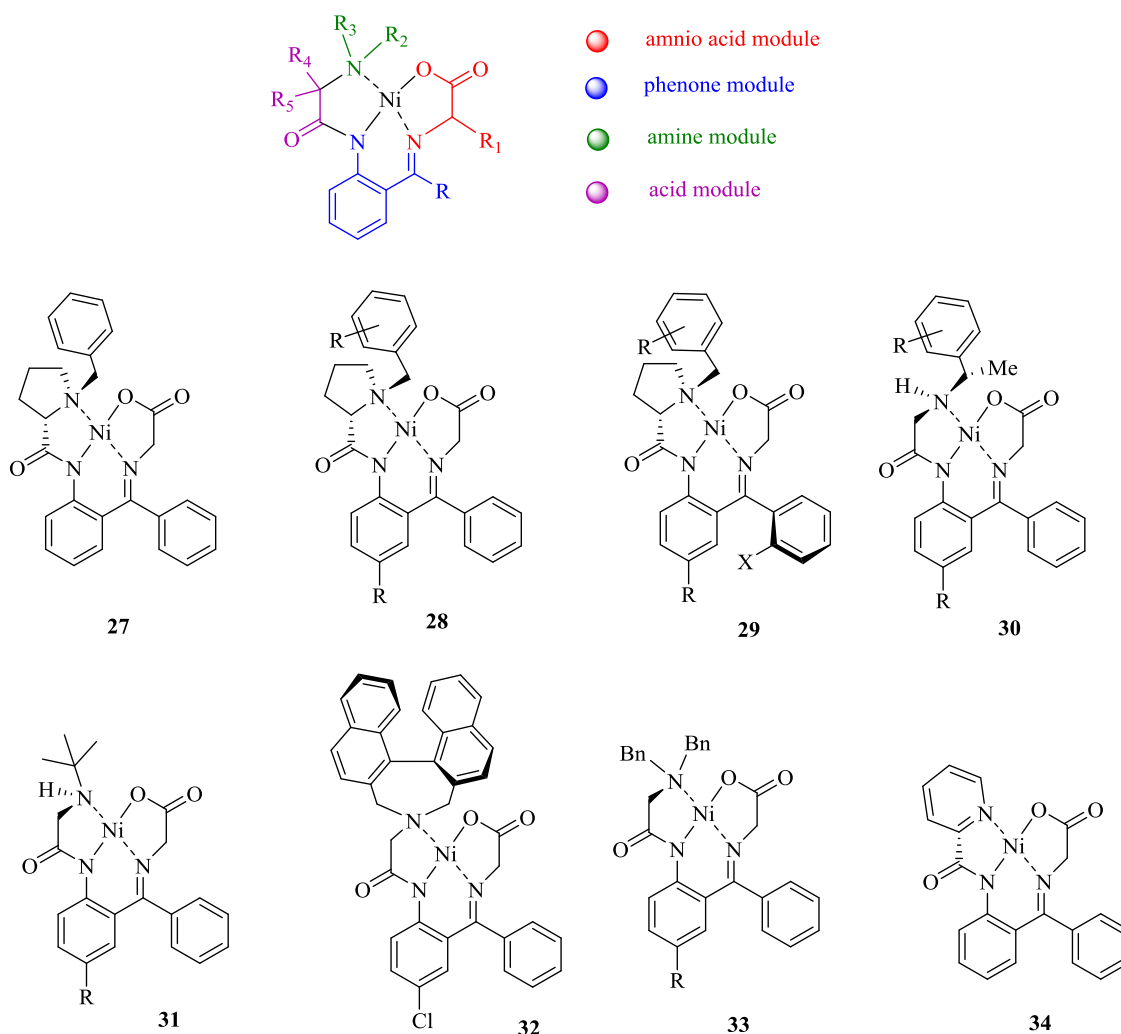
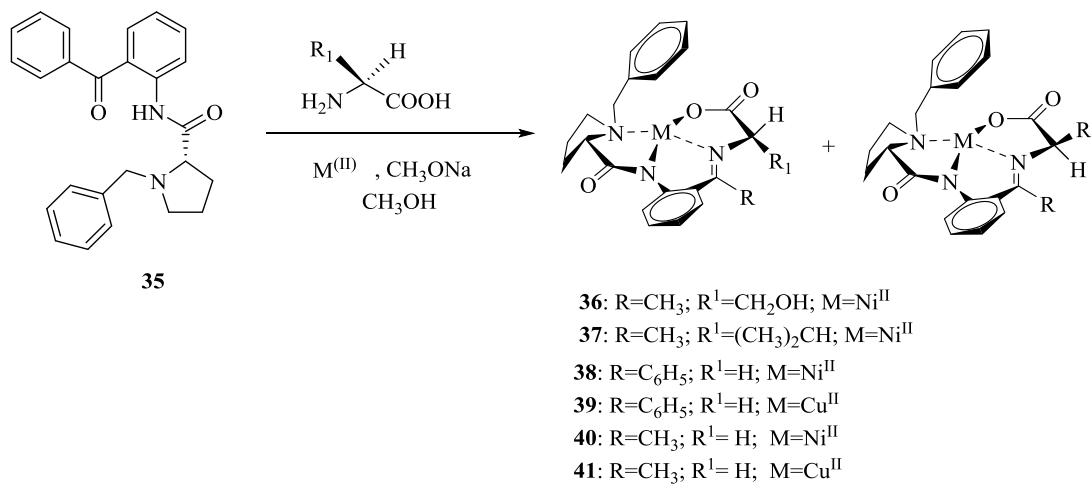


Figure 1.20: Modular design of Ni^{II} -complexes of amino acids and structure of glycine complexes.

The first method was discovered by Izumi *et al.* (1978) to synthesise of the new amino acids via Ni^{II} complexes of Schiff bases has been demonstrated.⁹¹ In 1985, Belokon *et al.* investigated the differential impact of using same ligand with different metals, for example Ni^{II} and Cu^{II} . Both of them formed a square planar complexes. The Cu^{II} complex showed a diamagnetic properties, whilst the Ni^{II} complex showed a paramagnetic properties, however, the polarimetric analysis and the CD spectra were used to compare the complexes. In spite of obtaining a yield of more than 60 % for both complexes, the

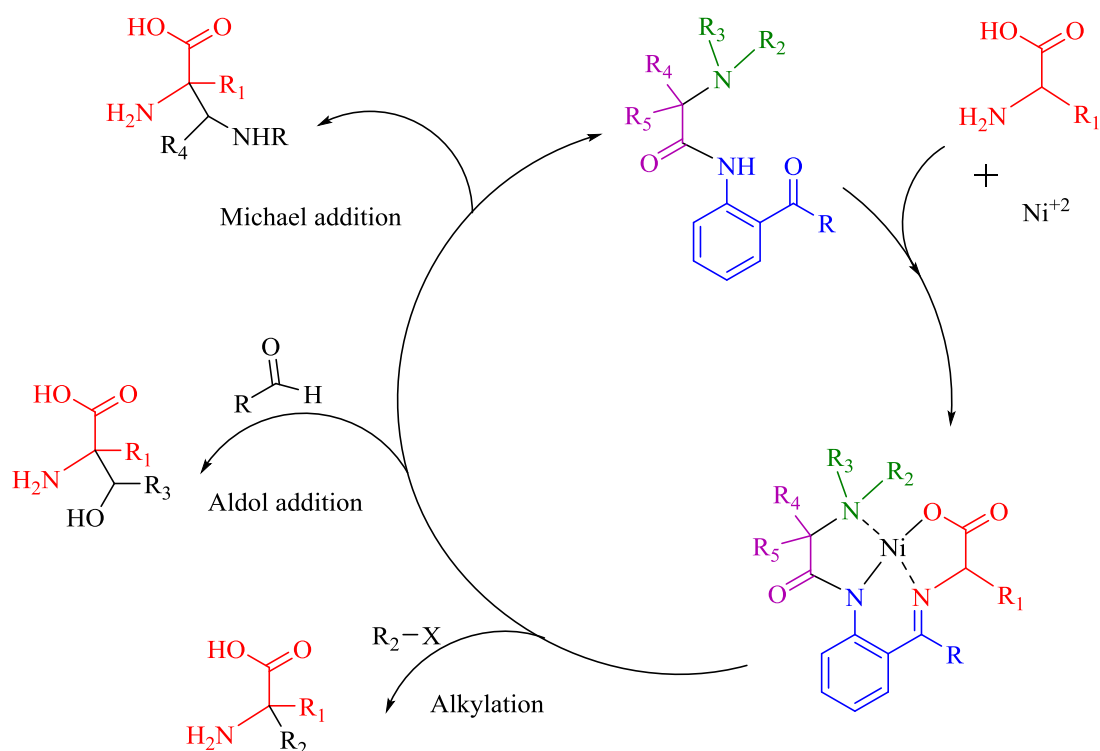
ee values for the new amino acids had been between 80-95 % the Cu^{II} preferred to form the R configuration in contrast to the Ni^{II} complexes, favouring S.⁵⁰



Scheme 1.3: Preparation of the complex with two metals a) Ni^{II} b) Cu^{II} .

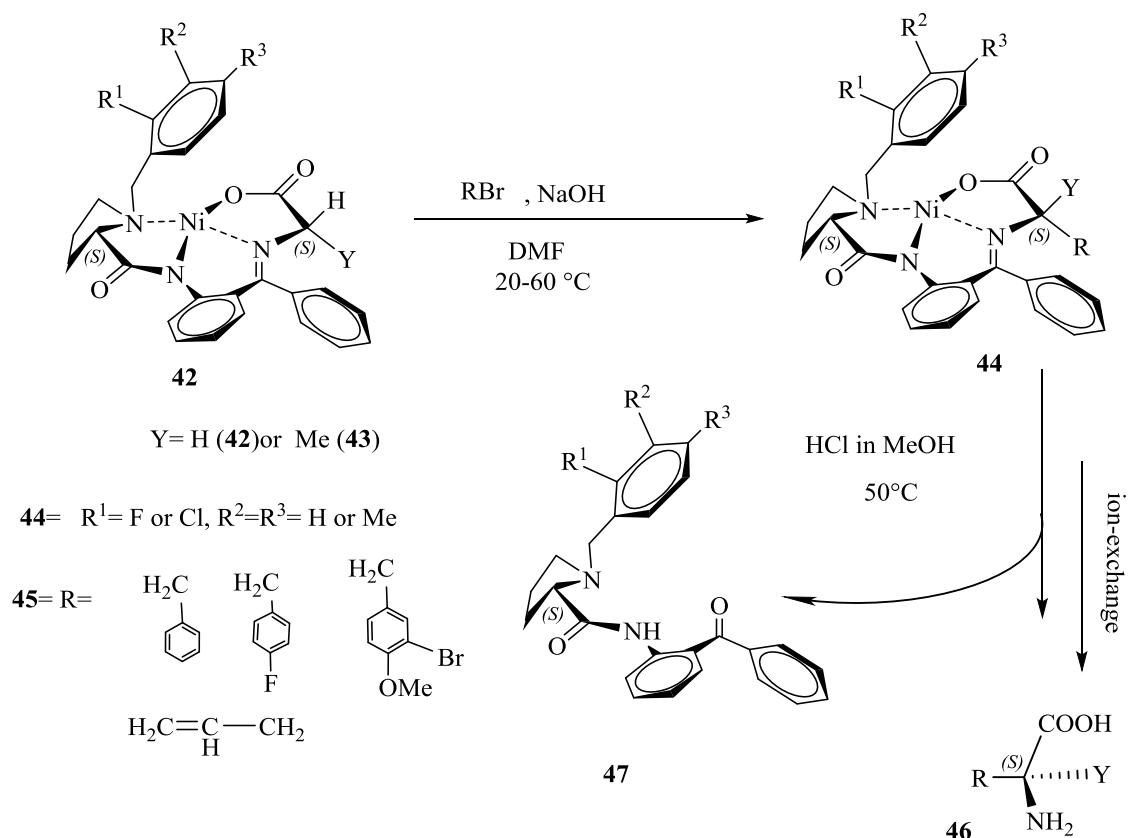
1.9.2 Application of Ni^{II} Schiff base complexes in amino acids synthesis

Synthesising unnatural amino acids using symmetric Ni^{II} Schiff base complexes have been accomplished by three major routes (Scheme 1.4): Alkylation, Aldol, Mannich addition reactions. These reports using these reactions are increasing and the methodologies developed to obtain higher yields with better enantioselectivities.^{92, 93}

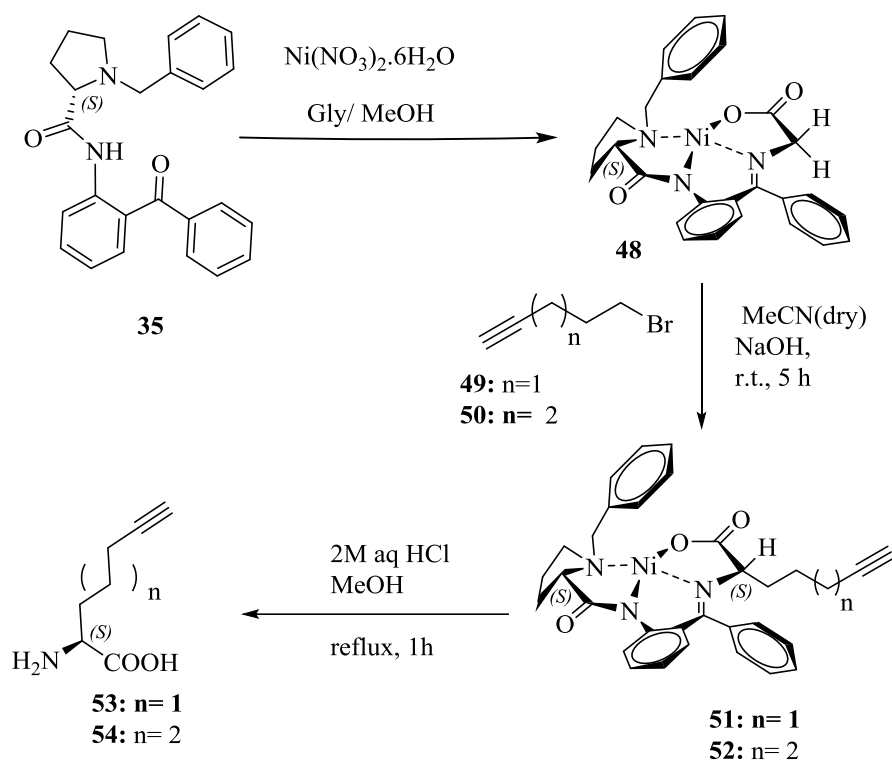


Scheme 1.4: Synthesis of the unnatural α -amino acids via Ni^{II} complexes of Schiff bases.

A successful application of the asymmetric alkylation reaction is that between the Ni^{II} complex of alanine and alkyl halides. There have been many attempts by several researchers to increase the diastereoselectivity of the alkylation step using different types of Ni^{II} complex and different types of benzyl group starting from proline as a chiral auxiliary. In 2006, Saghyan and co-workers presented the replacement of the hydrogen with a halogen such as chlorine or fluorine at the 2-position of the benzene ring which led to an increase in the rate of reaction together with a higher stereoselectivity (Scheme 1.5).⁹⁴

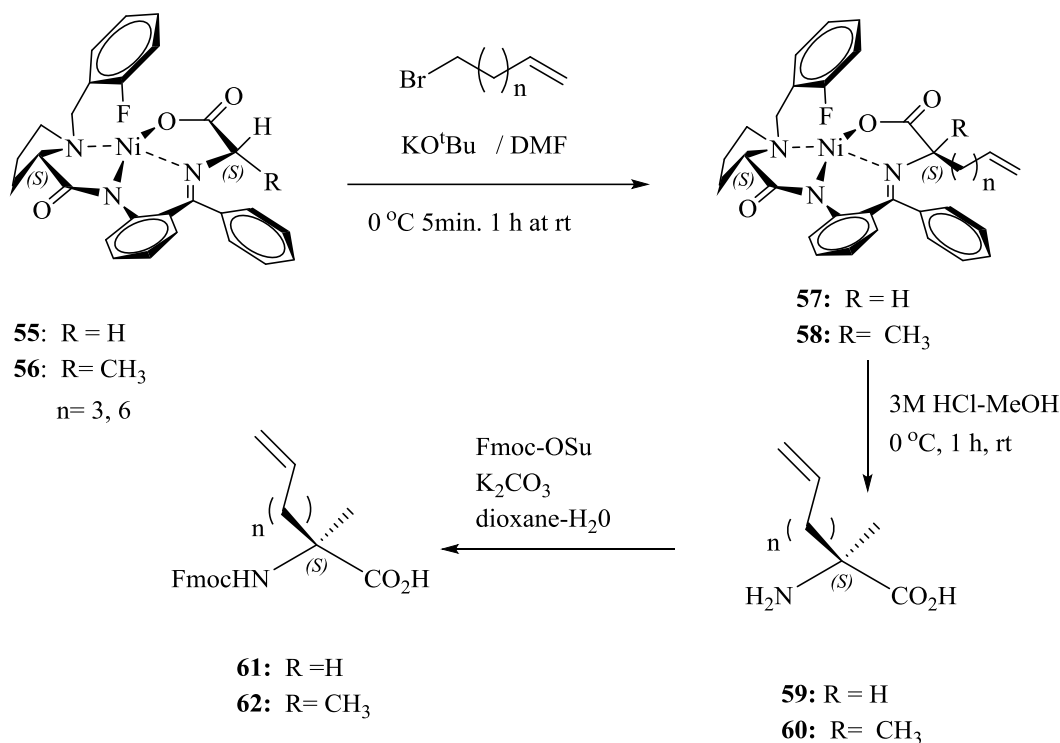
Scheme 1.5: Synthesis of the complex and alkylation in the alpha position⁹⁴

Moreover, according to Saghiyan *et al.* (2010), a new generation of chiral auxiliaries substituted on BPB can raise the enantioselectivity by using fluorine in different positions on the benzene ring.⁹⁵ In 2008, Isaad and co-workers reported the synthesis of monosubstituted Ni^{II} complexes incorporating glycine, using different chain lengths of the alkyl halide, where the C₅ and C₆ groups include triple bonds, with the diastereomeric ratio for C₅ = 71:29 (*SS/SR*), yield = 59 % and for C₆ = 88:12 (*SS/SR*), yield = 68 % (Scheme 1.6).⁹⁶



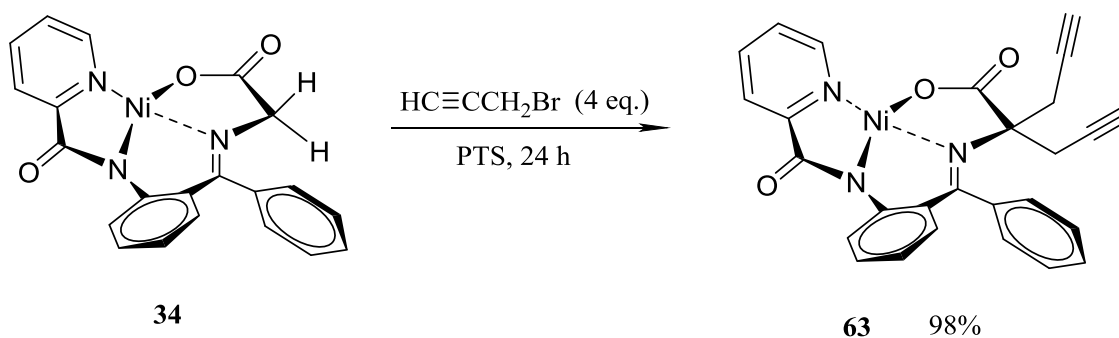
Scheme 1.6: Asymmetric synthesis of (S)- ω -alkynyl- α -amino acids.⁹⁶

In recent years, Jamieson *et al.*⁴⁸ reported the synthesis of new amino acids by alkylation of alanine and glycine Ni^{II} Schiff base complexes using different alkyl bromides. The group reported that there was a higher yield with the glycine complex than with the alanine one. Interestingly, the work also demonstrated a good ratio of complexes stereoselectivity (dr. 95:5) while previous workers reported dr. 88:12 or 89:11. The 5-bromopentene starting material, in both types of complex (alanine and glycine), produced higher yields than 8-bromooctene in the alkylation reaction. Subsequently, the complex was hydrolysed with HCl and the resulting free amino acid protected with the Fmoc reagent (Scheme 1.7).⁴⁸



Scheme 1.7: Synthesis of unnatural amino acids according to Jamieson.⁴⁸

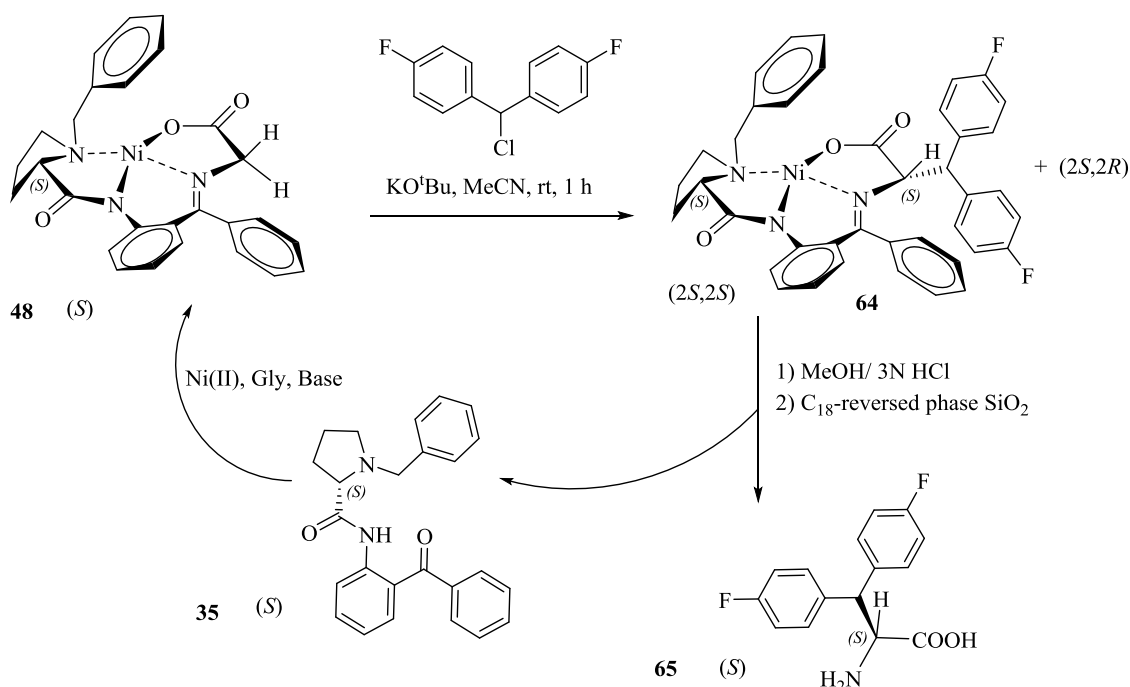
One of the main problem in the work occurred for the glycine complex during the alkylation when the di-substituted product was also observed since it has two α -hydrogen atoms. Belokon *et al.* examined the conditions required to prepare mono- or di-substituted products at the alpha position of the glycine Ni^{II} complex using alkyl halides that have double or triple bonds, or aromatic substituents. Benzyltriethylammonium bromide was used as a catalyst under basic PTS conditions at room temperature (Scheme 1.8).⁹⁷



Scheme 1.8: Di-substitution on a glycine Ni^{II} Schiff base complex.⁹⁷

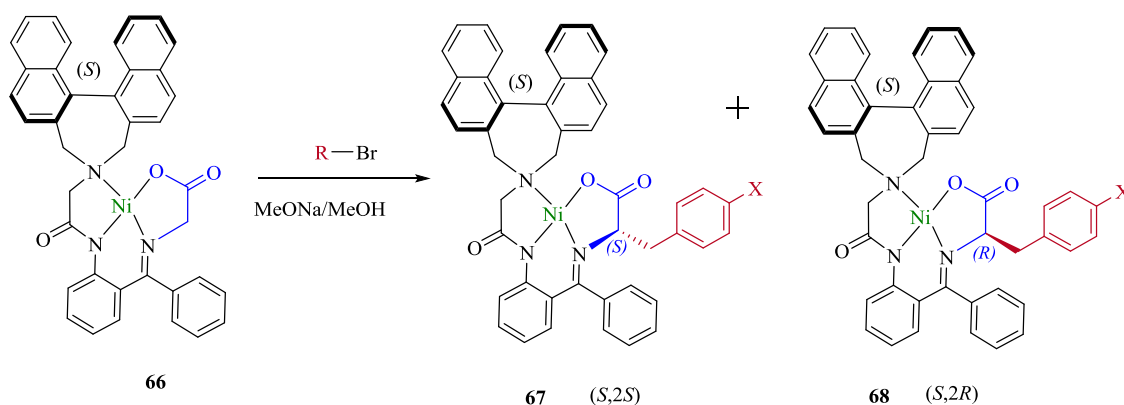
1.9.3 Synthesis of Fluorinated α -Amino Acids

In 2009, Soloshonok and Ono have reported alkylation reaction conditions for a glycine Ni^{II} Schiff complex using an alkyl chloride, with fluoroarene substituents, and tert-butoxide as a base in acetonitrile for one hour. The reaction could be scaled up to multi-gram scale to yield product with a high enantiomeric purity (95 % de) and in a high yield 90 % outcome of the alkylation of the glycine complex (Scheme 1.9).⁹⁸ The main importance of the amino acid product is that it is required to synthesis the Denagliptin medicine (for treatment of diabetes). This can be compared to a previous synthetic route to generate the amino acid in 55 % yield and 60 % ee.⁹⁹



Scheme 1.9: Asymmetric synthesis of (S)-2-amino-3,3-bis-(4-fluorophenyl)propionic acid

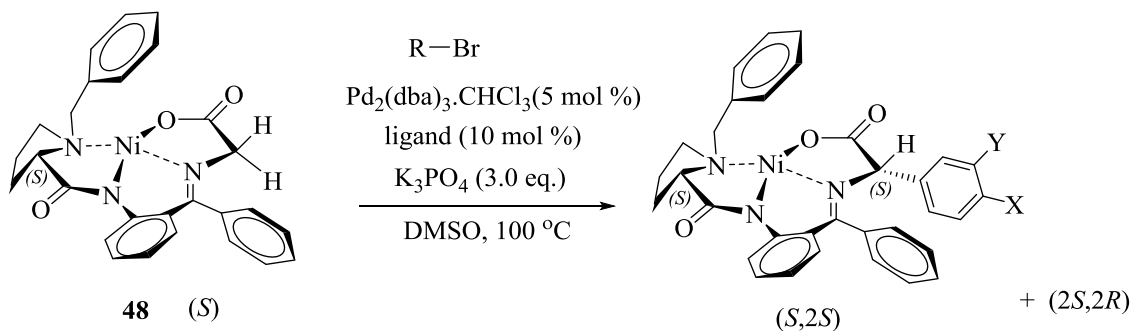
Recently, Liu and co-workers demonstrated a new type of ligand to synthesise α -amino acids with high enantiomeric purities. The alkylation reaction was undertaken with a glycine Ni^{II} Schiff base complex. The resulting enantiomer was easily purified. The reaction was optimised under different conditions of basicity, solvent and temperature to obtain the highest yields (85.5 %) with NaOMe/MeOH at 0 °C (Scheme 1.10).¹⁰⁰



X	H	F	Me
de (S:S):(S:R)	99:1	98:2	99:1

Scheme 1.10: Synthesis of amino acids using new ligands

Elsewhere, a new method of alkylation has been identified by Sun and co-workers. They presented a synthesis using palladium to catalyse the alkylation of α -arylated bromides of the glycine Ni^{II} Schiff base complex. The work described formation of pure products with 85-90 % yield for all the synthesised derivatives. They also improved the diastereoselectivity to obtain (20:1 dr (S,S)/(S,R)). Furthermore, the aryl starting materials used included 4-CN, 4- CF_3 , 4- CO_2Me , 4-F, 4- NO_2 , 4-CHO, 3,4- F_2 (Scheme 1.11).¹⁰¹



X	CN	CF_3	F	NO_2	F
Y	H	H	F	H	H
dr	4.6:1	5:1	4.4:1	6.3:1	1.1:1

Scheme 1.11: Pd-catalysed-arylation of chiral Ni^{II} glycinate complex with aryl bromides.

1.10 Application of alkynyl derivatives of amino acids in peptide synthesis

Synthesis of amino acid alkyne moieties with high stereochemistry became one of the researcher's targets. The alkyne amino acids have previously been used in two ways in peptides synthesis: Firstly, synthesis of triazole bridges, secondly, synthesis of macrocycle peptides or diene peptides by 1,3-diyne ring closure.

1.10.1 Synthesis of triazoles

Alkynyl derivatives of amino acids have been used to form triazole bridges by reacting with another amino acid with an azide group on the side chain (1,3-dipolar cycloaddition reactions) by using Cu(I) as a catalyst. This reaction concept of Cu(I)-catalysed azido-alkyne cycloaddition (CuAAC) was introduced for first time by Sharpless (2001). It shows great stability under acidic and basic conditions, and also oxidative and reductive conditions.¹⁰² Interestingly, the work also showed that the triazole bridged peptides had good biological activity compared to the native peptides.¹⁰³ However, the triazole bridged-peptides showed two configurations: i) 1,4-disubstituted 1,2,3-triazole; ii) 1,5-disubstituted 1,2,3-triazole (*E* and *Z* configurations) (Figure 1.21).

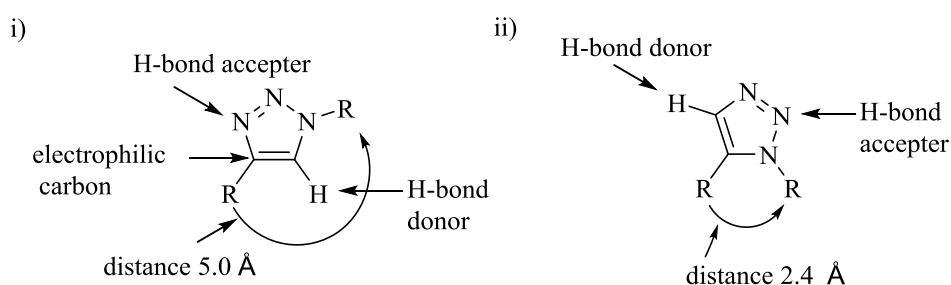
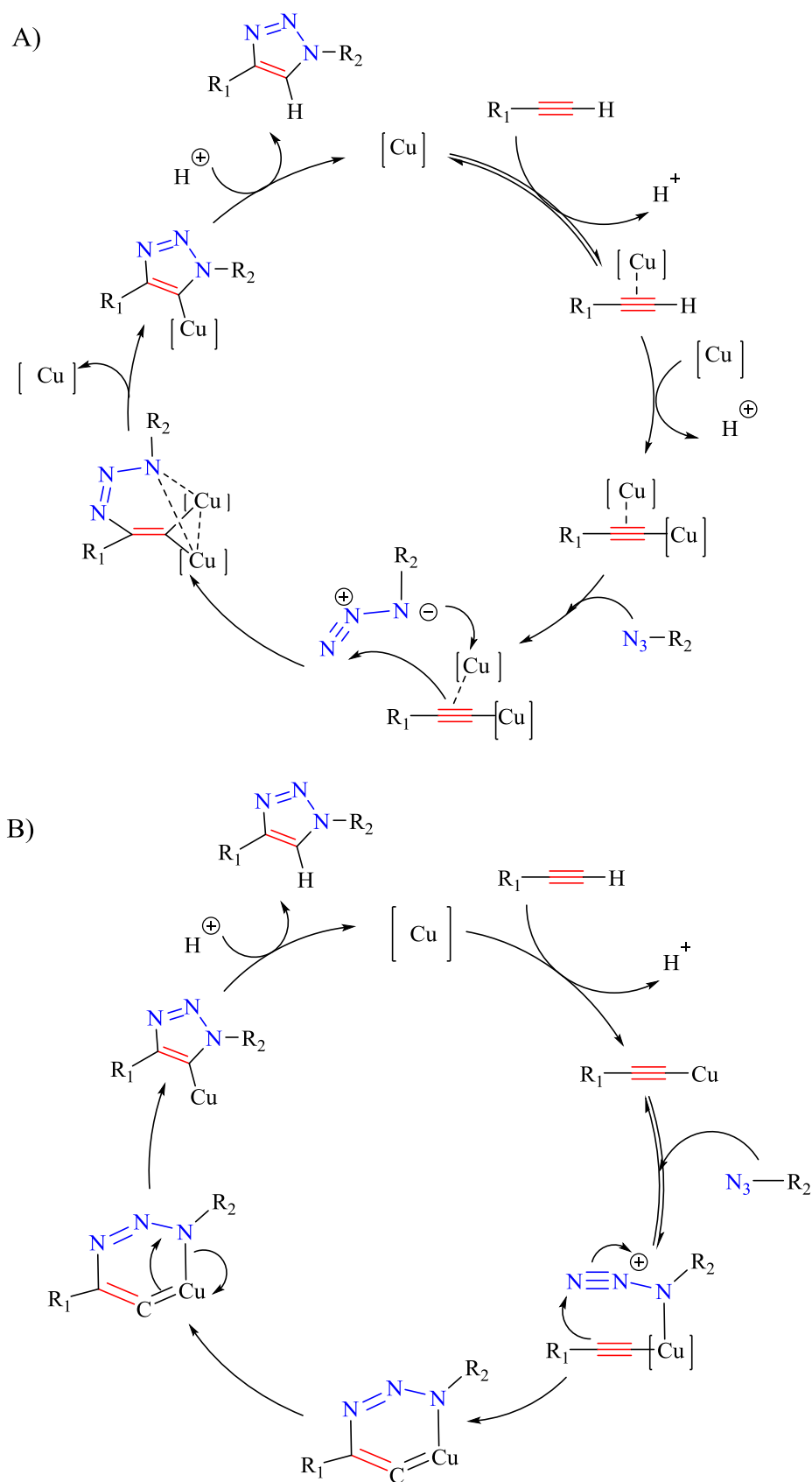


Figure 1.21: Triazole configurations: i) 1,4-disubstituted 1,2,3-triazole; ii) 1,5-disubstituted 1,2,3-triazole.

The click reaction mechanism, using Cu(I) as a catalyst in this reaction, showed only the 1,4-disubstituted synthetic pathway, but via two mechanisms, to form 1,2,3-triazoles as the final product (Scheme 1.12).¹⁰⁴



Scheme 1.12: Proposed catalytic model for the CuAAC with a) two copper atoms b) one copper atom

D'Ursi and co-workers reported the first example of the synthesis of 1,2,3-triazolyl helical structures stapled using the CuAAC reaction in positions i , $i+4$ for a parathyroid hormone-related peptide.¹⁰⁵ They used various lengths of alkynyl chains $(\text{CH}_2)_{1-4}$. In this case, the positions of the amino acids to be coupled were changed and swapped. The studies showed that all triazole staples enhanced the stability of the helices compared to those of the native peptide (Figure 1.22).¹⁰⁵

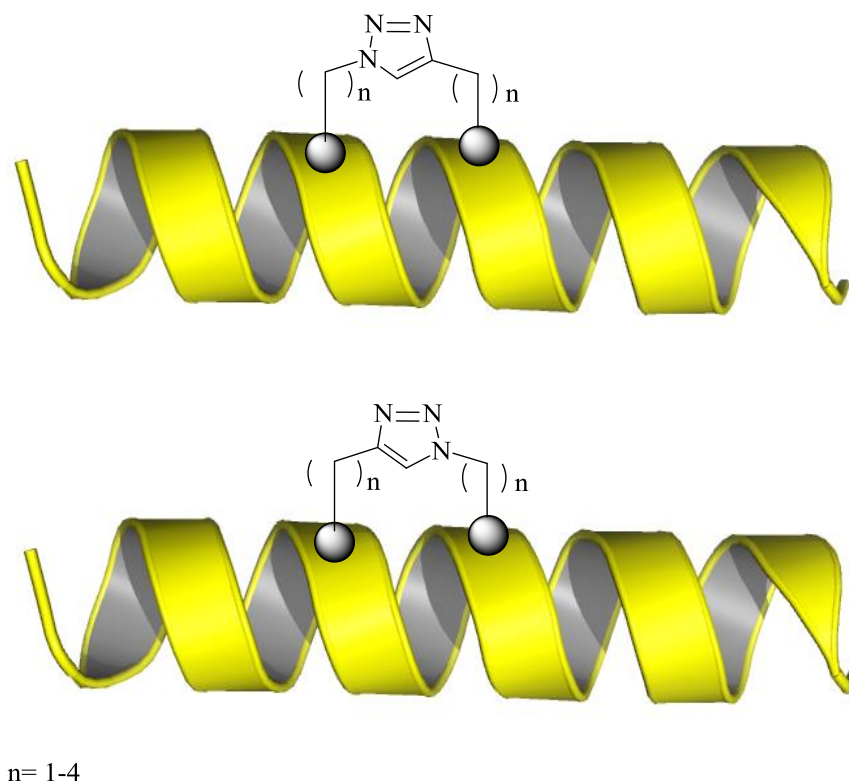


Figure 1.22: Synthesis of the triazole groups in peptides.¹⁰⁵

1.10.2 Preparation of 1,3-diyne group.

Recently, researchers have shown an increased interest in 1,3-diyne group in peptide synthesis. They used the Glaser and Eglinton reaction method between alkynyls under mild conditions by using copper as a catalyst (in other words, oxidative acetylenic coupling) to synthesise a variety of di-peptides and macropeptides and then examined their stabilities.^{106, 107} Inouye *et al.* (2008) mentioned the significant relationship between the 1,3-diyne group as a bridge for peptide synthesis. They found that RCM using the 1,3-diyne group increased the activity of the two amide groups on both sides of the linker. Also, these new types of bridges had different rigidities and lengths of the associated helices, particularly increasing the stability of short peptides. The series of peptides

included diaminopropionic acid (Dap), diaminobutyric acid (Dab), ornithine (Orn) and Lys in different positions, namely i , $i+4$; i , $i+7$ or i , $i+11$. One of the significant findings in this study arises from the ring closure, which was suitable for the creation of stable helical structures up to > 95 % (Figure 1.23).¹⁰⁸

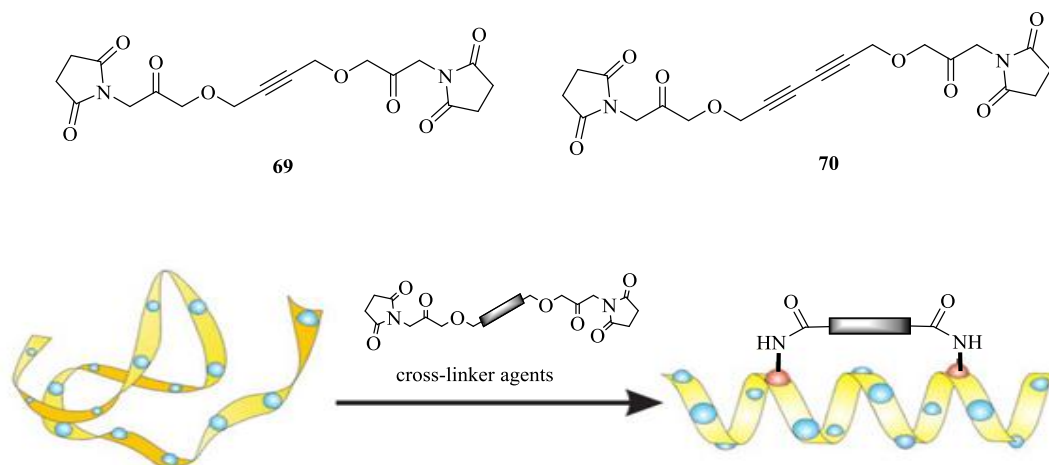
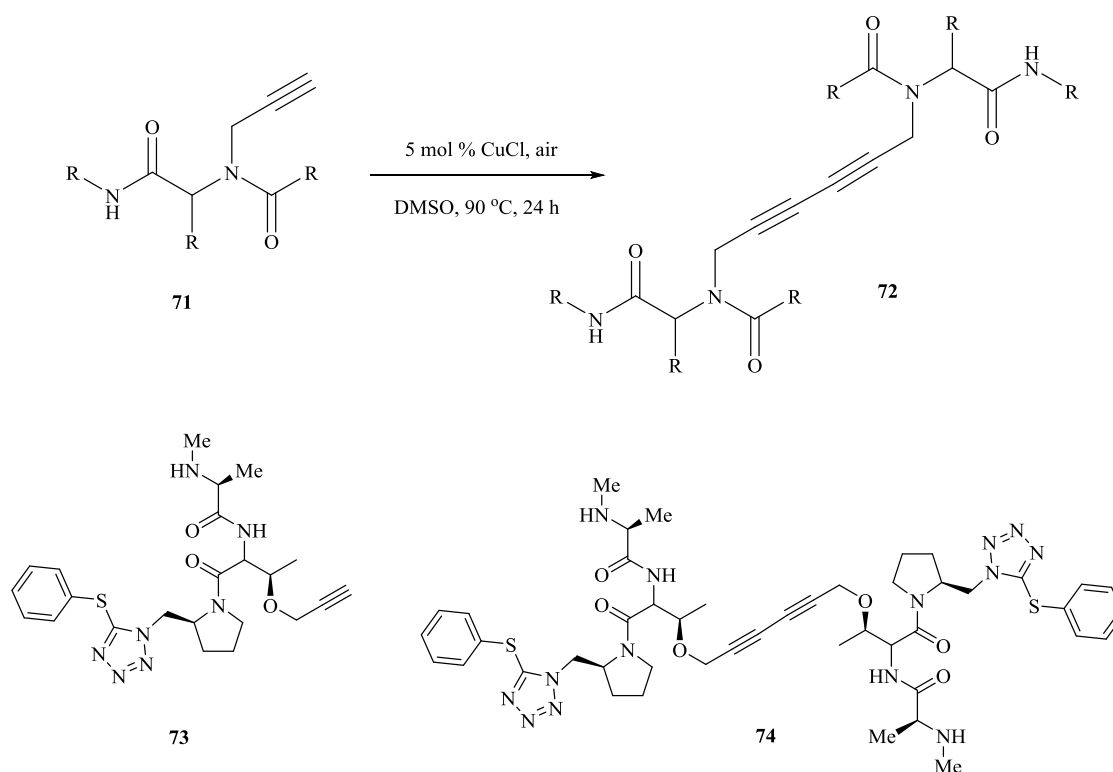


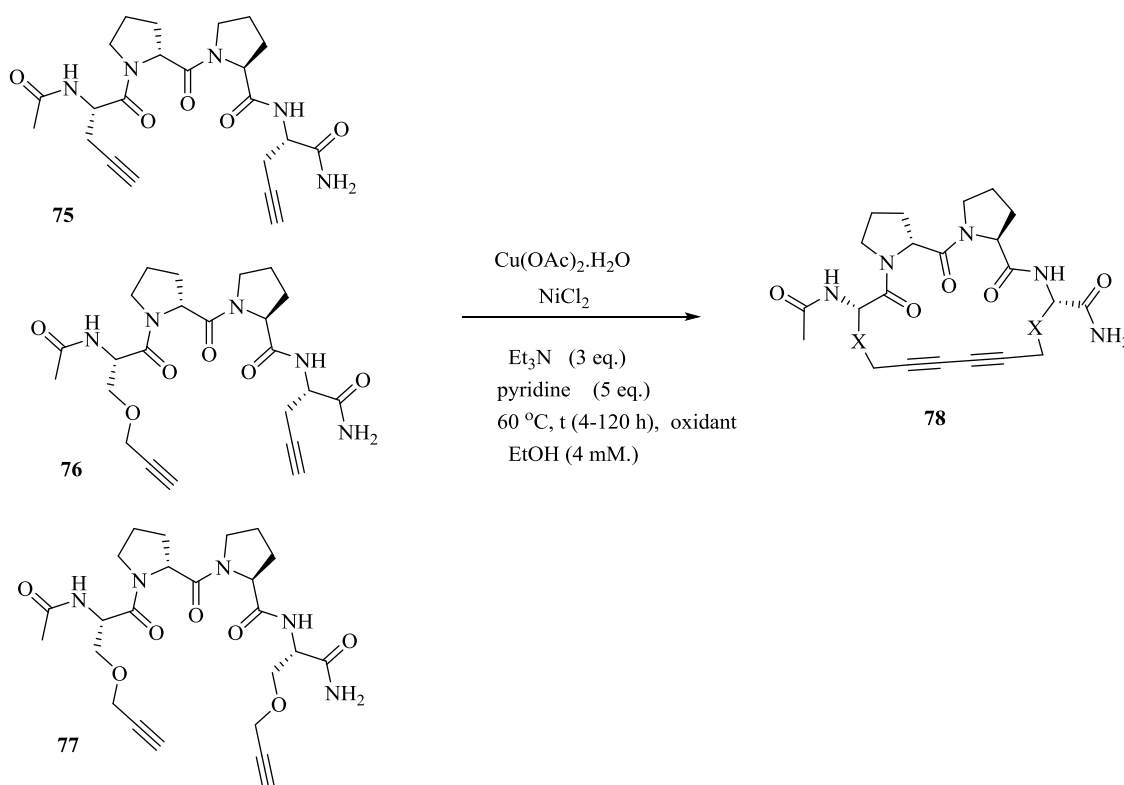
Figure 1.23: Synthesis a bridge between 1,3-diyne linker sides and the two amide groups

Recent cases, as reported by Wessjohann *et al.* (2015), concerned the 1,3-diyne. They reported that a dimeric peptoid species could be used to synthesise six-compound-libraries of homo- and di-heterodimer peptides. They also supported the idea that dimeric peptoids showed reasonable antibacterial activity (Gram-positive bacterium bacillus) (Scheme 1.13).¹⁰⁹



Scheme 1.13: Apoptosis inducer C2-symmetric 1,3-diyne-linked peptide.¹⁰⁵

The finding is consistent with past and indeed more recent studies. For example, Verniest *et al.* (2015) demonstrated the influence of 1,3-diynes on the synthesis of cyclic peptides, also known as macrocyclisations. The group reported more than 50 different sets of reaction conditions; for example, temperature, copper catalyst and co-catalyst (NiCl₂), base, solvent and oxidant (Scheme 1.14).¹¹⁰

Scheme 1.14: Oxidative 1,3-diyne macrocyclization¹¹⁰

These findings are consistent with the study by Auberger *et al.* who examined new methods by which to synthesise macrocyclic peptides. The Glaser–Eglinton reaction has been used to synthesise hexa- and octa-cyclic peptides. The peptide is constrained by a 1,3-diyne (butadiyne) bridge and lactam cyclized hexapeptides. This work also used both propargylglycine (Pra), or N-propargylated amino acids (NPro) amino acids to make the RCM under the same conditions (Figure 1.24).¹¹¹

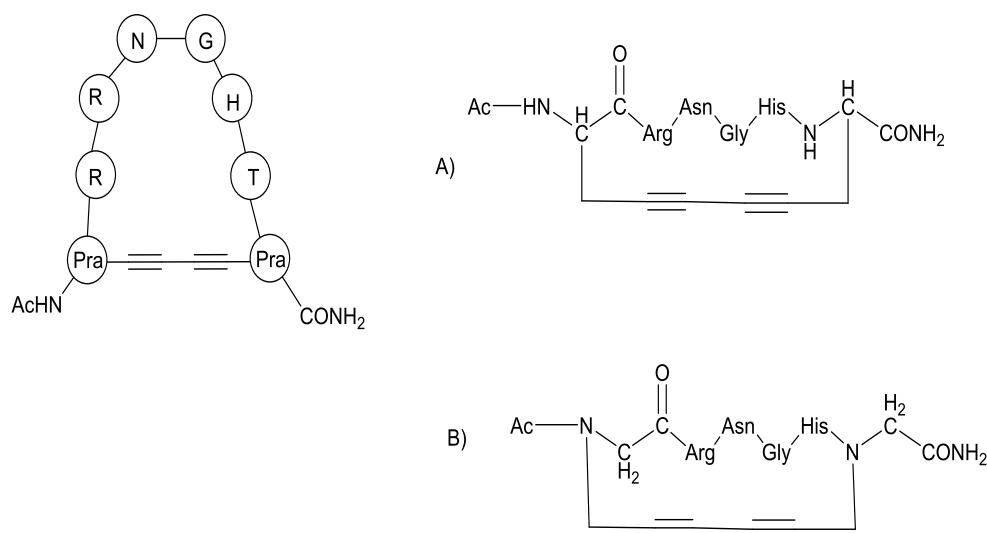


Figure 1.24: Preparation 1,3-diyne of cyclic hexapeptides between two L-Pra amino acids and between NPra amino acids¹¹¹

1.11 Peptide synthesis

Peptide synthesis can be classified into two types: liquid phase and solid phase. The latter type has become the principal means by which to synthesise peptides.

1.11.1 Solid phase peptide synthesis

Bruce Merrifield (1960) obtained a Nobel prize for the creation of a new method called solid phase peptide synthesis (SPPS).¹¹² Peptides are prepared from the C-terminal to the N-terminal. The main requirements for this method to become commonplace are its relatively low cost, high efficiency and ease of use, and compatibility with liquid methods. The main principle of the SPPS technique is the attachment of the first amino acid to an insoluble polymeric support. Amino acids are sequentially added to the polymer-attached amino acid/growing peptide. This strategy makes the synthesis of peptides straightforward, without requiring purification after each step. Furthermore, removing starting materials (unreacted) and waste is easy through repeated washing with solvents followed by drying to become ready for next step in the reaction sequence, because the peptide-resin remains in the reaction vessel (Figure 1.25).^{113, 114}

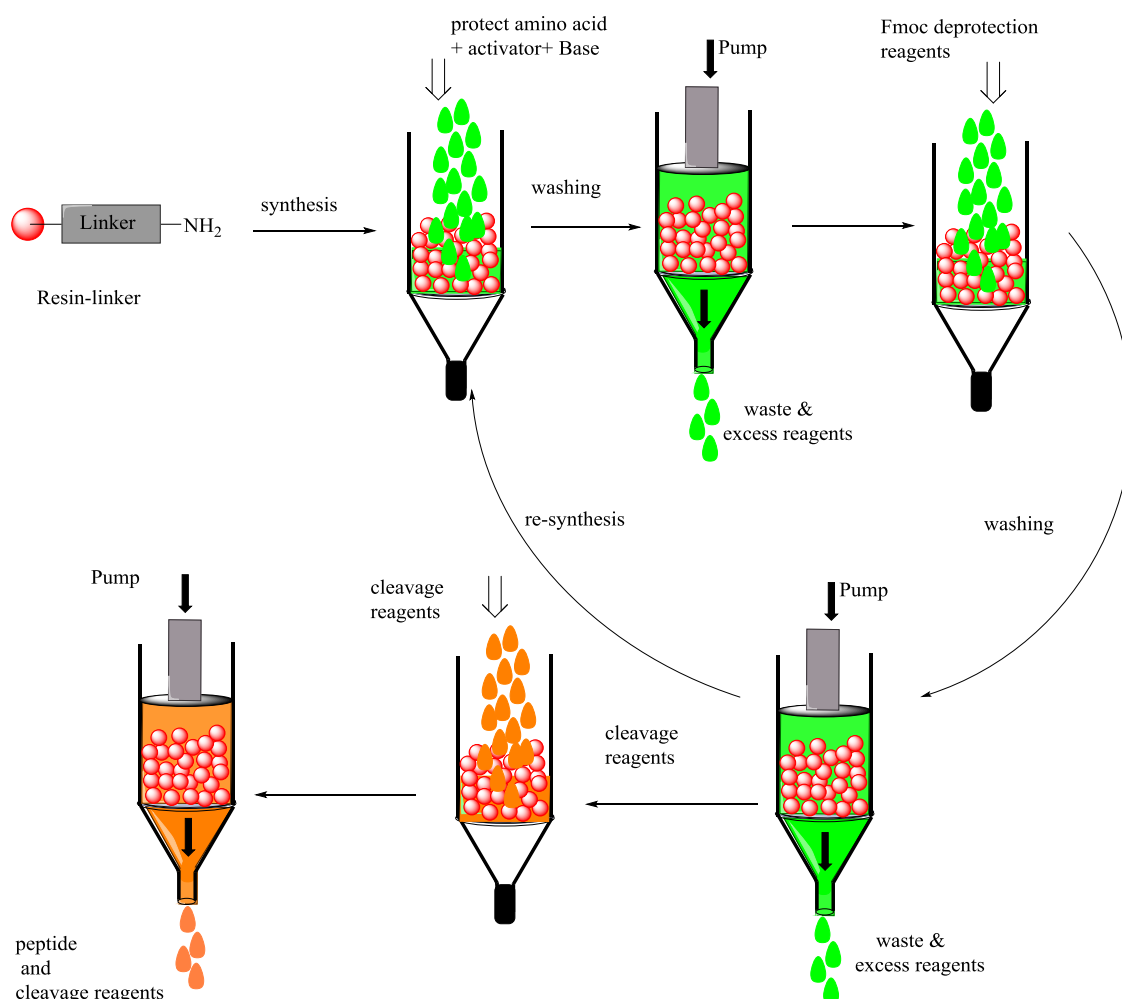


Figure 1.25: Solid phase peptide synthesis (SPPS)

Many solvents are used in peptides synthesis, such as acids, bases, polar and nonpolar solvents; the resin should not be soluble in any one of them. Moreover, the resin has one functional group (linker) to react with the free functional group of the amino acid. The linker group is the connector between the resin and the amino acid. The capacity of resin is measured in mol/gm which is required to determine the number of moles of peptides present following reaction. There are several types of resin that can be used in peptides synthesis. They can be classified into two kinds; the resin reacts with carboxylic acid to form the C-terminus [e.g. 1) Merrifield resin; 2) Wang resin *p*-alkoxybenzyl alcohol (PABA)] and with the amine to form the N-terminus [e.g. 3) Tentagel resin; 4) 2-chlorotrityl chloride; 5) Rink resin 4-methylbenzhydrylamine (MBHA); 6) Rink resin aminomethyl (AM)] (Figure 1.26).¹¹⁵⁻¹¹⁷

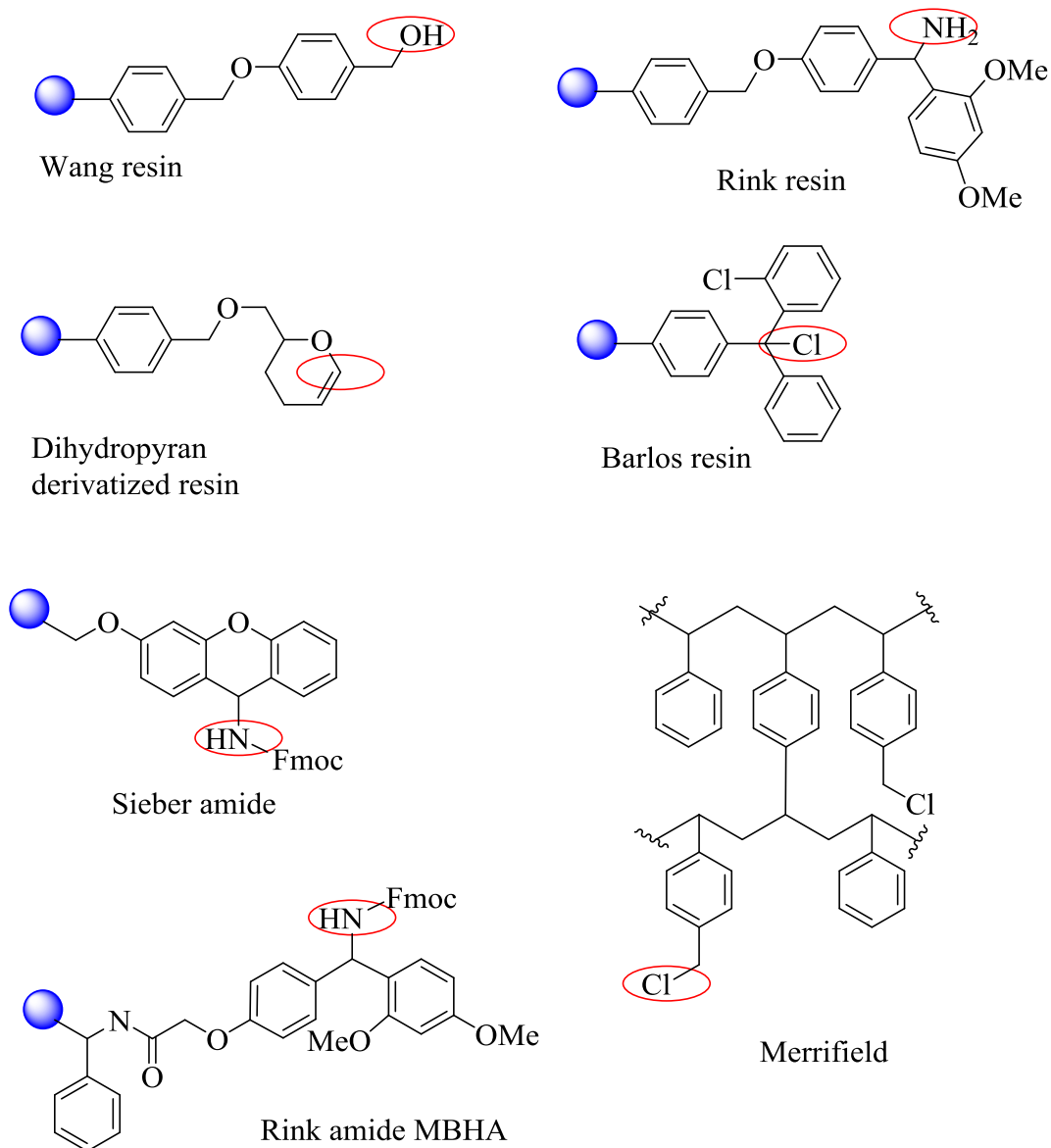
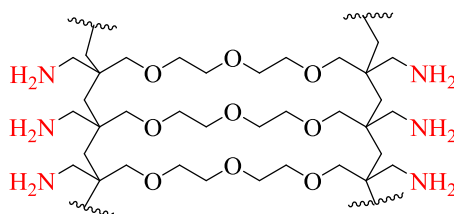


Figure 1.26: Types of resin with the linkage.

However, there are a few weaknesses in using some of these peptide-resins, such as the Wang-resin which can be cleaved under mild acid conditions and the Merrifield resin which cannot be used for a long-sequence peptide because of the acidity of the resin. Recently, various resins have been developed in the SPPS field to cover the demands of peptide synthesis such as ChemMatrix® and SpheriTide®.¹¹⁴ Throughout, all of these coupling and decoupling reactions need a long time to go to completion and many steps are needed to obtain a pure peptide in high yield. In addition, there are some couplings to amino acids that needed double steps, whilst unnatural amino acids need longer reaction times than natural amino acids for many reasons including the fact that unnatural amino

acids may cause more steric hindrance different than native amino acids. Accordingly, the use of microwaves for heating has been introduced to improve and assist peptide synthesis. Yu and co-workers (1992) reported the first successful use of microwaves (local microwave oven) in organic reaction. In recent times, microwave techniques have been developed to cover the requirements of certain organic reactions, such as microwave power and reaction temperature. Recent cases reported by Smith *et al.* (2003) also report the use of the microwave in new methods for peptide synthesis, including in an Fmoc-deprotection reaction as well as in coupling reactions.¹¹⁸ More recently, automated peptide synthetic methods have been developed making them easier to use, whilst manual techniques have been improved as well (Figure 1.27).¹¹⁹

1) ChemMatrix®



2) SpheriTide®

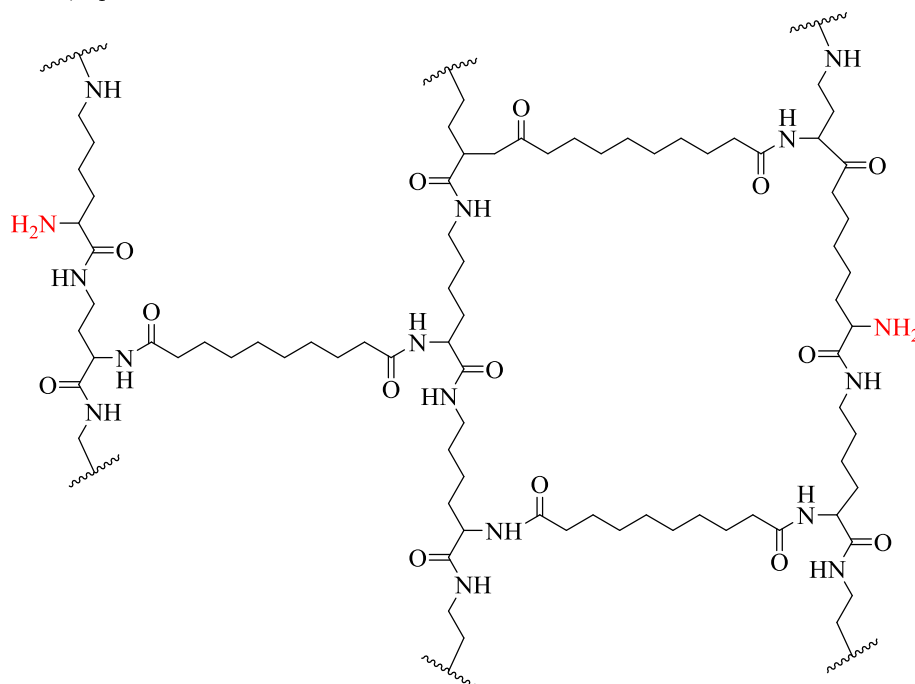


Figure 1.27: Peptide Resin 1) ChemMatrix® and 2) SpheriTide®.

1.12 Project aims

The rationale behind this project is that a highly rigid side-chain to side-chain 1,3-diyne bridge (Figure 1.28) would act as an extremely effective configurational constraint thus

providing peptides with high degrees of α -helical structure and improved binding affinity (through protein-protein interactions) and physicochemical properties. The project was undertaken to design and develop a novel hydrocarbon peptide α -helix and then to evaluate model systems via circular dichroism CD.

The specific aims of the project are:

- 1) Synthesis of novel chiral Ni^{II} Schiff base complexes and development of the synthetic methods to increase the yield and the purity using both of *S* and *R* enantiomers of a fluorinated ligand. Here, the fluorinated ligand would aid in establishing the diastereoselectivity of the products.
- 2) Synthesis of novel chiral unnatural fluorinated amino acids and alkynyl amino acids via alkylation of the Ni^{II} Schiff base complexes and development of the synthetic methods of the alkylation reaction using alkyl iodides and alkyl bromides.
- 3) Synthesis of model linear peptides incorporating the unnatural alkynyl amino acid using automated microwave assisted solid phase peptide synthesis and an Fmoc protection strategy on Rink resin.
- 4) Synthesis of model 1,3-diyne bridged peptides from the alkynyl-functionalised model linear peptides using the Glaser-Hay ring closing metathesis reaction.
- 5) Conformational analysis of the linear and the 1,3-diyne bridged peptides using circular dichroism spectroscopy to make a comparison between these model systems and to determine the arrangement that creates the highest % helicity. Subsequently, the best peptide model will be applied in the synthesis of open and ring closed Bim peptide analogues and undertake a conformational analysis of these peptides.

Throughout the project all products will be thoroughly characterised by a range of appropriate analytical and spectroscopic techniques.

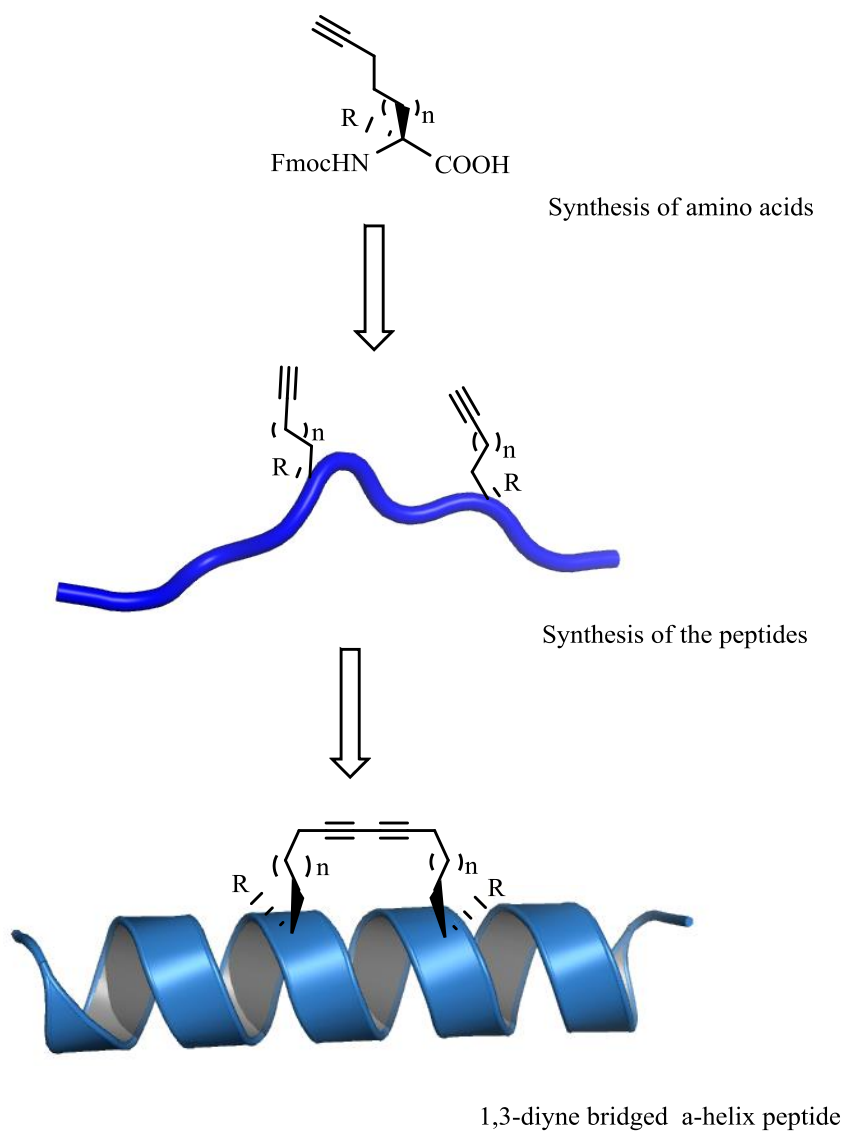


Figure 1.28: The aim of the project

Chapter 2

Synthesis of Schiff Base Ni^{II} Complexes



UNIVERSITY OF
LEICESTER

2.1 Introduction

The synthesis of new unnatural amino acids has become a significant strategy since they can be used to produce peptide-mimics and to advance peptide synthesis and properties. The synthesis of enantiomerically pure amino acids is the primary target and this can be achieved by using different catalysts or different chiral compounds such as Ni^{II} Schiff base complexes. The new amino acids have modified side chains and can be used as starting materials in the peptidomimetic process. The majority of researchers in this field are focused on the synthesis of these amino acids to make α -helix peptides and to study their protein–protein interactions (PPIs). Moreover, these workers have demonstrated new features of the peptides, such as increased stability, increased bioavailability and enhanced physicochemical and pharmacological properties.^{120, 121}

Synthesis of the new amino acids started firstly by synthesising amine compounds, which were then used in alkylation reactions. In 1976, Stork *et al.* presented the first types of protected nucleophilic amino acid (glycine) suitable for alkylation reactions; these were achiral products (Schiff bases). They protected the amine group with either benzaldehyde or benzophenone **69**, **80**. These compounds were developed, by O'Donnell in 1978, who presented new modifications by protecting the carboxylic acid with t-Bu **82** instead of ethyl group. In recent years the methods developed have yielded products with high enantioselectivities, mostly quaternary ammonium salts (new catalysts) were used to obtain (99 % ee). However, the main problem of these methods is that the instability of the starting materials and the products are low (Figure 2.1).⁹²

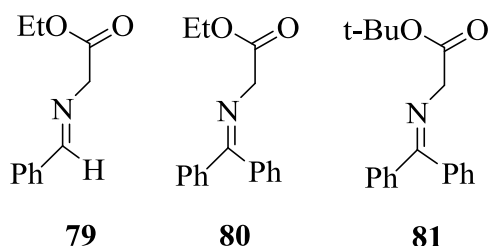


Figure 2.1: Achiral nucleophilic glycine substrates

The second generation of synthetic routes to unnatural amino acids started in 1983, when Schollkopf *et al.* demonstrated a new method to synthesise bislactams, as chiral starting materials for alkylation reactions of new derivatives **83-86**.¹²² However, whilst this method represents progress, it still has many disadvantages, such as the hydrogens on α -

C have low acidity. This property means that harsh reaction conditions, such as a strong base and low temperatures, for example *n*-BuLi at -78°C under anhydrous conditions, are required (Figure 2.2).¹²³

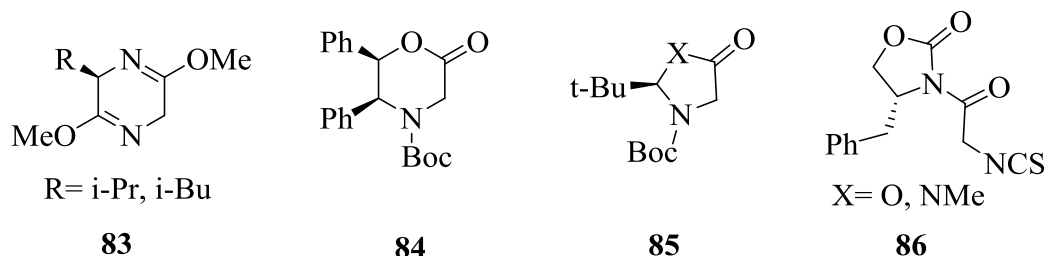


Figure 2.2: Chiral nucleophilic glycine

Also in 1983 another synthetic method was reported by Belokon *et al.*, a novel method by using a transition metal to make a complex with glycine-based Schiff bases. Cu^{II} was used, with a chiral ligand (*S*)-2-[N-(NO-benzylpropyl)amino]-benzophenone (BPB) and different amino acids, such as glycine, to make the complex.¹²⁴ However, whilst this method gave a good yield with high diastereoselectivity, Ni^{II} complexes showed higher stabilities and better reactivities than those of Cu^{II} . Furthermore, the Cu^{II} complexes are unsuitable for analysis by NMR spectroscopy due to their paramagnetic character.^{50, 125} Many researchers have built upon this method and have found it to be suitable for reactions as good nucleophiles in alkylation reactions,⁵⁰ e.g. the Michael reaction,¹²⁶ Aldol reaction¹²⁷ and Mannich reaction.¹²⁸ There are many types of Ni^{II} Schiff base complexes which have been synthesised following this discovery, and these can be divided into four types as outlined in Scheme 1.4. There are several factors that make this method one of the best: (i) The metal complexes can be easily purified by chromatography on SiO_2 or by crystallization. (ii) The starting material (ligand) can be re-used. (iii) The product under any reaction conditions can be purified and analysed using NMR spectroscopy, because the complexes are diamagnetic in character. The diamagnetic character can be easily recognised from the red colour of the complexes. This is related to their square planar geometry of the Ni^{II} metal centre ($3d^4s^4p^2$ hybridisation) rather than tetrahedral ($4s^4p^3$ hybridisation) which are green (Figure 2.3). In addition, the geometry has been confirmed by single crystal X-ray structure determinations of many of the complexes.

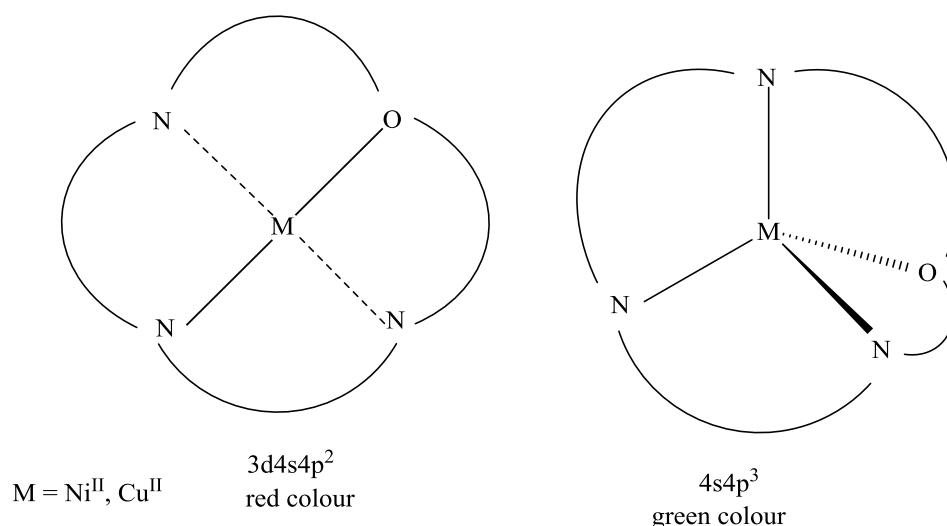
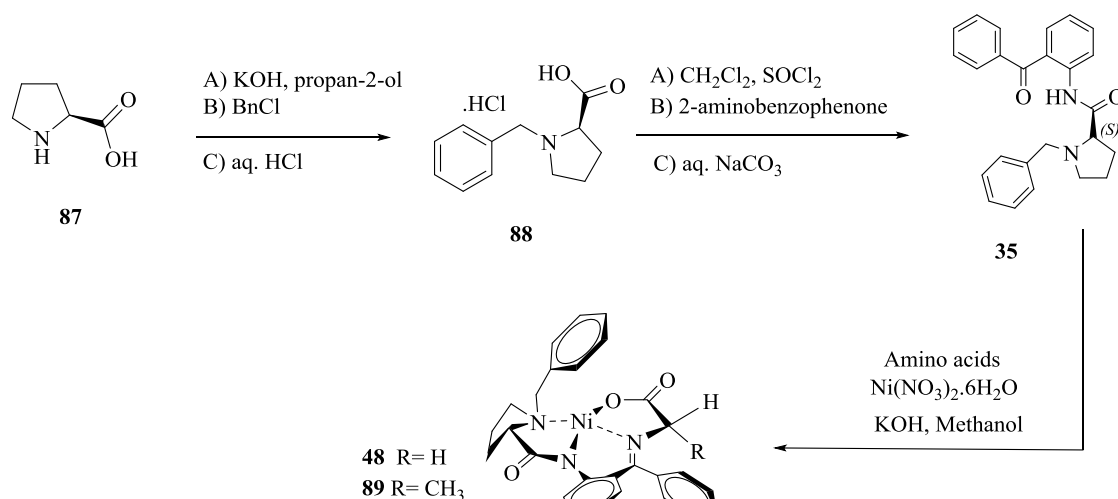


Figure 2.3: Shapes of the Ni^{II} and Cu^{II}

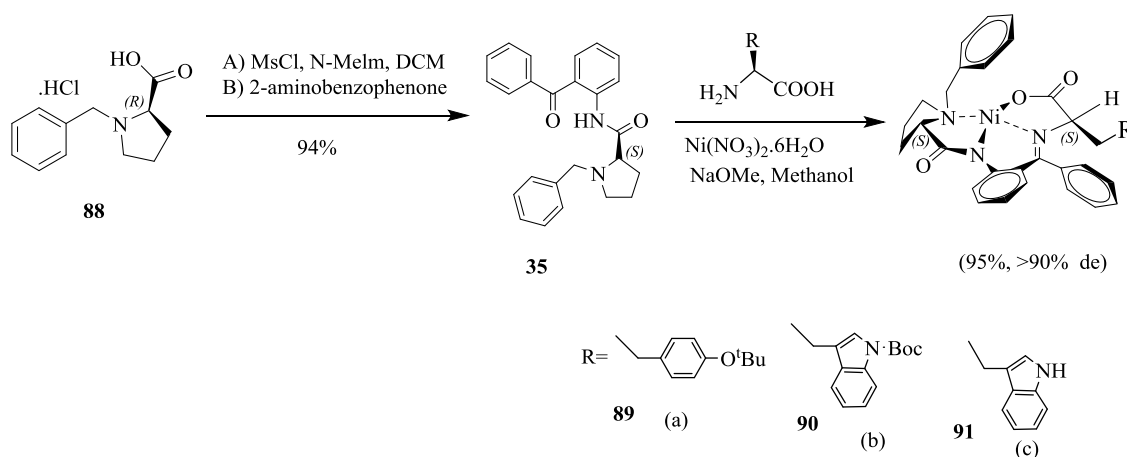
2.2 Synthesis of Ni^{II} complexes of Schiff base derivatives

Popkov *et al.* suggested that the benzene ring on the top of the Ni^{II} atom in these complexes can provide additional conformational stability. They assumed that there is a weak interaction from above the Ni^{II}-N,N,N,O plane between the benzene ring in the ligand and the Ni atom. Although this suggestion could not be accepted in the absence of the crystallographic data or theoretical calculations, they suggested that the benzene ring could have an effect on the Ni-X distances in the square plane.¹²⁹ In related work, Jamieson *et al.* proposed that there is, indeed, an interaction between the 2-fluorobenzene group in the ligand with the Ni^{II} atom. Although they could not confirm that there was an interaction between the fluorine atom and the Ni atom, they did obtain single crystal X-ray structural data on their complexes.⁴⁸

Belokon *et al.* published the first synthetic procedure in this research field (Scheme 2.1). After reacting *N*-benzylproline with SOCl₂, to form the acyl chloride, reaction with *O*-aminobenzophenone produced (*S*)-2-[*N*-(*N'*-benzylprolyl)amino]benzophenone (BPB). The reaction was driven to get 81 % yield by using a fifty percent excess of the pre-ligand to achieve this yield of the ligand. The complex was synthesised using glycine and alanine amino acid, Ni^{II} complexes of Schiff's bases derived from BPB and amino acids were prepared using KOH as a base to obtain a 90-91 % isolated yield with 90 :10 diastereoselectivity.¹³⁰

Scheme 2.1: Synthesis of the Ni^{II} Schiff base complexes

Ueki *et al.* demonstrated a high conversion in the reaction of pre-ligand with *O*-aminobenzophenone to obtain a 94 % isolated yield by increasing the reaction temperature to 40-45 °C under anhydrous conditions (Scheme 2.2).¹³¹ developed this method by reacting the *N*-benzylproline with MsCl, to make a good leaving group, before reaction with *O*-aminobenzophenone in DCM. The pre-ligand **2.m** can be isolated by crystallisation from an ethanol solution or precipitation from an acetone solution acidified with HCl.



Scheme 2.2: Synthesis of different complexes

The Ni^{II} Schiff base complexes can then be synthesised, in a single step, from reaction of the pre-ligand with a Ni^{II} salt in the presence of an amino acid under basic conditions.

The complexes were obtained diastereomerically pure, with 95 % yield. Synthesis of complexes with various substituents on the benzene ring have been reported by De and Thomas,¹³² Ueki *et al.*,¹³¹ Belokon *et al.*,⁹⁷ Saghiyan *et al.*,^{94, 95} and Popkov *et al.*¹³³ Throughout, the chiral centre of the proline starting material was shown to efficiently control diastereoselectivity.

2.3 The aims of this chapter are:

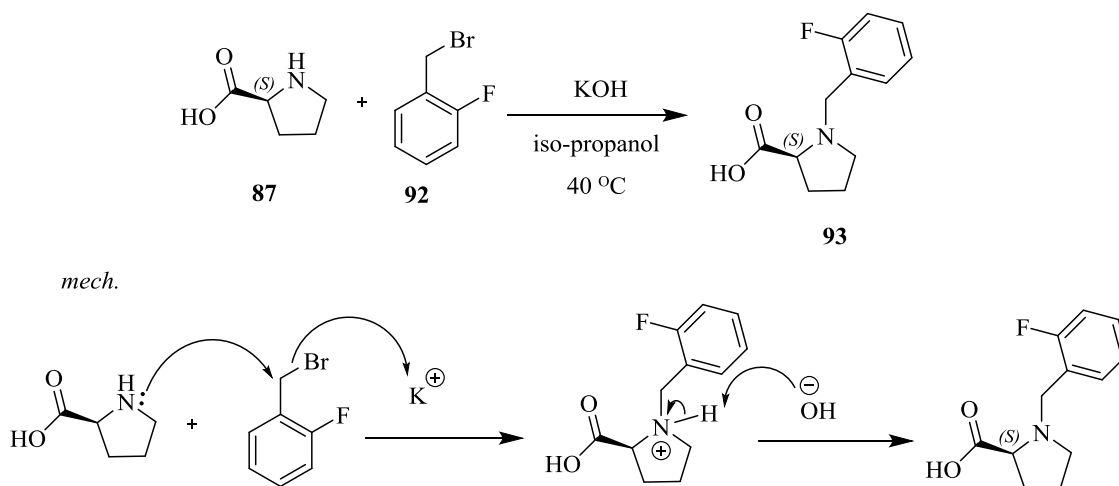
To synthesise Ni^{II} Schiff base complexes which would then be used in the work in the following chapters to synthesis novel derivatives of amino acids derived from glycine, alanine, valine, leucine and phenylalanine. Beyond this, the aims included the development of routes to synthesise both *S* and *R* pre-ligands, by starting with D or L-proline, to allow different diastereomeric metal complexes. Throughout, a fluorinated benzyl starting material would allow the reactions to be monitored with respect to both purity and the diastereomeric composition of the complexes.

2.4 Synthesis of a chiral Ni^{II} Schiff base complexes

The synthesis of Ni^{II} complexes used the modified procedure of Jamison *et al.*,⁴⁸ which was adapted from the work of Belckon *et al.*^{130, 134} The synthesis consisted of three steps: alkylation reaction, amide coupling reaction and complexation.

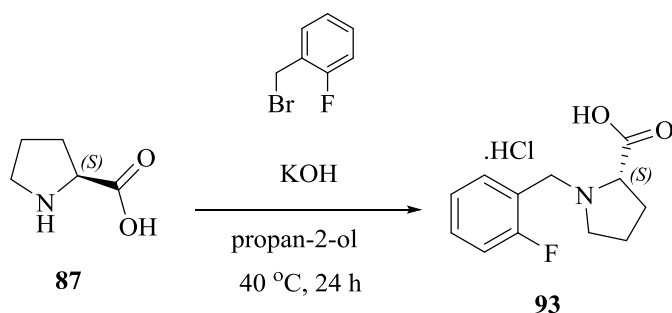
2.4.1 Alkylation reaction

The general procedure of Jamieson was followed to synthesise of 1-(2-fluorobenzyl)pyrrolidine-2-carboxylic acid (FBPB) from the reaction of 2-fluorobenzyl bromide with L-proline in basic conditions (KOH), in isopropanol at 50 °C (Scheme 2.3). A strong base is essential for this reaction. Following the reaction, neutralisation of the reaction mixture with hydrochloric acid is a key step in the work up. In contrast to the literature that reports, the product was a waxy yellow solid,⁴⁸ here recrystallisation of the crude product twice from dry acetone yielded the product as a white powder in high purity (as determined by ¹H NMR spectroscopy).



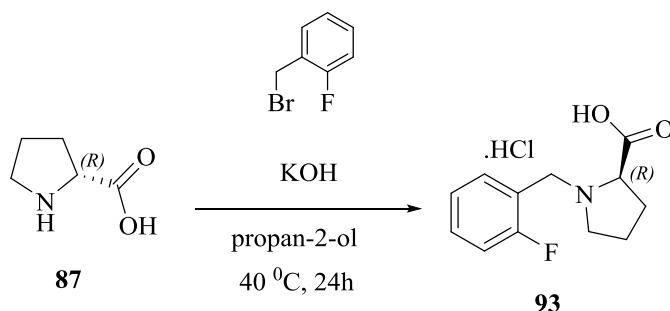
Scheme 2.3: Reaction and mechanism of alkylation reaction on the proline

2.4.1.1 (S)-1-(2-fluorobenzyl)pyrrolidine-2-carboxylic acid



Specifically, L-proline was reacted with 2-fluorobenzyl bromide to produce (S)-1-(2-fluorobenzyl)pyrrolidine-2-carboxylic acid **93**, as a white powder, following recrystallisation from acetone, in a 74 % yield. The product was characterised by ^1H NMR and ^{13}C NMR spectroscopy and in the ^{19}F NMR spectrum a single peak at -116.0 ppm is typical for the single *ortho*-fluorine. In the LC-MS and HRMS-ESI a parent ion peak at 224.1087 supported the characterisation. The synthetic route could be successfully scaled up to the 25 g scale.

2.4.1.2 (*R*)-1-(2-fluorobenzyl)pyrrolidine-2-carboxylic acid



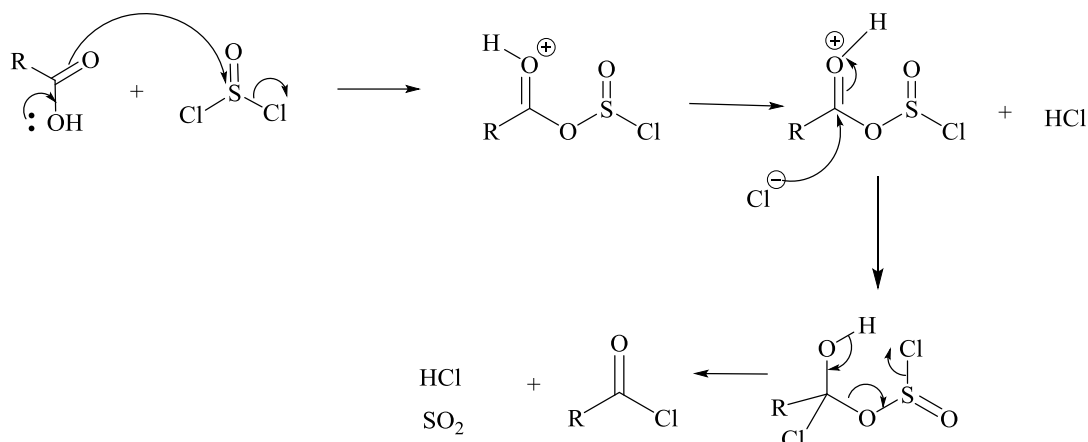
The same procedure was used to synthesise the (*R*)-1-(2-fluorobenzyl)pyrrolidine-2-carboxylic acid **2.2** enantiomer from *D*-proline and 2-fluorobenzyl bromide, also the reaction could also be scaled up to give 25 g of the product. The ^{19}F NMR spectrum showed a single peak for both enantiomers, which can not be distinguished by NMR spectroscopy. The enantiomers were characterised by chiral HPLC which allowed separation of the *S* and the *R* enantiomers. The product was obtained in a 74 % yield and was identified by ^1H NMR and ^{13}C NMR spectroscopies. Further confirmation of the identity of this species came from the LC-MS and HRMS-ESI. These results are consistent with those reported by Jamieson.¹⁵

2.4.2 Synthesis of (*S*)-*N*-(2-benzoylphenyl)-1-(2-fluorobenzyl)pyrrolidine-2-carboxamide (pre-ligand (FBPB)) **95**

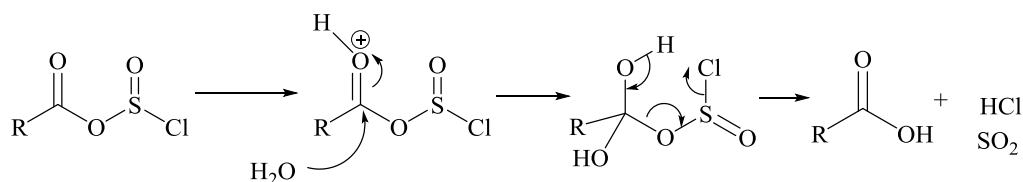
A variety of conditions were attempted to develop and modify the Jamieson method to increase the yield in this reaction. However, the highest yield of the isolated pre-ligand after recrystallization was 55 %. In general, to synthesise (*S*)-*N*-(2-benzoylphenyl)-1-(2-fluorobenzyl)pyrrolidine-2-carboxamide **95**, two different routes were followed. Firstly, (*S*)-1-(2-fluorobenzyl)pyrrolidine-2-carboxylic acid **93** was dissolved in dry dichloromethane under an inert atmosphere and reacted at 0 °C with thionyl chloride, because the reaction is very sensitive to air and moisture. The thionyl chloride should be added dropwise to the reaction mixture at 0 °C because the reaction is exothermic.¹³⁵ This formed the acid chloride which is a more reactive group than a carboxylic acid. 2-Aminobenzophenone, dissolved in the same solvent, was added to the reaction mixture dropwise to maintain the reaction conditions. This reaction gave the desired product **95** as white crystals in a 32 % yield. In a second attempt using this approach, to try to increase the yield from the reaction, extra thionyl chloride was used as both solvent and reactant

and the reaction was heated to 45 °C. However, no reaction was observed during monitoring the reaction with ^{19}F NMR spectroscopy (Scheme 2.5).

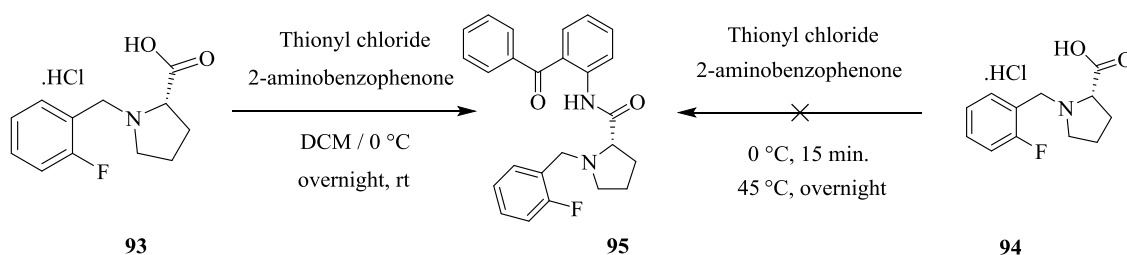
A) Synthesis



B) Hydrolysis



Scheme 2.4: Mechanism of the acid chloride synthesis and the hydrolysis¹³⁵

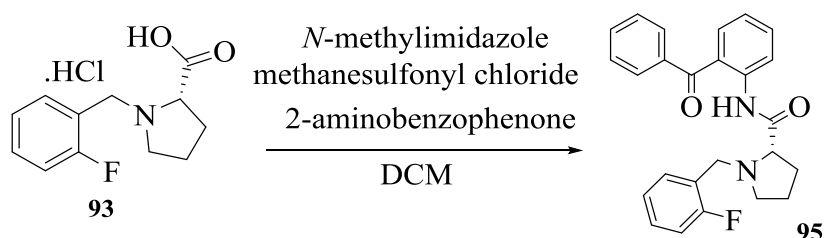


Scheme 2.5: Synthesis of (*S*)-*N*-(2-benzoylphenyl)-1-(2-fluorobenzyl)pyrrolidine-2-carboxamide **95**

In the second route to synthesise (*S*)-*N*-(2-benzoylphenyl)-1-(2-fluorobenzyl)pyrrolidine-2-carboxamide **95**, methanesulfonyl chloride (1 equivalent) was added to a solution of (*S*)-1-(2-fluorobenzyl)pyrrolidine-2-carboxylic acid (1 equivalent) and *N*-methylimidazole (2.2 equivalents) in dry dichloromethane at 0 °C, followed by 2-

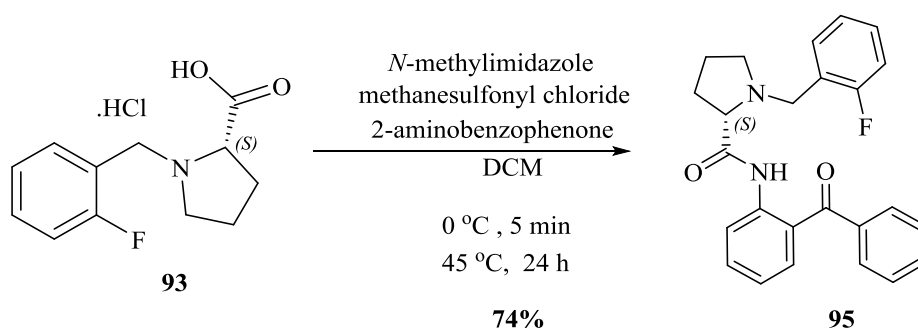
aminobenzophenone (0.9 equivalents). The reaction mixture was heated at 45 °C overnight (16-19 hours). Table 2.1 shows the optimisation of the reaction conditions to obtain the best results, through changing the time duration, the temperature and equivalents of *N*-methylimidazole. The reaction conditions (Table 2.1, Entry 5) that gave the best yield required an increase in the equivalents of *N*-methylimidazole from 2.2 to 3.2 for 24 hours instead of 16 hours, and the product was isolated as white crystals in a 74 % yield. It was identified by ^1H and ^{13}C NMR spectroscopy, also, ^{19}F NMR spectroscopy showed a single peak at -117.6 ppm and by HRMS-ESI which showed a parent ion peak at 403.1822. It was also identified by chiral HPLC which showed the high enantiomeric purity.

Table 2.1: Synthesis of the pre-ligand **2.3** by using different equivalent reagent, time and temperature



Entry	Quantity (g)	Temp. (°C)	Time (h)	Eq. of <i>N</i> -methylimidazole	Yield (%)
1	0.1	45	18	2.2	25
2	0.1	50	18	2.2	35
3	0.1	45	18	3.2	55
4	1	45	24	3.2	70
5	27	45	24	3.2	74

Following the reaction by TLC allowed the exact time necessary for the reaction to reach completion to be identified. To purify the product, two methods were used. Firstly, the acidification of the product with concentrated hydrochloric acid to obtain a salt which was then collected as a precipitate after allowing crystallization in the fridge for 24 hours to give a 74 % yield. Secondly, the product was isolated by extraction from the reaction mixture with dichloromethane, followed by purification using column chromatography (15 % ethyl acetate/hexane) (Scheme 2.6).⁴⁸

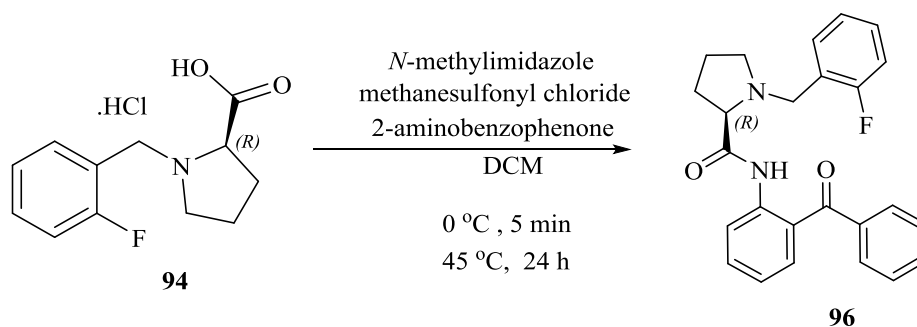


Scheme 2.6: Synthesis of (*S*)-*N*-(2-benzoylphenyl)-1-(2-fluorobenzyl)pyrrolidine-2-carboxamide **95**

However, the enantiomeric purity (97-98 % ee) of the 2-FBPB **95** after column chromatography was acceptable. Therefore, the product was recrystallized from hexane and few drops of ethyl acetate to increase the amount of the target enantiomer product to > 99 % ee. The purity was demonstrated via the HPLC technique which showed a single peak at 15.2 minutes (Figure 2.5). Crystals suitable for a single crystal X-ray structure determination were grown by slow evaporation of the compound from ethylacetate that confirmed the (*S*) stereochemistry of the product.

In comparison to the literature,⁴⁸ the reaction conditions and the equivalents of reagent had been modified; these new conditions gave higher yields and better enantiomer purity (ee) than previously reported. The fluorine at (*S*)-*N*-(2-benzoylphenyl)-1-(2-fluorobenzyl)pyrrolidine-2-carboxamide **95** could be one of the factors leading to a greater overall yield for this reaction.

2.4.3 Synthesis of (*R*)-*N*-(2-benzoylphenyl)-1-(2-fluorobenzyl)pyrrolidine-2-carboxamide **96**



The reaction between the (*R*)-1-(2-fluorobenzyl)pyrrolidine-2-carboxylic acid **94** and 2-aminobenzophenone was carried out under the same reaction conditions and the reaction

was scaled up to 25 g. The reaction was monitored by ^{19}F NMR spectroscopy to show a single peak for the pure product at -117.5 ppm. The product was purified via column chromatography and recrystallization from hexane and a few drops of ethyl acetate, and was isolated in a 78 % yield as pale orange crystals. It was further characterised by ^1H NMR and ^{13}C NMR spectroscopies, and by HRMS-ESI mass spectrum which showed a characteristic peak at 403.1822 (calcd for $\text{C}_{25}\text{H}_{24}\text{N}_2\text{O}_2\text{F}^+$ $[\text{M}+\text{H}^+]$ 403.1822) ($\Delta = 0.0$ ppm); HPLC (OD-H column, hexane (5 %)/ i PrOH isocratic): 13.05 min. A single crystal X-ray structure determination was carried out on crystals grown by slow evaporation of a solution of the compound in ethylacetate which confirmed the chirality of the pre-ligand as (*R*) (Figure 2.4).

Here, both enantiomers have been synthesised which allows a comparison to be made between the *S* and *R* compounds. The chiral HPLC showed distinct peaks for the two enantiomers at 15.2 and 13.5 minutes respectively; there is a different retention time for each. When the two enantiomers are mixed, the chiral HPLC reveals both peaks (Figure 2.6). The X-ray structures of both enantiomers were also determined (Figure 2.5).

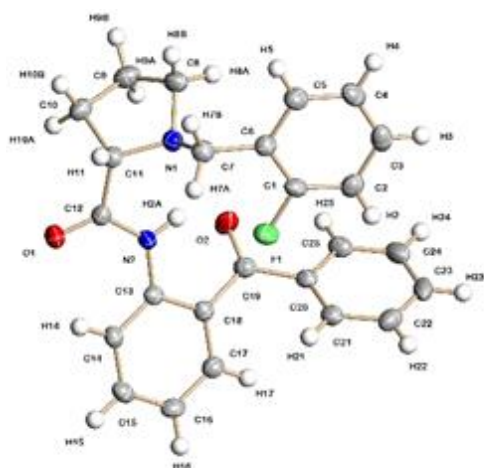
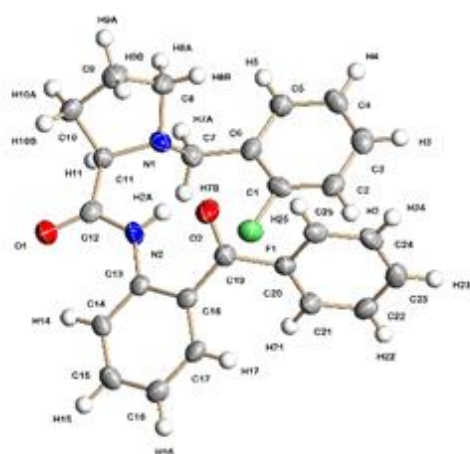
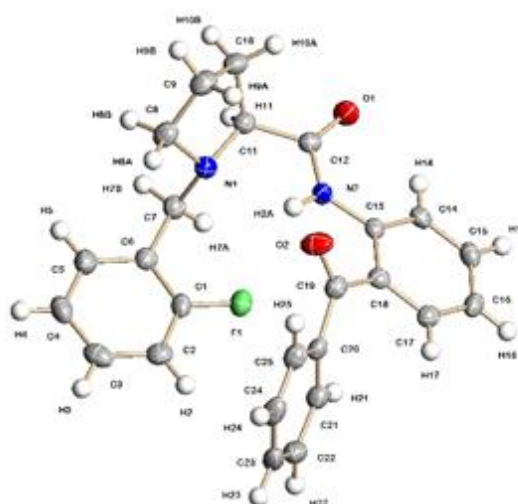
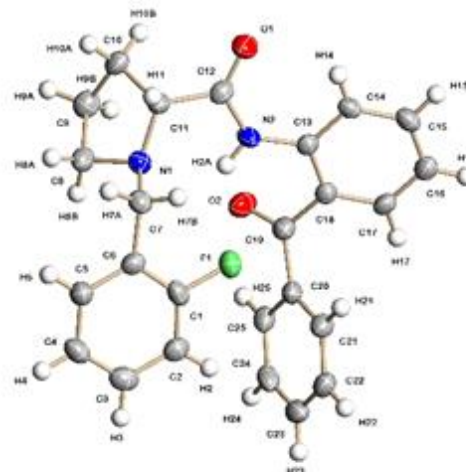
a) *S* ligand 95b) *R* ligand 96

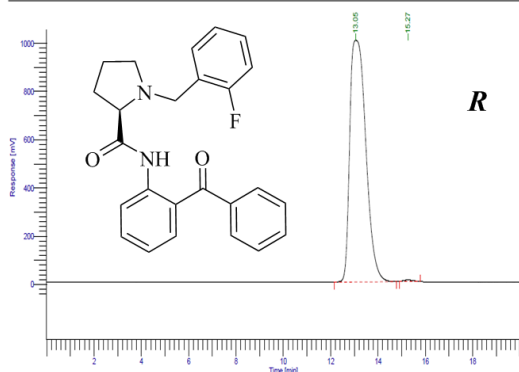
Figure 2.4: Crystal structure of compounds: 95 and 96

Page 1 of 1

Software Version : 6.2.1.0.104.0104
 Sample Name : emad1
 Instrument Name : PerkinElmer_HPLC
 Rack/Vial : 1/1
 Sample Amount : 1.000000
 Cycle : 1

Date : 09/11/2015 16:40:00
 Data Acquisition Time : 09/11/2015 16:59:07
 Channel : A
 Operator : emad
 Dilution Factor : 1.000000

Result File : C:\PE200A\Emad\data\emad1001.rst
 Sequence File : C:\PE200A\Emad\sequence\Chiral Default.seq



Chiralcel OD-H

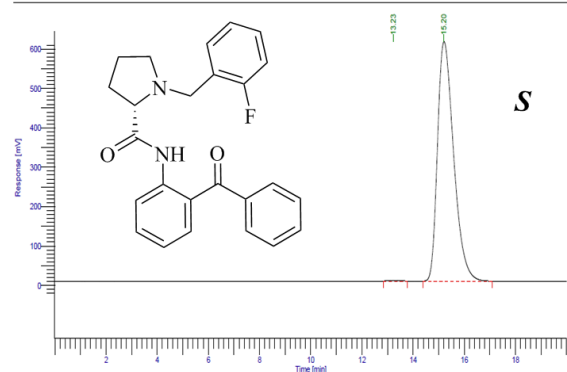
Peak #	Time [min]	Area [uV*sec]	Height [uV]	Area [%]	BL
1	13.05	47281747	1002611	99.6	MM
2	15.27	181616	6072	0.4	MM
47463363 1008683 100.0					

Page 1 of 1

Software Version : 6.2.1.0.104.0104
 Sample Name : emad1
 Instrument Name : PerkinElmer_HPLC
 Rack/Vial : 1/1
 Sample Amount : 1.000000
 Cycle : 1

Date : 09/11/2015 17:06:38
 Data Acquisition Time : 09/11/2015 16:27:14
 Channel : A
 Operator : emad
 Dilution Factor : 1.000000

Result File : C:\PE200A\Emad\data\emad1001-20151109-164725.rst
 Sequence File : C:\PE200A\Emad\sequence\Chiral Default.seq



Chiralcel OD-H

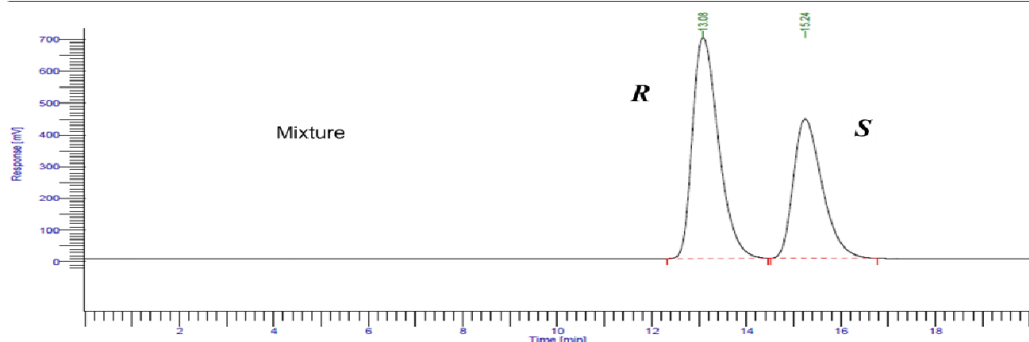
Peak #	Time [min]	Area [uV*sec]	Height [uV]	Area [%]	BL
1	13.23	60403	1948	0.2	MM
2	15.20	26716945	608487	99.8	MM
26777348 610435 100.0					

Page 1 of 1

Software Version : 6.2.1.0.104.0104
 Sample Name : emad1
 Instrument Name : PerkinElmer_HPLC
 Rack/Vial : 1/1
 Sample Amount : 1.000000
 Cycle : 1

Date : 09/11/2015 17:10:52
 Data Acquisition Time : 09/11/2015 16:50:13
 Channel : A
 Operator : emad
 Dilution Factor : 1.000000

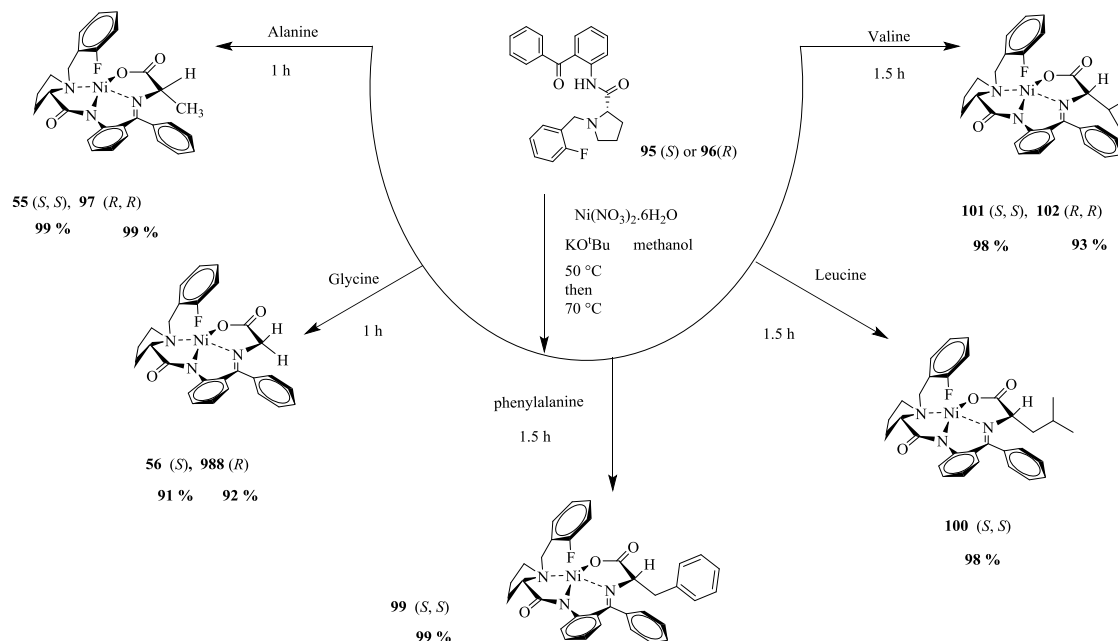
Result File : C:\PE200A\Emad\data\emad1001-20151109-171024.rst
 Sequence File : C:\PE200A\Emad\sequence\Chiral Default.seq



Chiralcel OD-H

Peak #	Time [min]	Area [uV*sec]	Height [uV]	Area [%]	BL
1	13.08	26598244	694785	58.9	BB
2	15.24	18587924	437909	41.1	BB
45186168 1132694 100.0					

Figure 2.5: Chiral HPLC chromatogram of (*S*) **95**, (*R*) **96** and mixture (*S* & *R*)-N-(2-benzoylphenyl)-1-(2-fluorobenzyl)pyrrolidine-2-carboxamide. (2-FBPB).

2.5 Synthesis of Ni^{II} Schiff base complexes

We were particularly interested in advancing the chemistry of Ni^{II} complexes of amino acid derived Schiff bases. The complexation of compounds **95** (*S*) or **96** (*R*) was carried out using nickel nitrate under basic conditions using the modified procedure of Jamieson by using freshly ground KO^tBu instead of KOH in methanol in the presence of a series of amino acids (glycine, alanine, valine, leucine, and phenyl alanine) to give the nickel Schiff base complexes. KO^tBu was used because it is easier to dissolve in methanol than the KOH pellets. Different types of amino acid were used which have different side chains. In general, this method gave more than 91-99 % yield for the complexation reaction as red crystals. All the complexes were formed in high purity and with excellent diastereoselectivity from 98 % to more than 99 % *de*. Only the glycine complexes needed to be purified using column chromatography. The progress of the reactions was monitored with ¹⁹F NMR spectroscopy and by TLC. The ¹⁹F NMR showed a characteristic peak for each complex. Mass spectrometry, ¹H NMR and ¹³C NMR spectroscopy provided the evidence for the formation of the complexes (Table 2.2).

(*S*)-({2-[1-(2-fluorobenzyl)benzyl]pyrrolidine-2-carboxamide]-phenyl}phenyl methylene)-alaninato-*N,N',N'',O*} nickel(II) **55** has been obtained in a 99 % yield. The product was identified with ¹⁹F NMR spectroscopy, which showed a single peak at -113.9 ppm

(*R*)-({2-[1-(2-fluorobenzyl)benzyl]pyrrolidine-2-carboxamide]-phenyl}phenyl methylene)-*R*-alaninato-*N,N',N'',O*} nickel^{II} **97** has been prepared in a 99 % yield. The complex was identified via ¹⁹F NMR spectroscopy, which showed a single peak at -113.9 ppm and by ¹H NMR and ¹³C NMR spectroscopies and mass spectrometry..

(*S*)-({2-[1-(2-fluorobenzyl)benzyl]pyrrolidine-2-carboxamide]-phenyl}phenyl methylene)-glycinato- *N,N',N'',O*} nickel(II) **56** has been synthesised in a 91 % yield. The product was indicated via ¹⁹F NMR spectroscopy, which showed a single peak at – 113.7 ppm and by ¹H NMR and ¹³C NMR spectroscopies and mass spectrometry.

(*R*)-({2-[1-(2-fluorobenzyl)benzyl]pyrrolidine-2-carboxamide]-phenyl}phenylmethylene)-glycinato-*N,N',N'',O*} nickel^(II) **98** has been achieved in a 92 % yield. The product indicated via ¹⁹F NMR spectroscopy, which showed a single peak at -113.6 ppm and by ¹H NMR and ¹³C NMR spectroscopies and mass spectrometry.

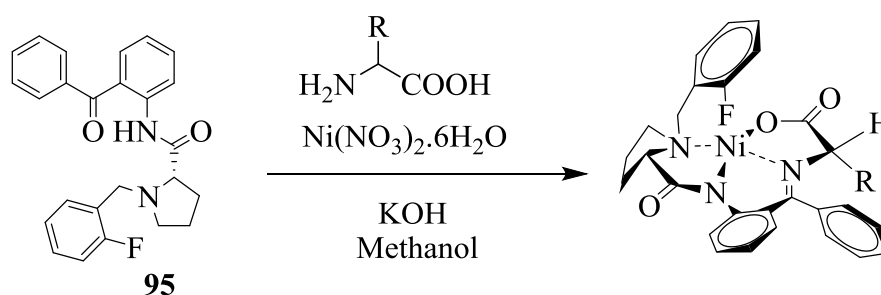
(*S*)-({2-[1-(2-fluorobenzyl)benzyl]pyrrolidine-2-carboxamide]-phenyl}phenyl methylene)-phenylalaninato-*N,N',N'',O*} nickel^(II) **99** has been achieved in a 99 % yield. The product identified via ¹⁹F NMR spectroscopy, which showed a single peak at -113.9 ppm and by ¹H NMR and ¹³C NMR spectroscopies and mass spectrometry.

(*S*)-({2-[1-(2-fluorobenzyl)benzyl]pyrrolidine-2-carboxamide]-phenyl}phenyl methylene)-(*S*)-leucinato-*N,N',N'',O*} nickel^(II) **100** has been achieved in a 98 % yield. The product identified via ¹⁹F NMR spectroscopy, which showed a single peak at -113.9 ppm and by ¹H NMR and ¹³C NMR spectroscopies and mass spectrometry.

(*S*)-({2-[1-(2-fluorobenzyl)benzyl]pyrrolidine-2-carboxamide]-phenyl}phenyl methylene)-*S*-valinato-*N,N',N'',O*} nickel^(II) **101** has been achieved in a 99 % yield. The product identified via ¹⁹F NMR spectroscopy, which showed a single peak at -113.8 ppm and by ¹H NMR and ¹³C NMR spectroscopies and mass spectrometry.

(*R*)-({2-[1-(2-fluorobenzyl)benzyl]pyrrolidine-2-carboxamide]-phenyl}phenylmethylene)-*R*-valinato-*N,N',N'',O*} nickel^(II) **102** has been achieved in a 94 % yield. The product identified via ¹⁹F NMR spectroscopy, which showed a single peak at -113.8 ppm and by ¹H NMR and ¹³C NMR spectroscopies and mass spectrometry.

Table 2.2: General Complexation Reactions

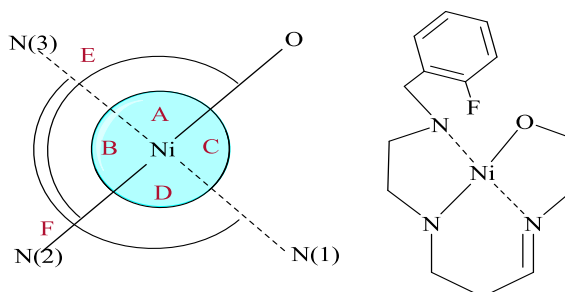


Entry	Compound	Amino acid	dr (<i>S</i> : <i>R</i>)	Product	¹⁹ F NMR	Yield (%)
1	<i>S</i> -ligand	glycine	-----	55	-113.93	99
2	<i>R</i> -ligand	glycine	-----	97	-113.91	99
3	<i>S</i> -ligand	<i>L</i> -alanine	98:2	56	-113.65	91
4	<i>R</i> -ligand	<i>D</i> -alanine	98:2	98	-113.63	92
5	<i>S</i> -ligand	<i>L</i> -phenylalanine	99:1	99	-113.92	92
6	<i>S</i> -ligand	<i>L</i> -leucine	99:1	100	-113.94	98
7	<i>S</i> -ligand	<i>L</i> -valine	99:1	101	-133.80	99
8	<i>S</i> -ligand	<i>D</i> -valine	98:2	102	-113.82	94

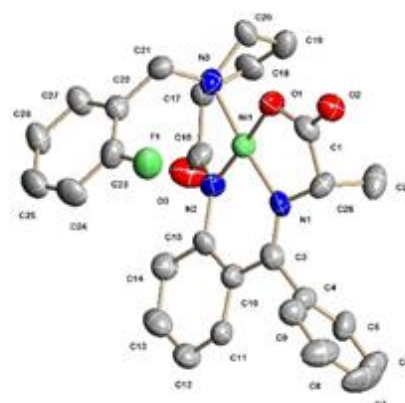
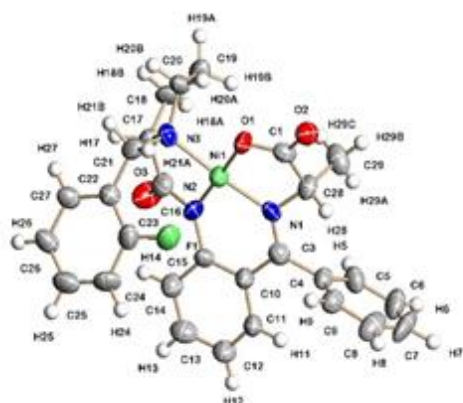
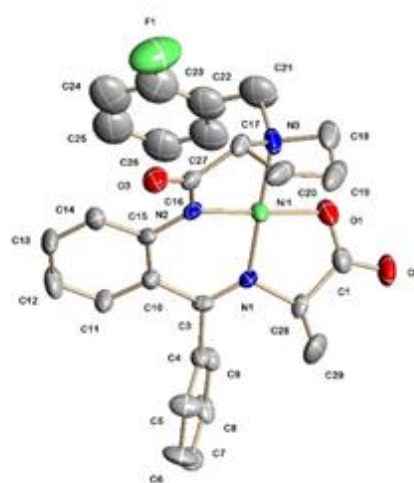
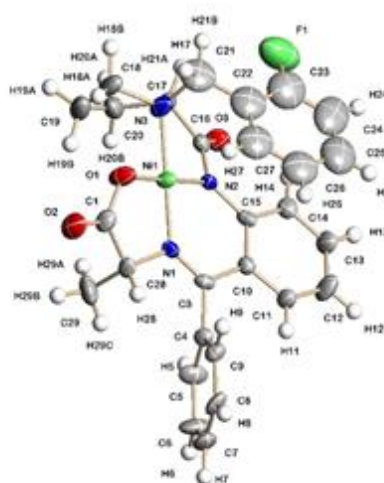
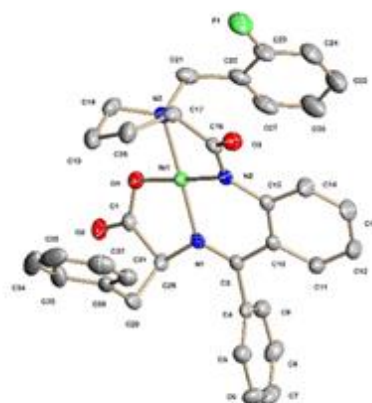
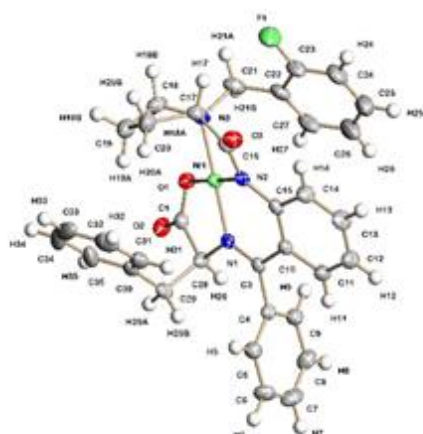
Forming crystals suitable for X-ray crystallography studies was achieved for the compounds **55**, **97**, **99-102**, (Figure 2.6). Their solid-state structures showed a Ni^{II} centre supported by an unsymmetrical *N, N, N, O* pincer ligand in a distorted square planar geometry. The bond lengths and angles around nickel are compared in Table 2.3, and show only slight differences between the complexes which are than 0.03 Å. These data are comparable to those seen for other Ni^{II} Schiff base complexes. The Ni(1)-N(2) bond lengths showed the longest in **97** is 1.857(5) Å, however, the shortest shown in **55** is 1.825(7) Å, The Ni(1)-O(1) bond lengths showed the longest in **55** is 1.872(5) Å, however the shortest was shown in **101** and is 1.851(2) Å. The Ni(1)-N(1) bond lengths showed the longest in **100** is 1.852(5) Å, however the shortest shown in **97** is 1.835(5) Å. The Ni(1)-N(3) bond lengths showed the longest in **100** is 1.942(5) Å, however the shortest shown in **97** and is 1.835(5) Å. Furthermore, these determinations show that the intramolecular interaction between the Ni^{II} and the fluorine atom on the benzyl group are all different and all longer than that reported by Jamieson.¹⁵ All the bond angles around the Ni^{II} centres showed some deviation from the right angle expected for a regular square

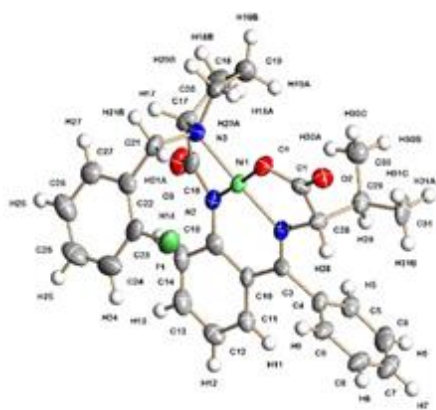
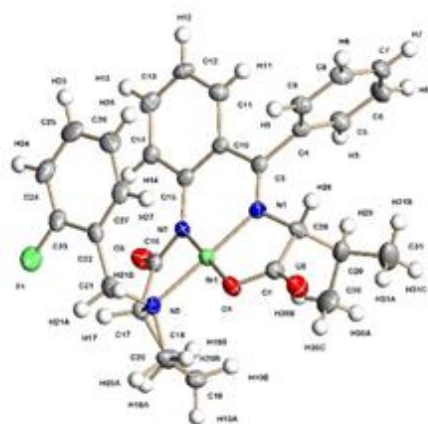
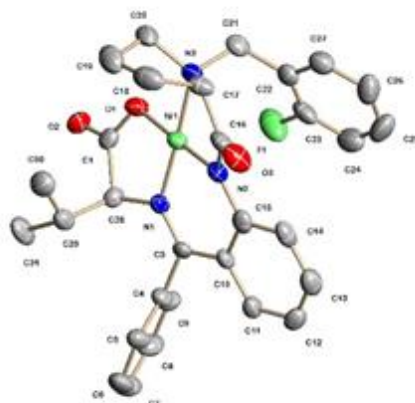
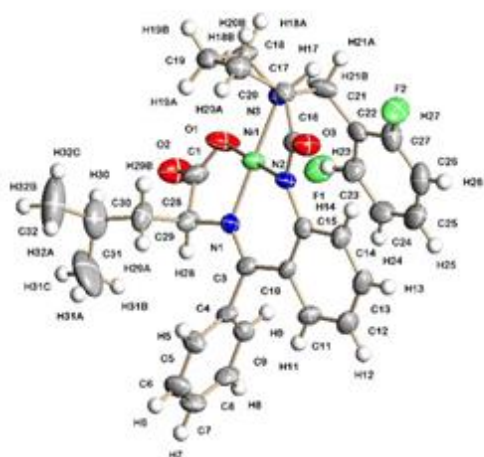
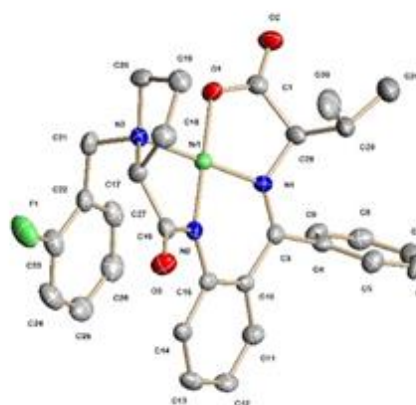
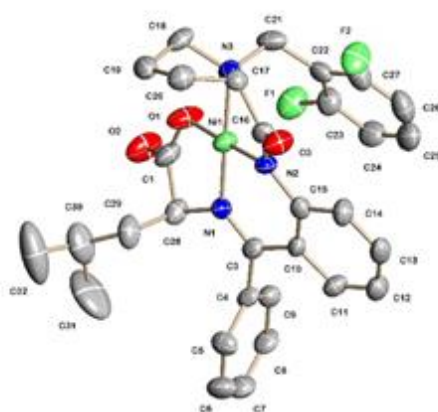
planar coordination geometry. Overall the angles are within $\pm 5^\circ$ of the right angle. As expected, the angles are all slightly strained due to presence of the heteroatoms in each corner of the square (Table 2.3).

Table 2.3: Key bond lengths (Å) and angles ($^\circ$) for **2.5**, **2.6**, and **2.9-2.12**



Compound	Bond Lengths (Å)					
	Ni(1)-N(2)	Ni(1)-O(1)	Ni(1)-N(1)	Ni(1)-N(3)	Ni(1)...F(1)	
55	1.825(7)	1.872(5)	1.836(6)	1.925(7)	3.1	
97	1.857(5)	1.861(5)	1.835(5)	1.940(6)	3.1	
99	1.833(4)	1.857(4)	1.837(4)	1.934(4)	3.1	
100	1.840(5)	1.854(4)	1.852(5)	1.942(5)	3.1	
101	1.847(3)	1.851(2)	1.843(3)	1.935(3)	3.0	
102	1.833(4)	1.857(4)	1.837(4)	1.934(4)	3.1	
Compound	Bond Angles (°)					
	O(1)-	N(2)-	O(1)-	N(2)-	N(2)-	N(1)-
	Ni(1)-	Ni(1)-	Ni(1)-	Ni(1)-	Ni(1)-	Ni(1)-
	N(3) A	N(3) B	N(1) C	N(1) D	O(1) E	N(3) F
55	91.2(3)	87.4(3)	86.7(3)	94.9(3)	177.0(3)	175.3(3)
97	92.3(2)	86.4(2)	86.8(2)	94.5(2)	178.2(3)	179.1(3)
99	91.97(18)	87.06(19)	86.57(18)	94.36(19)	178.4(2)	177.8(2)
100	91.58(19)	86.7(2)	86.80(18)	94.9(2)	178.3(2)	177.2(2)
101	92.22(10)	87.06(11)	86.49(10)	94.25(11)	178.9(11)	177.7(11)
102	91.97(18)	87.06(19)	86.57(18)	94.36(19)	178.4(2)	177.8(2)

A) Alanine complex **55** (*S, S*)B) Alanine complex **97** (*R, R*)C) Phenylalanine complex **99** (*S, S*)

D) Valine complex **100** (*S, S*)E) Valine complex **101** (*R, R*)F) Leucine complex **102** (*S, S*)Figure 2.6: Crystal structure of compounds: **55**, **97**, **99-102**

2.6 Conclusions

The synthesis of both *S* and *R* 1-(2-fluorobenzyl)pyrrolidine-2-carboxylic acid **2.1** and **2.2** as a white crystals, in high purities, has been achieved by recrystallization from acetone.

Synthesis of the ligands **95** and **96**, as pure, with high enantiomeric purity (>99 %) has been achieved by a modification of the Jamieson method by increasing the equivalents of *N*-methylimidazole to 3.2 and by increasing the reaction time to 24 h. Here, enantiomers were distinguished via chiral HPLC.

Synthesis of the eight examples of Ni^{II} Schiff base complexes from the pre-ligands, a nickel(II) salt and an amino acid has been achieved. Some of these are diastereoisomers of others, such as: (*S,S*) **55** and (*S,R*) **97**; (*S,S*) **101** and (*S,R*) **102**; (*S,S*) **56** and (*S,R*) **98**. The diastereoisomers will be used in the alkylation reaction and aldol reaction in Chapters 3 and 4 for the synthesis of unnatural amino acids and to study any effect of steric hindrance on the reactivities of these complexes.

Chapter 3

Synthesis of novel alkynyl derivatives of amino acids via Ni^{II} Schiff base complexes



UNIVERSITY OF
LEICESTER

3.1 Introduction

Alkynyl amino acids have found extremely wide application in peptide synthesis by use in (i) click reaction, (ii) synthesis of 1,3-dyne dimer, (ii) synthesis of macrocyclic peptides. The newest field for the alkynyl amino acids is using the Sonogashira reaction to modify the alkynyl derivatives. In general, there are two types of amino acid that have been used for these reactions with different lengths of the side chain of the amino acids (Figure 3.1).

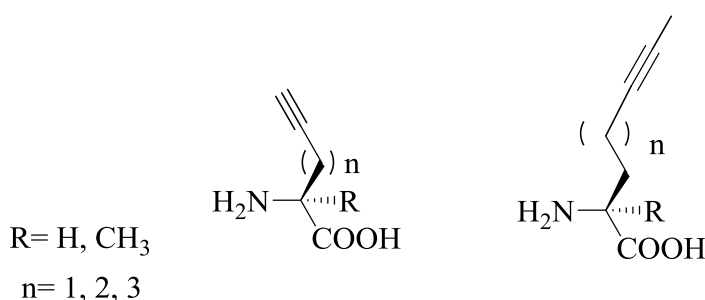
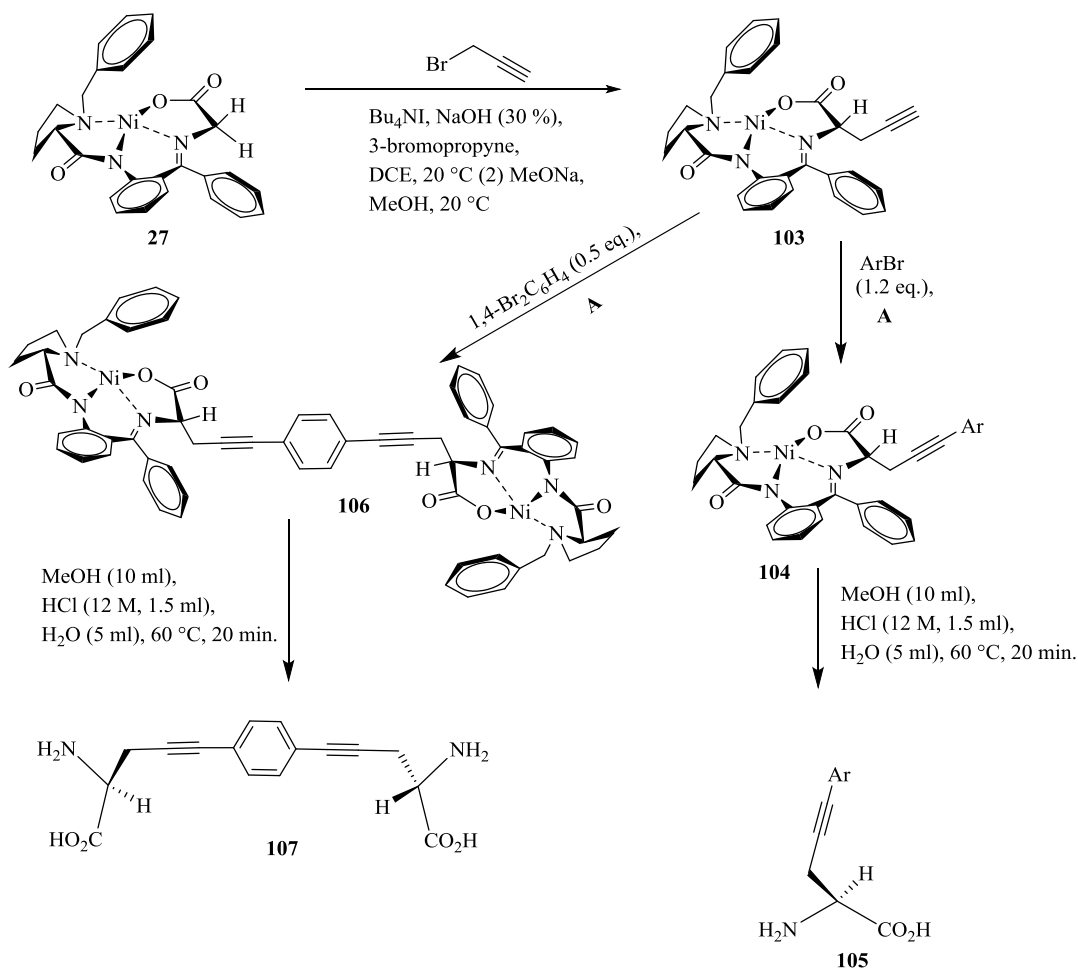


Figure 3.1: Types of alkynyl derivatives of amino acids

3.2 Synthesis of alkynyl derivatives of amino acids

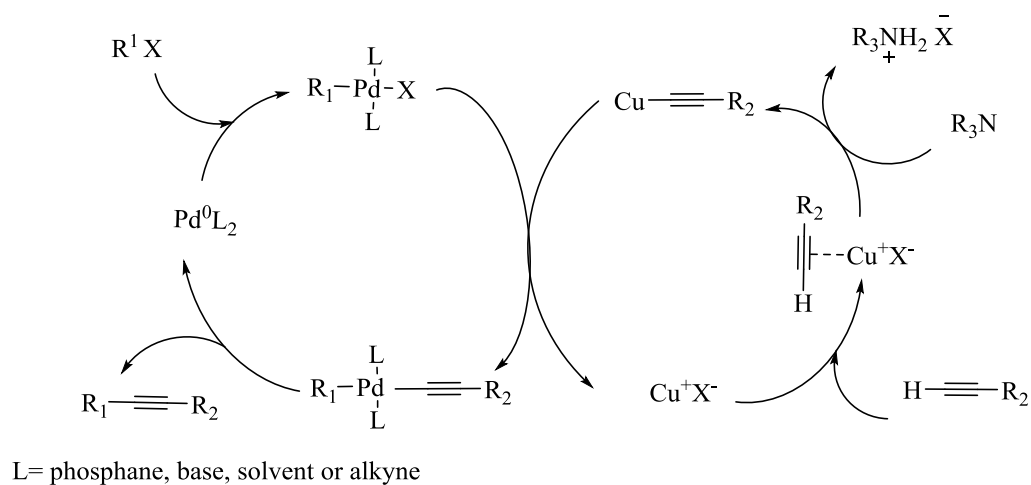
In 2015, Langer and co-workers introduced the synthesis of optically pure alkynyl amino acids derivatives ((*S*)-2-amino-5-pent-4-ynoic acids) using different procedures to synthesise the new amino acid via alkylation. They synthesised ((*S*)-2-amino-5-pent-4-ynoic acids) by an alkylation reaction on the glycine Ni^{II} Schiff base complex under phase-transfer conditions (PTC) followed by Sonogashira coupling reactions (Scheme 3.2)¹³⁶ with either aryl bromides and or 1,4-dibromobenzene to synthesise the dimer. The products were shown to be good selective inhibitors for both ALR1 (aldehyde reductase) and ALR2 (aldose reductase), enzymes which play important roles in the polyol and glucose metabolism pathways (Scheme 3.1).¹³⁷



A = $\text{Pd}(\text{PPh}_3)_4$ (5 mol %), CuI (10 mol %), HNiPr_2 (1 ml/0.25 mmol),
 1,4-dioxane (1 ml/0.25 mmol), 90°C , 3–4.5 h.

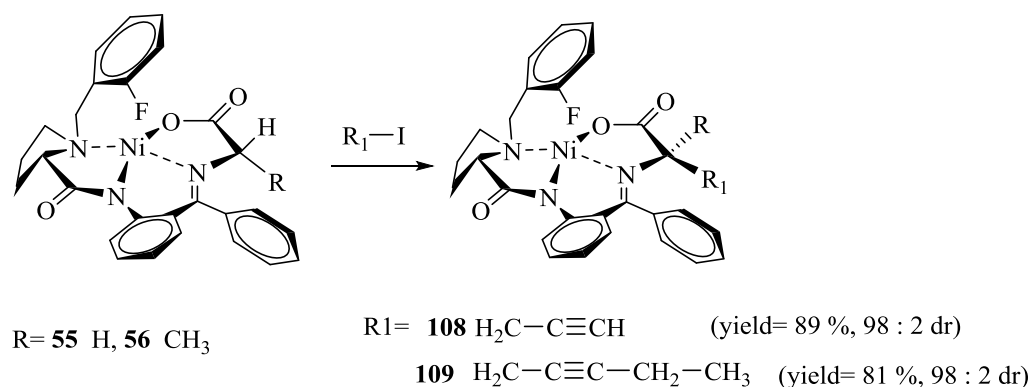
Ar = Phenyl, 4-Fluorophenyl, 4-Chlorophenyl, 4-(Trifluoromethyl)phenyl, 3-Methoxyphenyl,

Scheme 3.1: Synthesis of mono and bis-aryl-alkyne amino acids by Sonogashira Coupling reactions



Scheme 3.2: Sonogashira coupling reaction mechanism¹³⁶

In 2014, Soloshonok and co-workers¹³⁸ presented the synthesis of different types of the alkynyl amino acids, such as (2-aminohex-5-ynoic acid), and fluorinated amino acids using a different type of glycine Ni^{II} Schiff base derivative. The reaction was carried out under PTC conditions and used a few different alkynyl halides to synthesis the amino acid derivatives. The reactions gave good yields, with high diastereoselectivity (>98 : 2 dr), as determined by ¹H NMR spectroscopy (Scheme 3.3).



Scheme 3.3: Synthesis alkyne amino acids

Many researchers have investigated methods to increase the side chain length of the alkyne by introducing alternative spacer groups,¹³⁹ either by acylation or alkylation reactions. In general, the alkylation reaction was carried out on the side chain of protected amino acids such as serine^{140, 141}, threonine¹⁴² and tyrosine¹⁴³ (Figure 3.2), whilst the acylation reactions were performed on acidic or basic amino acids such as lysine, aspartic acid and glutamic acid.¹³⁹

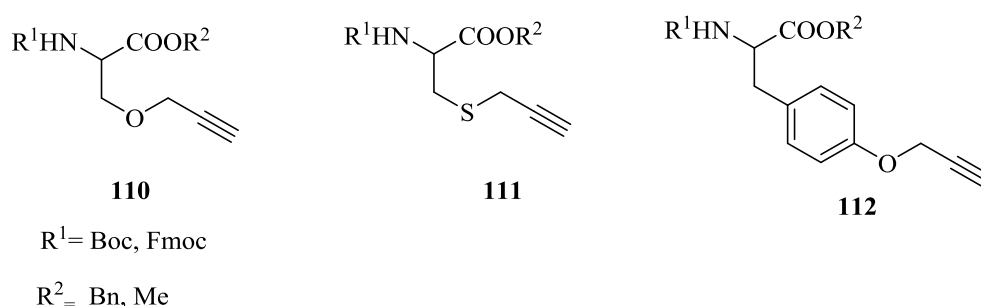
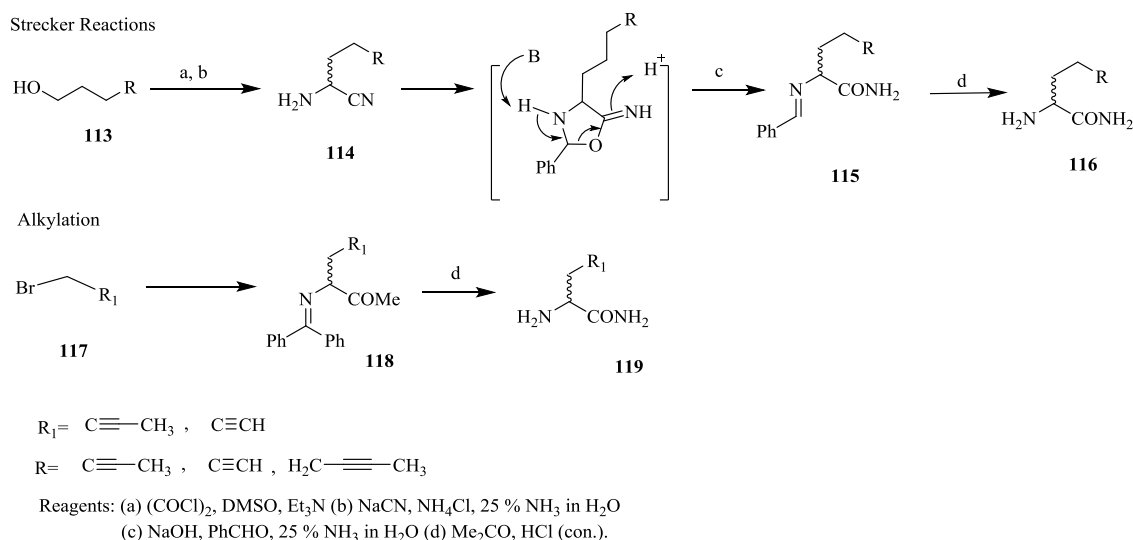


Figure 3.2: Derivatives of amino acids: a) serine b) threonine c) tyrosine

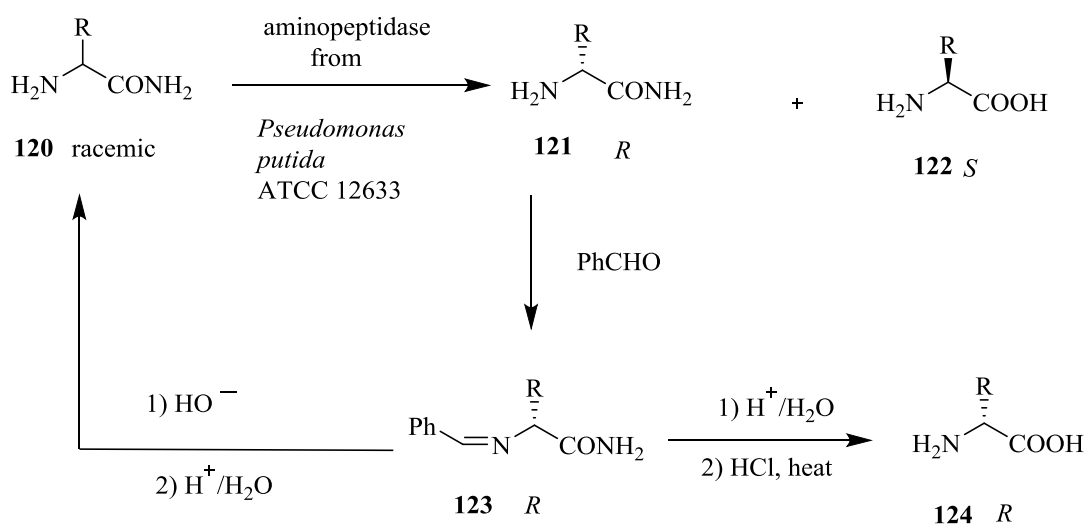
Rutjes and co-workers have prepared alkynyl amino acids by alkylation of methyl-*N*-(diphenylmethylene)glycinate or by Strecker reaction and subsequent partial hydrolysis

of the cyanide to the amide (Scheme 3.4).¹⁴⁴ The racemic mixture of the amino acids was treated with *Pseudomonas putida* ATCC 12633 and a genetically modified



Scheme 3.4: Synthesis of amino acid via Strecker reaction and alkylation reaction

organism, leading to the enantiomers pure (*S*)-acids and (*R*)-amides. The main significance in this paper was being able to scale up the enzymatic pathways route to form enantiomerically pure un-natural amino acids (Scheme 3.5).



Scheme 3.5: General biocatalytic pathway

3.3 Aims of Chapter 3

The fundamental aim of the work in this chapter is the synthesis of novel enantioenriched mono- and di-substituted alkynyl amino acids by the use of chiral Ni^{II} Schiff base complexes. New types of alkynyl amino acids have become one of the main target in peptides synthesis. The unnatural amino acids afford new starting materials to prepare new peptidomimetics for exploration and for use as staples to stabilise peptide structures. Some alkynyl amino acids are commercially available, but these contain small side chains such as propargylglycine and 2-aminohex-5-ynoic acid. For peptide stapling, the distance between the positions i , $i+4$, i , $i+7$ and i , $i+11$ (used to make the 1,3-diyne bonds) are longer than the length of the side chains in these amino acid, such that they are only suitable for creating peptides (eg. dimer¹⁰⁹; Scheme 1.13) or macrocyclic peptides¹¹¹ (Scheme 1.14) not staple-bridged peptides. Here, different chain lengths are needed for different types of alkynyl amino acids, all with high diastereoselectivities. The longer side chains will be used to synthesise novel 1,3-diyne stapled peptides, and different long side chains are required for different positions in the peptides: i , $i+4$, i , $i+7$ and i , $i+11$ (Figure 3.3). Three types of iodoalkyne have been used in the alkylation reaction in this work (C5, C6, and C7) to generate side chains on the glycine, alanine, valine, leucine and phenylalanine Ni^{II} Schiff base complexes. The glycine and alanine derivatives C6 and C7 have been synthesised with good yields and excellent diastereoselectivities, and, therefore, these have been selected for the synthesis of the novel 1,3-diyne stapled peptides.

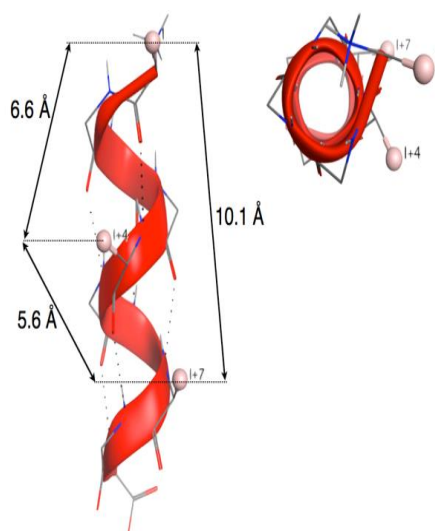
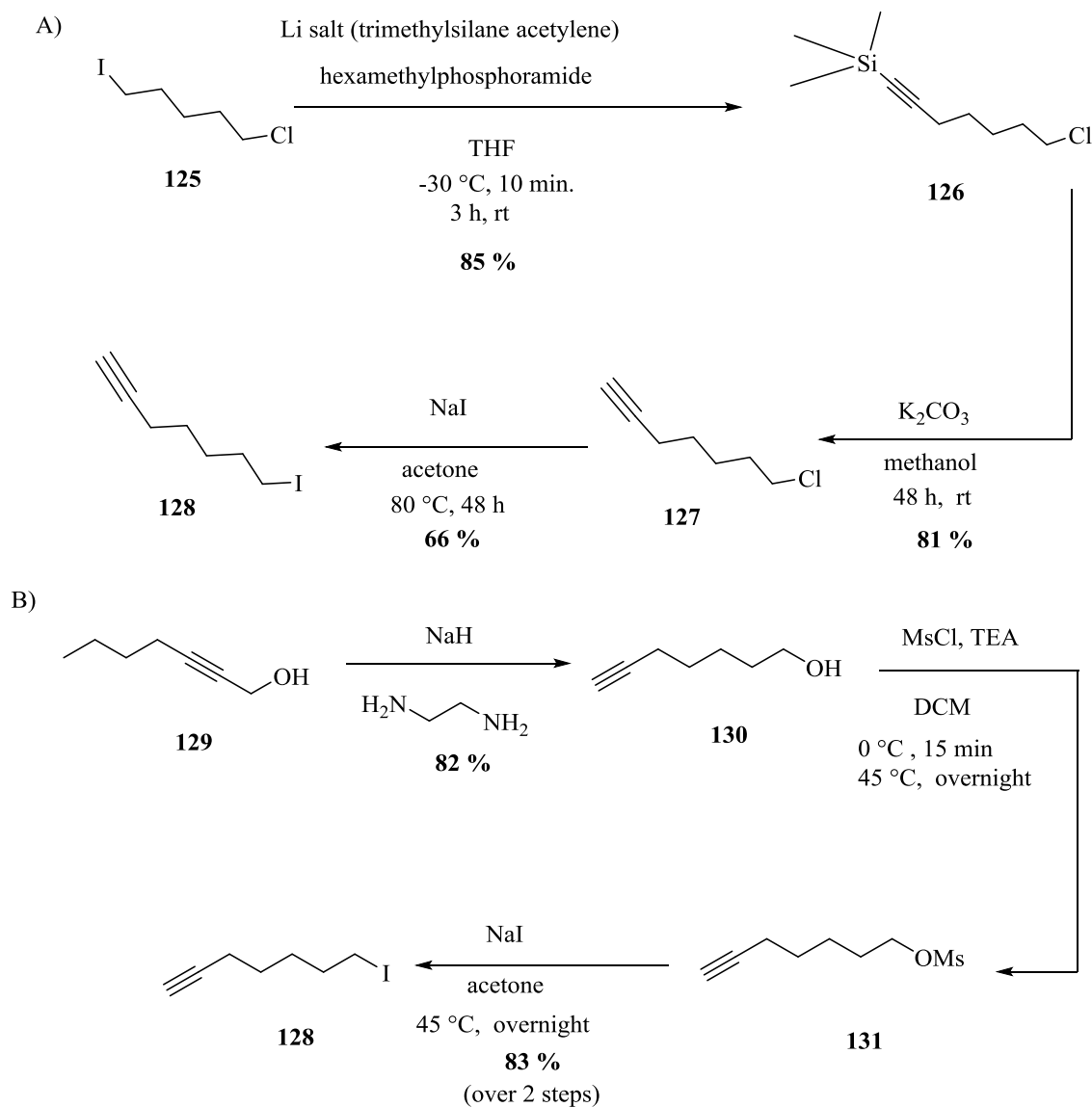


Figure 3.3: Distances between i , $i+4$, i , $i+7$ in peptide α -helix

3.4 Synthesis of the iodoalkyne electrophiles

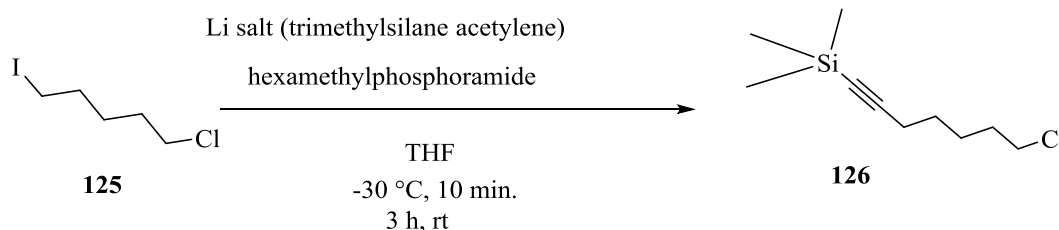


The key starting materials required for the preparation of the alkynyl derivatives of amino acids are the electrophilic alkynyl iodides: 5-iodopent-1-yne (C5) and 7-iodohept-1-yne (C7). In contrast, 6-iodohex-1-yne (C6) is commercially available. Whilst bromoalkynes have been used in the alkylation reaction of Ni^{II} Schiff base complexes in the previous studies, the iodoalkynes are stronger electrophiles than either bromoalkynes or chloroalkynes, which is related to the electronegativity of the halides (I>Br>Cl). 7-Iodohept-1-yne (C7) has been prepared by two methods:

3.4.1 Method A

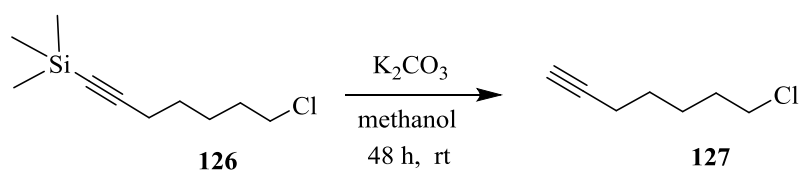
Here, the synthesis of 7-iodohept-1-yne was carried out in three steps according to a literature procedures from 1-chloro-5-iodopentane.¹⁴⁵

3.4.1.1 Synthesis of 7-chlorohept-1-yn-1-yl trimethylsilane



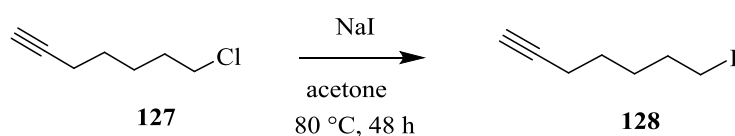
Hexamethylphosphoramide (HMPA) was added to dry THF then 1-chloro-5-iodopentane **125** was added to the reaction mixture. HMPA was used as both a Lewis base catalyst for the reaction¹⁴⁶ as well as the solvent. It is a highly polar solvent and aprotic solvent. The iodine is more reactive than the chlorine in nucleophilic substitution reactions of alkyl halides.¹⁴⁷ A commercially available 0.5 M solution of the lithium salt of trimethylsilyl acetylene in THF was added to the reaction mixture dropwise at low temperature, before the reaction mixture was allowed to warm to room temperature to improve the yield. The reaction was monitored by GC every 30 minutes until all the starting material had been converted. A saturated aqueous ammonium chloride solution was added to quench the reaction mixture. The reaction afforded 91 % of the crude (7-chlorohept-1-yn-1-yl)trimethylsilane **126** which was higher than the reported literature value of 76 %. Mass spectrometry showed a peak in the ESI⁺-MS spectrum at m/z 202 as expected for the product as $M+H^+$. ¹H NMR spectroscopy showed that the triplet peak at 3.1 ppm in the starting material, which is assigned to the CH₂ neighbouring the iodine, had disappeared and a singlet (integral 9) at 0 ppm for the SiMe₃ group had appeared. Purification by column chromatography was extremely hard because the product and the starting material are not UV active.

3.4.1.2 Synthesis of 7-chlorohept-1-yne



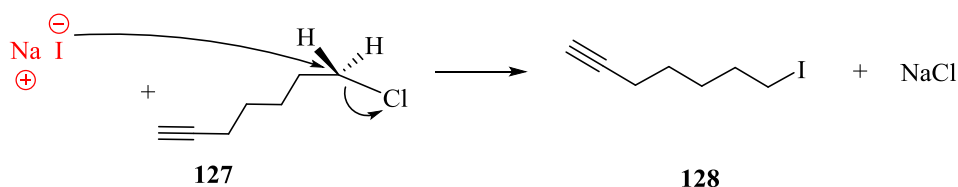
The crude product (7-chlorohept-1-yn-1-yl)trimethylsilane **126** was added to a solution of K_2CO_3 in methanol at room temperature and the terminal alkyne group generated by removal of the protecting group "SiMe₃" (TMS) under these basic conditions. The reaction was monitored by GC which showed that the reaction was not complete during the time detailed in the literature. So, the reaction time was increased from overnight to 48 h at room temperature to give the target terminal acetylene **127** in good purity in 86 % yield. The ESI⁺-MS spectrum gave a peak at m/z 131 for the product assigned as $\text{M}+\text{H}^+$, whilst the ¹H NMR spectroscopy showed the disappearance of the singlet (integral 9) at 0 ppm for the SiMe₃ group.

3.4.1.3 Synthesis of 7-iodohept-1-yne



The main reason to carry out this reaction is that, for alkyl halides, iodides react faster than chlorides, which is necessary in the alkylation reaction of the Ni^{II} Schiff base complexes.¹⁴⁸ In other words, the iodide is a better leaving group than the chloride in alkylation reactions. The reaction to form the alkyl iodide is known as the Finkelstein reaction; it is an S_N2 nucleophilic substitution reaction. NaI is soluble in acetone that gives I⁻. Crude 7-chlorohept-1-yne **127** was dissolved in acetone as an aprotic solvent. The reaction mixture was stirred in a sealed tube at 80 °C for 48 h; the reaction was done under high pressure to reduce the time and to increase the conversion. The reaction was monitored by GC to complete conversion. The solvent used for extraction was changed from ethyl acetate that was described in the literature to diethyl ether, to allow easier removal *in vacuo*. ¹H NMR spectroscopy showed the appearance of a triplet peak at 3.1 ppm for the CH₂ group neighbouring the iodine. In contrast, the triplet peak at 3.4 ppm for the CH₂ group neighbouring the chlorine had disappeared. The final alkynyl iodide was isolated in an 81 % yield and used in the subsequent alkylation reactions without

further purification. The product was an oily pale-yellow colour. However, method A used here to synthesise 7-iodohept-1-yne **128** from 1-chloro-5-iodopentane **125**, the product could not be purified and, therefore, it was used as a crude product in the alkylation reactions with the Ni^{II} Schiff base complexes.

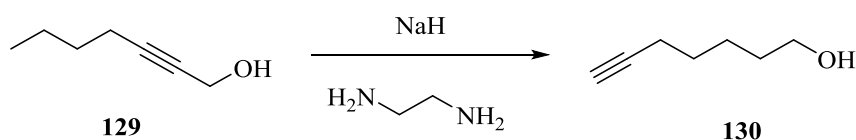


Scheme 3.6: Alkylation substitution reaction.

3.4.2 Method B

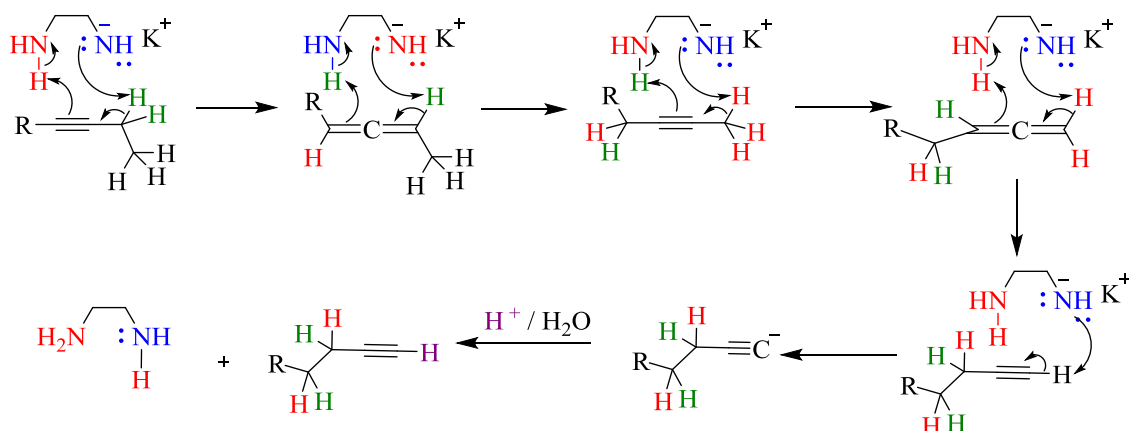
An alternative strategy involved the synthesis of 7-iodohept-1-yne according to a different literature procedure from hept-2-yn-1-ol via the Zipper reaction.¹⁴⁹ In 1975, Brown and Yamashita demonstrated the first alkyne Zipper reaction using potassium 3-aminopropylamide (KAPA), which had been prepared immediately from potassium hydride as a strong base and 3-aminopropylamide in dry trimethylenediamine solvent.¹⁵⁰ The synthesis was carried out in three steps:

3.4.2.1 Synthesis of hept-6-yn-1-ol **130**



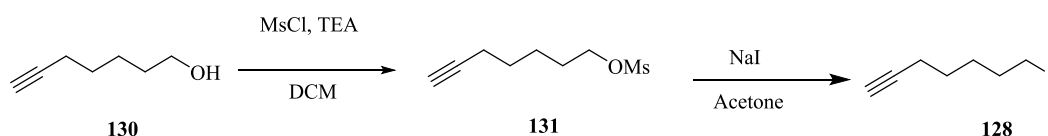
Sodium hydride (60 % in mineral oil) was added, in small portions due to the exothermic reaction, to ethane-1,2-diamine at 0 °C under nitrogen. Hept-2-yn-1-ol **129** was added at 40 °C and the reaction monitored by TLC and stained with potassium dichromate. When 100 % conversion of the starting material was achieved, the reaction mixture was quenched with water followed by 2 N HCl at 0 °C, since the acid-base reaction is exothermic; the reaction generates hydrogen gas, NaCl and *N1,N2*-dichloroethane-1,2-diamonium salt. After extraction with diethyl ether, the combined organic phases were extracted with Na₂SO₄ to remove unreacted ethane-1,2-diamine, which is water soluble. After purification by flash column chromatography hept-6-yn-1-ol **130** was obtained in an 80 % yield. ¹H NMR spectroscopy showed a triplet at 3.1 ppm has appeared, which is

assigned to the $\text{CH}\equiv\text{C}$ and a triplet peak at 0.96 ppm had disappeared, which is related to the CH_3 group (Scheme 3.7).



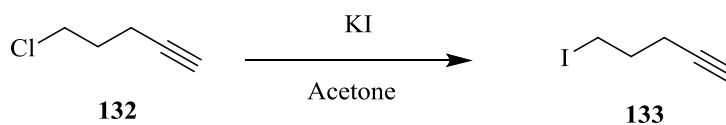
Scheme 3.7: Mechanism of the alkyne zipper reaction

3.4.2.2 Synthesis of 7-iodohept-1-yne **128**



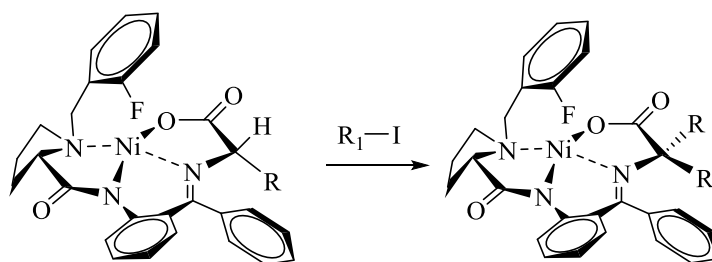
The hydroxyl group is not a good leaving group, so methanesulfonyl chloride in DCM, in the presence of triethylamine as a base, was used to convert create a good leaving group. An excess of methanesulfonyl chloride (1.5 eq.) was added to ensure 100 % conversion of the starting material. The reaction was quenched with water to get rid of the excess of methanesulfonyl chloride. The crude product was then used in a Finkelstein reaction to form the desired alkyl iodide by reaction with NaI in acetone. The crude oil product was purified by Biotage column chromatography (hexanes/ethyl acetate 80:20) to obtain the product, 7-iodohept-1-yne **128**, in 84 % yield. ^1H NMR spectroscopy showed the appearance of a triplet peak at 3.2 ppm for the CH_2 group neighbouring the iodine. The product was also identified by LC-MS and HRMS-ESI mass spectrometry with an ion peak at 222.9979.

3.4.3 Synthesis of 5-iodopent-1-yne **133**



Finkelstein reaction conditions were also used to synthesise 5-iodopent-1-yne from 5-chloropent-1-yne. The progress of the reaction was monitored by TLC stained with potassium chromate until 100 % conversion of the starting material was reached. The crude oil product was purified via Biotage column chromatography (hexanes/ethyl acetate 80 : 20) to obtain the product **133** in 99 % yield. The product identity was confirmed by LC-MS and HRMS-ESI mass spectrometry with a parent ion peak at 194.9665 (calc. for $[M+H]^+$ 194.9671) ($\Delta = -3.1$ ppm) and ^1H NMR spectroscopy.

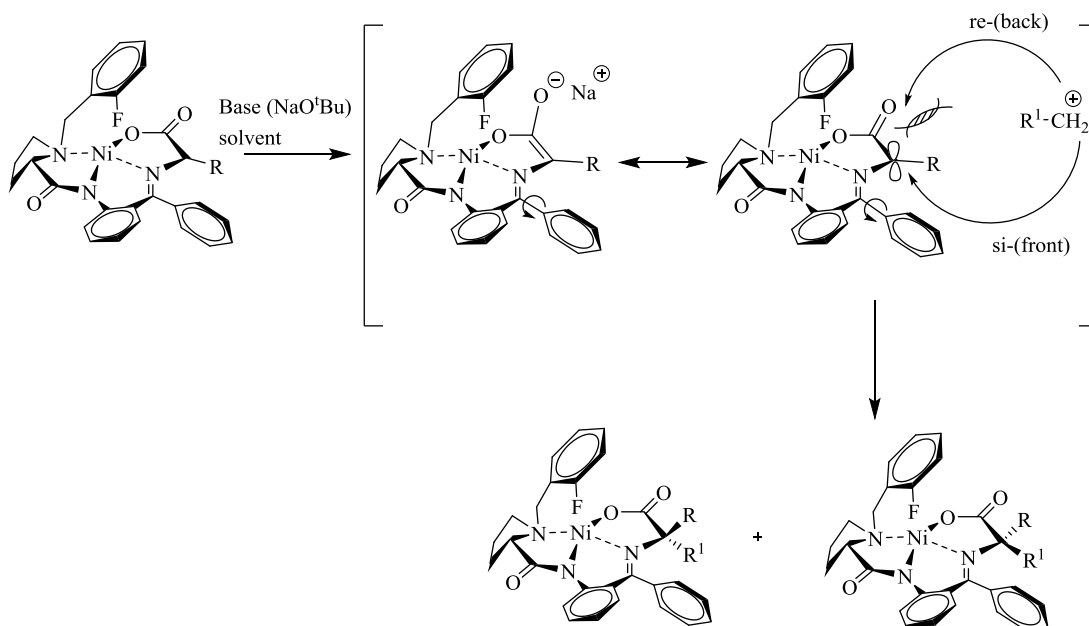
3.5 Alkylation reaction



The initial aim was to synthesise novel unnatural amino acids via alkylation reactions with different electrophiles, such as alkynyl iodides and alkynyl bromides, to generate appropriate amino acids required for i , $i+4$ and i , $i+7$ peptide hydrocarbon staples. The amino acids unsaturated moiety, with different side chain lengths, was the target for subsequent peptide synthesis because of their wide scope through click reactions and 1,3-dyne dimerisation.^{78, 147, 151-155} The key step of the alkylation reaction requires the generation of an enolate, as an intermediate, at the beginning of the reaction. Several bases, such as NaOH, KOH, NaH, NaOMe, NaO^tBu and KO^tBu, in different solvents, such as DMF, acetonitrile, MeOH and DCM, have previously been used in this type of study. The general mechanism, via the enolate,¹⁵⁶⁻¹⁵⁸ shows the possibility for diastereoselectivity (Scheme 3.8).¹⁵⁸

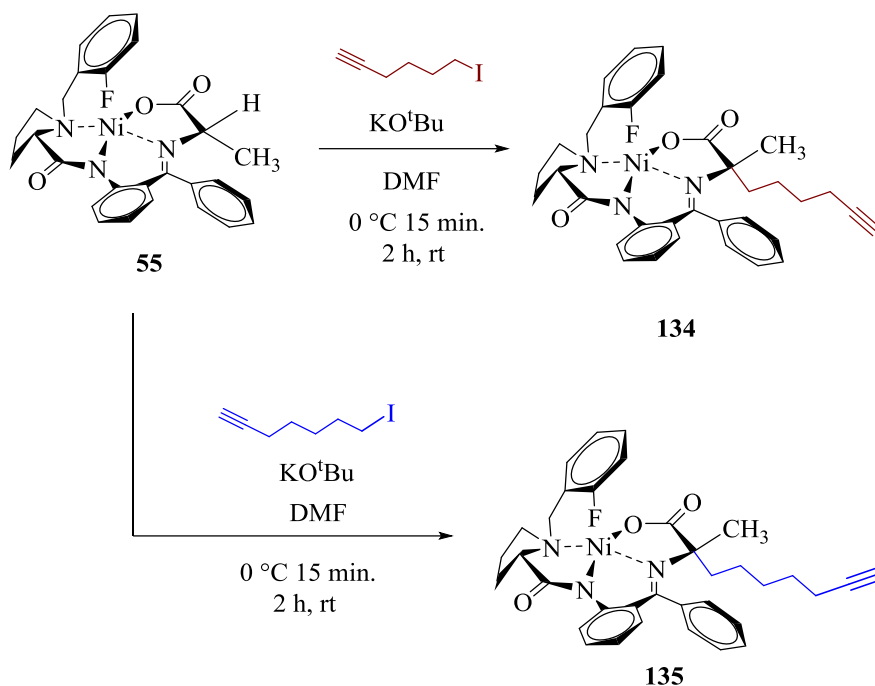
In this work, the alkylation of various Ni^{II} Schiff base complexes initially involved the formation of the enolate, as an intermediate, under strong basic conditions, followed by

addition of the electrophilic alkyl halide under S_N2 reaction mechanism. Generally, the reaction could be optimised to give the desired products in good yields with high diastereoselectivities (>95 : 5 dr). While many of the reactions used KO^tBu as base in DMF, the results showed that the glycine Ni^{II} Schiff base complex required less harsh reaction conditions.



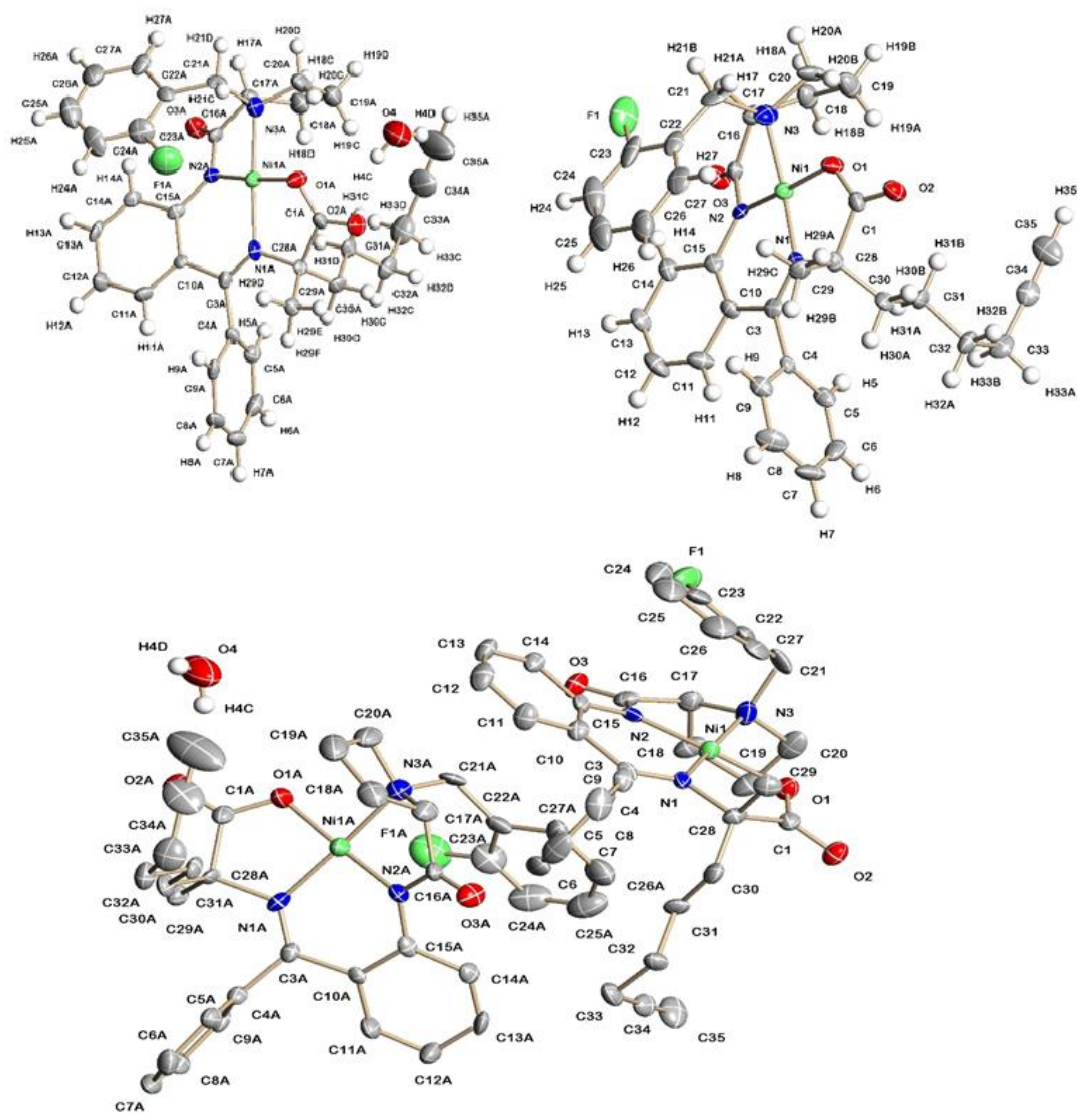
Scheme 3.8: Possibility of alkylation reaction re or si substitution

3.5.1 Alkylation of alanine Ni^{II} Schiff base complex

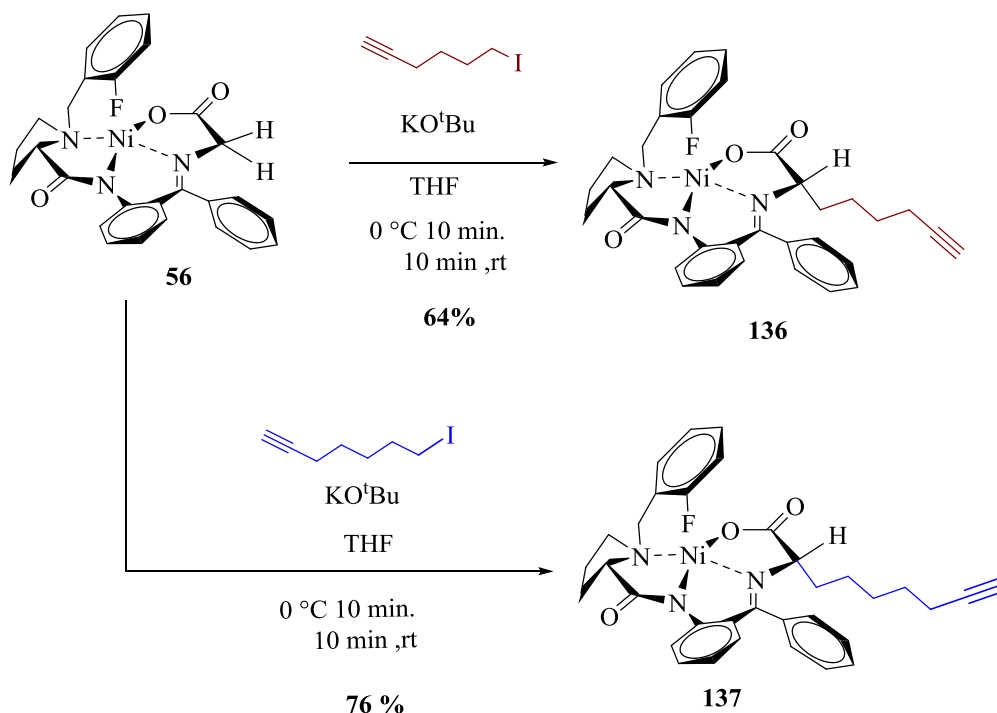


The alkylation of the alanine Ni^{II} Schiff base complex has only one possibility because the alanine already has one group substituted (Me) and has only one α -proton; so the reaction can only form an unsymmetrical α,α -di-substituted product. When it was first attempted with 4 equivalents of KO^tBu in DMF and 3 equivalents of the electrophile for 1 h at 50 °C,⁴⁸ the reaction formed both the 2*S* diastereoisomer (major) and 2*R* diastereoisomer (minor) as a mixed product. The reaction conditions were modified by increasing the time to 2h at room temperature. The reaction gave pure 2*S* diastereoisomer in a good yield.

The reaction was scaled up under the optimum conditions to 4.2 g of alanine Ni^{II} Schiff base complex with 6-iodohex-1-yne to synthesis compound with high diastereoselectivity (>99 : 1 dr) in 64 % yield. Similarly, 7-iodohept-1-yne was used to synthesis **134** under the scaled up optimum conditions using 3.5 g of the alanine Ni^{II} Schiff base complex to form the disubstituted complex in a 70 % yield and with high diastereoselectivity (>98 : 2 dr).

Figure 3.4: X-ray crystallography for the compound **134**

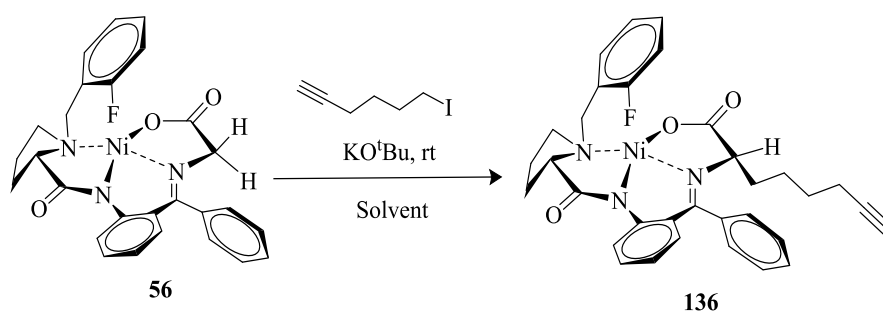
3.5.2 Alkylation of glycine Ni^{II} Schiff base complex



During the alkylation of glycine Ni^{II} Schiff base complexes there are two possibilities for substitution because there are two hydrogen atoms on the α -carbon. The reaction can be controlled, by the use of different bases with different pK_as, to form either the α -mono- or the α,α -di-substituted product. The first α -proton has pK_a 11, which can be easily deprotonated under basic conditions, whilst the second α -proton has a higher pK_a of 15.⁴⁸ When the glycine Ni^{II} Schiff base complex was first reacted under the literature conditions, 4 equivalents of KO^tBu in DMF and 3 equivalents of the 6-iodohex-1-yne (electrophile) at room temperature for 15 min,⁴⁸ the reaction gave a mixture of both α -mono- and α,α -di-substituted alkylation products. The product was shown to be a mixture (2.2:1) by ¹⁹F NMR spectroscopy. Attempts to obtain pure products from this mixture were not successful because they have nearly identical R_f values (0.19) in a EtOAc : DCM 1:1 eluent system. The main reason a mixture was obtained here is that the alkyl iodide is more reactive than the alkyl bromide used in the literature.²⁷ Decreasing the reaction time to 5 min gave a similar result (Table 3.1, Entry 2). Reducing the amounts of the electrophile to 2 equivalents and 1.2 equivalents also gave similar results (Table 3.1, Entries 3 and 4). These results are similar to those reported by Belokon and co-workers for the alkylation reaction, however they used NaH as the base and reported a 70 % yield of the bis-substituted product.⁹⁷ Changing the solvent to MeCN with 2 or 1 equivalents of the alkyl iodide gave similar results (Table 3.1, Entries 5 and 6), whilst reducing the

electrophile to 1 equivalent and the KO^tBu to 1 equivalent in MeCN gave the mono-substituted product, but in a low conversion (23 %) and with many other unknown side products which made it difficult to purify (Table 3.1, Entry 7). On changing the solvent to THF (Table 3.1, Entry 8), the amount of side products had been reduced and that the product had been formed with excellent diastereoselectivity (>90 : 10) in a good yield after a short reaction time (5min.).

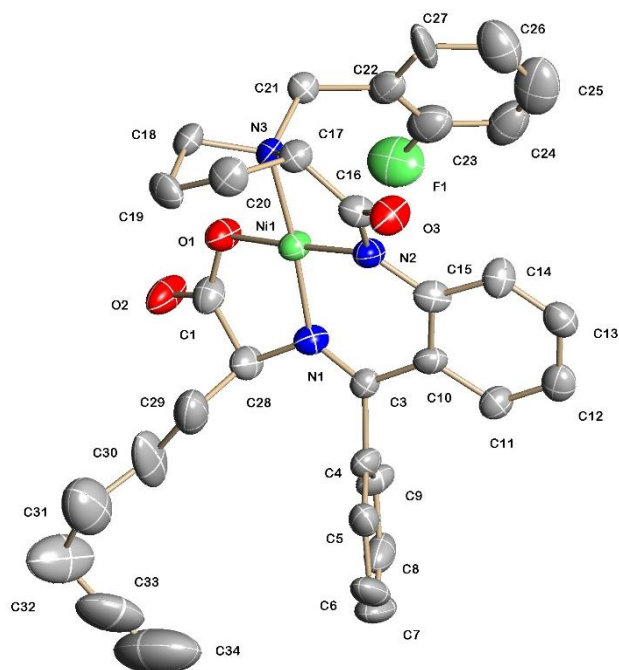
Table 3.1: Alkylation of glycine Ni^{II} complex



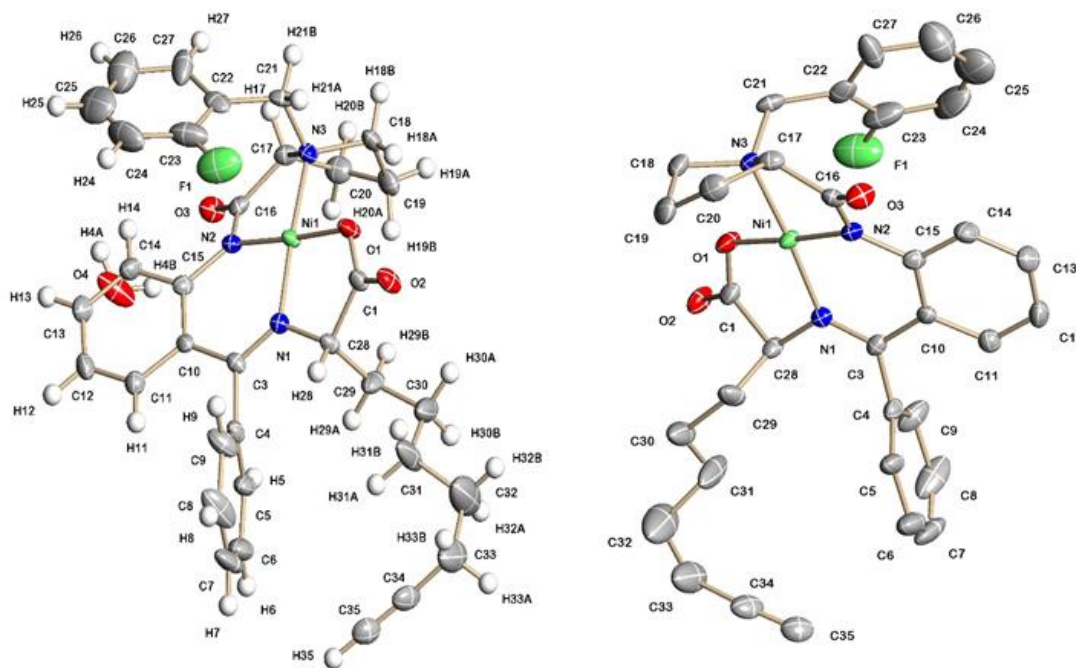
Entry	Electrophile (eq.)	KO ^t Bu(eq.)	solvent	Time (min.)	Product (S:R)
1	3	4	DMF	15	1.75: 1
2	3	4	DMF	5	2.16:1
3	2	4	DMF	5	2.2:1
4	1.2	4	DMF	5	2.1:1
5	2	4	MeCN	5	5.5:1
6	1	4	MeCN	5	6.5:1
7	1	1	MeCN	5	8.5:1
8	1	1	THF	5	51:1

The reaction was scaled up under the optimum conditions to 4 g of the glycine Ni^{II} Schiff base complex and 6-iodohex-1-yne to synthesise the mono-substituted amino acid (**136**) with high diastereoselectivity (>95 : 5 dr) in a 64 % yield. Similarly, using 0.9 equivalents of 7-iodohept-1-yne (to reduce the possibility of forming the disubstituted complex) was used to synthesis **137** under the optimum conditions on a 5 g scale.

Crystals suitable for X-ray crystallographic analysis were achieved for the compounds **134** and **135** (Figure 3.5). The solid-state structures of these compounds showed that they adopt square planar geometries related to the parent Ni^{II} complex. The Ni^{II} centres are coordinated by unsymmetrical *N, N, N, O* pincer ligands, with a distorted square planar geometry in which the Ni-X bond lengths and the bond angles are nickel are not equal.



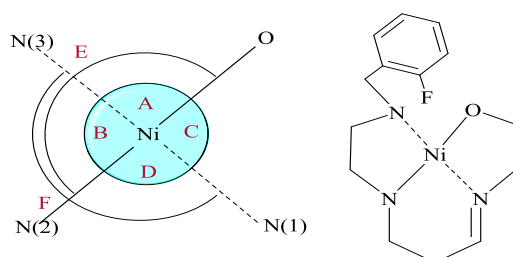
a) Solid-state structure of $\text{C}_{26}\text{H}_{28}\text{N}_3\text{O}_3$ **136**

b) Solid-state structure of C7(H) **137**Figure 3.5: X-ray crystal structures for the compounds **136** and **137**

Crystals suitable for X-ray crystallographic analysis were analysed for **134** (Figure 3.4). Selected bond lengths and bond angles for **134**, together with those for the related glycine-containing complexes **136** and **137**, are given in Table 3.2. For **134**, there are two slightly different complexes within the unit cell, but both show the nickel^{II} metal centre supported by an unsymmetrical *N, N, N, O* pincer ligand in the anticipated distorted square planar geometry. The crystallographic showed the Ni(1)-N(2), Ni(1)-N(3) and Ni(1)-O(1) bonds length are longer in complex **137** 1.848 Å, 1.941 Å and 1.857 Å respectively more than in the **134** and **136** complexes. Wilts in the **134** complex showed Ni(1)-N(1) bond length 1.872 Å, which is longer than the length bond in **136** and **137** complexes (Table 2.2), however, the bonds are between the same element and in same type of the complexes. Moreover, the angles was also different between them, complex **134** showed the largest angle in N(2)-Ni(1)-N(3) and N(2)-Ni(1)-O(1) angles 87.4(2) and 177.1(2) respectively than in the **136** and **137** complexes. Wilts complex **136** showed the largest angle in O(1)-Ni(1)-N(1) and N(2)-Ni(1)-N(1) angles 87.7(2), and 97.4(3) respectively than in the **134** and **137** complexes. While the **136** complex showed the larger angles in O(1)-Ni(1)-N(3) and N(1)-Ni(1)-N(3) 92.37(3) and 175.8(2) than **134**

and **136** complexes. The solid states for compound **134** as a dimer and the $F\cdots Ni^{II}$ showed different lengths 3.153 and 4.417 (Å).

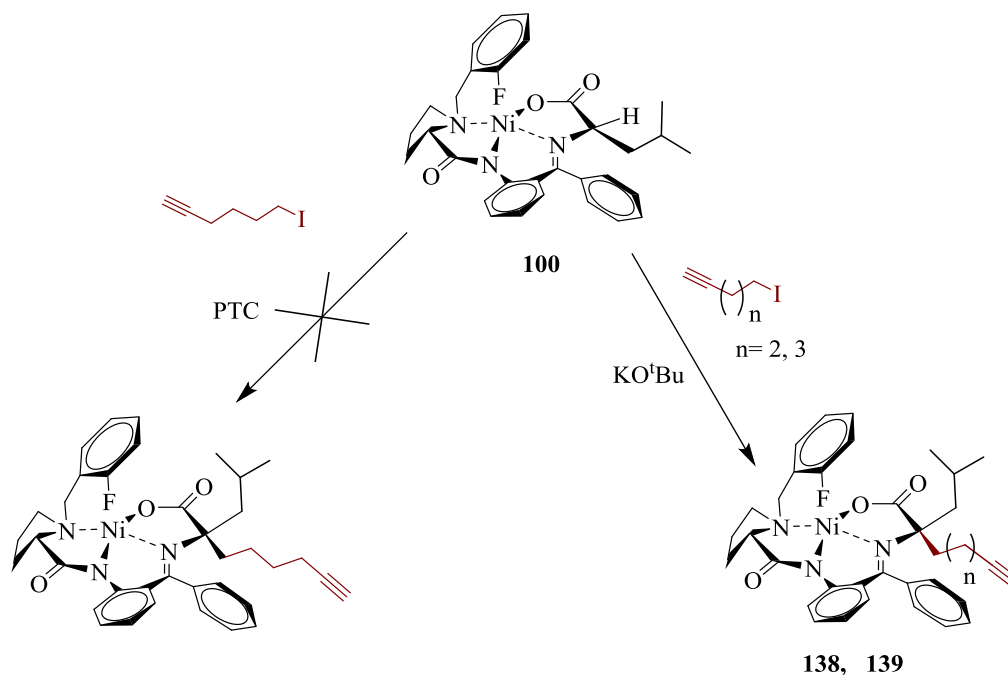
Table 3.2: Comparison between bond lengths and angles around the Ni^{II} centres for compounds **134**, **136** and **137**



Compound	Bond Lengths (Å)				
	Ni(1)-N(2)	Ni(1)-O(1)	Ni(1)-N(1)	Ni(1)-N(3)	Ni(1)...F(1)
134	1.832(5)	1.849(4)	1.872(5)	1.919(5)	4.417(6) & 3.153(6)
136	1.843(6)	1.841(5)	1.855(6)	1.942(6)	2.985(5)
137	1.848(4)	1.857(4)	1.865(4)	1.941(5)	3.023(5)

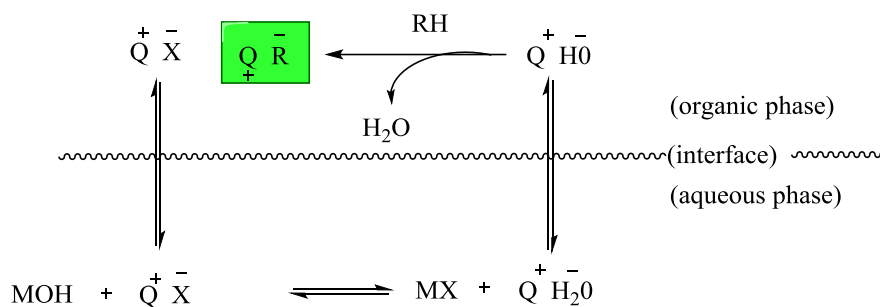
Compound	Bond Angles (°)					
	O(1)-Ni(1)-N(3) A	N(2)-Ni(1)-N(3) B	O(1)-Ni(1)-N(1) C	N(2)-Ni(1)-N(1) D	N(2)-Ni(1)-O(1) E	N(1)-Ni(1)-N(3) F
134	91.9(2)	87.4(2)	86.6(2)	94.3(2)	177.1(2)	174.8(2)
136	89.9(3)	85.8(3)	87.7(2)	97.4(3)	172.9(3)	172.5(3)
137	92.37(17)	85.77(19)	86.86(18)	95.22(19)	176.4(2)	175.8(2)

3.5.3 Alkylation of leucine Ni^{II} Schiff base complex

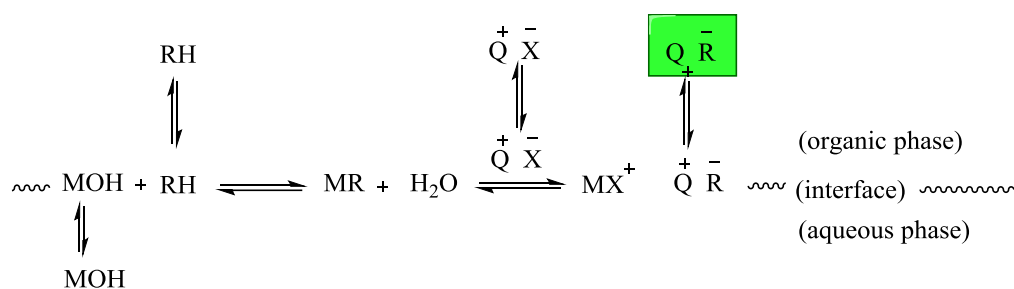


The general reaction procedure was used and also the optimum conditions were used in attempts to synthesise compound **138** by alkylation of the leucine Ni^{II} Schiff base complex using the literature conditions (4 equivalents of KO^tBu and 3 equivalents of 6-iodohex-1-yne in DMF at 50 °C) were unsuccessful (Table 3.3, Entry 10). The ¹⁹F NMR spectrum of the crude reaction product showed only unreacted starting material. Changing the solvent to dry THF under the same good conditions (Table 3.3, Entry 2), changing the temperature by increasing it to 70 °C for 2 h (Table 3.3, Entry 3) or by decreasing it to room temperature for 2 h (Table 3.3, Entry 1) or to -30 °C for 4 h or overnight (Table 3.3, Entries 4 and 5) had no impact on the reaction, with starting material identified in all cases.

Alkylation under phase-transfer catalysis (PTC) conditions is a common alternative, reaction method, first presented by Starks in 1971. In general, the reaction mechanism has been shown to proceed in two ways: Starks' extraction mechanism (Scheme 3.9, 1)¹⁵⁹ and Makosza's interfacial mechanism (Scheme 3.9, 2).¹⁶⁰



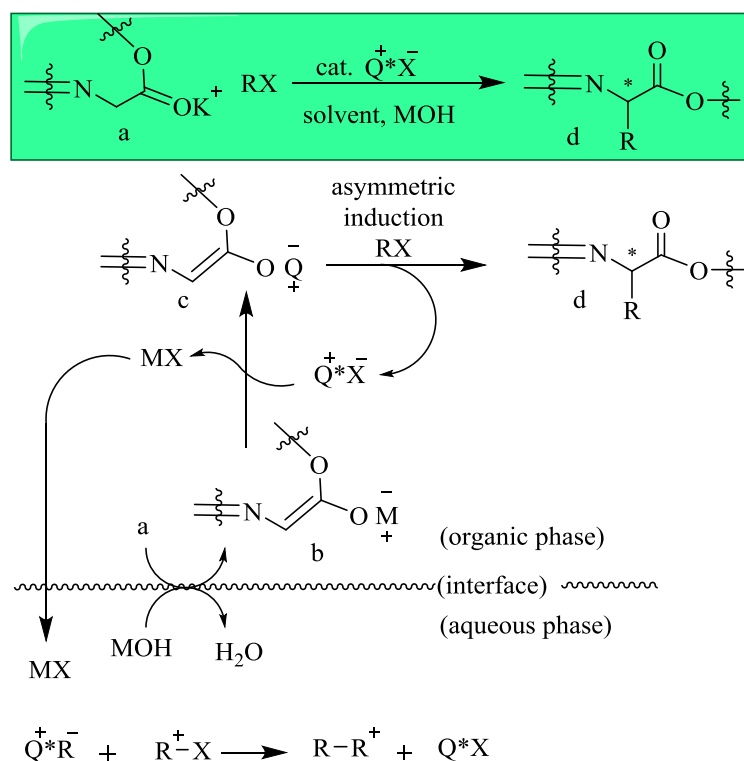
1) Starks extraction mechanism



2) Makosza interfacial mechanism

Scheme 3.9: The PTC reaction mechanism 1) Starks extraction mechanism 2) Makosza interfacial mechanism

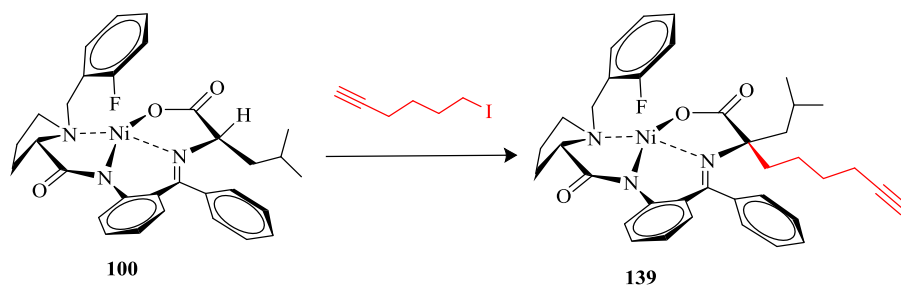
Since the previous reactions had all failed, the PTC method was attempted as an alternative approach for the alkylation of the leucine Ni^{II} Schiff base complex using the literature conditions.^{161, 162} Generally, these conditions are relatively mild and had previously led to formation of mono-alkylation products.⁹² However, here, a variety of PTC conditions were attempted in order to promote this alkylation reaction. Decreasing the reaction temperature, using tetrabutylammonium bromide (TBAB) or tetrabutylammonium fluoride (TBAF) as phase-transfer catalysts with 30 % aqueous NaOH and DCM, or increasing the reaction time, failed to give product in all cases (Table 3.3, Entries 6-9).



Scheme 3.10: Alkylation reaction leucine Ni^{II} Schiff base complex under PTC conditions (refer to Scheme 3.10 in the text)

Returning to the general conditions (3 equivalents of electrophile and 4 equivalents of base in DMF solvent) but at low temperature (0-5 °C) (Table 3.3, Entry 11) was also unsuccessful. Reducing the temperature further to -30 °C and leaving the reaction at this temperature for much longer (48 h) finally generated the desired product. Analysis by ¹⁹F NMR and ¹H NMR spectroscopy showed the crude product to be 1: 1 mixture of diastereomers in a 56 % conversion. On scaling the reaction up to a 1 g scale, the yield was increased to 66 %. The ¹⁹F NMR spectrum showed two peaks for the crude diastereomeric mixture: *S, S* (-133.9): *S, R* (-113.7) in a 2.9 : 1 ratio. Unfortunately, these diastereomers could not be separated by flash column chromatography.

Table 3.3: Alkylation of leucine Ni^{II} Schiff base complex with 6-iodohex-1-yne

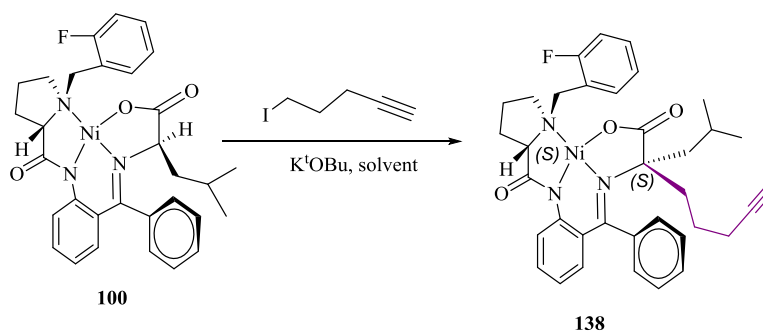


Entry	Electrophile (eq.)	Base (eq.)	solvent	Time (h)	Temperature (°C)	Outcome
1	3	(4) KO ^t Bu	THF		rt	n/r
2	3	(4) KO ^t Bu	THF	2	50	n/r
3	3	(4) KO ^t Bu	THF	2	70	n/r
4	3	(4) KO ^t Bu	THF	4	-30	n/r
5	3	(4) KO ^t Bu	THF	18	-30	n/r
6	3	(1)TBAI, NaOH 30 % in 5 ml,	DCM/ H ₂ O	4	rt	n/r
7	3	(1)TBAI, NaOH 30 % in 5 ml	DCM/ H ₂ O	4	50	n/r
8	3	(1)TBAI, NaOH 30 % in 5 ml	DCM/ H ₂ O	18	50	n/r

9	3	(0.25)TBAF NaOH 30 % in 5 ml	DCM/ H ₂ O	4	-30	n/r
10	3	(4) KO ^t Bu	DMF	1	50	n/r
11	3	(4) KO ^t Bu	DMF	3	0-5	n/r
12	3	(4) KO ^t Bu	DMF	4	-30	n/r
13	3	(4) KO ^t Bu	DMF	18	-30	n/r
14	3	(4) KO ^t Bu	DMF	24	-30	n/r
15	3	(4) KO ^t Bu	DMF	48	-30	56 %
Scale up to 1g	3	(4) KO ^t Bu	DMF	48	-30	66 %

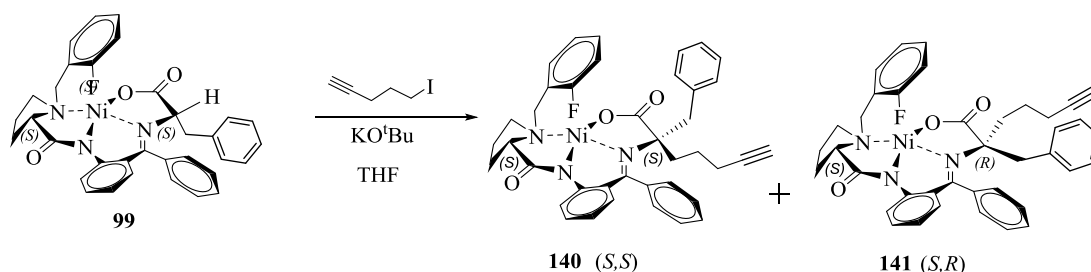
Changing the electrophile to 5-iodopent-1-yne using DMF at -30 °C for 48 h allowed the desired product to be formed, but again as a crude diastereomeric mixture. Again, purification by flash column chromatography was unsuccessful but a small amount could be purified using the Biotage instrument. The two separated products were not pure but one had an 11.8:1 ratio of the *S, S* : *S, R* diastereomers whilst the second has a 6.2:1 ratio of the *S, R* : *S, S* diastereomers from ¹⁹F NMR spectroscopy. The overall yield of the products was 66 % when carried out on a 1 g scale.

Table 3.4: Alkylation reaction for the leucine complex under different conditions



Entry	solvent	Time (h)	Outcome
1	DCM	24	n/r
2	DCM	48	n/r
3	DMF	24	n/r
4	DMF	48	66 %

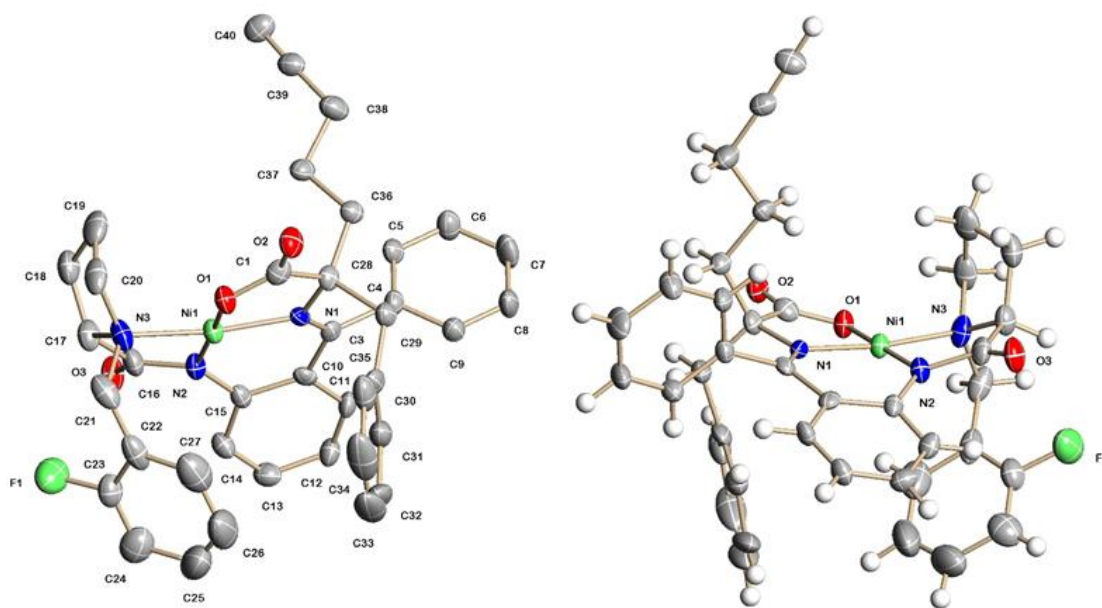
3.5.4 Alkylation of phenylalanine Ni^{II} Schiff base complex



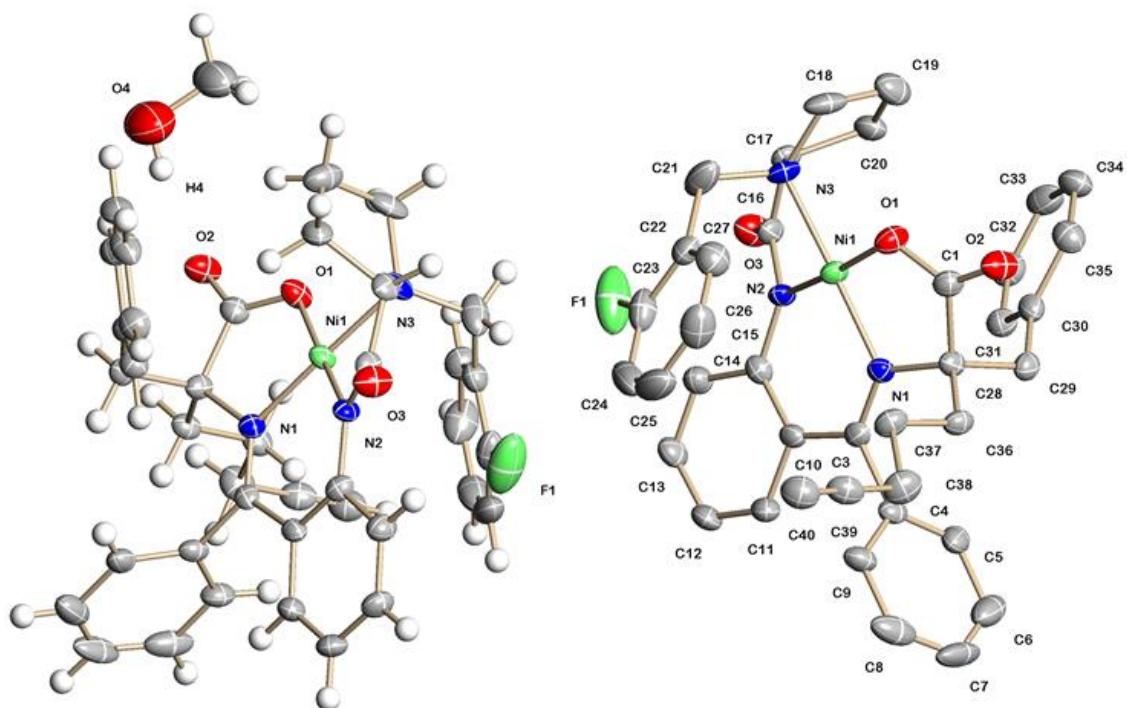
The general reaction procedure was used successfully in this alkylation reaction under the same reaction conditions used previously (4 equivalents of KO^tBu and 3 equivalents of 6-iodohex-1-yne in DMF at 50 °C) to synthesis compound **140** on a 1 g (of the phenylalanine complex starting material) scale. The product was obtained in a good yield (80 %) but with poor diastereoselectivity. The ¹⁹F NMR spectrum showed the diastereomers in a 1.8 : 1 ratio of the *S*, *S* (-114.6 ppm): *S*, *R* (-113.8 ppm). The main reason for getting a mixture results from the steric hindrance of the benzyl group of the amino acid which looks like one hand of the main rotor blade of a helicopter. However, purification could not be achieved by column chromatography but the product was purified using the Biotage instrument (EtOAc/DCM 1:1) to give the product **140**, in a 68 % yield as a reddish-orange solid as the pure *S*, *S* diastereomer (-114.6 ppm) by ¹⁹F NMR

spectroscopy. Moreover, the ^{19}F NMR spectrum of the residue showed a mixture of diastereomers, although the majority was the *S, R* diastereomer.

The formation of crystals suitable for X-ray crystallographic studies was achieved for both the purified *S,S* diastereomer of **140** and from the residue after separation of the *S,R* diastereomer of **140** (Figure 3.6). These solid states structures of *S,S* **140** and *S,R* **141** diastereomers showed the expected Ni^{II} centre supported by an unsymmetrical *N, N, N, O* pincer ligand in a distorted square planar geometry. The bond lengths and bond angles around the Ni centres for both crystals were very similar, showing on minor differences, which might be expected since the complexes are the same with only different chiral centres at the α -carbon only (Table 3.5). However, the crystal structure showed significant differences in the non-bonding $\text{F}\cdots\text{Ni}$ distances arising from the configurational differences between the diastereomers.



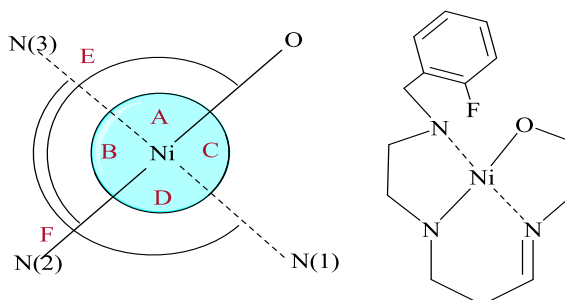
a) Solid-state structure of **140** (*S,S*)



b) Solid-state structure of 141 (*S,R*)

Figure 3.6: Single crystal X-ray structures for showing a) (*S,S*) **140** and b) (*S,R*) **141** configurations

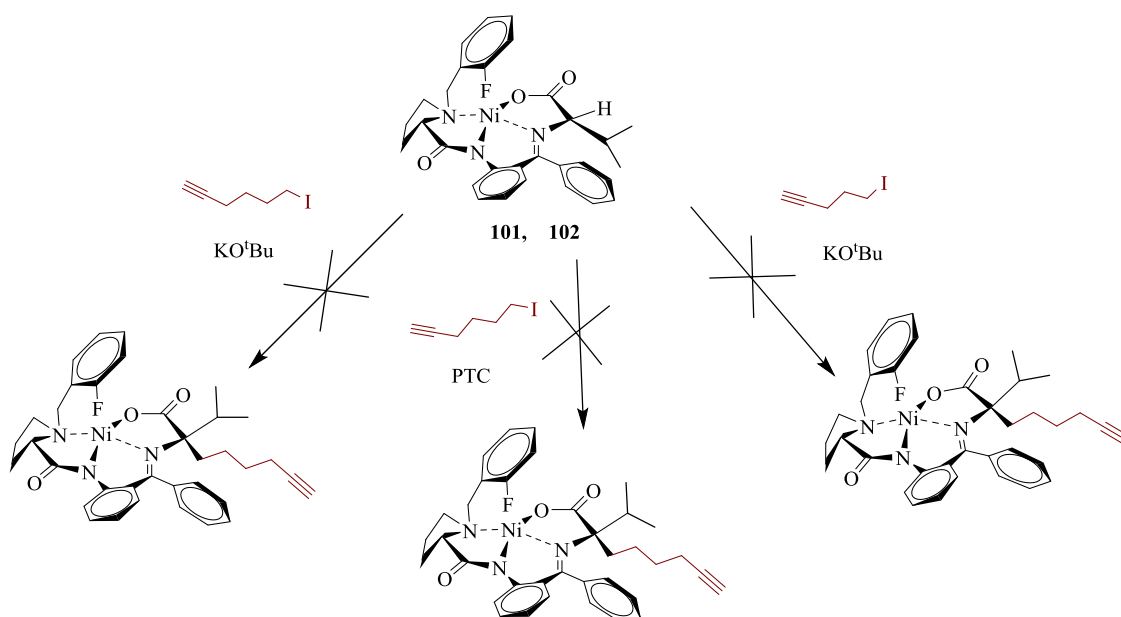
Table 3.5: Comparison of bonds length and the angles around the Ni^{II} centres between the a) (*S,S*) **140** and b) (*S,R*) **141** configurations for **140**



Compound	Bond Lengths (Å)				
	Ni(1)-N(2)	Ni(1)-O(1)	Ni(1)-N(1)	Ni(1)-N(3)	Ni(1)...F(1)
140 (<i>S,S</i>)	1.833(4)	1.847(4)	1.879(4)	1.952(4)	4.612
141 (<i>S,R</i>)	1.844(3)	1.838(3)	1.878(3)	1.946(3)	3.881

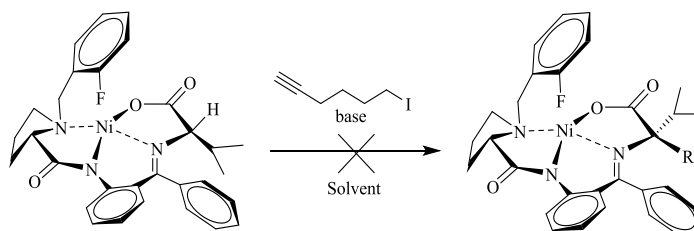
Compound	Bond Angles (o)					
	O(1)- Ni(1)-N(3) A	N(2)- Ni(1)-N(3) B	O(1)- Ni(1)- N(1) C	N(2)- Ni(1)- N(1) D	N(2)- Ni(1)- O(1) E	N(1)- Ni(1)- N(3) F
140 (<i>S,S</i>)	89.34(18)	86.93(19)	87.61(17)	96.39(19)	175.47 (18)	172.83 (19)
141 (<i>S,R</i>)	91.47(13)	84.62(14)	87.73(13)	96.42(13)	173.06 (14)	177.49 (14)

3.5.5 Alkylation of valine Ni^{II} Schiff base complex



The general reaction procedure was followed in this alkylation reaction under the same reactions conditions to synthesise new valine derivatives. All the reactions were monitored by ¹⁹F NMR spectroscopy, TLC and mass spectroscopy. Unfortunately, all of the reaction conditions failed to yield alkylated products. This included (Table 3.6): reactions at room temperature for 1 h and 2 h; increasing the reaction temperature to 50 °C for 2 h; decreasing the reaction temperature to 0 °C for 2 h; changing the solvent to dry THF and repeat the other conditions that were used in the previous entries: the PTC method under the literature conditions;^{161, 162} PTC using tetrabutylammonium bromide (TBAB) or tetrabutylammonium fluoride (TBAF) as catalysts for 1, 2, 3 and 4 h; PTC using tetrabutylammonium bromide (TBAB) at room temperature for 1 2, 3 and 4 hrs; changing the electrophile from 6-iodohex-1-yne to 1-(bromomethyl)-4-(trifluoromethyl)benzene for 1, 2 and 3 h. Unfortunately, all the reactions to obtain valine Ni^{II} complex (*S*) derivatives under 27 different sets of conditions were unsuccessful. Lastly, changing the complex from the valine Ni^{II} complex (*S*) to the valine Ni^{II} complex (*R*) as a final alternative was investigated. The reaction mixture was heated for 2 h at 50 °C, but again this reaction was unsuccessful. Hence, all the reaction conditions showed that it is too hard to alkylate, under either PTC conditions or in dry solvents, either the valine Ni^{II} complex (*S*) or the valine Ni^{II} complex (*R*), using either alkyl bromides or alkyl iodides as electrophiles.

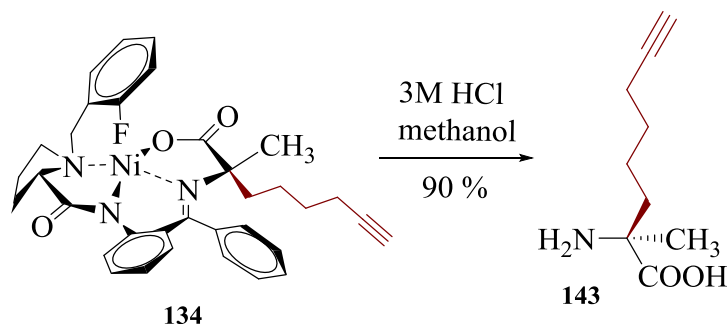
Table 3.6: Alkylation reaction with valine complex in different condition



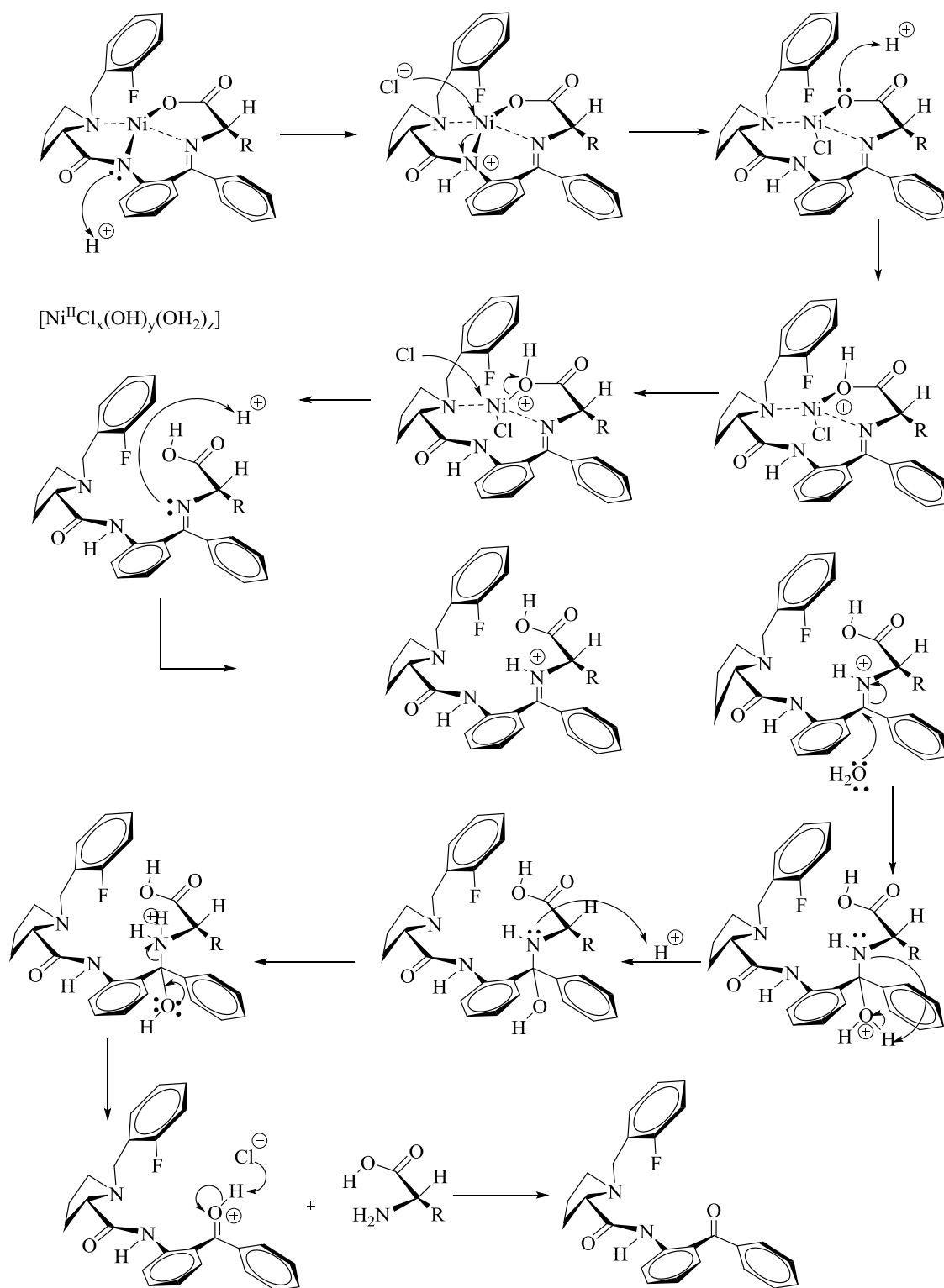
Entry	Base (4 eq.)	solvent	Time(h)	Temp.(°C)
1	KO ^t Bu	DMF	1	rt
2	KO ^t Bu	DMF	2	rt
3	KO ^t Bu	DMF	1	50
4	KO ^t Bu	DMF	2	50
5	KO ^t Bu	DMF	1	0
6	KO ^t Bu	DMF	2	0
7	KO ^t Bu	THF	1	rt
8	KO ^t Bu	THF	2	rt
9	KO ^t Bu	THF	1	50
10	KO ^t Bu	THF	2	50
11	KO ^t Bu	THF	1	0
12	KO ^t Bu	THF	2	0
13	(0.25) TBAF NaOH 30 % in 5 ml	DCM/H ₂ O	1	rt
14	(0.25) TBAF NaOH 30 % in 5 ml	DCM/H ₂ O	2	rt
15	(0.25) TBAF NaOH 30 % in 5 ml	DCM/H ₂ O	3	rt
16	(0.25) TBAF NaOH 30 % in 5 ml	DCM/H ₂ O	4	rt
17	(1 eq)TBAI, NaOH 30 % in 5 ml	DCM/H ₂ O	1	rt
18	(1 eq)TBAI, NaOH 30 % in 5 ml	DCM/H ₂ O	2	rt
19	(1 eq)TBAI, NaOH 30 % in 5 ml	DCM/H ₂ O	3	rt
20	(1 eq)TBAI, NaOH 30 % in 5 ml	DCM/H ₂ O	4	rt
21	(1 eq)TBAI, NaOH 30 % in 5 ml	DCM/H ₂ O	4	50
22	(1 eq)TBAI, NaOH 30 % in 5 ml	DCM/H ₂ O	18	50
valine complex(R)				
23	KO ^t Bu	DMF	2	50

3.6 Hydrolysis or decomplexation of Ni^{II} Schiff base complexes

3.6.1 Acidification hydrolysis



Generally, the Ni^{II} Schiff base complexes are stable under base conditions and, vice versa, they are decomposed under moderately strong acids such as 1-6 N HCl.^{163, 164} These properties are significant factors for the creation of new amino acids via substitution reactions under base conditions, such as alkylation, Aldol reaction and Mannich reaction. The second step in this sequence is hydrolysis of the complexes to release the newly formed amino acids; the side product is the ligand that can be re-used again. Mostly researchers achieve the hydrolysis of the complexes in acidic conditions, such as HCl in methanol heated to reflux for 30-60 min (Scheme 3.11). Here, a literature route to decomplexation has been followed.^{48, 165} After hydrolysis, the ligand was removed from the crude product by extraction three times with DCM. The most difficult step was the separation of the aqueous layer mixture of components; these include the new amino acid and Ni^{II} salts. The mixture was separated with an ion-exchange column used Dowex 50WX2 200 H⁺ resin and used specific eluents 20 % NH₄OH–EtOH (1:1 (v/v)) as a liquid carrier (base eluent) to purify the amino acid and leave behind the NiCl₂ salt on the column. Generally, this method is cheap but it includes several steps in the workup to obtain pure amino acids.

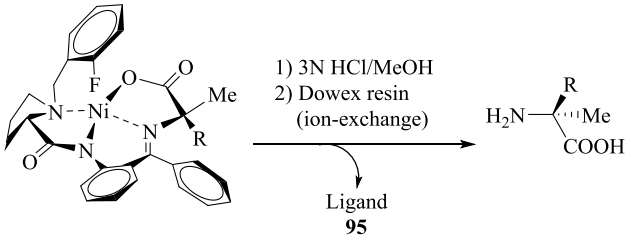
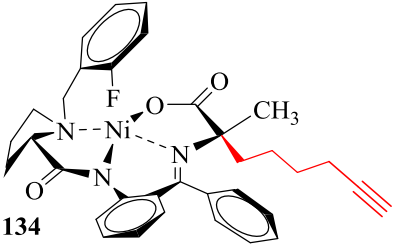
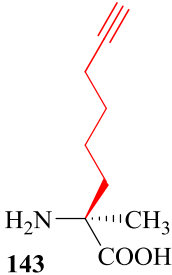
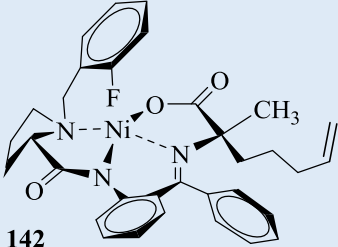
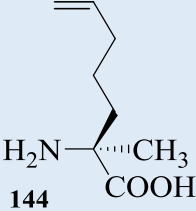


Scheme 3.11: Hydrolysis of the complexes under acid conditions

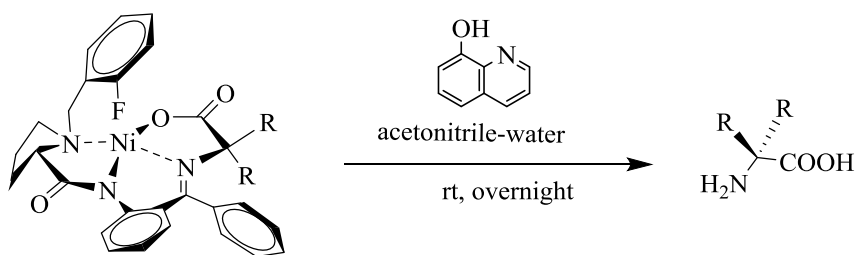
Compound **134** was decomplexed under acidic conditions using HCl in methanol. The red colour of the starting material changed to green during heating at reflux for 20-30 min, but the heating was continued for up to 1 h to ensure that all of the complex had

decomplexed. The methanol was removed by evaporation leaving aqueous solution. The ligand was removed by extraction with DCM. The aqueous layer was purified by column chromatography with ion-exchange resin. Before attempting the separation, the resin was washed with water: ethanol (1:1) which was checked with litmus paper until the pH reached 7. The amino acid was purified with base eluents 20 % NH_4OH –EtOH (1:1 (v/v)). The pure fractions were collected and the solvent evaporated under high vacuum. The identity of the product was determined by mass spectrometry and ^1H NMR spectroscopy. Compound **143** was obtained and purified in an 84 % yield after ion-exchange and freeze dried. It is important to keep the product in the fridge because the new amino acid is unstable at room temperature. The same procedure was used to de-complex compound **142** to produce compound **144** in a 63 % yield.

Table 3.7: Hydrolysis of the complexes under acid conditions

			
Entry	Starting material (alanine NiII complex)	Product	Yield (%)
1	 134	 143	84
2	 142	 144	63

3.6.2 Hydrolysis of the complexes under neutral conditions (chelation)



During this research, another method, published in a patent,^{166, 167} was seen as an alternative approach to the decomplexations using HCl by the use of 8-hydroxyquinoline as a chelator. There are many organic compounds that can be used for chelation to nickel, such as tartaric acid, oxalic acid, EDTA, acetylacetone and 8-hydroxyquinoline. The patent showed that 8-hydroxyquinoline is the most effective for the hydrolysis of the Ni^{II} Schiff base complexes. Using this method would decrease the number of steps required for the workup in the previous method (hydrolysis under acidic conditions). Furthermore, the patent showed that an excess of 2 equivalents of the chelator were required to hydrolyse the Ni^{II} complexes at room temperature. The procedure was modified by increasing the amount of 8-hydroxyquinoline to three equivalents, the time to 24 h and the temperature to 30 °C (**Error! Reference source not found.**). The reaction was monitored by ¹⁹F NMR throw convert the complex to the ligand peak at $\delta -117.6$ (s). After the 24 h the reaction mixture was extracted with DCM, EtOAc and diethyl ether respectively. The combined organic layers were collected and the solvents removed *in vacuo*. The residue included the ligand and the Ni^{II} salt as a bis-hydroquinoline, [Ni(hydroquinoline)₂], which was purified by column chromatography to re-use the ligand. The aqueous layer was dried by freeze drying to obtain the pure amino acid which made the purification simpler than that by the acidic hydrolysis method.

Table 3.8: Hydrolysis of the complexes under mild conditions

<p>8-hydroxyquinoline</p> <p>MeCN/ H₂O</p> <p>30 °C, 24 h</p> <p>Ligand 95</p>			
Entry	Starting material (Ni(III) complex)	Product	Yielda (%)
1	<p>136</p>	<p>145</p>	84
2	<p>135</p>	<p>146</p>	73
3	<p>137</p>	<p>147</p>	75
4	<p>140</p>	<p>148</p>	80

In entry 1 after the decomposition of compound **136** and extraction, the ^{19}F NMR spectrum of the aqueous layer did not show any fluorine peak whilst the organic layer had a single peak associated with the *S*-ligand **95**. (*S*)-2-aminooct-7-ynoic acid **145**, isolated from the aqueous phase, was obtained as a white powder in 84 % yield. The identity of the amino acid **145** was determined by the ^1H NMR and ^{13}C NMR spectroscopies, LC-MS mass spectrometry and the HRMS-ESI mass spectrum.

In entry 2, compound **146** was formed from the decomposition of **135**. (*S*)-2-amino-2-methylnon-8-ynoic acid **146** was obtained as a white powder in 73 % yield. The ^1H NMR, ^{13}C NMR and the spectrum. LC-MS demonstrated the purity of the product and the HRMS-ESI mass spectrum had a parent ion at 184.1339.

(*S*)-2-aminonon-8-ynoic acid **147** (Entry 3) was obtained as a white powder in a 75 % yield from compound **137** by hydrolysis under the same conditions. The new amino acid was identified by the ^1H NMR and ^{13}C NMR spectroscopies, and the LC-MS and HRMS-ESI mass spectrometry showing a parent ion peak at 170.1178.

On hydrolysis of (*S*)-({2-[1-(2-fluorobenzyl)benzyl]pyrrolidine-2-carboxamide]-phenyl}phenylmethylene)-(*S*)-1-pentyl-leucinato-*N,N,N',O*}nickel^(II) **140** (Entry 4) the amino acid (*S*)-2-amino-2-benzylhept-6-ynoic acid **148** was generated. The product was analysed via The ^1H NMR and ^{13}C NMR spectroscopies, The new amino acid was also identified by LC-MS and HRMS-ESI mass spectrometry with a parent ion at 232.1342.

3.7 Protection of Amino acids

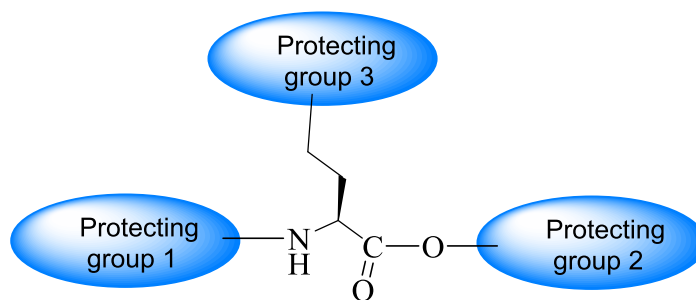


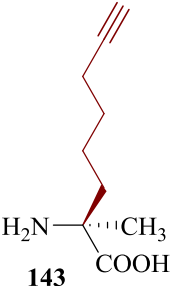
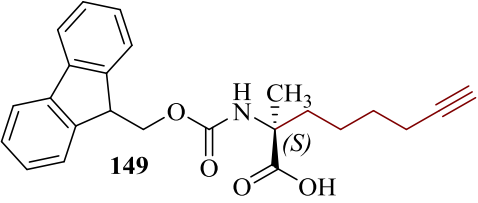
Figure 3.7: General protecting groups for amino acids for using in SPPS

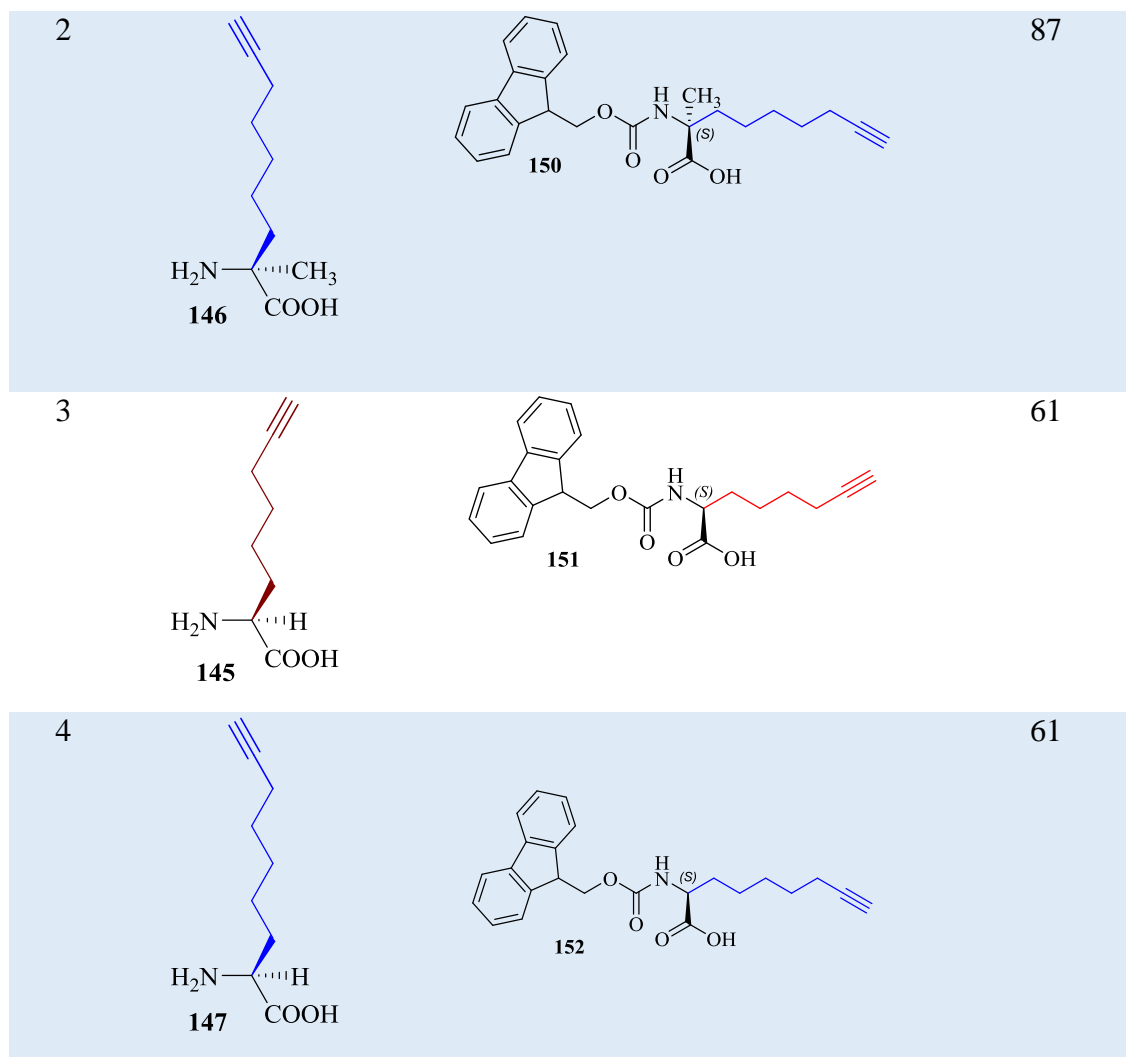
Generally, amino acids have three active groups, two (carboxylic acid and amine) of which need to be protected to become ready for peptide synthesis (Figure 3.7). The main purpose for these protections is to force the reaction in the SPPS synthesis to only have

one reaction with the resin. Protecting group three is used when the amino acid has an active group in side chain such as hydroxyl, amine or carboxylic group. The second group of protection (such as methyl, t-butyl or benzyl) is used when the resin used in the SPPS has a carboxylic group free to react with the amine group of the amino acid in the coupling reaction. The first group of protection is used when the resin (Rinke resin) has a free amine group, which reacts with the free carboxylic acid in the coupling reaction, and include groups such as t-butyl carbamate (Boc), benzyl carbamate (Cbz) and 9-fluorenylmethyl carbamate (Fmoc). In this work, Fmoc will be used to protect the amine group in the new amino acids for many reasons;

- (i) The resin to be used in SPPS is Rinke amide.
- (ii) All the reactions in the peptide synthesis were carried out under acidic conditions
- (iii) Fmoc is easy to remove, as necessary, under mild basic conditions.

Table 3.9: General procedure for Fmoc protection of amino acids

$ \begin{array}{c} \text{R}_1 \\ \\ \text{H}_2\text{N}-\text{C}-\text{R} \\ \\ \text{COOH} \end{array} \xrightarrow[\text{H}_2\text{O, Dioxane, 24h at 30 }^\circ\text{C}]{\text{Fmoc-OSu, potassium carbonate}} \begin{array}{c} \text{R}_1 \\ \\ \text{FmocHN}-\text{C}-\text{R} \\ \\ \text{COOH} \end{array} + \text{H}-\text{O}-\text{N} \begin{array}{c} \diagup \diagdown \\ \text{O} \quad \text{O} \end{array} $			
Entry	amino acid	Product(Fmoc-AA)	Yield(%)
1	 <p>143</p>	 <p>149</p>	50



The new amino acids prepared in this work were reacted under basic conditions with Fmoc-OSu N-(9H-Fluoren-9-ylmethoxycarbonyloxy)succinimide, one of Fmoc reagents. In general, the reaction results in the protection of the amine group with production of *N*-hydroxy-succinimide as a side-product. An excess of Fmoc-OSu was used in the reactions to promote them and to increase the conversion to the desired products. The reactions were monitored with TLC using ninhydrin as a stain. At the end of the reaction, the mixture was extracted with ethylacetate to remove the excess of Fmoc-OSu and the side product as the Fmoc-amino acids are more soluble in water as salts. Then, the aqueous layer was acidified to pH = 1 to regenerate the Fmoc-amino acids which were extracted with ethylacetate three times. The resulting Fmoc-amino acids were fully characterised with LC-MS, and ^1H NMR and ^{13}C NMR spectroscopies, and also tested negative with ninhydrin indicator.

(*S*)-2-amino-2-methylnon-8-ynoic acid **143**, entry 1 (Table 3.9), was also reacted under the same conditions to give (*S*)-2-((((9H-fluoren-9-yl)methoxy)carbonyl)amino)-2-methyloct-7-ynoic acid **149** as a white powder in a 50 % yield. This new Fmoc-amino acid **149** was identified similarly by LC-MS and HRMS-ESI. Furthermore, on HPLC only one peak was observed: (OD-H column, hexane (50 %)-iPrOH isocratic +0.1 % AcOH): 5.55 min.

In entry 2, (*S*)-2-((((9H-fluoren-9-yl)methoxy)carbonyl)amino)-2-methylnon-8-ynoic acid **150** was obtained, from reaction of (*S*)-2-amino-2-methylnon-8-ynoic acid **146** under the same, as a white powder in a 61 % yield. The new Fmoc-amino acid **150** was also identified by LC-MS and HRMS-ESI. Furthermore, on HPLC only one peak was observed: (OD-H column, hexane (50 %)-iPrOH isocratic +0.1 % AcOH): 5.58 min.

(*S*)-2-Aminooct-7-ynoic acid **145** Entry 3, was reacted under the same conditions to produce (*S*)-2-((((9H-fluoren-9-yl)methoxy)carbonyl)amino)oct-7-ynoic acid **151** as a white powder in a 70 % yield. The new Fmoc-amino acid **151** was also identified by LC-MS and HRMS-ESI. Furthermore, on HPLC only one peak was observed: (OD-H column, hexane (50 %)-iPrOH isocratic +0.1 % AcOH): 6.43 min.

In entry 4, (*S*)-2-((((9H-fluoren-9-yl)methoxy)carbonyl)amino)non-8-ynoic acid **152** was obtained from reaction of (*S*)-2-aminonon-8-ynoic acid **147** as a viscous colourless oil in a 87 % yield. In the ¹H NMR spectrum, multiple peaks for 8H are assigned to the aromatic CH, and the ¹³C NMR spectrum show the expected number of related peaks for aromatic carbon. The new Fmoc-amino acid **152** was also identified by LC-MS and HRMS-ESI. Furthermore, on HPLC only one peak was observed: (OD-H column, hexane (50 %)-iPrOH isocratic +0.1 % AcOH) in 6.27 min.

3.8 Conclusions

Three iodo-alkynes have been used in this work. 7-Iodohept-1-yne has been prepared by two methods: As a crude product, in three steps, by method A, but, unfortunately, the yield was poor. Method B was used as an alternative, to give 7-iodohept-1-yne in good yield and high purity in three reaction steps (alkyne zipper reaction; Conversion of the hydroxyl group to a good leaving group: Finkelstein reaction). 5-Iodopent-1-yne was synthesised in one step via a Finkelstein reaction. 6-Iodohex-1-yne was commercially available.

The new Ni^{II} Schiff base complexes **134-152** have been synthesised by alkylation reactions of Ni^{II} Schiff base complexes described in Chapter 2 (containing glycine, alanine, valine, and leucine and phenylalanine amino acids). The alkylation of the alanine Ni^{II} Schiff base complex **55** was successful following the Jamieson group procedure,⁴⁸ using alkyl iodides instead of alkyl bromides, to give the desired products in great yields and high diastereoselectivity. Compound **134** was formed by alkylation with 6-iodohex-1-yne whilst 7-iodohept-1-yne was used in the synthesis of **135**.

However, these reaction conditions were unsuccessful for the alkylation of the other Ni^{II} Schiff base complexes. The method was modified for reaction of the glycine Ni^{II} Schiff base complex **56** by changing the solvent from DMF to THF, using just one equivalent of the base (KO^tBu) and one equivalent of the alkyne iodide for 5 min at room temperature to synthesise the mono-substituted compounds **136**, on reaction with 6-iodohex-1-yne, and **137**, on reaction with 7-iodohept-1-yne.

Compound **139** was synthesised by reaction of the phenylalanine Ni^{II} Schiff base complex with 5-iodopent-1-yne under these new conditions in good yield and with high diastereoselectivity. Unfortunately, compounds **138** and **139**, which were synthesised by reacting the leucine Ni^{II} Schiff base complex with 5-iodopent-1-yne and 6-iodohex-1-yne respectively, had low diastereoisomers. Finally, the valine Ni^{II} Schiff base complex **101** is unsuitable for these alkylation reactions, presumably because of steric hindrance of the two methyl groups.

Two methods for the de-complexation of the Ni^{II} Schiff base complexes to generate new amino acids have been investigated.

A) Hydrolysis of the complexes under acid conditions.

B) Hydrolysis of the complexes under neutral conditions (chelation).

Both methods were good, but the second had an easier work up to obtain the amino acids. However, the diastereoisomeric products could interconvert if the products were heated to reflux for a long time under acid conditions. Compounds **143** and **144** were obtained by method (A) with good yields and high diastereoselectivities, whilst compounds **137**, **145-147** were obtained via method (B).

Protection of the amino acids **149-152** were achieved by reaction with N-(9-fluorenylmethoxycarbonyloxy) succinimide under base conditions (potassium carbonate), since a Rinke amide resin is going to be used for peptide synthesis, to find the best 1,3-diyne staple peptides, using the SPPS method in Chapter 5. The peptide syntheses will be done under acidic conditions and the Fmoc protection group is straightforward to remove under mild basic conditions.

Chapter 4

Synthesis of Fluorinated Aromatic Amino Acids via Schiff Base Ni^{II} Complexes



UNIVERSITY OF
LEICESTER

4.1 Introduction

Drug candidates containing the element fluorine have become one of the most common categories of industrial pharmaceutical. This small halogen, with the highest electronegativity in the periodic table, has a remarkable impact on the chemical reactivity and physical properties of organic molecules, especially in terms of their metabolic stability, binding affinity and particular physicochemical properties. There have been various reviews published in latest few years on the new fluorine-containing pharmaceutical compounds, which have impact on different therapeutic modes (activate or inhibit the activities).^{65, 168-170} The inclusion of fluorine can result in highly stable intermolecular interactions (hydrogen bond) whilst the carbon-fluorine displays increased lipophilicity compared to that of the carbon-hydrogen bond, both of which impact upon their physicochemical characteristics. The main significant advantages from substituting fluorine atom(s) in the medicines (peptides) are enhanced metabolic stability, improved physicochemical properties and altered binding affinities.⁶⁵

Metabolic solubility is another significant factor affecting drug discovery. Substituting fluorine into organic compounds increases the polarity of the compounds. In general, the halogen increases any dipole moment due to its electronegativity, which leads to an increase in polarity. Alternatively, fluorine has been used as a label in compounds to show the purity, or follow metabolic pathways, including rates, routes or extent of the metabolism of the medicine. In 1954, the U.S. Food and Drug Administration (FDA) presented the first steroid containing a fluorine moiety, which was approved as a new type of medicine, (9 α -fluorohydrocortisone acetate) (Figure 4.1).¹⁷¹

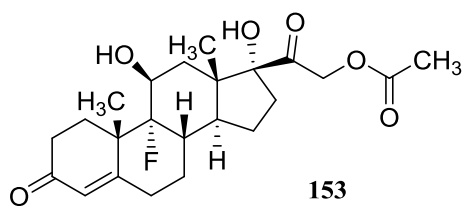


Figure 4.1: Structure of 9 α -fluorohydrocortisone acetate

Also, fluorine has become a common component in protein design with the creation of non-natural fluorinated amino acids. The design of new fluorinated amino acids is intended to increase the stability of the peptides. In general, hydrophobic amino acids that include fluorine atom(s) will change the stability and functionality of the protein

structure. The solubility of the proteins influenced the polar side chain residues of the amino acids, which will have an effect on the types of methods used to separate them from other proteins, with non-polar residues, during purification. Hydrogen bonds are among the strongest intermolecular interactions, because of the large difference in the electronegativities of the atoms. Hydrophobicity affects both entropic (ΔS) and the Gibbs free energy (ΔG) of a system.

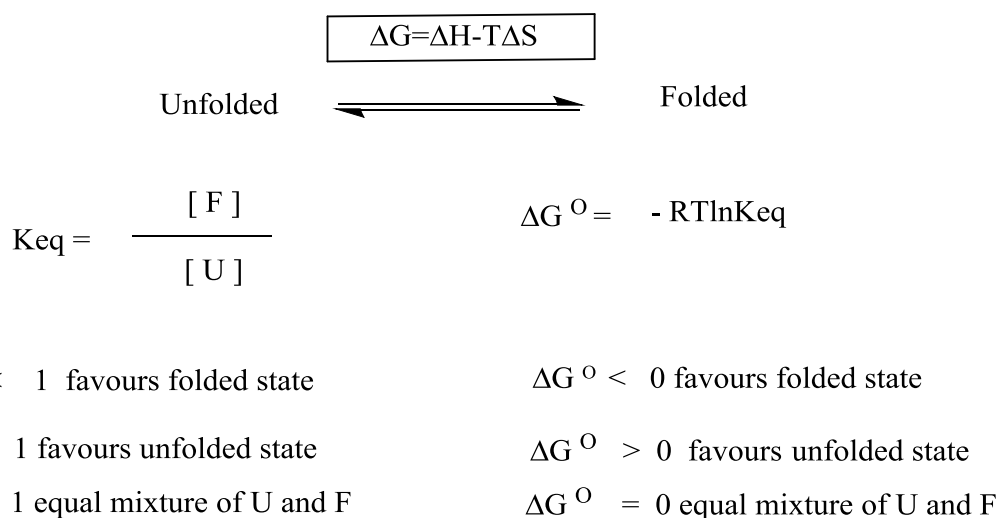


Figure 4.2: Gibbs equation for folded and unfolded proteins

The Gibbs free energy (Figure 4.2) of folding becomes more favourable as the hydrophobicity of the protein increase. The surface area of the hydrophobic residues results in spontaneous folding. Fluorinated side chains amino acids generally increase the stability of the folded structure and, as a result, increase the thermodynamic stability of the protein.^{73, 172} In general, an aliphatic side chain has a lower hydrophobicity than an aromatic side chain. When the aromatic side chain has mono-, di- or tri-fluorination(s) dipole-dipole moment interactions inside the protein increase, and also there is a greater tendency to form hydrogen bonds, and thus the proteins favour the folded conformation to achieve greater stability.¹⁷³⁻¹⁷⁵

Another area in which fluorinated organic compounds are being used is to decrease the pKa of organic compounds such as trifluoroacetic acid (TFA) (strong acid), where pKa decreases with increasing numbers of fluorine atoms.¹³⁵ In addition, this phenomenon can also be seen in alcohols and amines (Figure 4.3).¹⁷⁶

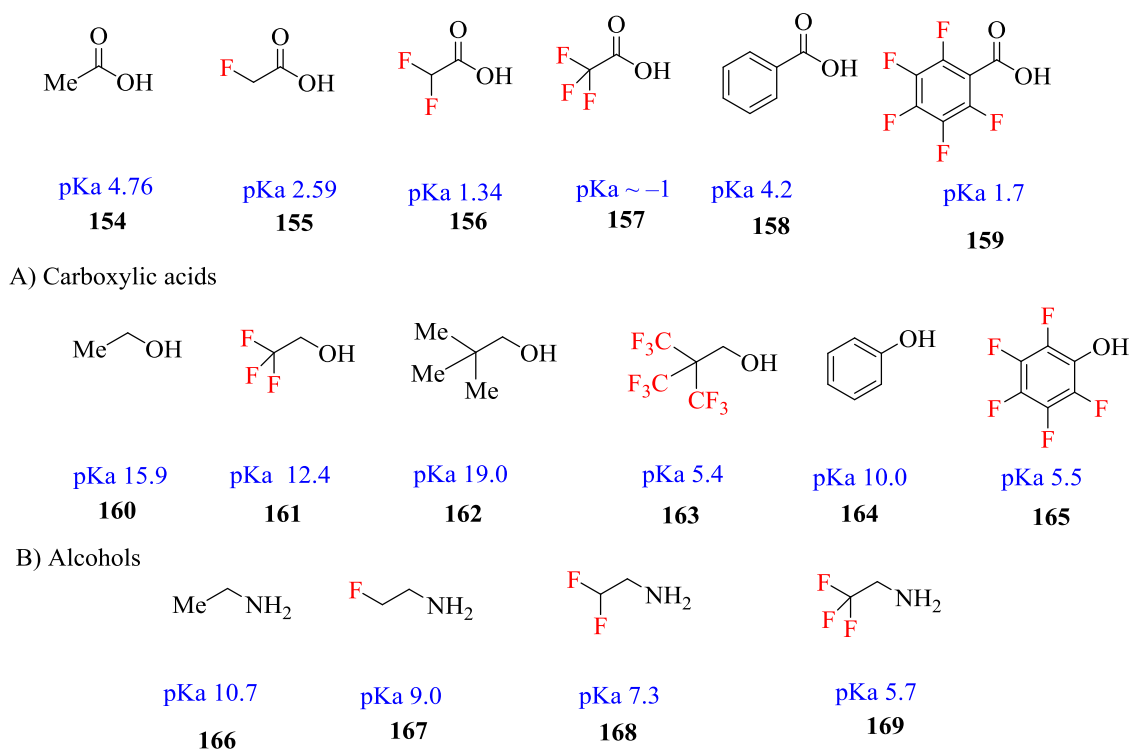


Figure 4.3: Effect of increasing fluorine atom number on pKa

Elsewhere, fluorinated side chain amino acids have become a significant strategy to monitor the behaviour of proteins in complex mixtures by working as an indicator. For examples: analysis, following purifications, studying proteins interactions and optimising biopharmaceutical properties *in vivo* and *in vitro* using ^{19}F NMR spectroscopy (Figure 4.4; Figure 4.5). This technique is appropriate methodology, especially for large proteins, as a probe of biological protein-protein or peptide-protein interactions, which is easier to undertake and interpret than either ^{15}N or ^{13}C NMR spectroscopies. In addition, the diffusion coefficient can be used to determine the mass of the peptide using UV-Vis spectroscopy,¹⁷⁷⁻¹⁷⁹ and this technique can also be used to study conformations of peptides, such as α -helices or β -sheets, as well as other biological interactions of peptides (Figure 4.5).¹⁷⁹

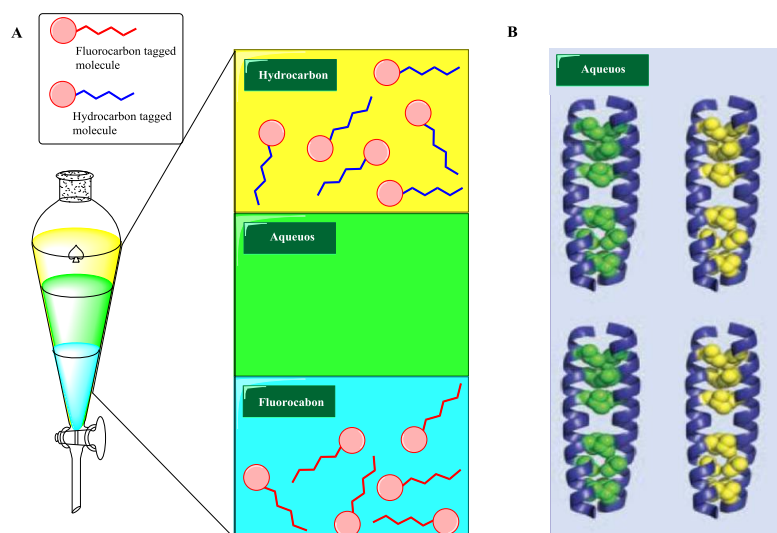


Figure 4.4: Purification of the proteins with and without fluorine

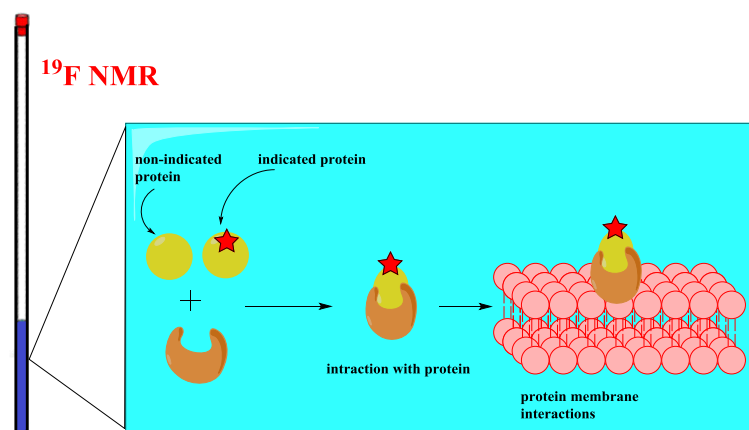


Figure 4.5: Probing Biological Interactions (fluorinated peptides) using ^{19}F NMR Spectroscopy¹⁷⁹

4.2 Fluorination in peptide and protein

The ^{19}F nucleus has spin $\frac{1}{2}$ and the abundance in nature is 100 %, NMR properties that are comparable to those of the proton, which means that it has excellent sensitivity in 1D NMR spectroscopy. The significant benefits of ^{19}F NMR spectroscopy include this substantial sensitivity, the virtual absence of fluorine in nature and that its chemical shift depends on the local chemical environment. Moreover, the span of ^{19}F NMR chemical shifts is ~ 400 ppm, which is greater than that in ^1H NMR spectroscopy (~ 15 ppm). For this reason, since the local chemical environment of the peptide can be affected by a large number of factors, the ^{19}F NMR signal can be used as an excellent protein probe.¹⁸⁰ Therefore, there are a large numbers of the benefits of ^{19}F NMR spectroscopy for studies in the biological molecules especially the proteins. Moreover, the fluorine in the aromatic

system acts as a withdrawing group, which have been ordered by arranging electron withdrawing effectiveness depending on the substitution position in the aromatic system: $m\text{-F} > o\text{-F} > p\text{-F}$. Relating to distance, $o\text{-F}$ substitution has the strongest σ -withdrawing effect than $p\text{-F}$ substitution. Whilst, the $m\text{-F}$ has a strongest electron acceptor and the others are weaker electron acceptor, as a result of this fact, the fluorine atom work as an electron withdrawing inductive effect because of the resonance positions in the benzene ring (Figure 4.6).¹⁸¹

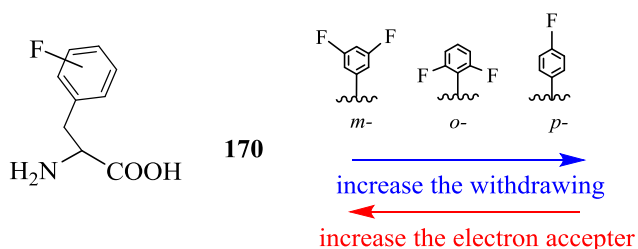


Figure 4.6: Fluorinated aromatic amino acid

A new report, published in 2017 by Oberlies *et al.* described the synthesis of a new modification of the peptides of fungal strains MSX70741 and MSX57715 (Figure 4.7), which had been labelled with a fluorinated amino acid (2 or 3-fluoro-DL-phenyl alanine). The new peptide derivatives showed improved and excellent activity against human cancer cells than the native peptide. The peptides were fully characterised via NMR spectroscopy including ^{19}F NMR, 1D and 2D NMR. The fluorinated amino acid was used as an indicator to monitor the biological activity, which has played a pivotal role in increasing their potential as anticancer agents.

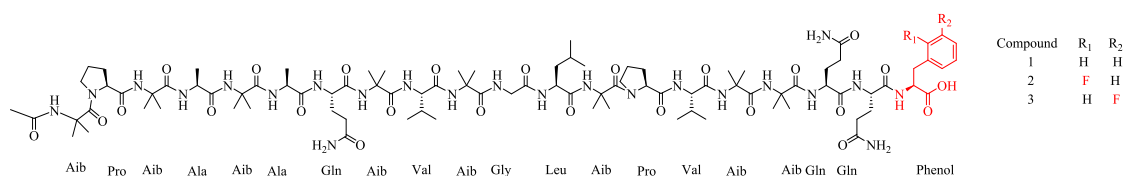


Figure 4.7: Structures of MSX70741 and MSX57715 connected with a substituted α - and β -fluoro-amino acid¹⁸²

There are many other factors that could be affected by the presence of fluorinated amino acids in the peptides, including conformational pre-organization (gauche effects), interactions with other phenyl groups (π - π stacking) and hydrogen bonding.

4.2.1 Conformational pre-organization (gauche effects)

Michel and co-workers have presented the best example to date of using a fluorinated aromatic amino acid in a collagen peptide. The new derivatives of collagen showed a higher stability than the original collagen to high temperature, as a result of the gauche effects of the fluorinated amino acid. The collagen peptide consists of three amino acids (Glu, Pro and Hyp), with this triplet repeated. They used 4(*R*)-fluorinated proline instead of normal proline with the aim of improving the stability of the peptide. However, they also discovered that the melting point had increased from 69 °C to 91 °C. Here, increasing the stability arises from the proline in an *exo*-conformation and the backbone amide bond in a *trans*-conformation due to the gauche effect, which was subsequently demonstrated by NMR spectroscopy (Figure 4.8).¹⁸³

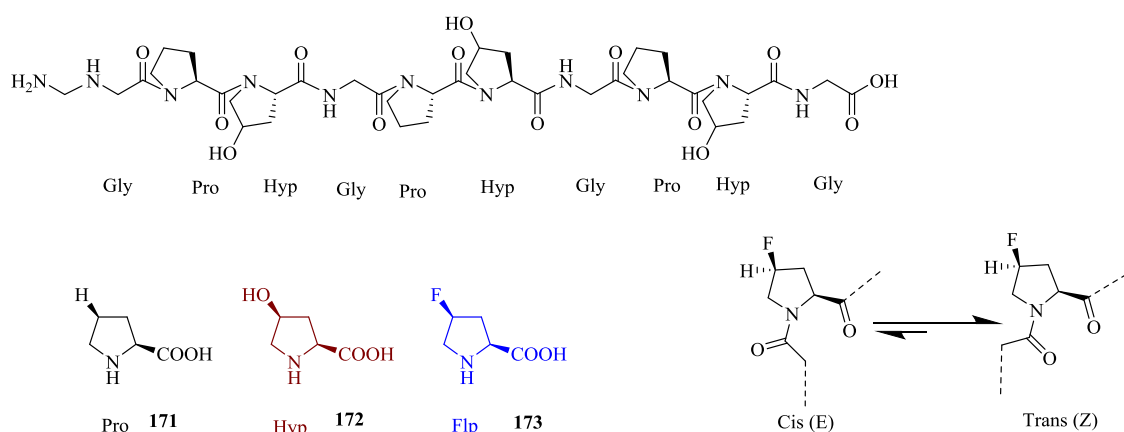


Figure 4.8: The effect of fluorine in the proline ring in the gauche form as a mimic for collagen peptides.

4.2.2 Substituted aromatic amino acids interaction (π - π stacked)

In sp^2 hybrid aromatic systems (benzene) the carbon atoms have higher electronegativities than the hydrogens they are bonded to ($C = 2.75$ and $H = 2.48$).¹⁸¹ In benzene, the centre of the ring has a partial negative charge and the outside of the ring (the hydrogen atoms) have a partial positive charge. A polar- π interaction in such aromatic molecules is one of the most common factors that increase the stability of a large number of the organic compounds. This phenomenon can be used positively in peptides synthesis for extra stability from both protein-protein interactions and peptide folding.

In recent years, several studies have been published that show the advantages of using fluorinated aromatic amino acid instead of the solely hydrogen containing aliphatic or aromatic amino acids. There are a large number of examples in the literature related to the synthesis of the fluorinated aromatic amino acids, leading to studies of the biological activity of peptides after modification. Of particular interest have been protein-protein interactions. Generally, benzene rings can form π - π interactions with other benzene rings in three possible ways: offset-stacked, edge-face stacked and face-face stacked with respect to the other two. For example, Pace and Gao (2012) demonstrated the effectiveness of using different types of fluorinated aromatic amino acids in the synthesis of HP35 peptides, in which they replaced the amino acids in the sequences at positions 6, 10 and 17. Their studies showed that the fluorinated amino acid side chains allowed new polar- π interactions between the dimeric helices. These interactions between the fluorinated aromatic amino acids affected the folding of the peptides, introducing new folding conformations that were non-existent in the original peptides. When the two fluorinated and non-fluorinated peptides were mixed they preferentially formed a heterodimer peptide instead of the homodimers, due to enhanced face-face interactions in the former (Figure 4.9).¹⁸⁴

These are influenced by the electronegativity of the benzene ring when it is substituted by fluorine atoms in comparison to unsubstituted benzene rings,¹⁸⁴ where the face-face stacked arrangement, as demonstrated by single crystal structure determinations, is disfavoured with respect to the other two arrangements. For example, Pace and Gao (2012) demonstrated the effectiveness of using different types of fluorinated aromatic amino acids in the synthesis of HP35 peptides, in which they replaced the amino acids in the sequences at positions 6, 10 and 17. Their studies showed that the fluorinated amino acid side chains allowed new polar- π interactions between the dimeric helices. These interactions between the fluorinated aromatic amino acids affected the folding of the peptides, introducing new folding conformations that were non-existent in the original peptides. When the two fluorinated and non-fluorinated peptides were mixed they preferentially formed a heterodimer peptide instead of the homodimers, due to enhanced face-face interactions in the former (Figure 4.10).¹⁸⁴

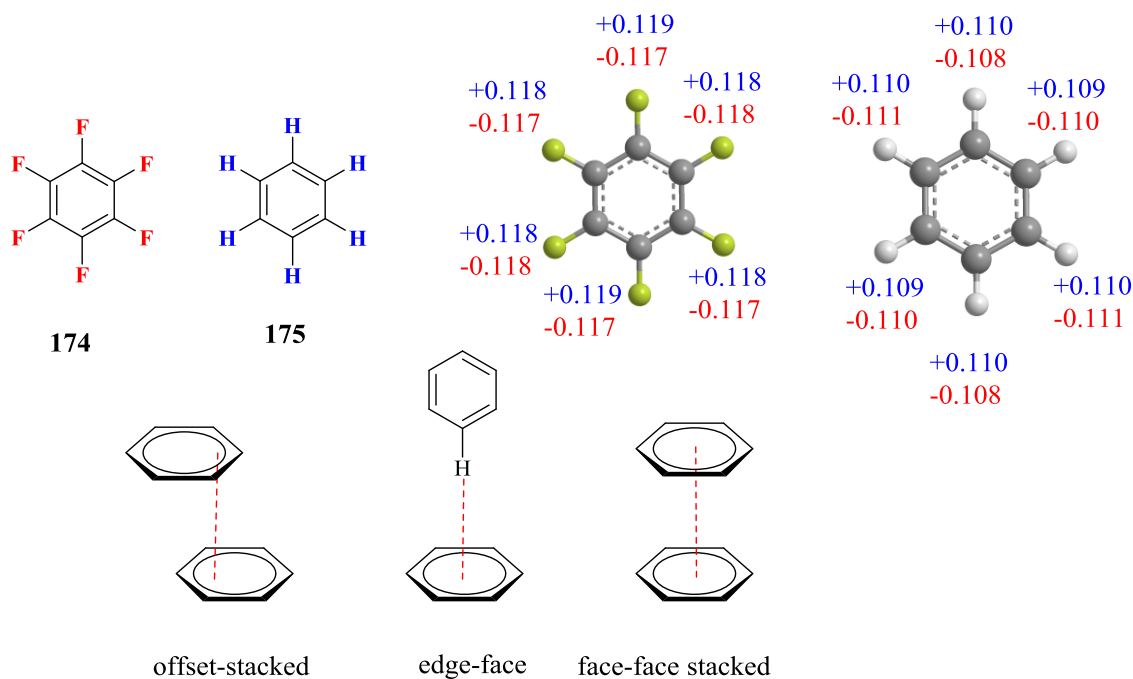


Figure 4.9: Benzene rings can form various possible π - π interaction, the blue numbers are for the C atoms and the red numbers for the hydrogen or fluorine atoms

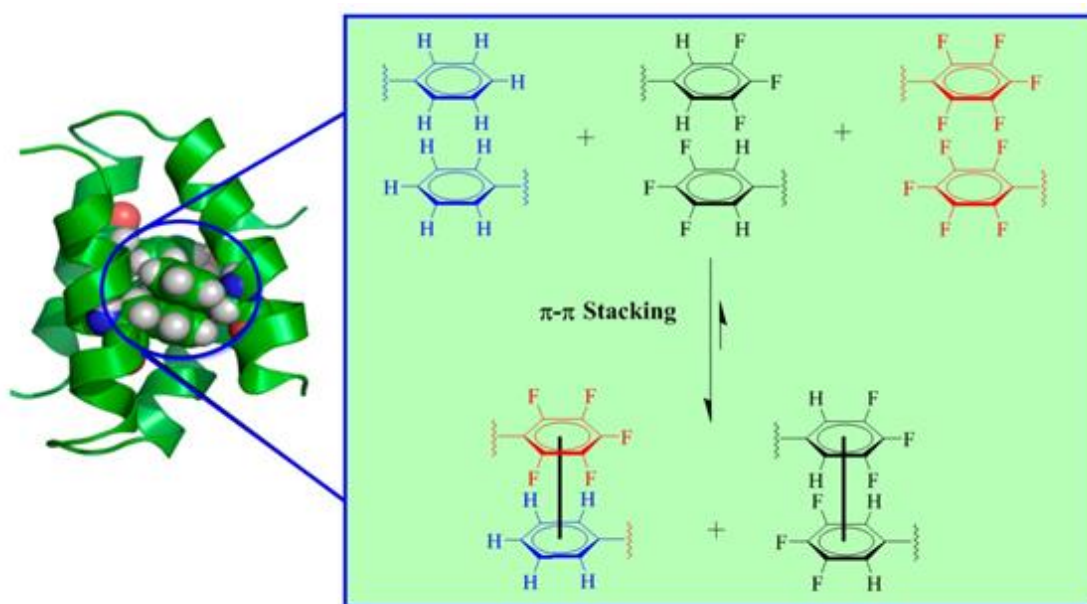


Figure 4.10: Polar- π interactions between dimeric helices

4.2.3 Effect of hydrogen bond between $\text{H}\cdots\text{F}$

It is well known that fluorine is strongly electron withdrawing in the fluoro-substituted organic compounds when compared to non-substituted compounds. These withdrawing groups are the main factors that increase the acidity of the organic compounds, which

have active groups such as hydroxyl, amine, amide and carboxylic acids. The fluorine atom also has three non-bonding lone pairs of electrons that can form strong hydrogen bonds; both inter-molecular and intra-molecular $\text{H}\cdots\text{F}$ interactions. Fluorine can form an electrostatic interaction with the hydrogen atom of an amine and the carbon atom of a carbonyl group. Oleson and co-workers showed a good example of these interactions with fluorine, when using a para substituted amino acid in peptide synthesis. Here, in the crystal structure of thrombin, between the ligand and the protein complex, there is an interaction between the fluorine and the hydrogen in the alpha position (CH) and the carbonyl group in the backbone of the Asp98 unit (Figure 4.11).¹⁸⁵

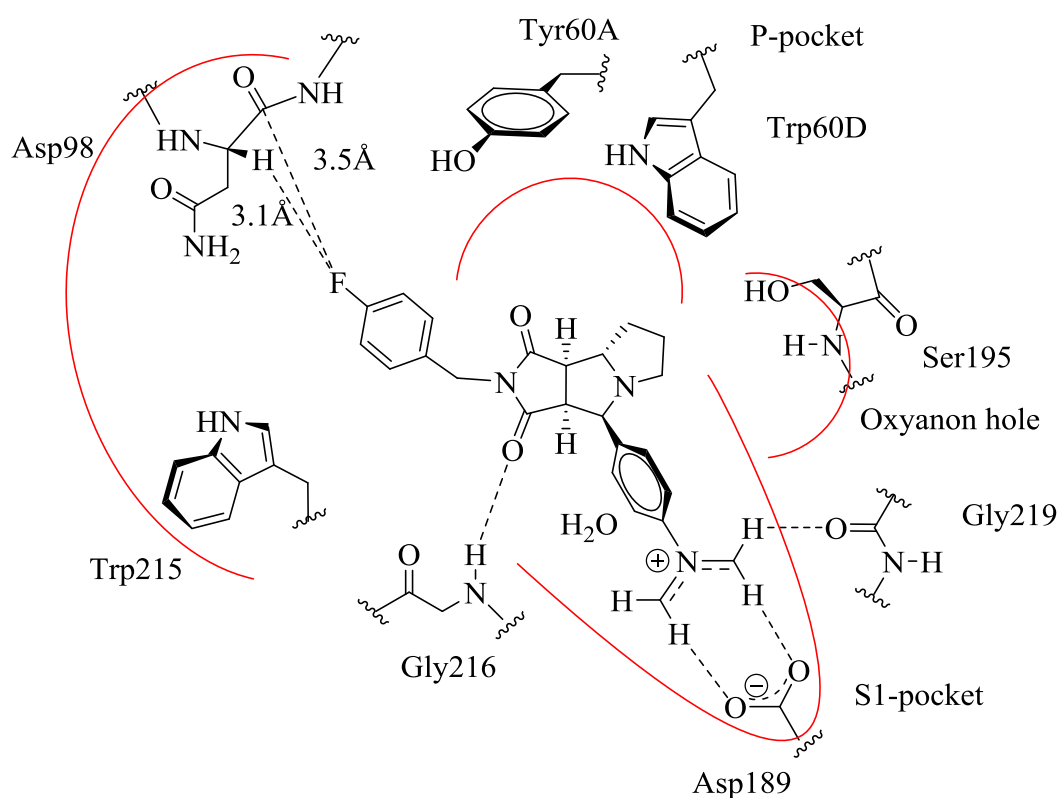
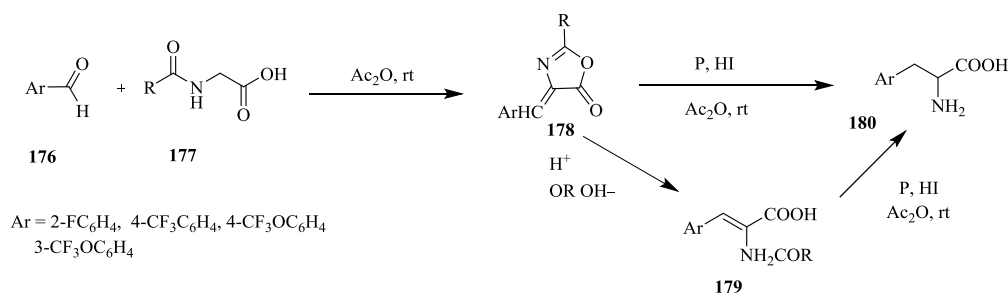


Figure 4.11: X-ray crystallographic study showing the binding of tricyclic thrombin inhibitor and the $\text{C-F}\cdots\text{HN}$ and $\text{C-F}\cdots\text{CO}$ interactions

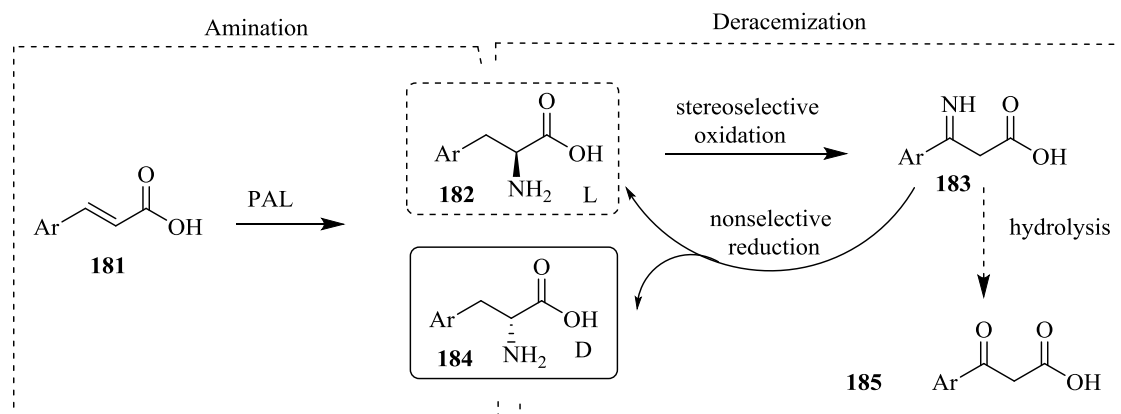
Although there are various methods to synthesise fluorine-substituted phenylalanine in good yield, in general a racemic mixture is obtained, from which it is extremely difficult or impossible to isolate the enantiomers. For example, Samet and co-workers developed a direct synthesis of fluorinated amino acids using a reduced number of steps which starts with the Erlenmeyer reaction to produce an azalactone and is followed by ring cleavage.

This new method is impressive in the sense of obtaining an acceptable yield in only two steps, but less useful in the sense that the product was a racemic mixture, (*S*)-2-amino-3-(2-fluorophenyl)propanoic acid was obtained in 42 % yield, whilst (2-amino-3-(4-(trifluoromethyl)phenyl)propanoic acid obtained in 32 % yield (Scheme 4.1).¹⁸⁶



Scheme 4.1: Samet's new amino acid synthetic method

In the last few years, several new procedures for the synthesis of fluorinated amino acids in high yields and excellent optical purities have been developed that make use of biocatalysts. One of the main primary methodologies to synthesise them via biocatalysts, for example, uses microbial cells or enzymes derived as catalysts in the amino acids synthesis.¹⁸⁷ In 2015, Turner and co-workers presented a new method to synthesise pure enantiomers amino acids in increased yield using derivatives of cinnamic acids and phenylalanine ammonia lyase (PAL) amination via chemoenzymatic deracemization. Whilst this new method is an acceptable means of achieving *D* or *L*-fluorinated amino acids, it can be only be used for small scale production (Scheme 4.2).¹⁸⁸ So, commercially, non-natural fluorinated amino acids remain expensive, especially when required in high enantiomeric purity (ee).



Scheme 4.2: Reaction of cinnamic acid derivatives by using PAL amination and LAAD/NH₃: BH₃ deracemization

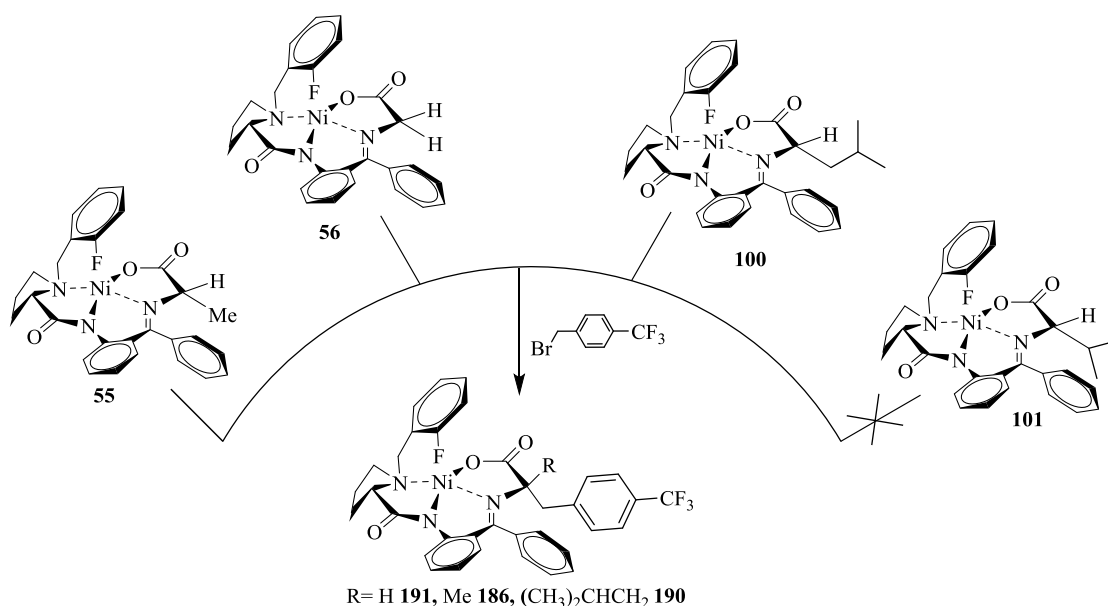
4.3 The aims of the work in this chapter are:

- (i) Using the Ni^{II} Schiff base complexes, that were synthesised in Chapter 2, to extend the methodology to synthesise new complexes via alkylation reactions with fluorine-containing aryl substrates such as 1-(bromomethyl)-4-(trifluoromethyl)benzene and 1-(bromomethyl)-2-fluorobenzene.
- (ii) Using these Ni^{II} Schiff base complexes derivatives to develop an alternative approach for the synthesis of new complexes via Aldol reaction with benzaldehyde or 2-phenyloxirane.
- (iii) Synthesis of new fluorinated amino acids in good yields and high enantioselectivity.

4.4 New Methodology for the synthesis of fluorinated aromatic amino acids

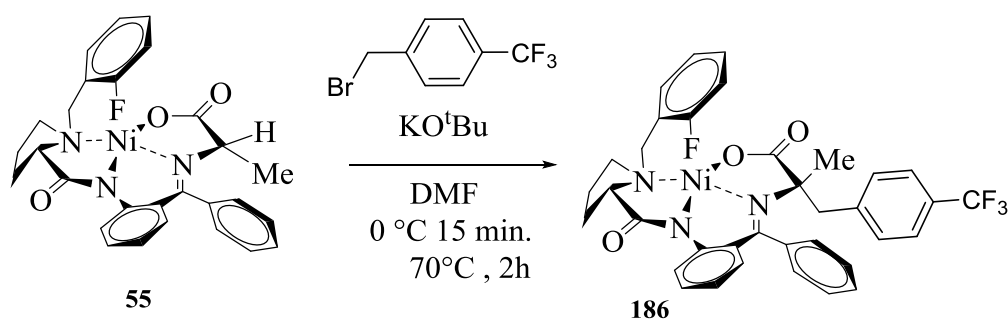
Gaining enantiomerically pure unnatural α -amino acids is a general problem in synthesis. Using Ni^{II} Schiff base complexes derivatives as starting materials for an alkylation reaction or an aldol reaction would form useful intermediates from which to synthesise new amino acids. Various types of ligands have been investigated in the synthesis of Ni^{II} Schiff base complexes, which have shown to offer a very attractive approach to the synthesis of unnatural amino acids with high chirality.

4.4.1 Alkylation with 1-(bromomethyl)-4-(trifluoromethyl)benzene



Here, the synthesis of new fluorinated amino acids derivatives via alkylation reaction using as glycine, alanine, valine and leucine Ni^{II} Schiff base complexes is described. This study allows a comparison between these complexes in the synthesis with a particular emphasis on the diastereoselectivity (*de*) and on the purity.

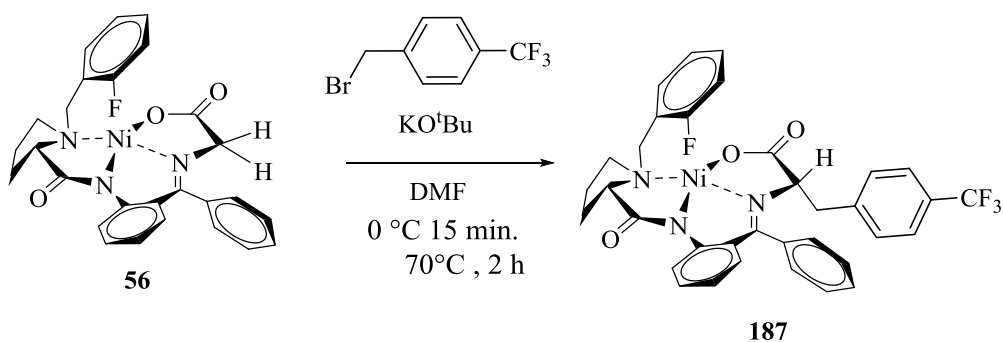
4.4.1.1 Alkylation of alanine Ni^{II} Schiff base complex



In the initial attempt at the synthesis of new derivatives compound (*S*) **186** via the alkylation reaction of the alanine Ni^{II} Schiff base complex **55** the same reaction conditions used for the alkylation reaction (room temperature for 1 hour) of the glycine-complex were followed, but the reaction was unsuccessful (Table 4.1, Entry 1). Increasing the time to 2 hours at room temperature was not successful (Table 4.1, Entry 2), whilst increasing the reaction temperature to 50 °C gave a limited improvement. Mass spectroscopy of the crude product revealed that there was some product, but only

in small amounts, and the starting material (the Ni^{II} Schiff base complex **55**) was still present. This was confirmed by ¹⁹F NMR spectroscopy with a large peak for the starting material. Increasing the reaction time to 2 hours at 50 °C had a remarkable impact on the product yield; almost all the starting material was converted to the product as shown by both mass spectroscopy and ¹⁹F NMR spectroscopy. The product was purified using the Biotage instrument. The identity of the compound, (*S*)-({2-[1-(2-fluorobenzyl)benzyl]pyrrolidine-2-carboxamide]phenyl} phenylmethylene)-(*S*)-4-(trifluoromethyl)benzyl-alaninato-*N,N,N',O*}nickel^(II) **186** confirmed the alkylation through two single fluorine peaks of the fluorine in the ¹⁹F NMR spectrum of the product with integrals of 1:2.6. The first singlet peak at $\delta = -133.6$ was attributed to the aromatic fluorine, whilst the second single peak at $\delta = -62.4$ to CF₃ group. ¹H NMR and ¹³C NMR spectroscopy further confirmed the identity of this species, as did the mass spectrum which showed peaks at 688.1754 and 690.1722. Furthermore, the reaction showed a good yield, with only the mono-substituted product, and a high diastereoselectivity (>99 *de*) (*S*).

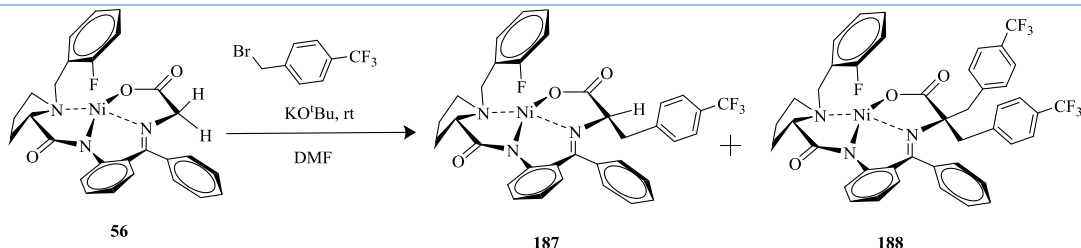
4.4.1.2 Alkylation of glycine Ni^{II} Schiff base complex



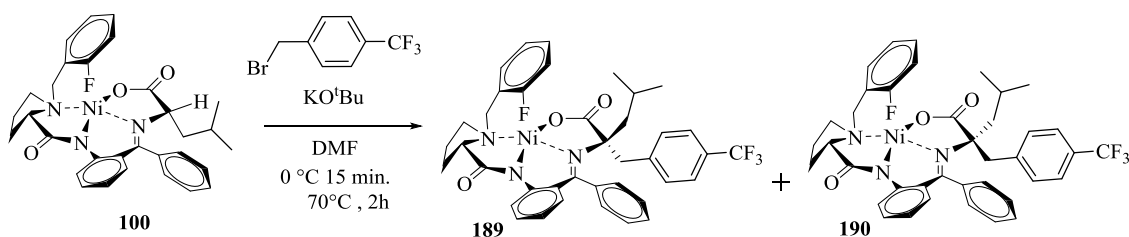
The key starting material required to synthesise the new fluorinated derivative is **187**, which can be formed via alkylation of compound **56** under basic conditions following general method **F**. Initially, the conditions for the alkylation reaction followed the literature route of Jamieson and co-workers,⁴⁸ using 3 equivalents of the alkyl bromide and stirring for 15 min. Unfortunately, this procedure was unsuccessful, with the subsequent ¹⁹F NMR spectrum of the crude product showing a number of species were present, which could not be separated by the flash column chromatography, since they have very similar R_f values from TLC. As an alternative, the amount of alkyl bromide

was decreased to 1.1 equivalents using the same amount (and concentration) of the base. The reaction was monitored via ^{19}F NMR spectroscopy until almost all the starting material had been consumed. The reaction was scaled up to a 1 gram scale, and the product yield was isolated in a reasonable yield (66 %) with a high diastereoselectivity (> 99: 1 *dr*). The identity of compound **187** was confirmed from the alkylation by two single fluorine peaks in ^{19}F NMR spectrum with appropriate integrations (1 : 2.88), where the first singlet peak was at $\delta = -133.7$ and was assigned to the *ortho*-aryl fluorine atom, whilst the second singlet peak, at $\delta = -62.4$, was assigned to the CF_3 group. In addition, the ^1H NMR and ^{13}C NMR spectral data were consistent with the desired product, and the which showed peaks at 696.1396, found 696.1406 ($\Delta = 1.4$ ppm) and 698.1351, found 698.1382 ($\Delta = 4.4$ ppm).

Table 4.1: Alkylation reaction with glycine complex under different reaction conditions

			
Entry	Electrophile (eq.)	Time (min.)	Outcome %
1	3	15	0
2	1.1	15	50, 6
3	1.1	60	66, 8

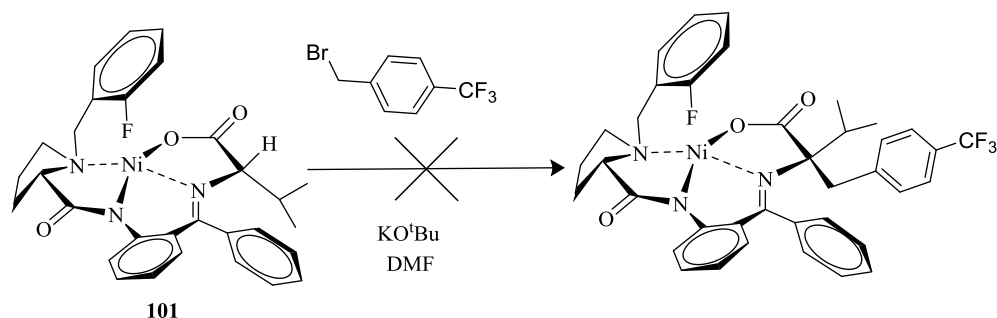
The by-product, the α,α -di-substituted derivative **188**, could also be formed as a reddish-orange solid. The ^{19}F NMR spectrum of **188** showed a singlet peak δ at -113.3 for the single fluoride and peaks at -62.4 and -62.3 for the two CF_3 groups. The by-product was isolated in an 8 % yield and characterised by its HRMS-ESI spectrum.

4.4.1.3 Alkylation of leucine Ni^{II} Schiff base complex

Synthesis of compound **189** was achieved by the alkylation of compound **100** using 1-(bromomethyl)-4-(trifluoromethyl)benzene. The same reaction conditions were followed, with the same equivalents of the base and the electrophile, but the reaction temperature was decreased to -30 °C for 48 hours, to optimise the synthesis of the pure compound in high yield. Almost all of the starting material was converted to product, as demonstrated by mass spectrometry and ¹⁹F NMR spectroscopy. The product was purified using the Biotage instrument. The major product of the alkylation reaction was the (S,S) diastereomer, isolated as (S)-({2-[1-(2-fluorobenzyl)benzyl]pyrrolidine-2-carboxamide}phenyl)phenylmethylene)-(S)-4-(trifluoromethyl)benzyl-leucinato-N,N',N'',O}nickel(II) **189** in a 66 % yield as a pure reddish-orange solid. The identity of the compound was demonstrated by two single fluorine peaks in the ¹⁹F NMR spectrum, with integrated values of 1:2.7. The first singlet peak at $\delta = -114.1$ was assigned to a single aromatic fluorine and the second singlet peak at $\delta = -62.4$ to a CF₃ group. Further confirmation of the product, and its stereochemistry, came from a single crystal X-ray structural determination on single crystals grown by slow evaporation from ethylacetate solvent; this showed the chirality of these crystals were the (S, S) complex. The purity of the product was identified and confirmed through ¹H NMR and ¹³C NMR spectroscopies. In the mass spectrum parent ion peaks at 752.2025 and 754.2008 were observed. Furthermore, the minor product, a reddish-orange solid isolated in a 17 % yield, was identified as the (S, R) diastereoisomeric product. ¹⁹F NMR spectroscopy indicated the purity of this product, with two signals at different chemical shifts to those for the (S,S) diastereomer; a singlet at $\delta = -113.5$ assigned to the aromatic fluorine and a singlet at $\delta = -62.5$ assigned to the CF₃ group. From the mass spectrum, parent ion peaks were observed at 752.2047 and 754.2019. One of the targets of the study was to demonstrate that the different stereoisomers had different ¹⁹F NMR chemical shifts, due to the slightly different environments, as shown for these products. ¹⁹F NMR spectroscopy is an

excellent indicator of the chirality in these compounds. Furthermore, we noted that the diastereoisomers can be isolated even when performing large-scale reactions (ca. 1 g).

4.4.1.4 Alkylation of valine Ni^{II} Schiff base complex



The synthesis of a new type of fluorinated valine amino acid derivative was attempted in the reaction of valine Ni^{II} Schiff base complex compound **101** and 1-(bromomethyl)-4-(trifluoromethyl)benzene. The general procedure of the alkylation reaction was followed, under the procedure described by Jamieson and the variations described above. However, monitoring the reactions by ¹⁹F NMR spectroscopy showed no evidence for the target product and only showed starting materials in the crude products.

Table 4.2: Alkylation reaction with the valine complex under different reaction conditions

101

Entry	Time (h)	Temperature (°C)
1	1	rt
2	2	rt
3	3	50

However, during these attempts a by-product was found, which was subsequently demonstrated by X-ray crystallography, for crystals grown by slow evaporation from ethylacetate/DCM, to be (*E*)-1,4-bis(4-(trifluoromethyl)phenyl)but-2-ene (Figure 4.12).

The main reason for obtaining this dimer is that under basic conditions the benzyl bromide can react with itself followed by an elimination reaction (Scheme 4.3).¹⁸⁹

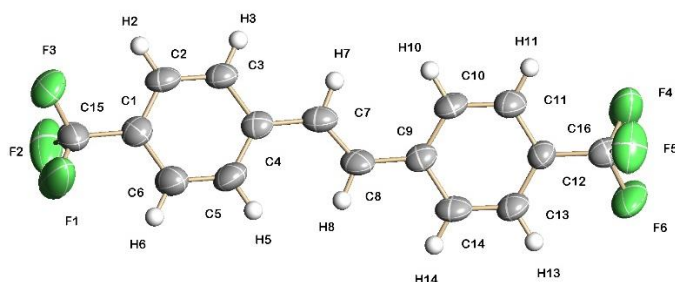
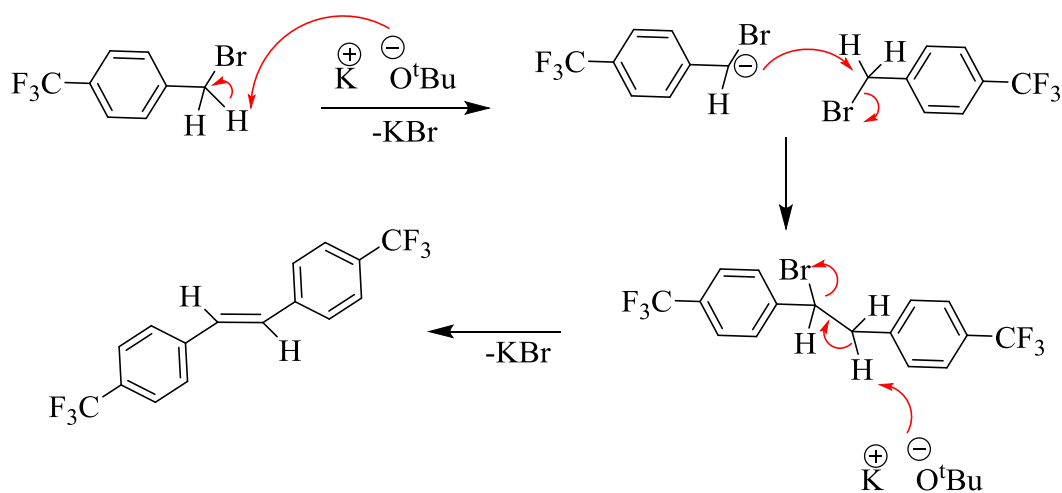
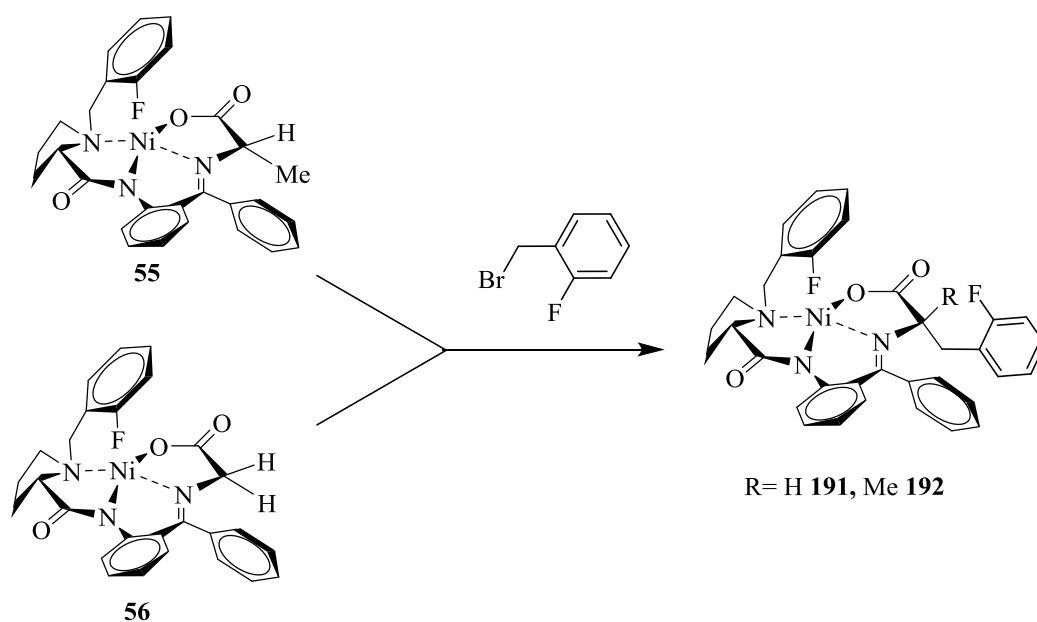


Figure 4.12: Solid-state structure of (*E*)-1,4-bis(4-(trifluoromethyl)phenyl)but-2-ene



Scheme 4.3: Mechanism of synthesis (*E*)-1,4-bis(4-(trifluoromethyl)phenyl)but-2-ene

4.4.2 Alkylation by using 1-(bromomethyl)-2-fluorobenzene

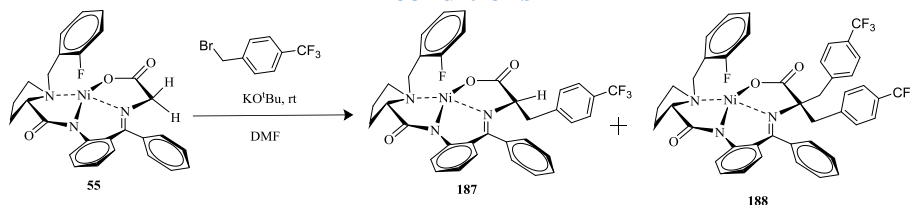


4.4.2.1 Alkylation of the glycine Ni^{II} Schiff base complex

(*S*)-({2-[1-(2-fluorobenzyl)benzyl]pyrrolidine-2-carboxamide}phenyl}phenylmethylene)-(*S*)-2-fluorobenzyl-glycinato-*N,N',N'',O*) nickel^(II) **191** was synthesised by the alkylation of the glycine Ni^{II} Schiff base complex **192** with 2-fluorobenzylbromide. The reaction conditions described by Jamieson and co-workers⁴⁸ were again initially followed. However, although these conditions were successful in achieving alkylation when using aliphatic electrophiles, they were unsuccessful with benzyl electrophiles. Alternatively, decreasing the equivalents of the electrophile to 1.1 equivalents gave a reaction that showed a good yield of the desired product, but with little diastereoselectivity (Table 4.3, Entry 2). The ¹⁹F NMR spectrum of the crude product showed four singlet peaks; the major (*S, S*) product peaks at $\delta = -115.3$ and -113.9 , and the minor (*S, R*) product peaks at $\delta = -115.0$ and -113.0 . Reducing the equivalents of the electrophile further to 1 allowed the pure product to be isolated with high diastereoselectivity (> 95:5dr) (Table 4.3, Entry 3). The reaction was monitored via ¹⁹F NMR spectroscopy until almost all of the starting material had reacted, when the reaction was stopped to prevent disubstitution, as the disubstituted product was expected to be difficult to separate from the target monosubstituted product. The reaction was scaled up to 1 g, and a higher yield (66 %) and higher diastereoselectivity (> 95:5 dr) were obtained. The identity of compound **188** was confirmed by two singlet fluorine peaks in the ¹⁹F

NMR spectrum and supported by the ^1H NMR and ^{13}C NMR spectral data, and the mass spectrum.

Table 4.3: Alkylation reaction with glycine complex under different reaction conditions



Entry	Electrophile (eq.)	Time (min.)	Temperature $^{\circ}\text{C}$
1	3	15	rt
2	1.1	15	rt
3	1.1	60	rt

4.4.2.2 Alkylation of alanine Ni^{II} Schiff base complex

Following the reaction conditions of Jamieson *et al.* (50°C for 2 hours) the new derivative, (*S*) **192**, was formed in a 69 % yield through the alkylation reaction of 2-fluorobenzylbromide with alanine Ni^{II} Schiff base complex **55**. The product was purified using the Biotage instrument. The reaction gave only the monosubstituted product with a high diastereoselectivity ($> 99:1$ *de*) (*S*, *S*). ^{19}F NMR spectroscopy was used to verify the identity of the compound as (*S*)-({2-[1-(2-fluorobenzyl)benzyl]pyrrolidine-2-carboxamide}phenyl}phenylmethylene)-(*S*)-2-fluorobenzenyl-alaninato-*N,N',N'',O*} nickel(^{II}) **192**, from the presence of two singlet fluorine peaks at $\delta = -113.7$ and -113.8 . ^1H NMR and ^{13}C NMR spectroscopy were consistent with this formulation and mass spectrometry showed an ion peaks at 638.1777 and 640.1752

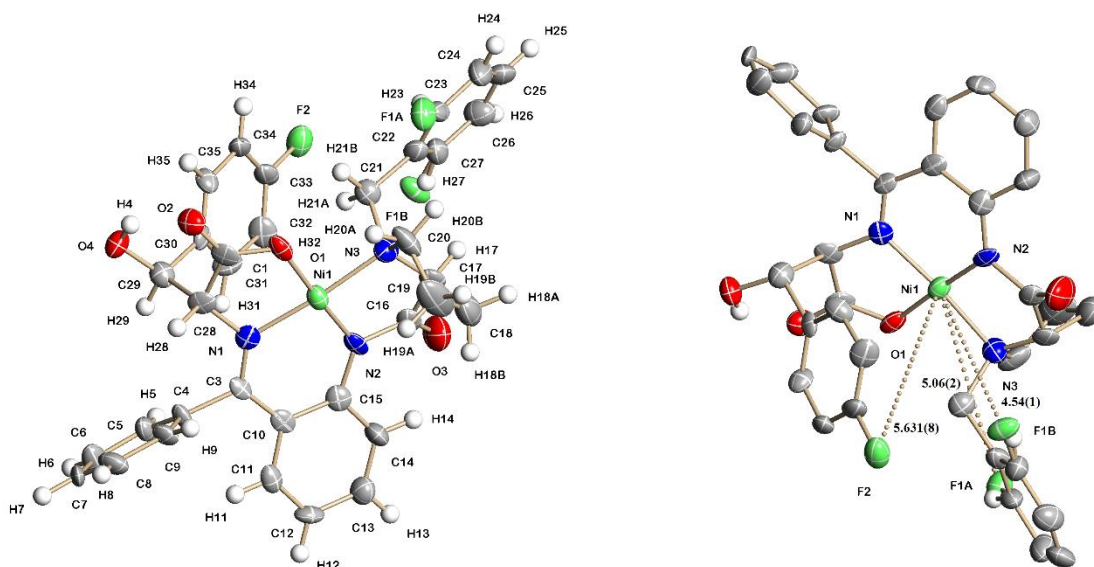
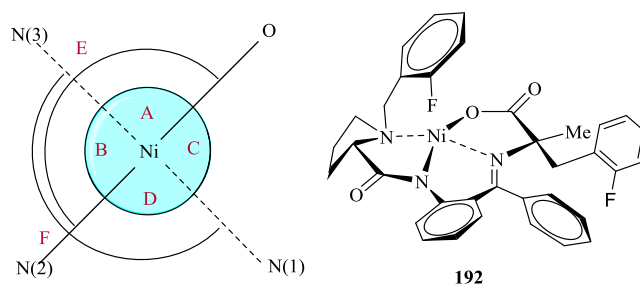


Figure 4.13: Crystal structure of compound

Crystals suitable for X-ray crystallography was grown for **192** (Figure 4.13). The bond lengths and bond angles (Table 4.4) illustrated the same distorted square planar structure as shown for the other Ni^{II} complexes with the metal centre supported by an unsymmetrical *N, N, N, O* pincer ligand.. There are slight differences between the Ni-X bond lengths, which are all within 0.03 Å.

Table 4.4: Key bond lengths (Å) and angles (°) for crystal structure of compound

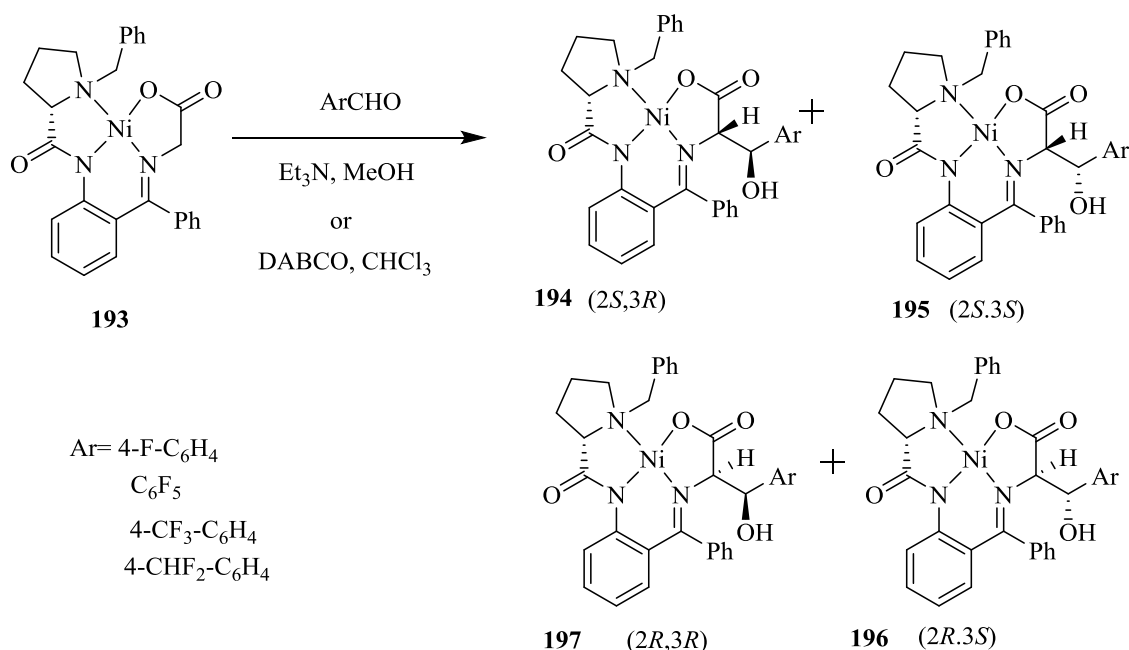


Bond Lengths (Å)		Bond Angles (°)	
Ni(1)-N(2)	1.844(4)	O(1)-Ni(1)-N(3) A	91.81(16)
Ni(1)-O(1)	1.838(3)	N(2)-Ni(1)-N(3) B	86.19(18)
Ni(1)-N(1)	1.861(4)	O(1)-Ni(1)-N(1) C	86.81(15)

Ni(1)-N(3)	1.941(4)	N(2)-Ni(1)-O(1) E	95.44(17)
Ni(1)...F(2)	2.881(4)	N(1)-Ni(1)-N(3) F	175.71(18)
Ni(1)...F(1B)	3.612(8)		
Ni(1).....F(1A)	4.921(5)		

4.5 Aldol reaction with glycine Ni^{II} Schiff base complex

The second target for the work in this chapter was the aldol reaction of the Schiff bases Ni^{II} complexes. The fluorines in the ligand and in the reagents were used as guides in the reaction to indicate conversion, and also to show the addition of the fluorinated aromatic group via the Aldol reaction to produce α -amino- β -hydroxy acids (Scheme 4.4). In the literature, formation of α -amino- β -hydroxy acids through the aldol reaction has only been reported with the glycine-containing Ni^{II} complex. In this chapter, the aldol reaction was also attempted on the alanine derivative.

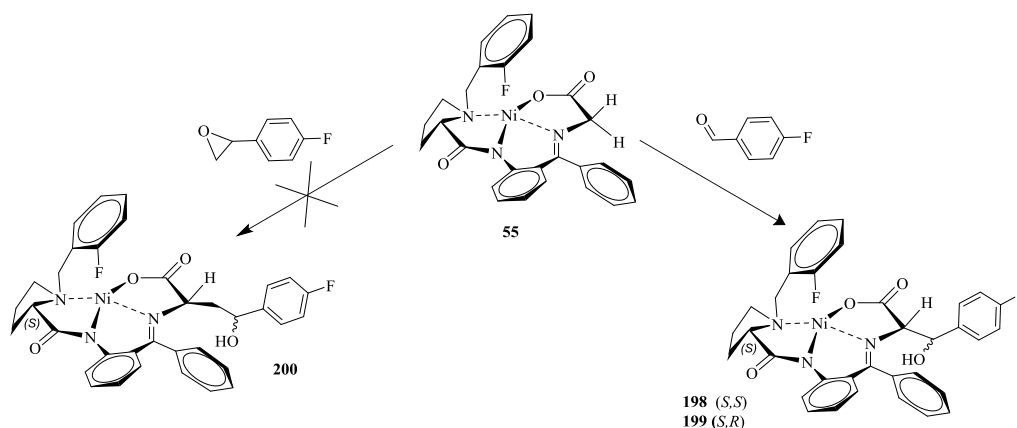


Scheme 4.4: Aldol reaction using Et_3N in methanol or DABCO in CHCl_3

Glycine Ni^{II} complexes Schiff base have been shown to react with aromatic aldehydes via the aldol reaction, which has the possibility of producing four diastereoselectively related products through the generation of new second and third chiral centres, the major

diastereomers being (2*S*, 3*R*) and (2*S*, 3*S*), and with the (2*R*, 3*R*) and (2*R*, 3*S*) diastereomers formed as minor products. Conversions of 90 % after several days (1-4 days) when using trimethylamine as a catalyst in a methanol solvent at 50 °C have been reported, however, the reaction time can be reduced to 2 h when using 1,4-diazabicyclo[2.2.2]octane (DABCO) as catalyst in a CHCl₃ solvent (Scheme 4.4).^{93, 190} These previous studies showed that the reaction was dependent on the type of catalyst that was used to increase the yield and also the purity and decrease the time. In 1995, a new method for the aldol reaction was introduced by Soloshonok and co-workers.¹⁹¹ Sodium methoxide in methanol at 24 °C was used instead of the previous catalysts with the same type of BPB glycine complex. With aliphatic aldehydes they obtained yields of > 90 % as the *syn*-(2*S*) and *syn*-(2*R*) diastereomers. These results demonstrated that each aliphatic aldehyde had a different reaction time, ranging from 0.5 minutes to 24 hours; however, some did not react (Scheme 4.4).¹⁹¹

We were interested to see if new fluorinated complex could be prepared using the 4-fluorobenzaldehyde with high diastereomers or used an alternative 2-(4-fluorophenyl)oxirane (Scheme 4.5). The reaction of the glycine Ni^{II} complex Schiff base (**2.7**) with 4-fluoro-benzaldehyde (2 eq.) was found to proceed best using sodium methoxide in methanol for 24 h at -10 to -15 °C under nitrogen. A fluorinated aromatic aldehyde was chosen with the aim of producing products with high diastereoselectivity. ¹⁹F NMR spectroscopy provided evidence for generation of the product and to monitor the reaction. After ten attempts to optimise the reaction conditions, finally the best reaction conditions were discovered.



Scheme 4.5: Aldol reaction of glycine complex.

In the first attempt, it was hoped that the reaction conditions would be essentially identical to the previous alkylation reaction conditions (Table 4.5, Entry 1). No reaction was observed, with only the presence of the starting material shown by ^{19}F NMR spectroscopy. The reaction was thereafter attempted by changing the solvent to MeCN and then increasing the temperature to 50 °C; however, the reactions in both of these circumstances were also unsuccessful (Table 4.5, Entry 2 and Entry 3). The reaction between the glycine Ni^{II} complex Schiff base **55** and 4-fluorobenzaldehyde was also repeated using THF (dry) at RT for both 2 hours (Table 4.5, Entry 4) and 4 days (Table 4.5, Entry 5); however, these reactions were also unsuccessful. The reaction was attempted at 50 °C for both 2 hours and 24 hours (Table 4.5, Entry 6 and Entry 7, respectively); however, ^{19}F NMR spectroscopy showed only the starting material and the decomposition of the ligand due to the effects of heating for 24 hours. The reaction was then attempted with increasing the amount of the electrophile (4-fluorobenzaldehyde) to 4 eq. at both RT and 50 °C, and again in both instances the reaction was unsuccessful (Table 4.5, Entry 8 and Entry 9). The last repeat of this reaction was carried out using sodium methoxide in methanol at a lower temperature (-10 to -15 °C) for 2 hours. Finally, (*S*)-({2-[1-(2-fluorobenzyl)benzyl]pyrrolidine-2-carboxamide]phenyl}phenylmethylene)-(*S*)-2-hydroxy-4-fluorobenzenyl-glycinato-*N,N',N'',O*} nickel^(II) **198** was observed via ^{19}F NMR spectroscopy in the crude product, along with unreacted starting material. The crude product was purified by column chromatography to give the desired product **198** (57 % yield) (Table 4.5, Entry 10) with high diastereoselectivity (> 99:1 *de*). In the final attempt, the reaction time was increased to 24 hours, and showed an increase in yield to 61 % when the reaction was scaled up. The identity of the product was determined via ^{19}F NMR spectroscopy, which showed two singlet peaks at -112.9 (-113.923) and -113.3 (-113.285), and also two singlet peaks at -112.9 (-113.909) and -113.3 (-113.271), and also via ^1H NMR and ^{13}C NMR spectroscopies.

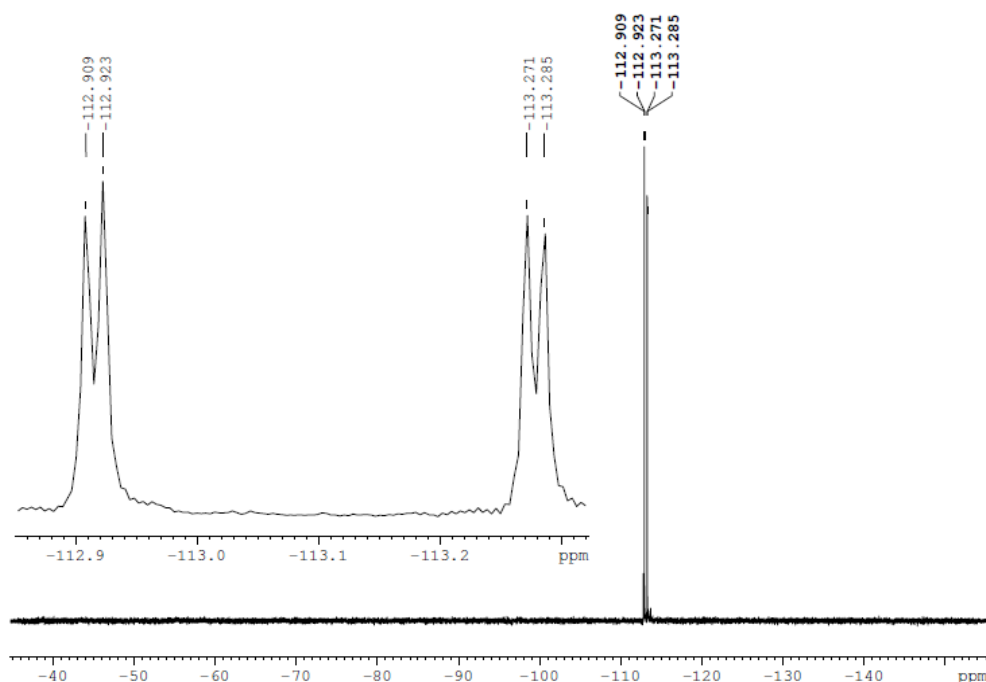
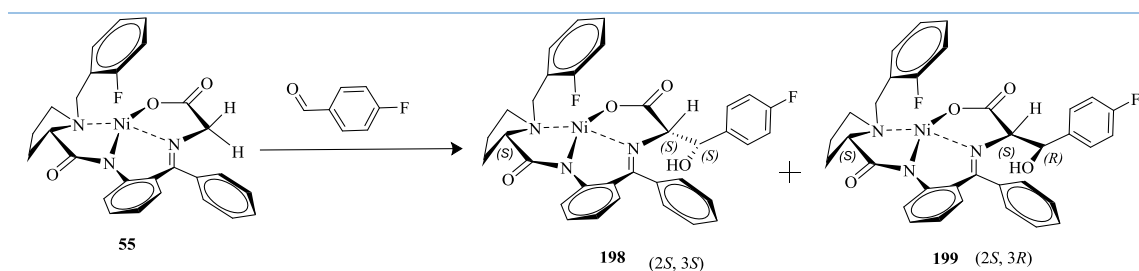


Figure 4.14: ^{19}F NMR spectroscopy for compound **198**

HRMS-ESI mass spectrometry also implied the desired product had been produced from peaks parent ion peaks at 640.1552 and 642.1528. Moreover, an X-ray crystallographic study of crystals grown by slow evaporation of an ethylacetate solution revealed the product with *syn* (2*R*) (1*S*, 2*R*, 3*S*) **198** configuration, and a second diastereoisomer with *syn* (2*S*)(1*S*, 2*S*, 3*S*) **199** configuration (Figure 4.15). The novelty of these synthesis reactions are in partial agreement with Soloshonok's discover by synthesis of diastereoisomers *syn* (2*R*) and *syn* (2*S*), the reaction conditions are modified to be suitable to apply for reaction with benzaldehydes rather than aliphatic aldehydes by decreasing the temperature to -10 to -15 °C for 24 hours.

Table 4.5: Aldol reaction with glycine complex under different reaction conditions



Entry	Base & solvent	Electrophile (eq.)	Time (h)	Temperature °C	Outcome
1	KO ^t Bu DMF	2	2	rt	----
2	KO ^t Bu MeCN	2	2	rt	----
3	KO ^t Bu MeCN	2	2	50	----
4	KO ^t Bu THF	2	2	rt	----
5	KO ^t Bu THF	2	4 days	rt	----
6	KO ^t Bu THF	2	2	50	----
7	KO ^t Bu THF	2	24	50	----
8	KO ^t Bu THF	4	24	50	----
9	KO ^t Bu THF	4	24	rt	----
10	NaOMe MeOH	2	2	-10 to -15	57
11	NaOMe MeOH	2	24	-10 to -15	61(after scaling up to 1g)

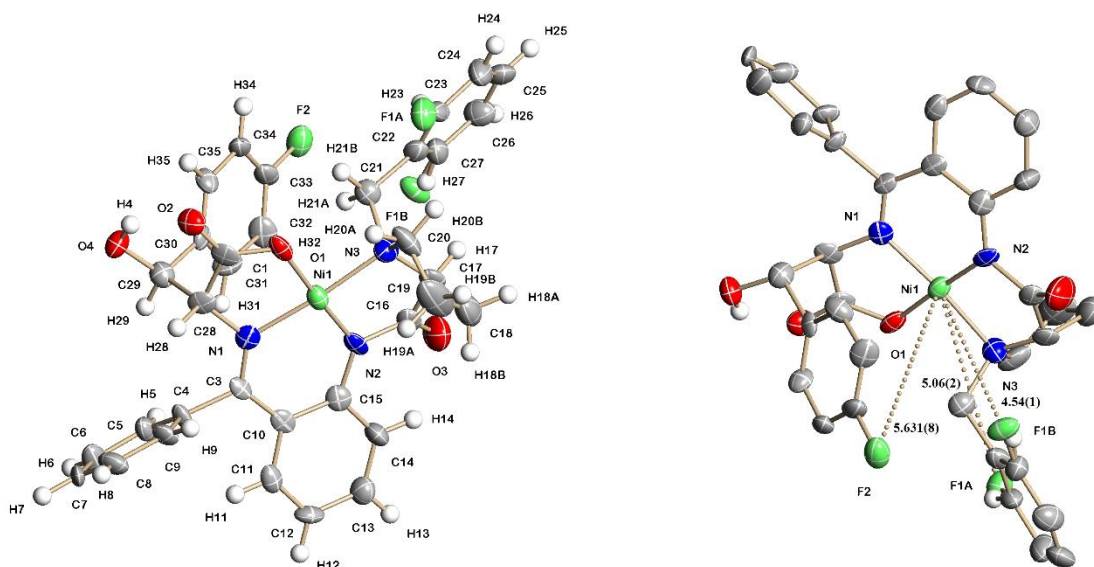
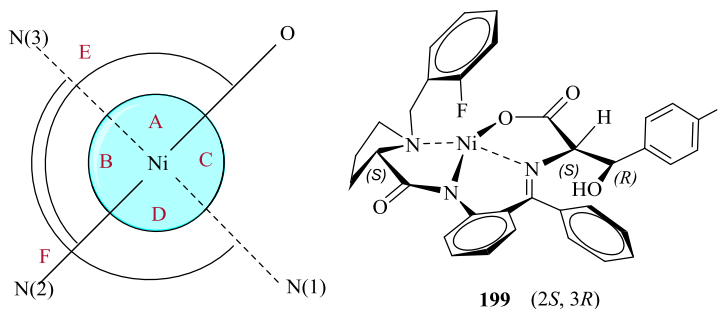


Figure 4.15: Crystal structure of compound

The solid state structure showed a Ni^{II} supported by an unsymmetrical *N, N, N, O* pincer ligand in a distorted square planar geometry. The bond lengths and bond angles, listed in Table 4.6, are similar to those found for the other Ni^{II} Schiff base complexes reported in this thesis.

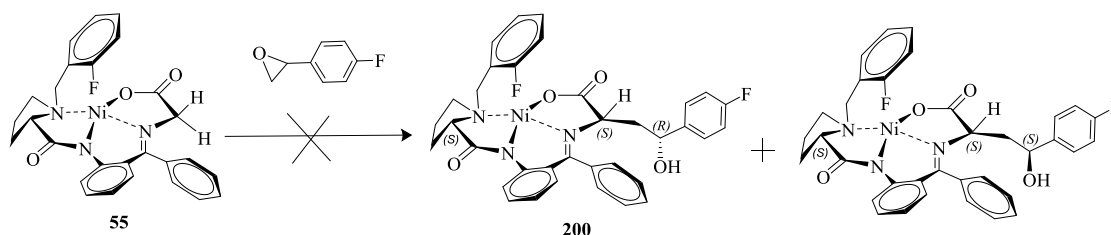
Table 4.6: Key bond lengths (Å) and angles (°) for compound **199**

Bond Lengths	(Å)	Bond Angles	(°)
Ni(1)-N(2)	1.821(9)	N(2)-Ni(1)-O(1)A	177.4(4)
Ni(1)-O(1)	1.836(7)	N(2)-Ni(1)-N(1)B	88.7(4)
Ni(1)-N(1)	1.939(10)	O(1)-Ni(1)-N(1)C	89.1(4)

Ni(1)-N(3)	1.865(10)	N(2)-Ni(1)-N(3)D	94.7(4)
Ni(1)....F(1)	4.612	O(1)-Ni(1)-N(3)E	87.5(4)
		N(1)-Ni(1)-N(3)F	175.0(5)

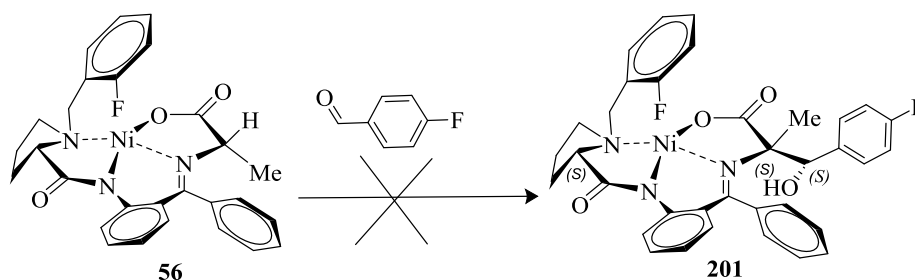
The reaction between glycine Ni^{II} complex Schiff base **55** and 2-(4-fluorophenyl)oxirane (as an electrophile) was used as an alternative to the aldehydes because it is a stronger electrophile. These reactions were unsuccessful under all the reaction conditions attempted (Table 4.7) with ¹⁹F NMR spectroscopy and mass spectrometry showing only unreacted starting materials.

Table 4.7: Attempted reaction between the glycine Ni^{II} complex and 2-(4-fluorophenyl)oxirane under different reaction conditions



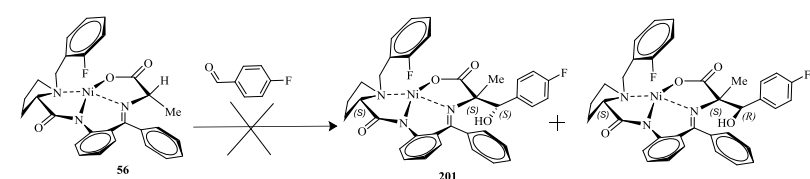
Entry	Electrophile (eq.)	Time (h)	Temperature °C	Outcome
1	3	1	rt	----
2	3	2	rt	----
3	1	1	50	----

4.5.1 Aldol reaction with alanine Ni^{II} Schiff base complex



Attempts were made to synthesise new types of α -amino- β -hydroxy acids using the alanine complex Ni^{II} Schiff base complex instead of that with glycine under a variety of reaction conditions. A fluorinated aromatic aldehyde was chosen as the electrophile to allow the progress of the reaction to be followed. In spite of repeated attempts through various changes to the procedure, including using different solvent protic and aprotic solvent (DMF, THF, MeOH), different bases and different equivalents of those bases (KO^tBu , NaH, KOH and NaOMe), changing the time (1, 2, 3, 6, 18 and 24 hours), and the temperature (0, 25, 50 °C) the reaction was unsuccessful. Unfortunately, analysis of the ^{19}F NMR spectrum of the crude product from these reactions indicated only the presence of starting materials. The main reason for this lack of success could be explained by the reaction mechanism of the glycine complex with the aldehydes during the rearrangement, as two hydrogens in the α -position are necessary in order to form the product.

Table 4.8: Aldol reaction with alanine complex under different reaction conditions

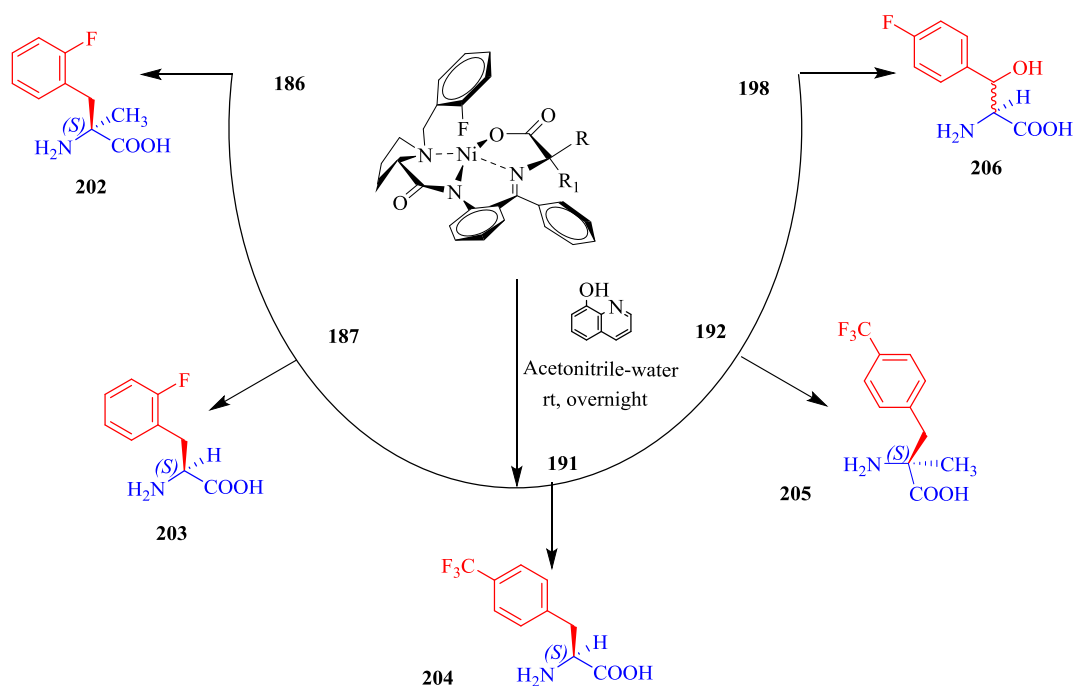


Entry	Base (eq.)	solvent	Electrophile (eq.)	Time (h)	Temperature °C
1	KO^tBu (4)	DMF	2	1h	50
2	KO^tBu (4)	DMF	20	1h	50
3	KO^tBu (8)	DMF	20	2h	50
4	KO^tBu (8)	DMF	20	3h	50
5	KO^tBu (8)	DMF	20	18	rt
6	KO^tBu (8)	MeOH	20	6	rt
7	KOH(8)	MeOH	20	6	rt
8	NaOMe(4)	MeOH	4	1	rt
9	NaOMe(4)	MeOH	4	2	rt
10	NaOMe(4)	MeOH	2	2	0

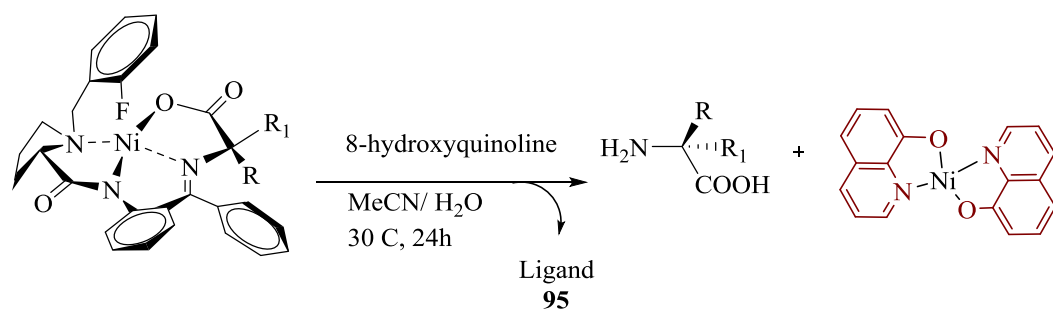
11	NaOMe(8)	MeOH	20	6	rt
12	NaOMe(72 (2.25 M))	MeOH	20	1	50
13	NaH(4)	THF	2	2	50
14	NaH(4)	THF	4	2	50
15	NaH(10)	THF	8	24	rt

The Aldol reaction with the alanine complex was unsuccessful because of the steric hindrance of the methyl group. α -CH₃ in this reaction.⁹³

4.5.2 Hydrolysis of the complexes under mild conditions



The hydrolysis of the fluorinated complexes has used the new, modified, procedure described in method (I). The reaction was performed under mild reaction conditions at 30 °C. In general, the number of the fluorine peaks in the ¹⁹F NMR spectra are expected to decrease, because one of the peaks arises from the ligand which is removed after the hydrolysis by the extraction with DCM, diethyl ether and ethylacetate. ¹⁹F NMR spectroscopy and the LC-MS and HRMS-ESI mass spectroscopy provided evidence for the synthesis of the products and allowed the reaction to be monitored and the resultant product purities to be determined.

Table 4.9: Hydrolysis of the Ni^{II} Schiff base complexes under mild conditions

Entry	Starting material (Ni ^{II} complex)	Product	Yield (%)
1	 192	 202	86
2	 191	 203	68
3	 187	 204	93
4	 186	 205	69
5	 198	 206	69

In entry 1, (*S*)-2-amino-3-(2-fluorophenyl)-2-methylpropanoic acid **202** was produced via hydrolysis of compound **192** under mild conditions. ^{19}F NMR spectroscopy showed a singlet peak at -115.7 (s). Moreover, the analysis of ^1H NMR, ^{13}C NMR and LC-MS and HRMS-ESI mass spectroscopy demonstrated the identity of the product.

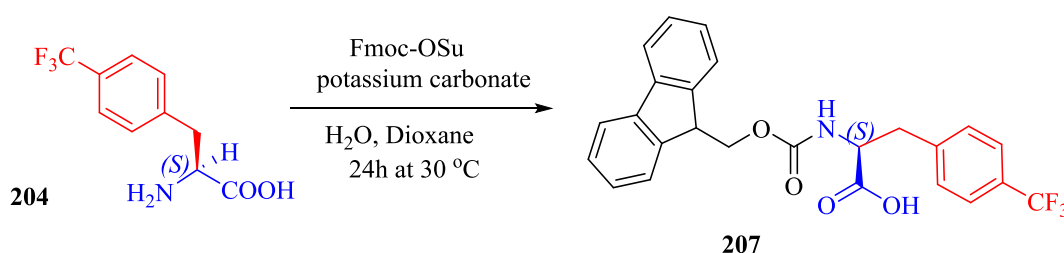
Complex **191** was decomposed and the fluorinated amino acid **203** was formed. The product was isolated in a 68 % yield and in high enantiomers. The ^{19}F NMR spectrum showed one peak at -117.7 (s), and along with ^{13}C NMR, ^1H NMR, LC-MS mass and HRMS-ESI mass spectroscopy demonstrated the identity of the product.

Complex **187** was hydrolysed under similar conditions to produce (*S*)-2-amino-3-(4-(trifluoromethyl)phenyl)propanoic acid **204**. The product was identified by ^1H NMR, ^{13}C NMR, LC-MS and HRMS-ESI mass spectroscopy and by ^{19}F NMR spectroscopy, which showed a singlet peak at -60.7 (s).

(*S*)-2-amino-2-methyl-3-(4-(trifluoromethyl)phenyl)propanoic acid **205** was synthesised by hydrolysis of **186**. The presence of the product was demonstrated by ^{19}F NMR spectroscopy, which showed a singlet peak at -62.4 (s), in combination with ^1H NMR and ^{13}C NMR spectroscopic data and LC-MS data and HRMS-ESI mass spectroscopy.

Similarly, the hydrolysis of complex **198** produced (*S*)-2-amino-3-(4-(trifluoromethyl)phenyl)propanoic acid **206** under the same reactions conditions. ^{19}F NMR spectroscopy showed a singlet peak at -114.9. Moreover, analysis of the ^1H NMR, ^{13}C NMR, HRMS-ESI mass spectrum, and LC-MS data demonstrated the identity of the product.

4.5.3 Fmoc-protection of a fluorinated amino acid



(*S*)-2-((((9H-fluoren-9-yl)methoxy)carbonyl)amino)-3-(4-(trifluoromethyl)phenyl)propanoic acid **207** was produced using a general procedure by reacting the (*S*)-2-amino-

3-(4-(trifluoromethyl)phenyl)propanoic acid at 30 °C under basic conditions (sodium carbonate) with (*S*)-2-amino-3-(4-(trifluoromethyl)phenyl)propanoic acid. The product was isolated in a 46 % yield. ^{19}F NMR spectroscopy showed a singlet peak at -60.8 (s), which helped confirm the identity of the product. ^1H NMR spectroscopy showed multiple peaks for 8H in the aromatic region, along with CH aromatic peaks in the ^{13}C NMR spectrum, assigned to the fluoren-9-yl group. The new Fmoc-amino acid 3.15 was also identified with the LC-MS and HRMS-ESI.

4.5.4 Conclusions

Fluorine has become a common component in protein design with the creation of non-natural fluorinated amino acids. The synthesis of new complexes, including a fluorine atom in new amino acids, has been achieved via Ni^{II} Schiff base complexes. The ^{19}F NMR data reveals that, after reaction of the Ni^{II} Schiff base derivatives, the signal(s) of the fluorine substituents have been shifted, which indicates that the environment has a strong effect on the position(s) of the peak(s). The results presented in this work suggest that ^{19}F NMR spectroscopy is a great probe to monitor these reaction and to give an indication of the purity of the products.

In this chapter the synthesis of fluorinated amino acids has been accomplished via two routes: Alkylation and aldol reactions on the Ni^{II} Schiff base complexes. The products showed high stability at the room temperature.

A) In the alkylation reaction two electrophiles were used:

1) 1-(Bromomethyl)-4-trifluoromethylbenzene

Synthesis of complexes **186**, **187** and **189** from **55**, **56** and **100** respectively in good yield and high diastereoisomers (>99 % de). Complex **101** was unreacted with 1-(bromomethyl)-4-trifluoromethylbenzene, however, many reaction condition were attempts.

2) 1-(Bromomethyl)-2-fluorobenzene

Synthesis of complexes **191** and **192** from **55** and **56** respectively in good yield and high diastereoisomers (>99 % de).

B) In the Aldol reaction also two electrophiles were used:

1) 4-Fluoro-benzaldehyde

Synthesis of complex **198** from **56** in a good yield. ^{19}F NMR spectroscopy showed the complex is a racemic mixture (*2S*, *3S*) and (*2S*, *3R*). Complex **55** was unreacted with 4-fluoro-benzaldehyde, however, fifteen different reaction conditions were attempted.

2) 2-(4-Fluorophenyl)oxirane

The attempts to react this electrophile with complex **55** under different reaction conditions were unsuccessful.

Hydrolysis of the complexes generated the fluorinated amino acids **202-207** from **186-187**, and **191-198** respectively in good yield and high diastereoselectivity (>99 % de).

Chapter 5

Synthesis of Novel Stapled Peptides



UNIVERSITY OF
LEICESTER

5.1 Introduction

In recent years, there has been an increasing interest in developing and improving the synthetic strategies to conformationally constrained peptides. There is a large volume of published studies describing the role of constrained stapled peptides. There are many types of helix constraints, as explained in Chapter 1. Staples are used to connect the two side chains, which should be on the same side and between them there should be one turn ($i, i+4$), two turns ($i, i+7$), or three turns ($i, i+11$) and the distance per turn in the α -helix has 3.6 residues.¹⁹² During the past 30 years much more information has become available on this topic, especially hydrocarbon stapled peptides. The olefin stapled peptides show good bioactive conformation leading to new physicochemical and pharmacological properties.

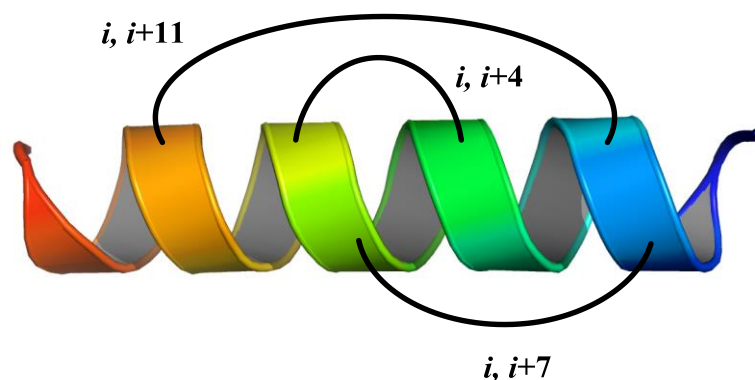


Figure 5.1: α -Helix staples at positions ($i, i+4$), ($i, i+7$) and ($i, i+11$)

In 2000, the first alkene stapled peptide was presented by Verdine *et al.*,⁶³ which was followed by many papers and reviews¹⁹³⁻¹⁹⁶ published over recent years on the design of new alkene hydrocarbon staples, because this approach showed positive impacts in both biological activity and helix stabilization properties, making it a very useful type of helix constraint. However, the alkene hydrocarbon staple has been confirmed to have two configurations (*cis* and *trans*). A strong relationship between the length of the alkene side chain and a conformational mixed set of products has been reported in the literature.¹⁹⁶

Throughout this chapter the $Ri,i+4S(x)$ term will be used to describe the staple and refers to the positions of the amino acids. Their distance apart (x) is the number of the carbon atoms in the bridge (linker length) and R and S refer to the chirality of the amino acids that form the bridge. The lengths of the carbon atom linkers are very significant in the

ring closing metathesis (RCM) reaction. A positive correlation has been found between the possibility of the ring closing and the length of the linker. There is a 98 % probability for RCM in an $i, i+4$ bridge for an 8 atom or more chain, whilst for an $i, i+7$ bridge 10 carbon atoms or more increase the probability of RCM to the same 98 %. There are several possible explanations for this result. For example, when the linker length has been increased to 12 carbon atoms or more, the possibility of forming either a *cis* and *trans* alkene configuration increases, and one isomer has greater stability than the other (18 %, vs 7 %).^{63, 197} Alternatively, there are weaknesses in the alkene staple, such as, when the bridge length increases it becomes more flexible and reduces the impact of the staple on the helical structure, especially in $i, i+7$ and $i, i+11$ staples. This leads to peptides having less effective conformational constraint and having an impact upon their physicochemical features.^{59, 198} For example, Futaki *et al.* reported work on alkene stapled hydrocarbons, formed by ring closing metathesis, using alkene side chains with different lengths of carbon atoms. S_5 and R_8 alkene amino acids were used in both positions $i, i+4$ and $i, i+7$ in numerous examples and compared with peptides such as: ATSP6935, SAHp53, SAHB, STAD, WAHM, and SAHM. The comparison between the stapled and the unstapled peptides showed the effect of the staple formation on these peptides. On the one hand, the work demonstrated that there was no correlation in the affinity (high in both sets) between cellular up-take and helix formation. However, results obtained from the preliminary analysis of biological activity between the ring opened and the ring closed peptides against HeLa cells (Figure 5.2) showed that the ring opened ones were more active than the ring closed ones.¹⁹⁹

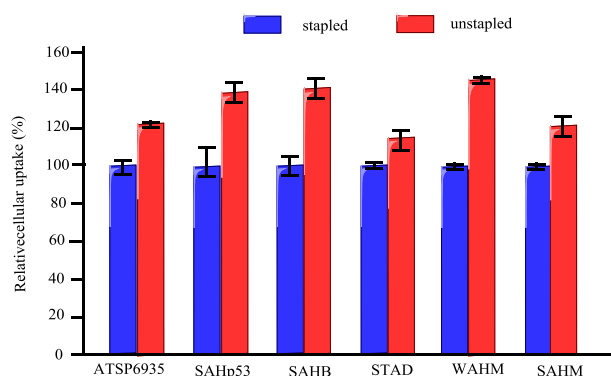


Figure 5.2: Stapled peptides showed less activity to HeLa cells than unstapled peptides when using (1 μ M) at 37 °C for 1 h

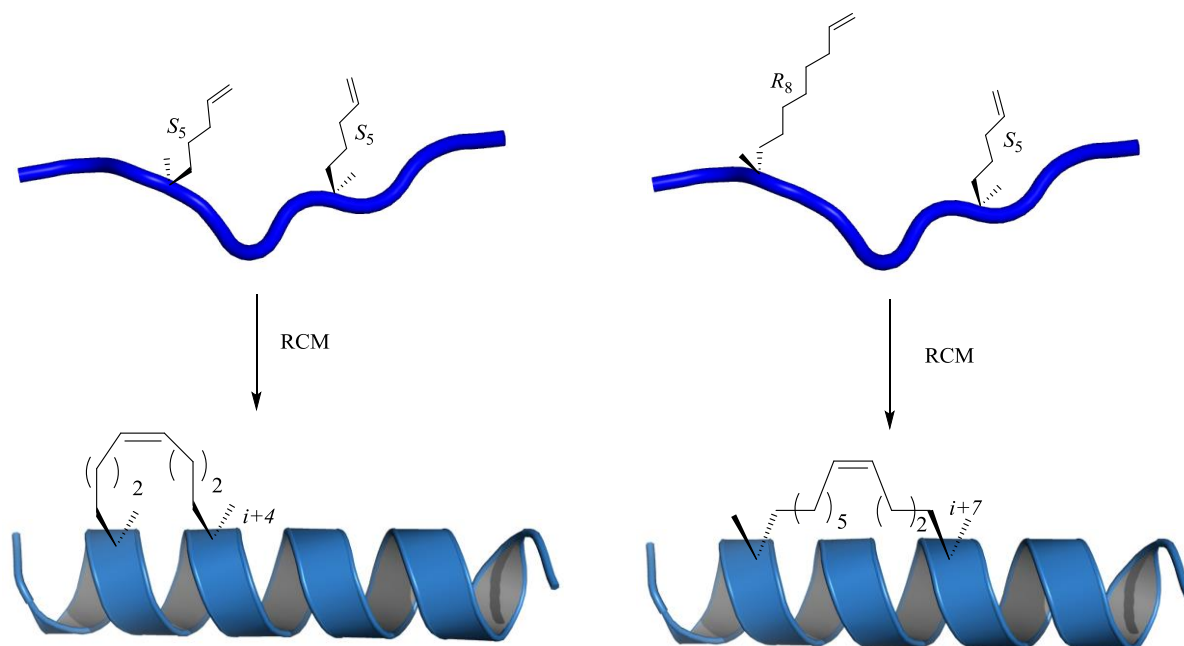


Figure 5.3: The structure of helical peptides through all-hydrocarbon staple formation

More recently, literature has emerged that offers alternative findings around developing new methods that increase the stability of the helix and helping to resolve the problem(s) that arise from using a single staple on the peptide by making a double stapled linker. An example of this is the study carried out by Chapuis and co-workers using olefin helix staples. They used both single and double staples in the α -helix in two types of anti-microbial peptides: lasioglossin III and melectin. They used two types of olefin in different positions in the peptide sequences for RCM by using two amino acids S_5 at positions i , $i+4$ and S_5 and R_8 at positions i , $i+7$. The single stapled peptides showed a greater resistance than the native peptides against proteolytic degradation, but the double stapled ones showed an even higher resistance than the single stapled ones. However, both the single and the double stapled anti-microbial peptide activities showed a reduction as compared to those of the native peptides.²⁰⁰

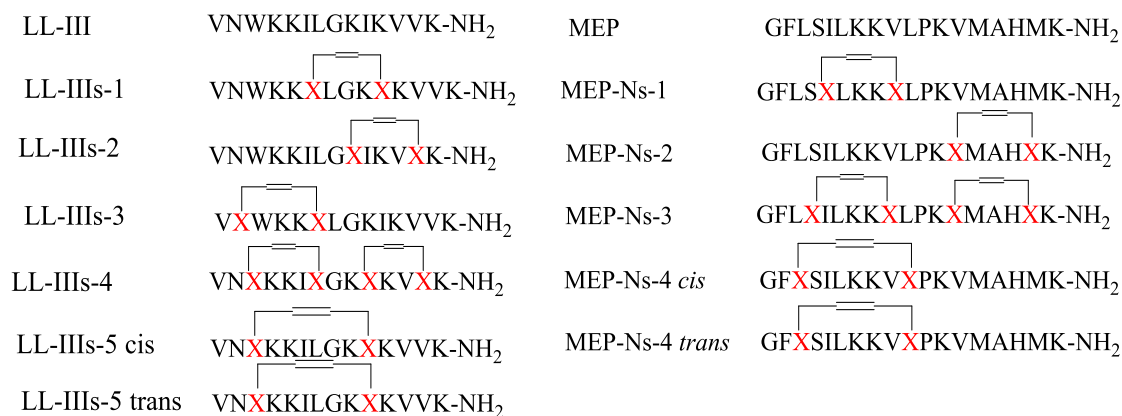


Figure 5.4: Stapled peptides on the lasioglossin (LL-III) and melectin (MEP-N)

5.2 Alkyne bonds

Recent developments in the field of stapled helices have led to a renewed interest in solving the problems of the *cis* and *trans* configuration issues of olefin staples over large distances such as $i, i+7$ and $i, i+11$ by making alkyne linkers instead of alkene ones. The alkyne group has a linear shape because the hybridisations of the carbon atoms are sp . Using an alkyne in the organic compounds can be viewed like a girder, which would avoid the conformational disadvantages of the alkene staples. This new type of hydrocarbon unit can be the initiator to use instead of alkenes in the synthesis of new stapled peptides. In 2016, Cromm and co-workers presented a new type of double stapled peptide using this new type of staple in bicyclic peptides containing a mixture of alkyne stapled and olefin stapled α -helices. The approach used both ring-closing olefin (RCM) and alkyne metathesis (RCAM). The new staple was used in positions $i, i+4$ by using molybdenum complexes (**208** and **209**) as catalysts for the ring closure. Different lengths of the alkyne side chain of amino acids were used (Figure 5.5). The work was applied to the small GTPase Rab8 bicyclic peptide and the resulting stapled peptides showed great activity as inhibitors.²⁰¹

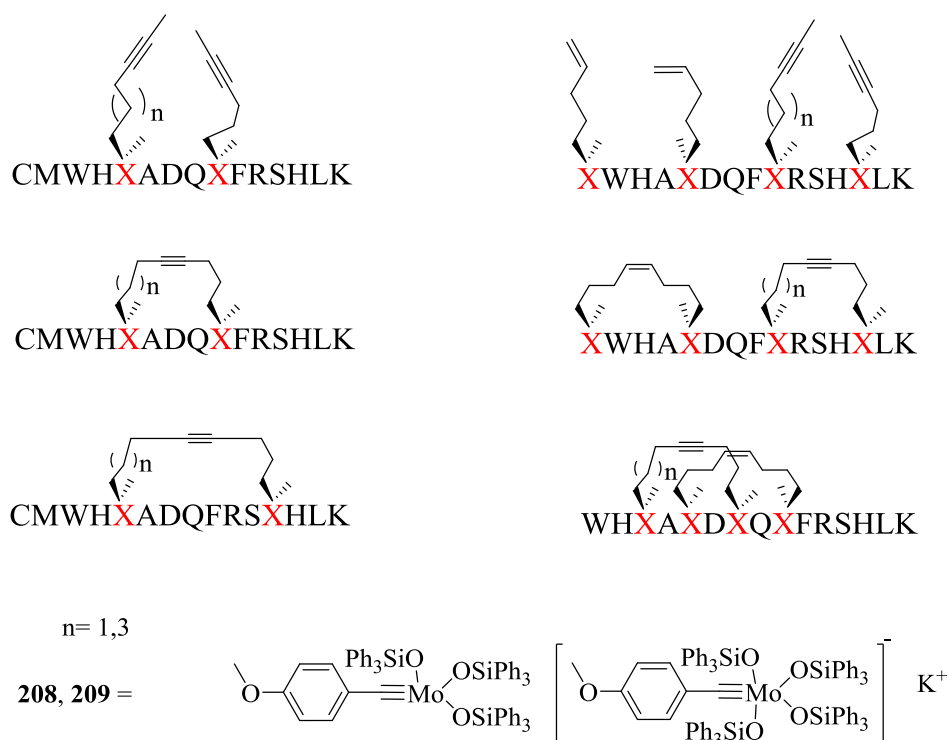


Figure 5.5: Synthesis of the bicyclic peptides using RCM and RCAM

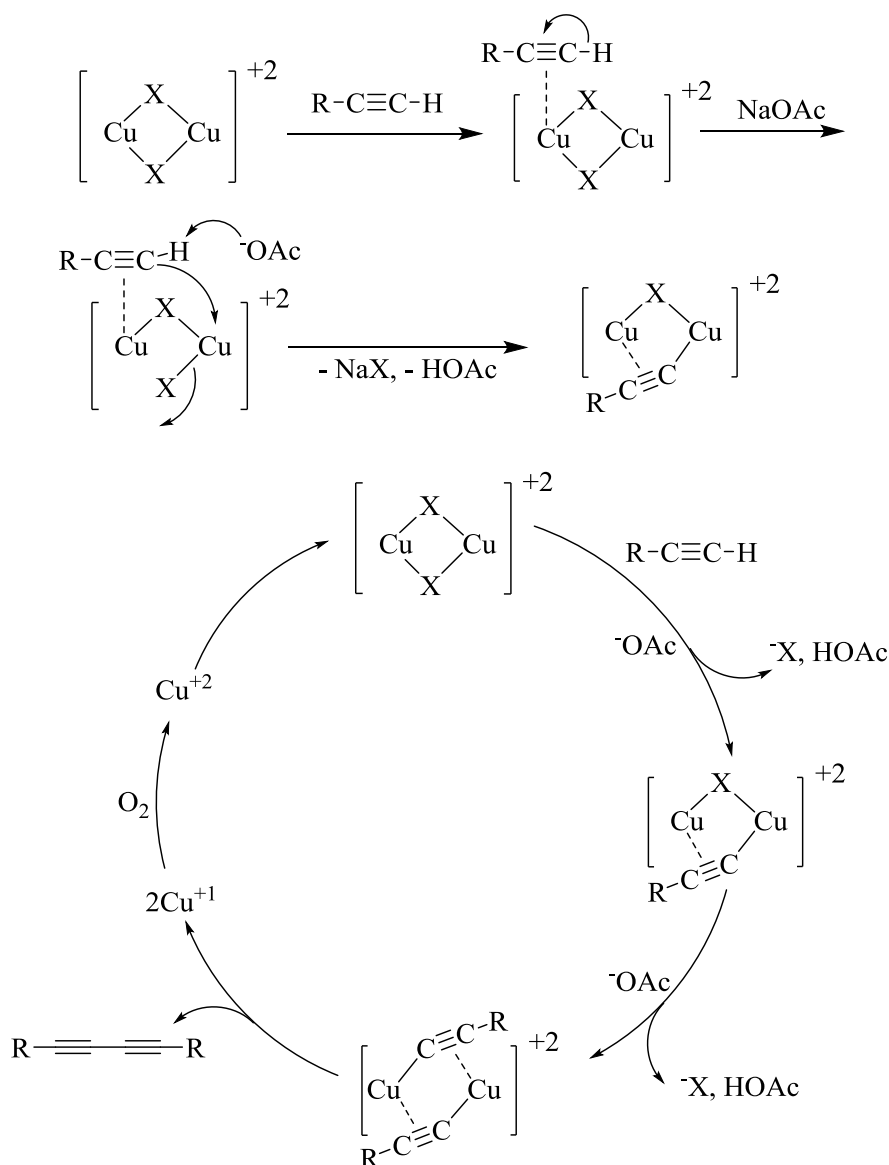
5.3 1,3-diyne bonds

A hundred years ago the Glaser coupling reaction was discovered, which was used to synthesise 1,3-diynes and has been used in a wide range of organic reactions.^{202, 203} In this reaction copper salts or expensive palladium salts were used as a catalyst with an amine base in an organic solvent. The Cu(X) catalytic activity depended on the counterion (X), which showed that the activity follows this order: $\text{I}^- > \text{Br}^- > \text{Cl}^- > \text{AcO}^- > \text{NO}_3^- > \text{SO}_2^-$. In a major study,^{110, 137} Li *et al.* showed a great example of the use of the Glaser coupling reaction to make a dimer of phenylacetylene by using $\text{CuCl}_2 \cdot 2\text{H}_2\text{O}$, NaOAc and polyethylene glycol (PEG) at different temperatures and for different reaction times. After optimising the reaction conditions and finding the best temperature, which was 120 °C, the reaction time was shown to be dependent on the aromatic and aliphatic substituents (Table 5.1) The proposed mechanism for the Glaser coupling reaction is shown in Scheme 5.1.²⁰³

Table 5.1: 1,3-diyne reaction conditions for aromatic and aliphatic alkynes

$$2 \text{ R}-\text{C}\equiv\text{C}-\text{H} \xrightarrow[\text{PEG-1000/ O}_2, 120 \text{ }^\circ\text{C}]{\text{CuCl}_2 \cdot 2\text{H}_2\text{O/ NaOAC}} \text{R}-\text{C}\equiv\text{C}-\text{C}\equiv\text{C}-\text{R}$$

Entry	R	Time	Yield (%)
1	C ₆ H ₅	1.5	99
2	<i>p</i> -CH ₃ C ₆ H ₄	1.5	86
3	<i>m</i> -CH ₃ C ₆ H ₄	3	99
4	<i>p</i> -CH ₃ OC ₆ H ₄	1.5	72
5	<i>p</i> -FC ₆ H ₄	1.5	97
6	<i>n</i> -C ₄ H ₉	12	52
7	<i>n</i> -C ₆ H ₁₃	48	95
8	<i>n</i> -C ₈ H ₁₇	48	73



Scheme 5.1: 1,3-Diyne reaction mechanism

5.4 Analysis of the conformation of peptides

Circular dichroism (CD) is a significant spectroscopic technique that can be used to investigate the conformation of the secondary structure of peptides in the solution.²⁰⁴ In CD compounds are irradiated in 178-250 nm region. The main important absorptions for the α -helix are at 222 and 208 nm in the negative ellipticity and also at 193 nm in the positive ellipticity. β -Sheets show a significant absorption at around 218 nm in negative ellipticity and around 195 nm in positive ellipticity, whilst random conformations show absorptions around 200 nm in negative ellipticity (Figure 5.6).

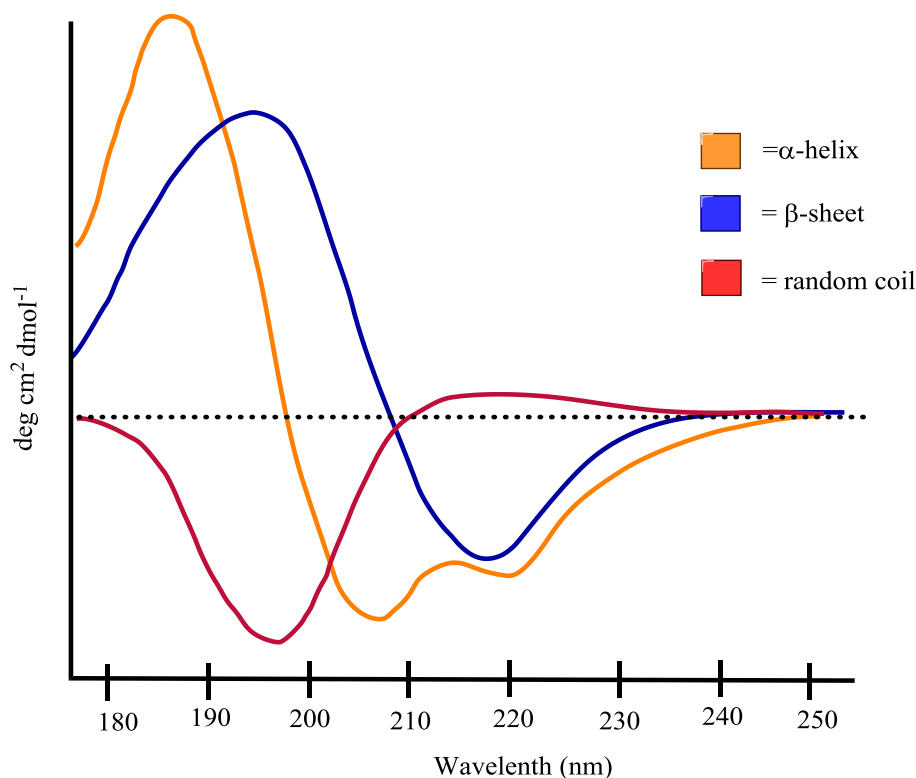


Figure 5.6: Peptide secondary structures: α -helix, β -sheet and random coil²⁰⁵

The region of the CD experiment (180-240 nm) is associated with the transitions of the non-bonding electrons, which can be divided into two types of transition: 1) $n \rightarrow \pi^*$, such as the electrons in the oxygen and nitrogen atoms at around 220 nm; 2) $\pi \rightarrow \pi^*$, for delocalized electrons in π -bonds at around 190 nm. Moreover, differences in the secondary-structures of peptides give an increase in the CD spectra in the far UV range, allowing a quantitative estimation of the peptide secondary structure. Consequently, this technique has become commonly used in peptide synthesis to estimate the structure of the peptide. In this technique $[\theta]$ is the mean residue molar ellipticity, with units $\text{deg.cm}^2.\text{dmol}^{-1}$, and it can be calculated using the equation below, where M_r is the molecular mass, l is the optical pathlength, c is the concentration of the peptide (mg/mL) and n is the number of residues in the peptide (amino acids).²⁰⁵

$$[\theta] = \frac{\theta \times 100 \times M_r}{c \times l \times n}$$

For a fully helical peptide the maximum value of $[\theta]$ at 222 nm is $-39,500 \text{ deg.cm}^2.\text{dmol}^{-1}$. So, using the equation below, this technique can be used to estimate the percentage of the α -helix for peptides through calculating $[\theta]$ for the absorption at 222 nm from the CD

spectrum; where i is the number of helices in the sample, n is the number of the residues (amino acids) and k is the wavelength specific constant, which is 2.57 at 222 nm.²⁰⁵

$$\% \alpha\text{-helicity} = \frac{[\theta]}{\theta_{222}^{\infty} \left[1 - \left(\frac{ik}{n} \right) \right]} \times 100$$

5.5 Apoptosis of peptides

Apoptosis is the control mechanism in genetic systems, which leads to cell death when the cell has achieved its mission or when the gene is damaged.¹⁹³ B cell leukemia/lymphoma 2 (Bcl-2) is a member of the apoptosis family. The Bcl-2 family can be sub-divided into two types: anti-apoptotic and pro-apoptotic member proteins. Pro-apoptotic proteins consist of Bcl-2 homology 3 domain (BH3) peptides and also consists of eight types: BAD, BIM, BID, PUMA, HRK, BIK, BMF and BAD (Figure 5.7).^{206, 207}

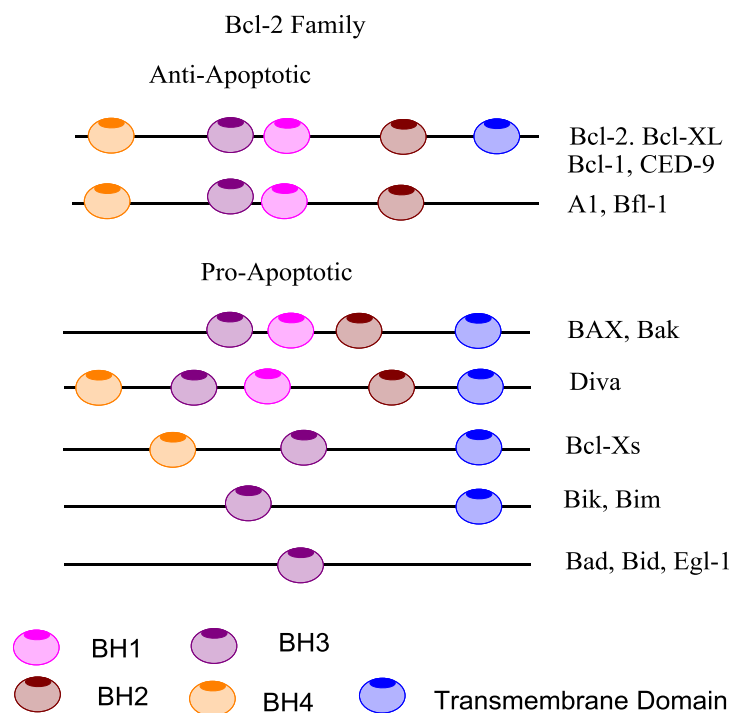
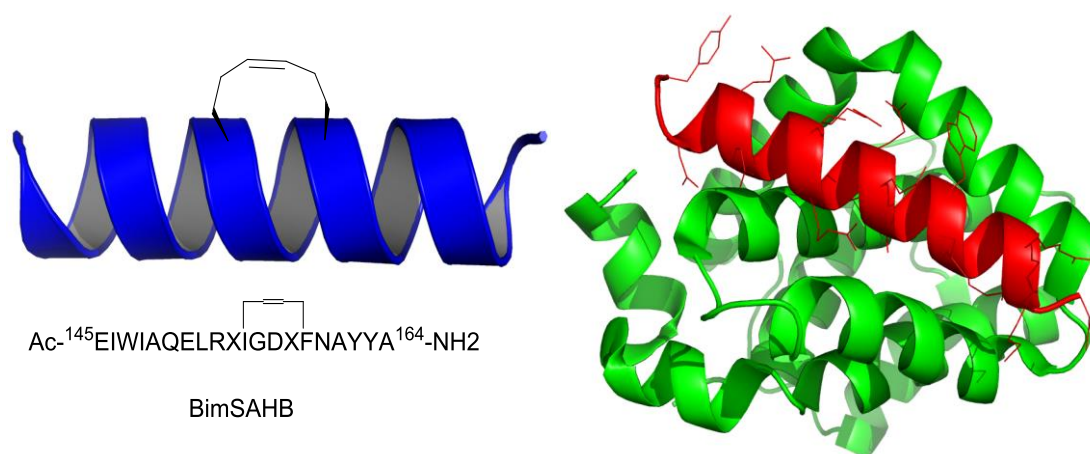


Figure 5.7: Bcl-2 Family showing Anti-Apoptotic and Pro-Apoptotic Proteins

During the past 30 years a large amount of new information has become available on pro-apoptotic, and especially, Bim peptides, such as the sequence and the activity. Several attempts have been made to synthesise the peptide with staples, including various

methods to increase the helicity and also the binding affinity. Different types of staples have been used and a few of these have shown great results.

Czaboter and co-workers presented a great example of a stapled Bim peptide with a hydrocarbon staple, which showed a great stability of the α -helix conformation relative to the native peptide. The stapled peptide used was *i, i+4* (Bim peptide sequence= 145-164 amino acids). However, the stapled peptide showed less affinity as a pro-apoptotic. The main reason for the loss of affinity is that there are intra-molecular interactions which affected the network stability. The new peptide had less apoptosis activity than the native Bim peptide.⁵⁹



Scheme 5.2: Images of the structure of the stapled Bim peptide⁵⁹

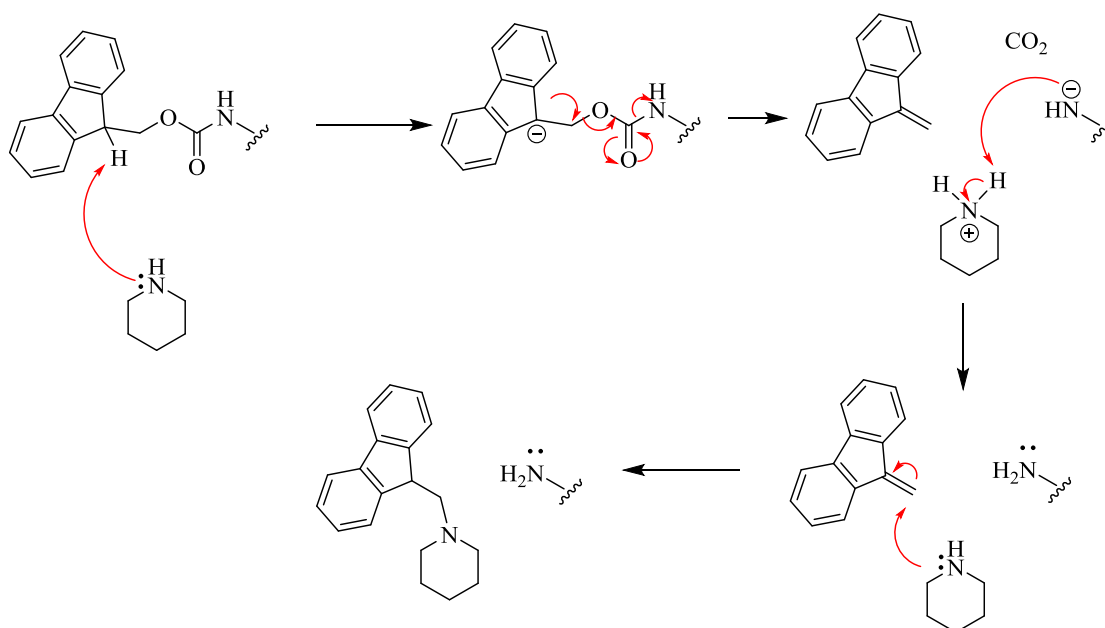
5.6 Synthesis of peptide models using the SPPS method

In general, solid phase peptide synthesis (SPPS) can be divided into two types: the Boc strategy and the Fmoc strategy dependent on the resin used. In this chapter the focus will be on the Fmoc strategy in SPPS. The main advantage of this strategy is the orthogonality with the protecting group on the side chain of the amino acids. Furthermore, in the Fmoc-based SPPS reaction, the deprotection of the Fmoc can be easily done using piperidine as a basic catalyst. This works under mild reaction conditions which do not affect the other protecting groups on the side chains of the amino acids. In contrast, in the Boc strategy, removal of the Boc protecting group needs a strong acid, such as trifluoroacetic acid

(TFA), which will also remove almost all of the protecting groups on the side chains of the amino acids in the peptide sequence.

5.7 Deprotection of the Fmoc group

The Fmoc group is one of the important protecting groups in peptide synthesis. The Fmoc group can be removed under base conditions because the deprotonation of the fluorenyl group is facilitated by the formation of the anion which generates an aromatic 14 π electron system. This means that Fmoc reacts easily with weak bases, such as piperidine, to form an aromatic cyclopentadiene-type intermediate, which directly undergoes β -elimination. This step forms dibenzofulvene (a highly reactive compound) which reacts with the excess of base to form a highly stable by-product (fulvene-piperidine) (Scheme 5.3).²⁰⁸

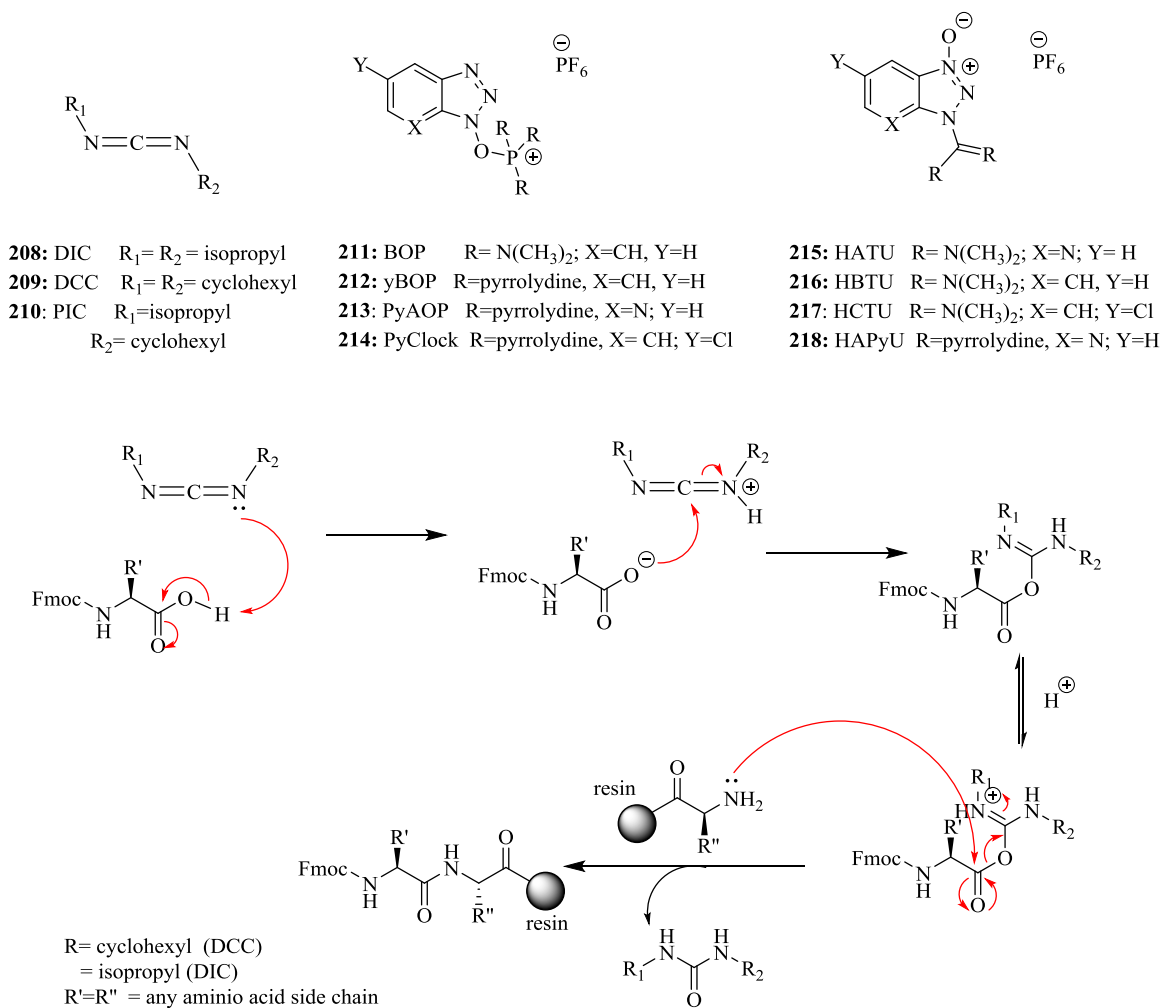


Scheme 5.3: Mechanism of Fmoc deprotection with piperidine

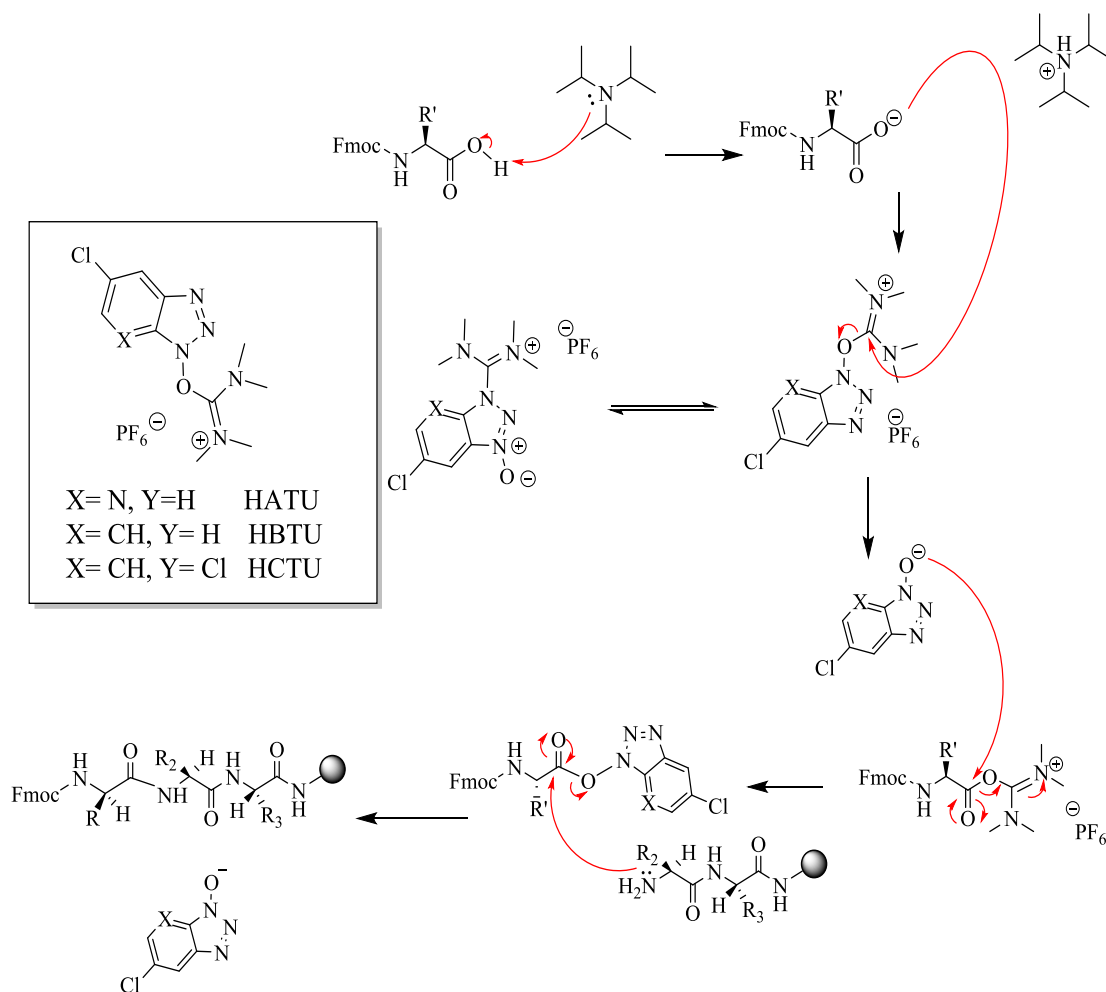
5.8 Coupling reaction in peptide synthesis

The free amine group on the peptide-resin undergoes a coupling reaction which is followed by Fmoc-deprotection of the newly added amino acid. In each step, the protected amino acid (Fmoc-amino acid) will be coupled with the de-protected amino acid on the peptide-resin, which has already been coupled with the resin. In this work, in

the coupling reaction *N,N,N',N'*-tetramethyl-*O*-(6-chloro-1*H*-benzotriazol-1-yl)uronium hexafluorophosphate (HCTU) is used as an activator to the Fmoc-amino acid, however, there are various other types of activator that have been used in peptide synthesis. A proposed amino acid coupling mechanism using carbodiimides as an activator is shown in Scheme 5.4.²⁰⁸



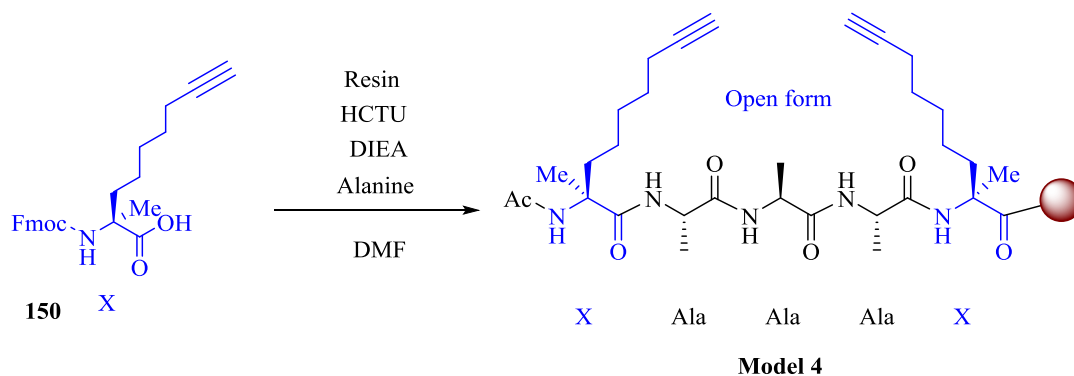
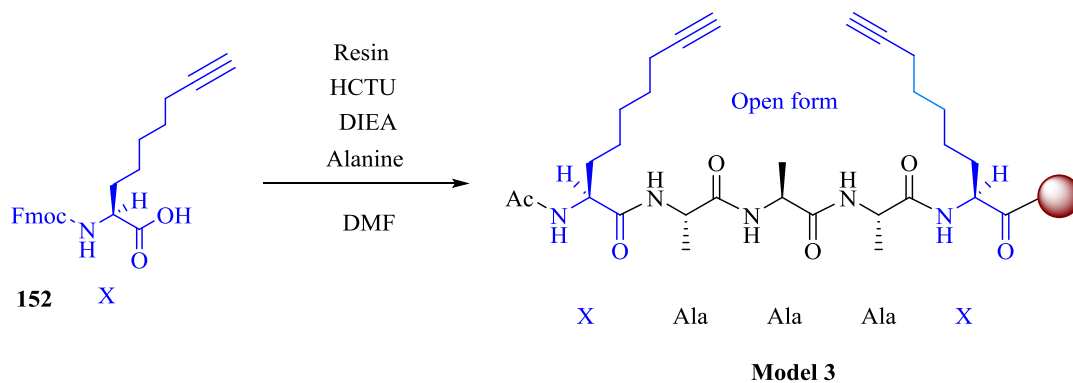
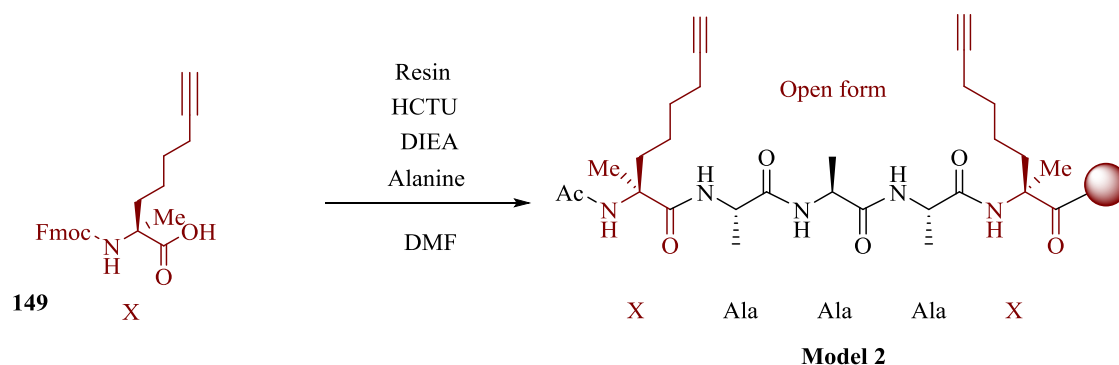
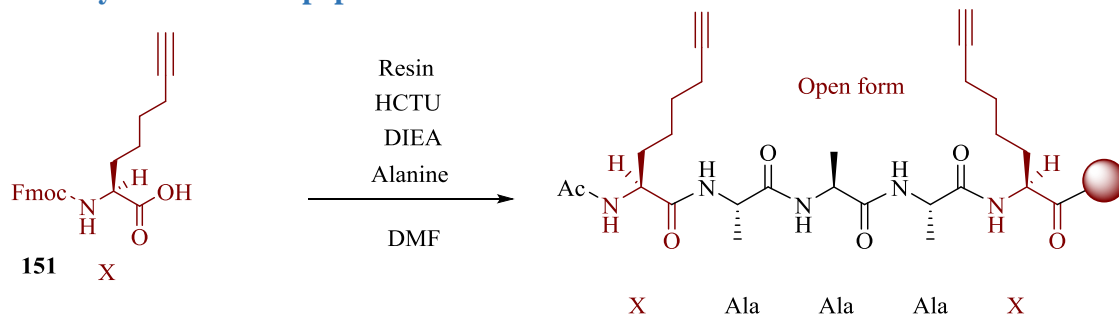
Scheme 5.4: Coupling agents used in peptide synthesis and the mechanism of the coupling reaction using carbodiimides



Scheme 5.5: Amino acid coupling mechanism

In the coupling reaction, (HCTU) is used under basic conditions, such as diisopropylethylamine (DIPEA). The function of using the base in the coupling reaction is removal of the acidic proton of the protected amino acid and formation of a negative charge. The carboxylate anion reacts as a nucleophile and attacks the HCTU. Finally, the amine of the amino acid on the peptide-resin attacks the carbonyl carbon atom in the activated amino acid with the elimination of 6-chloro-*O*-benzotriazole. The length of the peptide-resin is increased as an extra amino acid has been added (Scheme 5.5).²⁰⁸

5.9 Synthesis of the peptide models



A manual method has been used to synthesise the peptide models using a shaker instrument and microwave methods. Four amino acids were used as starting materials for synthesising these models, which were derivatives of glycine [C6 **151**, C7 **152**] and derivatives of alanine [C6 **149**, C7 **150**]. The shaker instrument method takes a long time

to synthesise the peptide. For example; a natural Fmoc-protected amino acid needed 15 minutes shaking in the coupling reaction, whilst the new unnatural Fmoc-protected amino acids required 3 hours for the same reaction. However, using the microwave method all the Fmoc-protected amino acids were coupled at 70 °C for 5 min.

In general, the first step was to activate the amino acid using two equivalents of HCTU. These were dissolved in DMF (dry) (0.2 M) and four equivalents of DIPEA and NMP were dissolved in DMF (dry), which was left for around 10 minutes to activate the Fmoc-amino acid. After each coupling reaction the deprotecting step followed. Generally, all the models consisted of two alkynyl amino acids, one on each side, and three alanine amino acids in the middle to allow one turn of an α -helix in the peptide. Finally the acetate group was introduced by reaction with acetic anhydride as a cap of the peptide-resin. After each step of the coupling and decoupling reactions, the peptide was tested using the Kaiser test as an indicator of the presence of free NH_2 groups. The peptides were analysed with LCMC and the reaction monitored by the cleavage test (using 5 mg of the peptide-resin dissolved in acetonitrile): water (1:1) (1-2 mL) to verify the conversion ratio of the product. Using a microwave reactor really reduced the reaction times, as did the use of RP-HPLC during purification to obtain high purity products.

Model 1 is a ring opened peptide, which was synthesised with the C6 alkynyl glycine derivative **151**. The crude peptide was purified by RP-HPLC $t_R = 18.837$ min, after cleavage with TFA, to give the product as a white powder in a 15 % yield. The HRMS-ESI showed a peak at 547.3257 (calcd. for $\text{C}_{27}\text{H}_{43}\text{N}_6\text{O}_6$ $[\text{M}-\text{NH}_2]^+$ 547.3244) ($\Delta = 2.4$ ppm). Furthermore, the analytical-HPLC showed a single peak which confirmed the purity of the product.

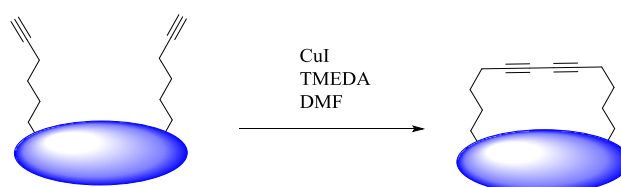
Model 2 is a ring opened peptide, which was synthesised with the C6 alkynyl alanine derivative **149**. The crude peptide was purified by RP-HPLC $t_R = 20.883$ min, after cleavage with TFA, to give the product as a white powder in a 23 % yield. The HRMS-ESI showed a peak at 597.3392 (calcd. for $\text{C}_{29}\text{H}_{46}\text{N}_6\text{O}_6\text{Na}$ $[\text{M}-\text{NH}_2]^+$ 597.3377) ($\Delta = 2.5$ ppm). Furthermore, the analytical-HPLC showed a single peak which confirmed the purity of the product.

Model 3 is a ring opened peptide, which was synthesised with the C7 alkynyl glycine derivative **152**. The crude peptide was purified by RP-HPLC $t_R = 20.810$ min, after

cleavage with TFA, to give the product as a white powder in a 12 % yield. The HRMS-ESI showed a peak at 575.3567 (calcd. for $C_{29}H_{47}N_6O_6$ $[M-NH_2]^+$ 575.3557) ($\Delta = 1.7$ ppm). Furthermore, the analytical-HPLC showed a single peak which confirmed the purity of the product.

Model 4 is a ring opened peptide, which was synthesised with the C7 alkynyl alanine derivative **150**. The crude peptide was purified by RP-HPLC $t_R = 22.953^a$ min, after cleavage with the TFA, to give the product as a white powder in a 9 % yield. The HRMS-ESI showed a peak at 625.3724 (calcd. for $C_{31}H_{50}N_6O_6Na$ $[M-NH_2]^+$ 625.3690) ($\Delta = 5.4$ ppm). Furthermore, the analytical-HPLC showed a single peak which confirmed the purity of the product.

5.10 Oxidative coupling



For all the stapled peptides models, ring closing metathesis is the cyclisation step of the peptide. The cyclisation step forms a 1,3-diyne group through the Glaser-Hay oxidative coupling reaction. For that reason CuI was used as a catalyst and TMEDA as a base in dry DMF; for the mechanism of the reaction see Scheme 5.1.²⁰⁹ The reaction was performed using the microwave for 2-3 hours at 75 °C at 50 W power. Using the microwave reactor really reduced the reaction time. The use of RP-HPLC during purification allowed a high purity product to be obtained.²⁰⁹

Model 5 is a ring closed peptide, which was synthesised with the C6 alkynyl glycine derivative. The crude peptide was purified by RP-HPLC $t_R = 64.134$ min, after cleavage with TFA, to give the product as a powder in a 21 % yield. The HRMS-ESI showed a peak at 567.2922 (calcd. for $C_{27}H_{40}N_6O_6$ $[M-H]^+$ 567.2907) ($\Delta = 2.6$ ppm). Furthermore, the analytical-HPLC showed a single peak which confirmed the purity of the product.

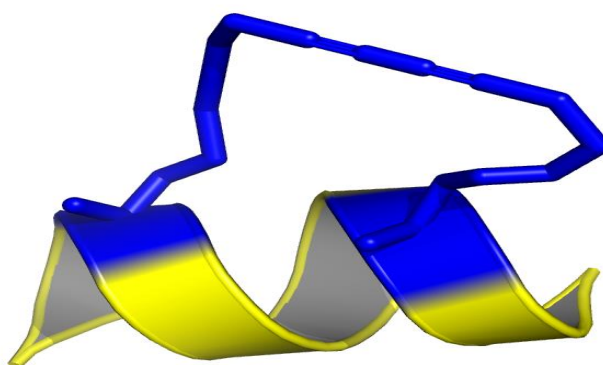
Model 6 is a ring closed peptide, which was synthesised with the C6 alkynyl alanine derivative. The crude peptide was purified by RP-HPLC $t_R = 20.883$ min, after cleavage with TFA, to give the product as a powder in a 27 % yield. The HRMS-ESI showed a

peak at 573.3409 (calcd. for $C_{29}H_{45}N_6O_6$ $[M+H]^+$ 573.3401) ($\Delta = 1.4$ ppm). Furthermore, the analytical-HPLC showed a single peak which confirmed the purity of the product.

Model 7 is a ring closed peptide, which was synthesised with the C7 alkynyl glycine derivative. The crude peptide was purified by RP-HPLC $t_R = 36.210$ min, after cleavage with TFA, to give the product as a powder in a 22 % yield. The HRMS-ESI showed a peak at 573.3403 (calcd. for $C_{29}H_{45}N_6O_6$ $[M+H]^+$ 573.3401) ($\Delta = 0.3$ ppm). Furthermore, the analytical-HPLC showed a single peak which confirmed the purity of the product.

Model 8 is a ring closed peptide, which was synthesised with the C7 alkynyl alanine derivative. The crude peptide was purified by RP-HPLC $t_R = 21.063$ min, after cleavage with TFA to give the product as a powder in a 13 % yield. The HRMS-ESI showed a peak at 623.3552 (calcd. for $C_{31}H_{48}N_6O_6Na$ $[M+Na]^+$ 623.3533) ($\Delta = 3.0$ ppm). Furthermore, the analytical-HPLC showed a single peak which confirmed the purity of the product.

5.11 Conformation analysis of the peptides models



The CD spectra for the stapled peptide models demonstrated that all four of the stapled peptides (models **5-8**) showed α -helical conformations; all the samples of the stapled peptide models were dissolved in deionised water and 10 % of TFE (v/v). It can be clearly seen that model **8** has the best helical conformation of these model peptides (59 %, Figure 5.8, orange coloured line). Comparing the data for the four models, in the presence of 10 % TFE, it can be seen that there is a great difference between the percentage helicities that can be reached in these $i, i+4$ peptides. However, these show that, even

with the stapled model 8, we have not been able to reach the maximum helicity possible for peptides with these 1,3-diyne staples.

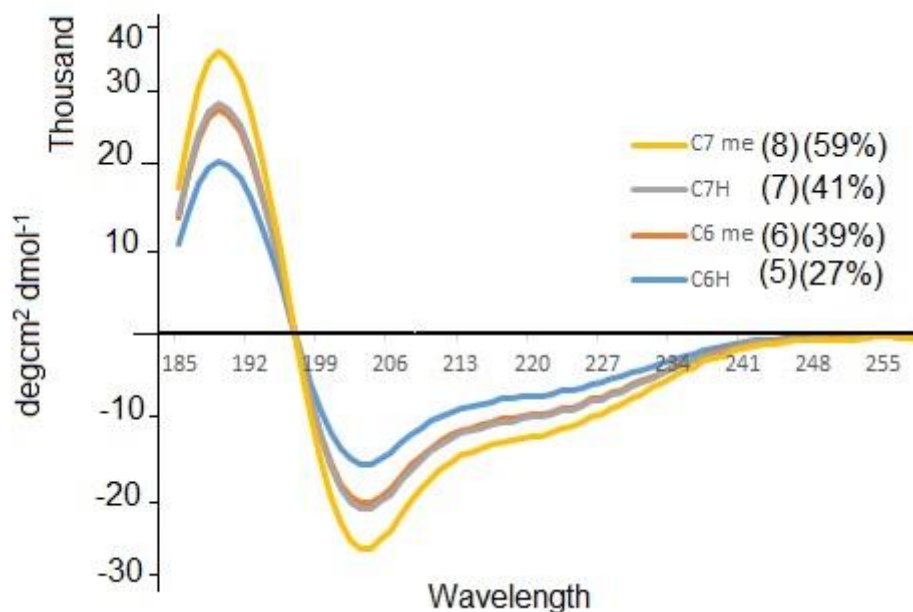


Figure 5.8: CD spectra of the stapled peptide models 5-8, scanned in 10 % TFE/H₂O

5.12 Application of the 1,3-diyne helices in peptides

Many stapled Bim peptides have been shown to have poor helicities. For example, Okamoto *et al.* have reported a Bim peptide, modified in the *i*, *i*+4 positions, for which the stapled peptide showed 21 % helicity compared with 39 % helicity for the unstapled linear peptide⁵⁹

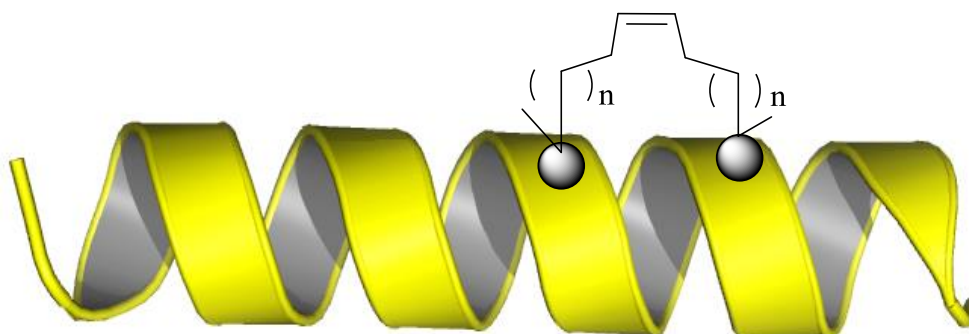
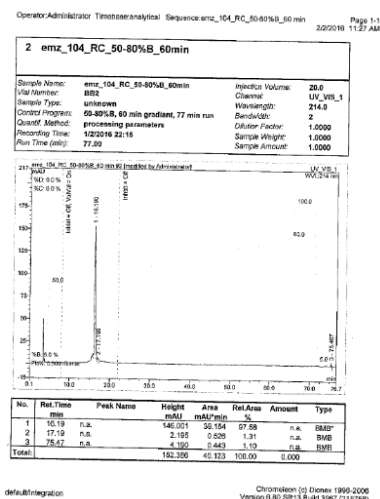
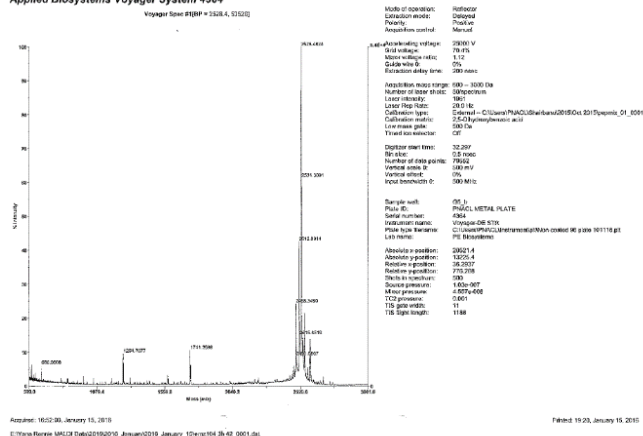


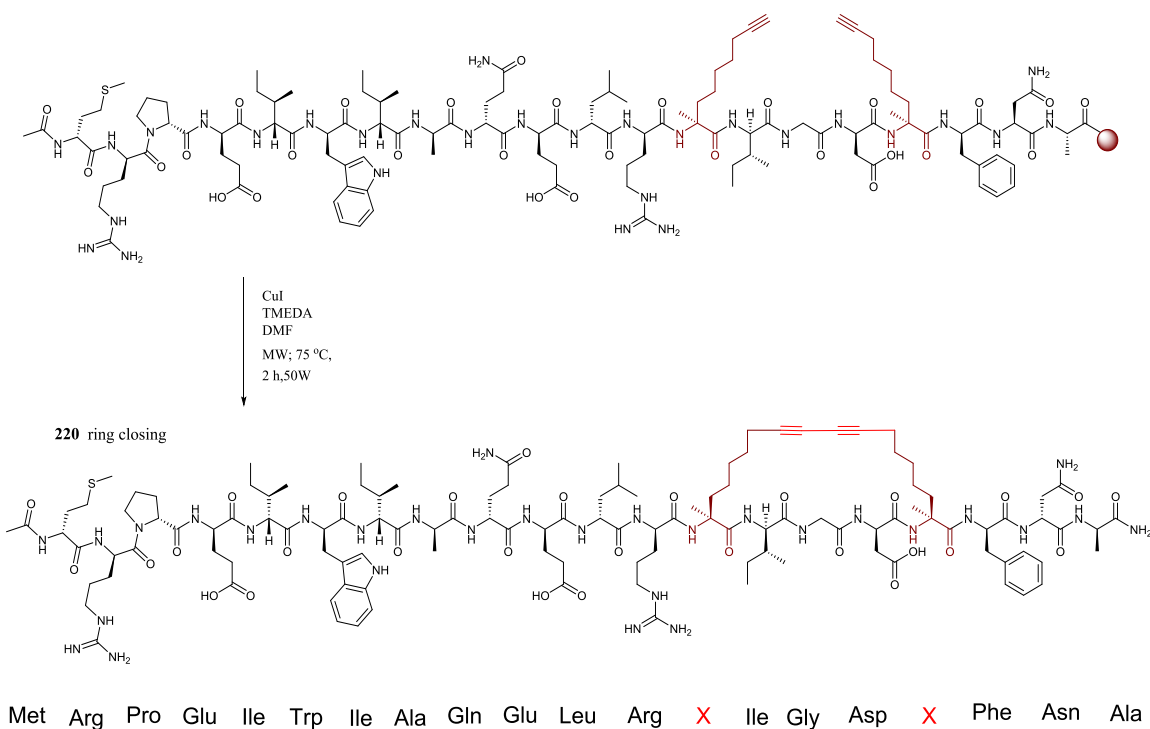
Figure 5.9: Bim peptide stapled via olefin ring closing metathesis

In this work, Bim peptide has been substituted with the C7-alkynyl-derivatised amino acid (**150**) since model 8 with this amino acid showed better helicity than the other models 5-7. The modified Bim peptide was synthesised on Rink amide MBHA resin using the Biotage microwave synthesis (automatic system). The new peptide (**219**) was substituted at positions 154, 158 appropriate for a $i, i+4$ stapled Bim peptide (142-164 residues). The product was obtained as a white powder after RP-HPLC; $t_R = 26.043$ minutes. The peptide was analysed with LC-MS and Maldi mass spectrometry showed a peak at 2531.3644 (calcd for $\text{C}_{119}\text{H}_{183}\text{N}_{30}\text{O}_{29}\text{S}$ $[\text{M}+\text{H}]^+$ 2531.3674) ($\Delta = 3.0$ ppm). In addition, the mass spectrum also showed peaks at 1266.17893 for $[\text{M}+2\text{H}]^{2+}$ and 844.4552 for $[\text{M}+3\text{H}]^{3+}$. The new ring open peptide was stapled using CuI and TMEDA in dry DMF for 3 hours in the microwave. The product was obtained as a white solid powder after RP-HPLC; at $t_R = 26.287$ minutes. The new peptide (**220**) was analysed by LC-MS, analytical HPLC and Maldi mass spectrometry also showed two peaks at 1265.1790 for $[\text{M}+2\text{H}]^{2+}$ and 843.7795 for $[\text{M}+3\text{H}]^{3+}$.



Scheme 5.6: Analysis of Bim peptide (220)Maldi and HPLC

219 ring opening



Scheme 5.7: Ring close of Bim peptide

The CD spectra for the Bim peptides demonstrates that both the open and ring-closed stapled peptides have α -helical conformations; the samples of the peptide models were dissolved in deionised water and 10 % of acetonitrile (v/v). It can be clearly seen that the ring-closed, stapled, Bim peptide has a better helical conformation (67 %) than the ring

open peptide (Figure 5.10, red coloured line). Comparing the data for the two Bim peptides, ring opened **219** and ring closed **220**, it can be seen that there are significant differences between the percentage helicities.

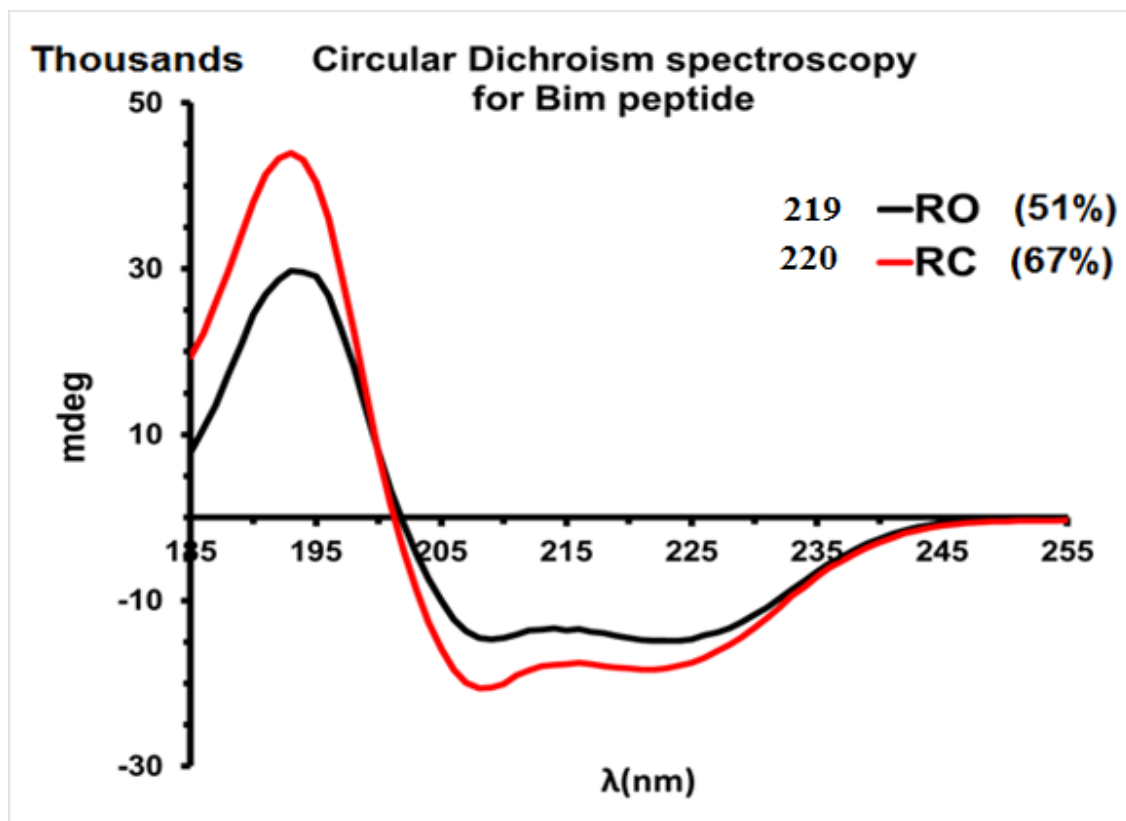


Figure 5.10: CD spectra of the Bim peptide ring opening and ring closure Bim peptide, stapled scan in 10 % acetonitrile /H₂O

5.13 Conclusions

Incorporating four of the new alkynyl-functionalised amino acids, **149-152**, as representative examples, a series of four model peptides have been synthesised. These peptides have five amino acids; cores made up of three alanines with alkynyl-functionalised amino acids at either end of the alanine chains. In these compounds the unnatural amino acids have been placed at approximately the right distance to allow the peptide to form one helical turn. Using the Glaser-Hay ring closing metathesis reaction, 1,3-diyne hydrocarbon stapled versions of each of these four models have been generated. CD spectroscopy has revealed the degree of helicity for these four model stapled peptides, with the greatest helicity shown by the model containing the unnatural amino acid based upon alanine with a C7 alkynyl side chain (**150**). This amino acid has

been introduced into the Bim peptide. CD spectra for the linear (unstapled) (**219**) and stapled (**220**) Bim peptides (Figure 5.11) demonstrate greater helicity (67 %) for the new 1,3-diyne stapled Bim peptide than that for the ring open Bim peptide (51 %).

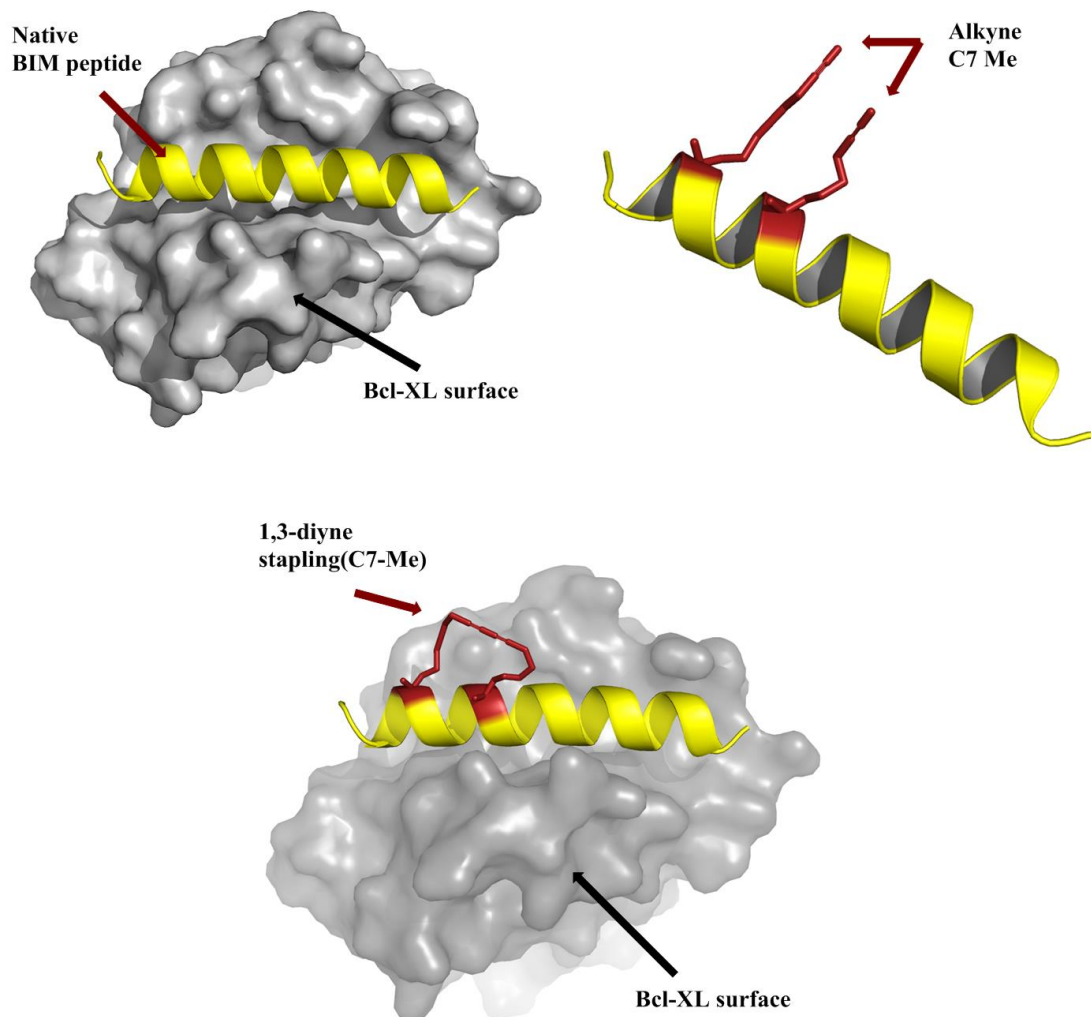


Figure 5.11: Bim peptide ring opening and ring closures

Chapter 6

Experimental



UNIVERSITY OF
LEICESTER

6.1 General information

All solvents and reagents used in this research were purchased from Sigma Aldrich or Novabiochem, and utilized as received without further purification. In general, the experiments were carried out under nitrogen, and the solvents were anhydrous. All amino acids (*L*-configuration) in the peptide synthesis were protected with Fmoc on the N-terminus. Analytical apparatus and requirements were as follows:

Thin layer chromatography plates (TLC) were carried out on a Merck Kieselgel 60 F254 with visualization via ultraviolet light and ninhydrin reagent.

Flash column chromatography was carried out using a Merck Kieselgel 60 (230-400 mesh).

Infra-red spectra were recorded on a Perkin Elmer System 100 as neat films using a universal ATR attachment accessory. Maximum absorbance (V_{\max}) are quoted in wavenumbers (cm^{-1}).

NMR spectra were recorded on Bruker DPX 500 (^1H , 500 MHz; ^{13}C , 125 MHz), DPX 400 (^1H , 400 MHz; ^{13}C , 100 MHz, ^{19}F , 376 MHz) and 300 (^1H , 300 MHz; ^{13}C , 75 MHz, ^{19}F , 282 MHz). The NMR chemical shifts (δ) are quoted in ppm TMS peak, and with coupling constants (J) quoted to the nearest 0.1 Hertz (Hz). Chiral HPLC were recorded on a Perkin Elmer system with a Chiralcel OD-H column (0.46 x 25 cm) eluted with hexane/*i*PrOH or hexane (1 % TF)/*i*PrOH.

PyMOL Molecular Graphics system, Version 1.2, was used to draw the peptide structures in 3D (α -helix).

X-ray crystallography was carried out on a Bruker Apex 2000 CCD diffractometer using graphite-monochromated Mo-K α radiation ($\lambda = 0.71073 \text{ \AA}$).

Melting points were determined with capillary tubes using a Gallenkamp Electrothermal Melting Point Apparatus.

High resolution mass spectra were recorded on a Kratos Concept with NBA as matrix.

GC autosystem XL (Perkin Elmer) flame ionisation detector (FTD). Carrier gas was He @ 1 ml/min., 1 ml injection 50:1 split ratio. Column 30 m x 0.25 mm 0.25 PE5.

The GC-MS autosystem XL turbomass mass spectrometer. GC method: 50 °C, 3 min. 10 °C/min (hold), 300 °C, ZB5. MS method (E1) 100-500 da.

HPLC reverse-phase / Dionex Ultimate 3000 system with a Phenomenex Gemini-NX 5µm C18 110Å AXIA packed column with dimensions 250 x 21.20 mm.

HPLC analytical reverse-phase/ Dionex Ultimate 3000 system with a Phenomenex Gemini-NX 5µm C18 110Å packed column with dimensions of 150 x 4.60 mm.

Lyophilisation/FreeZone Benchtop Freeze Dry System. It was conducted on an Edwards Modulyo lyophiliser.

Specific rotation $[\alpha]_D^{20}$ values are given in units $10^{-1} \text{ deg cm}^2 \text{ g}^{-1}$.

MALDI-TOF spectra were recorded following the procedure below. The sample was mixed 1:1 with a 10 mg/ml 2',4',6'-trihydroxyacetophenone monohydrate and 0.5 µL spotted on a stainless steel target plate. Analysis of complexes was carried out on a Voyager DE-STR MALDI-TOF mass spectrometer (Applied Biosystems, University of Leicester, UK) in positive ion reflection mode.

6.2 General methods:

6.2.1 Synthesis of 1-(2-fluorobenzyl)pyrrolidine-2-carboxylic acids (A)

Synthesis of 1-(2-fluorobenzyl)pyrrolidine-2-carboxylic acids using a modified literature procedure.⁴⁸ One equivalent of proline was added to a solution of three equivalents potassium hydroxide in isopropyl alcohol at 40 °C. After 20 minutes, aryl bromide (1.0 eq.) was added dropwise to the solution. The reaction mixture was warmed to 50 °C and stirred for 24 hours. The progress of the reaction was monitored via TLC (MeOH: (CH₂Cl₂:CH₃COOH (1 %)) 10: 90) and ¹⁹F NMR spectroscopy. After cooling to RT, 50 % removed *in vacuo* and concentrated hydrochloric acid (37 %) was added dropwise to the reaction mixture in an ice bath (0-5 °C) until the pH of the solution was in the range 5-6. The solution was filtered and concentrated *in vacuo*. The crude residue was recrystallised using acetone and the solution left in the fridge overnight. The solid was filtered, washed with cold acetone (3 x 50 mL) and dried *in vacuo* to generate the products as a white powder.

6.2.2 Synthesis of *N*-(2-benzoylphenyl)-1-(2-fluorobenzyl)pyrrolidine-2-carboxamids (B)

Synthesis of *N*-(2-benzoylphenyl)-1-(2-fluorobenzyl)pyrrolidine-2-carboxamid using a modified literature procedure.⁴⁸ One equivalent of (*S*)-*N*-(2-fluorobenzyl) proline was dissolved in dry freshly distilled DCM under a nitrogen atmosphere. The solution was heated for 20 min at 35 °C. 3.2 equivalents of *N*-methylimidazole were added and the mixture was stirred at the same temperature for 30 minutes. The reaction mixture was cooled to 0 °C in an ice bath; one equivalent of methanesulfonyl chloride was added dropwise. After 10 min, 0.9 equivalents of 2-aminobenzophenone was added, and the resulting solution was allowed to warm to room temperature. The mixture was heated for 24 h at 45 °C. The progress of the reaction was monitored via TLC (20 % ethylacetate/hexane). The mixture was left to cool to room temperature, saturated aqueous sodium hydrogen carbonate solution (60 mL) was added, the two layers separated, and the aqueous layer extracted with dichloromethane (3 x 100 mL). The combined organic layers were dried over anhydrous MgSO₄ and then concentrated *in vacuo*. Purification was achieved via flash column chromatography (15:85 ethyl acetate: hexane) followed by recrystallization with hexane and EtOAc (99:1) to give the products as light yellow crystals.

6.2.3 Synthesis of ({2-[1-(2-fluorobenzyl)benzyl]pyrrolidine-2-carboxamide}-phenyl}phenylmethylene)-(amino acid)ato-*N,N',N'',O*} nickel^{II} (C)

Synthesis of ({2-[1-(2-fluorobenzyl)benzyl]pyrrolidine-2-carboxamide}-phenyl}phenylmethylene)-(amino acid)ato-*N,N',N'',O*} nickel^{II} using a modified literature procedure.⁴⁸ One equivalent of *N*-(2-benzoylphenyl)-1-(2-fluorobenzyl)pyrrolidine-2-carboxamide and two equivalents of Ni(NO₃)₂·6H₂O and amino acids were dissolved in dried methanol at 50 °C in a 250 ml RBF. The mixture was stirred until all the solids had dissolved to give a green solution. Seven equivalents of freshly ground potassium hydroxide were added to the mixture. The temperature of the mixture was raised to 70 °C and stirred for 1-2.5 h. The colour changed to blood red. The progress of the reaction was monitored via TLC (ethylacetate: dichloromethane 1:1) and ¹⁹F NMR spectroscopy. The reaction mixture was cooled and then concentrated *in vacuo*. Water (150 mL) was added and the red product extracted with DCM (3 x 150 mL). The combined organic layers were collected and concentrated by 50 % *in vacuo*. The resulting residue was washed with water (3 x 100 mL) and a saturated aqueous sodium

chloride solution (3 x 100 mL), then dried with anhydrous MgSO_4 and concentrated *in vacuo*. Purification was achieved via flash column chromatography (50:50 ethylacetate: DCM or 5:95 MeOH: DCM) to give the products as red powders.

6.2.4 Alkylation of chiral Ni^{II} complexes Schiff bases using alkyl iodide (D)

Synthesis of new Ni^{II} complexes Schiff bases derivatives using a modified literature procedure.⁴⁸ Four equivalents of potassium tert-butoxide were taken up in dry DMF under an atmosphere of nitrogen. The mixture was cooled to 0 °C and one equivalent of ({2-[1-(2-fluorobenzyl)pyrrolidine-2-carboxamide]phenyl}phenylmethylene)-(aminoacid)ato- N,N',N'',O } nickel^{II} was added and the reaction mixture stirred for 15-20 minutes; the colour of the reaction mixture darkened. Three equivalents of alkyl iodide were added to the reaction mixture. The ice bath was removed after 15-20 minutes and the reaction mixture left to stir for 2 h at room temperature. The progress of the reaction was monitored via TLC (ethylacetate: dichloromethane 1:1) and ^{19}F NMR spectroscopy. Water (5-10 mL) was added to the reaction mixture to quench the reaction. The mixture was concentrated *in vacuo*, toluene (3 x 50 mL) was used as an azeotrope to remove the DMF the residue taken up in water (40-60 mL) and extracted with ethyl acetate (3 x 100 mL). The combined organic extracts were washed with aqueous lithium chloride solution (5 % w/v) (3 x 10 mL) and then with brine solution (3 x 10 mL), dried using anhydrous MgSO_4 and concentrated *in vacuo*. Purification was achieved via flash column chromatography (ethylacetate/ dichloromethane 1: 1) giving the product as a red-orange solid.

6.2.5 Alkylation of chiral glycine Schiff bases Ni^{II} complexes using alkyl iodide (E)

Synthesis of new Ni^{II} complexes Schiff bases derivatives using a modified literature procedure.⁴⁸ One equivalent of potassium tert-butoxide was taken up in dry THF under an atmosphere of nitrogen. The mixture was cooled to 0 °C and one equivalent of ({2-[1-(2-fluorobenzyl)pyrrolidine-2-carboxamide]phenyl}phenylmethylene)-glycinato- N,N',N'',O }nickel(II) was added and the mixture stirred for 10-15 minutes; the colour darkened. One equivalent of alkyl iodide was added to the reaction mixture. The ice bath was removed after 5-10 minutes and the mixture left at room temperature for 5-10 minutes, during which the colour changed to orange. The progress of the reaction was monitored via TLC (ethylacetate: dichloromethane 1:1) and ^{19}F NMR spectroscopy. Water (10-15 mL) was added to the reaction mixture to quench the reaction. The mixture

was concentrated *in vacuo* and taken up in water (40-50 mL) and extracted with dichloromethane (3 x 100 mL). The combined organic extracts were washed with brine solution (3 x 20 mL), dried using anhydrous MgSO_4 and concentrated *in vacuo*. Purification was achieved via flash column chromatography or the Biotage instrument (ethylacetate/ dichloromethane 1: 1), giving the products as reddish-orange solids.

6.2.6 Alkylation of chiral Schiff bases Ni^{II} complexes using alkyl bromide (F)

Synthesis of new Ni^{II} complexes Schiff bases derivatives using a modified literature procedure.⁴⁸ Four to ten equivalents of potassium tert-butoxide were taken up in dry DMF or THF under an atmosphere of nitrogen. The mixture was cooled to 0 °C and one equivalent of ({2-[1-(2-fluorobenzyl)pyrrolidine-2-carboxamide]phenyl}phenyl-methylene)(amino acid)ato- N,N',N'',O nickel^{II} was added and the mixture stirred for 10-20 minutes; the colour darkened. Three equivalents of alkyl bromide were added dropwise to the reaction mixture. The ice bath was removed after 20-30 minutes and the mixture stirred at room temperature for 1 h, during which the colour changed to orange. The progress of the reaction was monitored via TLC (ethylacetate: dichloromethane 1:1) and ^{19}F NMR spectroscopy. Water (40-50 mL) was added to the reaction mixture to quench the reaction. The mixture was concentrated *in vacuo* and extracted with dichloromethane (3 x 100 mL). The combined organic extracts were washed with brine solution (3 x 20 mL), dried using anhydrous MgSO_4 and concentrated *in vacuo*. Purification was achieved via flash column chromatography on the Biotage instrument giving the products as a reddish-orange solids.

6.2.7 Generation of amino acids by hydrolysis of the complexes (G)

Synthesis of new amino acids using literature procedure.⁴⁸ One equivalent of alkyl- Ni^{II} Schiff base complex was dissolved in methanol (50 mL) and hydrochloric acid (3 M, 15 mL at 50 °C) added dropwise over 10 minutes. The reaction mixture was heated at 70 °C for 40-50 minutes, during which the colour changed from dark red to a transparent greenish yellow. The mixture was then cooled to room temperature and the organic solvent removed *in vacuo*. Water (25.0 mL) was added to the residue and extracted with dichloromethane (3 x 50 mL). The combined organic extracts were dried using MgSO_4 and concentrated *in vacuo* to afford the ligand (*S* or *R*) for re-use. A Dowex 50WX2 200 H^+ column was pre-washed with H_2O to ensure it was neutralised by reaching pH 7. The aqueous solution was columned. The column was washed with H_2O -EtOH (1: 1 (v/v)),

250.0 mL) to remove the nickel salts. The amino acid was placed in the column and eluted with 20 % NH_4OH –EtOH (1:1 (v/v), 350.0 mL). Ninhydrin indicator was used to identify the fractions containing the product (new amino acid). The fractions were combined and concentrated *in vacuo*. The residue solution was put in a freeze dryer for 48 h to remove the water then triturated with diethyl ether to give as white powders.

6.2.8 Generation of amino acids by using 8-hydroxyquinoline (H)

Synthesis of new amino acids derivatives using a modified literature procedure.^{166, 167} One equivalent of amino acid and three equivalent of 8-hydroxyquinoline were dissolved in (20 mL) acetonitrile: water (3:1). The reaction mixture was left stirring for 24 h at 30 °C. Water (30 mL) was added to the reaction mixture and left to stir for 30 min at room temperature. The pale orange precipitate was filtered (8-hydroxyquinoline Ni^{II} complex) and washed with water (3 x 20 mL). The acetonitrile was removed in *vacuo* and the aqueous layer was extracted with dichloromethane (3 x 50 mL), ethylacetate (3 x 50 mL) and diethyl ether (3 x 50 mL). Approximately, half of the water was removed in *vacuo*. The resulting solution was put into the freeze dryer for 24-48h to remove the water. The resulting product was triturated with cold diethyl ether (3 x 20 mL) to give the products Fmoc-amino acids as either white powders or viscous yellowish oils.

6.2.9 Synthesis of Fmoc protected amino acids (I)

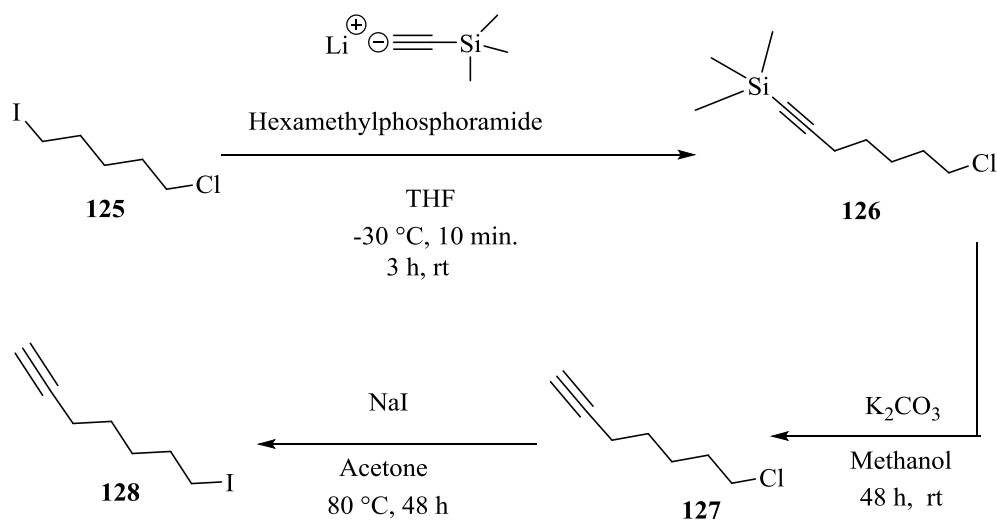
Synthesis of new Fmoc-amino acids using the literature procedure.⁴⁸ One equivalent of an amino acid and two equivalents of potassium carbonate were dissolved in water at room temperature. The reaction mixture was cooled to 0 °C. 1.5 equivalents of 9-fluorenyl-methyl-*N*-succinimidyl carbonate in dioxane or acetonitrile (10-20 mL) was added (dropwise over 30 minutes). The reaction mixture was warmed and left to stir for 24 hours at room temperature. Water (10-15 mL) was added and washed with ethyl acetate (3 x 50 mL). The combined organic phases were re-extracted with a saturated aqueous solution of sodium bicarbonate (30-50 mL), then the combined aqueous layers were acidified with HCl (3 M) until the pH 1 was reached. Thereafter, the solution was extracted with ethyl acetate (3 x 50 mL). The combined organic layers were dried over MgSO_4 and the solvent evaporated in *vacuo*. The resulting product was triturated with cold diethyl ether (3 x 20 mL). The residue solution was placed in a freeze dryer for 24-48 h to give the products as either white powders or viscous yellowish oils.

6.3 Synthesis of Starting materials

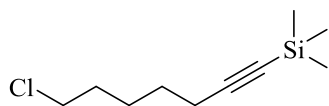
6.3.1 Synthesis of 7-iodohept-1-yne:

6.3.1.1 Method (1)

Synthesis of 7-iodohept-1-yne proceeded in three steps via a modified literature procedure.²¹⁰



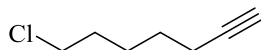
6.3.1.1.1 Synthesis of 7-chlorohept-1-yn-1-yl)trimethylsilane **126**



HMPA (4.864 mL, 29.095 mmol, 4.5 eq.) was added to dry THF (15 mL), in a dried 100 mL flask under an atmosphere of nitrogen, then 1-chloro-5-iodopentane **125** (1.5 g, 0.431 mmol, 1 eq.) was added to the reaction mixture. The mixture was cooled to $-25\text{ }^\circ\text{C}$ using a dry ice and acetonitrile bath. The Lithium salt of trimethylsilyl acetylene (0.5 M) solution in THF (0.9 mL, 7.759 mmol, 1.2 eq.), which is commercially available, was added dropwise to the reaction mixture over 30 min. The reaction mixture was stirred for 1 h, and then allowed to warm to room temperature gradually. Over the following 2 h, the starting materials were completely converted. The reaction was monitored by GC every 30 minutes. 10 mL of saturated aqueous ammonium chloride was added to the reaction mixture to quench the reaction, and the mixture was extracted with hexane (3 x 20 mL). The combined organic layers were extracted with water (2 x 20 mL), followed by brine (30 mL), dried with MgSO_4 and concentrated *in vacuo* to afford (7-

chlorohept-1-yn-1-yl)trimethylsilane **126** (1.18 g, 91 %). ^1H NMR (400 MHz, CDCl_3) δ 3.39 (2H, t, $^3J_{\text{HH}} = 6.7$ Hz, $\text{Cl}-\text{CH}_2$), 2.11-2.06 (2H, m, $\text{CH}\equiv\text{C}-\text{CH}_2$), 1.9 (2H, t, $^3J_{\text{HH}} = 6.7$ Hz, $\text{Cl}-\text{CH}_2$), 1.68-1.62 (2H, m, $\text{Cl}-\text{CH}_2-\text{CH}_2-\text{CH}_2$), 1.42-1.38 (2H, m, $\text{Cl}-\text{CH}_2-\text{CH}_2-\text{CH}_2-\text{CH}_2$), 0.0 (9H, s, 3 x CH_3).

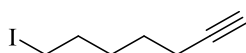
6.3.1.1.2 Prepare of 7-chlorohept-1-yne **127**



The product (7-chlorohept-1-yn-1-yl)trimethylsilane **126** (1.5 g, 6.466 mmol, 1 eq.) was added to a solution of K_2CO_3 (3 g) in methanol (15 mL) at room temperature.

The reaction mixture was stirred for 48 h at room temperature. The reaction mixture was quenched with water (20 mL) and extracted with a mixture of diethyl ether and hexane (1:1) (3 x 20 mL). The combined organic layers were extracted with water (3 x 25 mL), followed by brine solution and dried over MgSO_4 . The solvent was removed *in vacuo* to afford the crude acetylene in an, 86 % yield (655 mg). ^1H NMR (400 MHz, CDCl_3) δ 3.46 (2H, t, $^3J_{\text{HH}} = 6.7$ Hz, $\text{Cl}-\text{CH}_2$), 2.16-2.12 (2H, m, $\text{CH}\equiv\text{C}-\text{CH}_2$), 1.8 (1H, t, $^4J_{\text{HH}} = 2.7$ Hz, $\text{CH}\equiv\text{C}$), 1.7-1.63 (2H, m, $\text{ClCH}_2-\text{CH}_2$), 1.53-1.47 (4H, m, $\text{Cl}-\text{CH}_2-\text{CH}_2-\text{CH}_2-\text{CH}_2$).

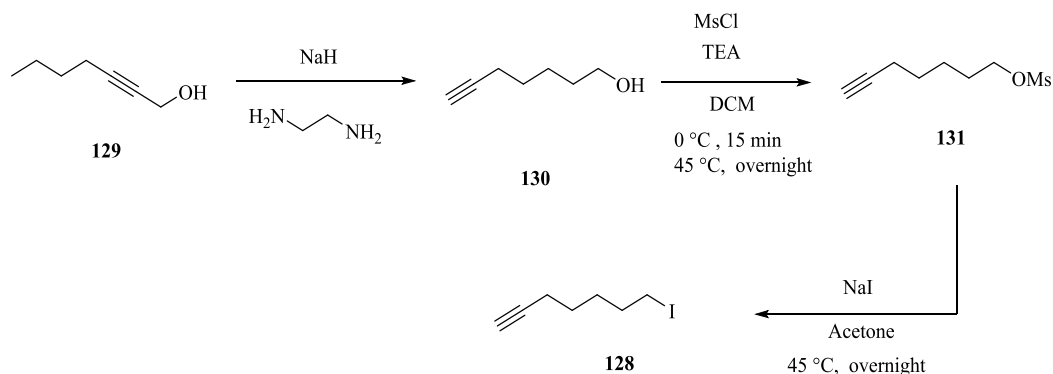
6.3.1.1.3 Synthesis of 7-iodohept-1-yne **128**



The 7-chlorohept-1-yne (650 mg, 1 eq.) **127** was dissolved in acetone (10 mL) and NaI (3.78 g, 5 eq.) was added at room temperature. The solution was stirred in sealed tubes at 80 °C for 2 days; the reaction was monitored by GC every 30 minutes until the GC showed complete conversion. The solvent was removed under reduced pressure and the mixture was dissolved in diethyl ether (30 mL) and filtered. After the evaporation of the solvent, the final iodoalkyne (825 mg) was isolated in an 81 % yield and used in alkylation reactions without purification. The product was oily, and a pale yellow colour. ^1H NMR (400 MHz, CDCl_3) δ 3.12 (2H, t, $^3J_{\text{HH}} = 7.0$ Hz, $\text{I}-\text{CH}_2$), 2.15-2.12 (2H, m, $\text{CH}\equiv\text{C}-\text{CH}_2$), 1.94 (1H, t, $^4J_{\text{HH}} = 2.8$ Hz, $\text{CH}\equiv\text{C}$), 1.82-1.75 (2H, m, $\text{I}-\text{CH}_2-\text{CH}_2$), 1.50-1.45 (4H, m, $\text{I}-\text{CH}_2-\text{CH}_2-\text{CH}_2-\text{CH}_2$).

6.3.1.2 Method (2)

Synthesis of 7-iodohept-1-yne proceeded via three steps using a modified literature procedure.²¹¹



6.3.1.2.1 Synthesis of hept-6-yn-1-ol **130**

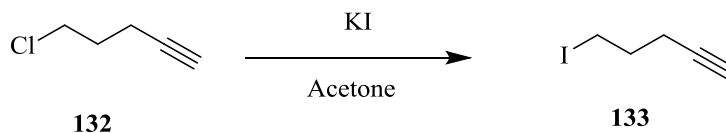
Ethane-1,2-diamine (70 mL) was added to a 250 mL three-neck round-bottomed flask which contained NaH (5.349 g, 222.87 mmol, 5.0 eq.) (60 % in mineral oil) in a dropwise manner and held carefully at 0 °C. The reaction mixture was stirred for 30 min at 0 °C and then left to warm to room temperature over 1 h, before being heated to 60 °C for another 1 h. The reaction was cooled to 40 °C. Hep-2-yn-1-ol **129** (5.0 g, 44.575 mmol, 1.0 eq.) was added dropwise and stirring continued for a further 1 h at the same temperature. Then the reaction mixture was stirred at 60 °C for another 1 h. Subsequently, the reaction mixture was cooled to 0 °C and water (100 mL) added dropwise to quench the reaction. Hydrogen chloride (10 mL, 3 M) was added dropwise and the mixture extracted with dichloromethane (3 x 150 mL). The combined organic extracts were washed with brine solution (3 x 20 mL), dried with anhydrous MgSO_4 and concentrated *in vacuo*. The crude oily product was purified via flash column chromatography (hexanes/ethyl acetate 7:3) to obtain the product **130** (4.6 g, 90 %) as a pale yellow oil. ^1H NMR (400 MHz, CDCl_3) δ 3.60 (2H, t, $^3J_{\text{HH}} = 6.7$ Hz, $\text{CH}_2\text{-OH}$), 3.22 (1H, s, OH), 2.16-2.13 (2H, m, $\text{HO-CH}_2\text{-CH}_2$), 1.92 (1H, s, $\text{HC}\equiv\text{C}$), 1.55-1.47 (2H, m, $\text{HC}\equiv\text{C-CH}_2$), 1.42-1.36 (4H, m, $\text{HO-CH}_2\text{-CH}_2\text{-CH}_2\text{-CH}_2$). ^{13}C NMR (100 MHz, CDCl_3) δ 84.4 ($\text{C}\equiv\text{CH}$), 68.3 ($\text{CH}_2\text{-OH}$), 62.4 ($\text{C}\equiv\text{CH}$), 32.1 ($\text{HO-CH}_2\text{-CH}_2$), 28.2 ($\text{HC}\equiv\text{C-CH}_2\text{-CH}_2$), 24.9 ($\text{HO-CH}_2\text{-CH}_2\text{-CH}_2$), 18.3 ($\text{HC}\equiv\text{C-CH}_2$).

6.3.1.2.2 7-Iodohypt-1-yne **128**

Et_3N (7.46 mL, 53.49 mmol, 2.0 eq.) followed by MsCl (3.104 mL, 40.118 mmol, 1.5 eq.) were added dropwise at 0 °C to oct-7-yn-1-ol (3.99 g, 26.745 mmol, 1.0 eq.) **130**, in DCM (20 mL). The reaction mixture was stirred overnight at room temperature.

After this time, volatiles were evaporated under reduced pressure. Water (10 mL) was added to the residue which was then extracted with EtOAc (3 x 100 mL). The combined organic extracts were washed with brine solution (3 x 40 mL), dried with anhydrous MgSO_4 and concentrated *in vacuo*. The crude intermediat **131** was dissolved in acetone (20 mL), NaI (18 g, 5.0 eq.) was added. The reaction mixture was stirred overnight at 60 °C. The mixture was allowed to cool to room temperature, and then extracted with EtOAc (3 x 100 mL). The combined organic extracts were washed with $\text{Na}_2\text{S}_2\text{O}_3$ (5 %, 3 x 40 mL), brine solution (3 x 40 mL), dried with anhydrous MgSO_4 and concentrated *in vacuo*. The crude oily product was purified via Biotage column chromatography (hexanes/ethyl acetate 80:20) to obtain the product **128** (16.581 g, 84 %) as a pale yellow oil. ^1H NMR (400 MHz, CDCl_3) δ 3.19 (2H, t, $^2J_{\text{HH}} = 7.2$ Hz, $\text{CH}_2\text{-I}$), 2.18 (2H, t, $^3J_{\text{HH}} = 7.1$ Hz, $\text{CH}_2\text{-C}\equiv\text{CH}$), 1.94 (1H, t, $^4J_{\text{HH}} = 2.8$ Hz, $\text{HC}\equiv\text{C}$), 1.86-1.79 (2H, m, $\text{I-CH}_2\text{-CH}_2$), 1.56-1.47 (4H, m, CH_2); ^{13}C NMR (100 MHz, CDCl_3) δ 84.0 (CH_2), 68.8 ($\text{C}\equiv\text{CH}$), 33.0 ($\text{C}\equiv\text{CH}$), 29.5 (CH_2), 27.7 (CH_2), 18.3 ($\text{CH}_2\text{-I}$), 6.8 (CH_2); HRMS-ESI (calcd for $\text{C}_7\text{H}_{12}^{127}\text{I}$ $[\text{M}+\text{H}]^+$) 222.9984, found 222.9979 ($\Delta = -2.2$ ppm).

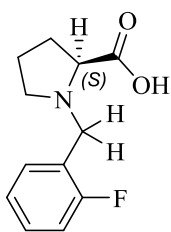
6.3.1.3 Synthesis of 5-iodopent-1-yne (**6**)



Chloropent-1-yne (10 g, 97.503 mmol, 1.0 eq.) was dissolved in acetone (20 mL), and NaI (43.844 g, 292.512 mmol, 3.0 eq.) added at room temperature. The reaction mixture was stirred overnight at 60 °C, allowed to cool to room temperature, then extracted with EtOAc (3 x 150 mL). The combined organic extracts were washed with $\text{Na}_2\text{S}_2\text{O}_3$ (5 %, 3 x 40 mL), brine solution (3 x 40 mL), dried with anhydrous MgSO_4 and concentrated *in vacuo*. The crude oily product was purified via Biotage column chromatography (hexanes/ethyl acetate 80 : 20) to obtain the product **3.aj** (18.810 g, 99 %) as a pale yellow oil. ^1H NMR (400 MHz, CDCl_3) δ ppm 3.27-3.32 (2H, m, I-CH_2), 2.20-2.35 (2H, m, $\text{CH}_2\text{-C}\equiv\text{CH}$), 1.97-2.03 (3H, m, $\text{I-CH}_2\text{-CH}_2$, $\text{C}\equiv\text{CH}$), ^{13}C NMR (100 MHz, CDCl_3) δ : 82.3 ($\text{C}\equiv\text{CH}$), 69.8 ($\text{C}\equiv\text{CH}$), 31.9 ($\text{I-CH}_2\text{-CH}_2$), 19.6 ($\text{CH}_2\text{-C}\equiv\text{CH}$), 5.5 (I-CH_2), HRMS-ESI (calcd for $\text{C}_5\text{H}_8\text{I}^{127}$ $[\text{M}+\text{H}]^+$) 194.9671, found 194.9665 ($\Delta = -3.1$ ppm).

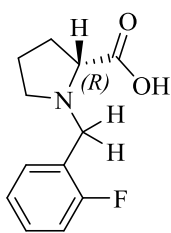
6.4 Experimental for Chapter 2

6.4.1 Synthesis of (S)-1-(2-fluorobenzyl)pyrrolidine-2-carboxylic acid 93



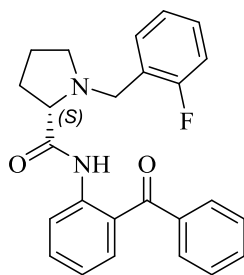
The general procedure (A) was followed using potassium hydroxide (36.6 g, 651.4 mmol) in isopropyl alcohol (200 mL), *L*-proline (25 g, 217.1 mmol) and 2-fluorobenzyl bromide (45.2 g, 189.0 mmol). Yield (42.21g, 75 %); m.p.: 85-87 °C (hexane–EtOAc)(lit: 70-80 °C)⁴⁸; $[\alpha]_D^{20} = -24.3$ (lit: -24.1) (c 0.01, CHCl₃) (lit: +1300.0(c 0.05, CHCl₃); ¹H NMR (400 MHz, D₂O) δ ppm 7.38-7.46 (2H, m, ArH), 7.10-7.22 (2H, m, ArH), 4.41 (2H, dd, ²*J*_{HH} = 9.6, ³*J*_{HH} = 9.6 Hz, Ar-CH₂-N), 4.08 (1H, q, ³*J*_{HH} = 4.0, ³*J*_{HH} = 4.1 Hz, α-CH), 3.58 (1H, ddd, ²*J*_{HH} = 11.3, ³*J*_{HH} = 7.3, ³*J*_{HH} = 3.9 Hz, δ(Pro)-CHH), 3.21-3.34 (1H, m, δ(Pro)-CHH), 2.38-2.50 (1H, m, β(Pro)-CHH), 1.84-2.12 (3H, m, β(Pro)-CHH, γ(Pro)-CHH); ¹³C NMR (100 MHz, D₂O) δ: 172.1 (C=O), 161.2 (d, ¹*J*_{CF} = 247.4 Hz, CF), 132.7 (d, ⁴*J*_{CF} = 3.1 Hz, Ar-CH), 132.6 (d, ³*J*_{CF} = 7.9 Hz, Ar-CH), 124.9 (d, ³*J*_{CF} = 3.2 Hz, Ar-CH), 116.3 (d, ²*J*_{CF} = 15.9 Hz, Ar-C), 115.7 (d, ²*J*_{CF} = 22.3 Hz, Ar-CH), 67.2 (α(Pro)-CH), 54.8 (δ(Pro)-CH₂), 51.7 (Ar-CH₂-N), 28.4 (β(Pro)-CH₂), 22.3 (γ(Pro)-CH₂); ¹⁹F NMR (375 MHz; D₂O) -116.0 (s); HRMS-ESI (calcd for C₁₂H₁₅NO₂F) 224.1087, found 224.1087 (Δ = 0.0 ppm).

6.4.2 Synthesis of (R)-1-(2-fluorobenzyl)pyrrolidine-2-carboxylic acid 94



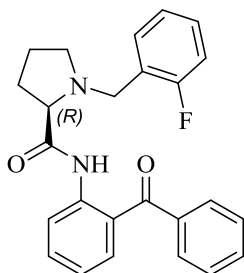
The general procedure (A) was followed using potassium hydroxide (36.6 g, 651.4 mmol) in isopropyl alcohol (200 mL), *D*-proline (25 g, 217.1 mmol) and 2-fluorobenzyl bromide (45.2 g, 189.0 mmol). Yield (41.81g, 74 %); m.p.: 85-87 °C (hexane–EtOAc)(lit: 78-80°C)⁴⁸; $[\alpha]_D^{20} = -24.3$, (lit: -24.1), (c 0.05, CHCl₃; ¹H NMR (500 MHz, D₂O) δ ppm 7.34-7.45 (2H, m, ArH), 7.07-7.19 (2H, m, ArH), 4.40 (2H, dd, ²*J*_{HH} = 9.6, ³*J*_{HH} = 9.6 Hz, Ar-CH₂-N), 4.21 (1H, t, ³*J*_{HH} = 8.64 Hz, α(Pro)-CH), 3.55 (1H, m, δ(Pro)-CHH), 3.19-3.31 (1H, m, δ(Pro)-CHH), 2.41-2.55 (1H, m, β(Pro)-CHH), 1.96-2.14 (2H, m, β(Pro)-CHH, γ(Pro)-CHH), 1.84-1.96 (1H, m, γ(Pro)-CHH); ¹³C NMR (100 MHz, D₂O) δ: 170.8 (C=O), 161.3 (d, ¹*J*_{CF} = 248.0 Hz, CF), 132.9 (d, ³*J*_{CF} = 9.0 Hz, Ar-CH), 125.1 (d, ³*J*_{CF} = 3.01 Hz, Ar-CH), 116.6 (d, ²*J*_{CF} = 15.06 Hz, Ar-C), 115.9 (d, ²*J*_{CF} = 21.08 Hz, Ar-CH), 66.3 (α(Pro)-CH), 54.9 (δ(Pro)-CH₂), 51.8 (Ar-CH₂-N), 28.1 (β(Pro)-CH₂), 22.0 (γ(Pro)-CH₂); ¹⁹F NMR (376 MHz; D₂O) -115.8 (s); HRMS-ESI (calcd for C₁₂H₁₅NO₂F [M+H⁺]) 224.1087, found 224.1085 (Δ = -0.9 ppm).

6.4.3 Synthesis of (S)-N-(2-benzoylphenyl)-1-(2-fluorobenzyl)pyrrolidine-2-carboxamide **95**



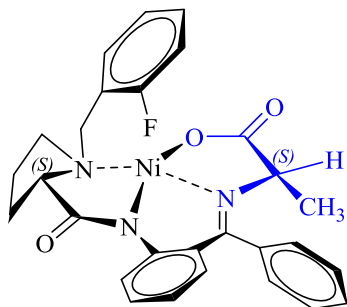
The general procedure (**B**) was followed using (S)-N-(2-fluorobenzyl) proline **93** (27 g, 103.96 mmol), N-methylimidazole (26.52 mL, 82.11 mmol) and methanesulfonyl chloride (8.05 mL, 103.96 mmol) and 2-aminobenzophenone (18.455 g, 93.57 mmol) to give the product as light yellow crystals (Crystals suitable for single crystal X-ray structure determination were grown by slow evaporation of the compound in ethyl acetate). Yield (27.89 g, 74 %). m.p.: 88-90 °C (lit: 88-90 °C);⁴⁸ $[\alpha]_D^{20} = -125.3$ (c 0.25, MeOH) (lit: -125.1 (c 0.05, CHCl₃)), ¹H NMR (400 MHz, CDCl₃) δ : 11.42 (1H, s, NH), 8.55 (1H, dd, ³J_{HH} = 8.4, ⁴J_{HH} = 0.8 Hz, ArH), 7.79-7.72 (2H, m, ArH), 7.64-7.56 (1H, m, ArH), 7.56-7.41 (5H, m, ArH), 7.16-7.04 (2H, m, ArH), 6.92 (1H, ddd, ³J_{HH} = 7.5, ³J_{HH} = 7.5, ⁴J_{HH} = 1.1 Hz, ArH), 6.83-6.74 (1H, m, ArH), 3.90 (1H, d, ²J_{HH} = 13.2 Hz, Ar-CHH-N), 3.73 (1H, d, ²J_{HH} = 13.2 Hz, Ar-CHH-N), 3.35 (1H, dd, ³J_{HH} = 10.1, ⁴J_{HH} = 4.5 Hz, α (Pro)-CH), 3.27-2.23 (1H, m, β (Pro)-CHH), 2.53-2.52 (1H, m, β (Pro)-CHH), 2.34-2.19 (1H, m, δ (Pro)-CHH), 2.02-1.89 (1H, m, δ (Pro)-CHH), 1.86-1.78 (2H, m, γ (Pro)-CH₂); ¹³C NMR (100 MHz, CDCl₃) δ 197.9 (C=O), 174.4 (C=O), 161.1 (d, ¹J_{CF} = 245.3 Hz, CF), 139.0 (Ar-C), 138.6 (Ar-C), 133.3 (Ar-CH), 132.5 (Ar-2CH), 131.7 (d, ³J_{CF} = 3.6 Hz, CH), 130.1 (Ar-2CH), 128.9 (d, ³J_{CF} = 8.4 Hz, Ar-CH), 128.3 (Ar-2CH), 125.6 (Ar-C), 124.9 (d, ²J_{CF} = 15.1, Ar-C), 123.9 (d, ⁴J_{CF} = 3.4, Ar-CH), 122.3 (Ar-CH), 121.5 (Ar-CH), 115.1 (d, ²J_{CF} = 22.7 Hz, CH), 67.9 (α (Pro)-CH), 53.8 (δ (Pro)-CH₂), 52.0 (Ar-CH₂-N), 31.1 (β (Pro)-CH₂), 24.3 (γ (Pro)-CH₂); IR (ν_{\max} /cm⁻¹, neat): 3273, 2968, 2823, 1682, 1646, 1577, 1511, 1489, 1443, 1286, 1266, 1245, 1227, 1183, 1101, 923, 779, 768, 754, 710, 697, 659; ¹⁹F NMR (376 MHz, CDCl₃) δ -117.6 (s); HRMS-ESI (calcd for C₂₅H₂₄N₂O₂F) 403.1822, found 403.1822 (Δ = 0.0 ppm); HPLC (OD-H column, hexane (5 %)/ ⁱPrOH isocratic): 15.19 min.

6.4.4 Synthesis of (R)-N-(2-benzoylphenyl)-1-(2-fluorobenzyl)pyrrolidine-2-carboxamide **96**



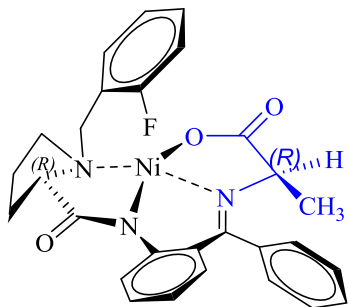
The general procedure (**B**) was followed using (S)-N-(2-fluorobenzyl) proline (41.00 g, 157.87 mmol), N-methylimidazole **94** (40.272 mL, 505.18 mmol), methanesulfonyl chloride (12.220 mL, 157.87 mmol), and 2-aminobenzophenone (28.02 g, 142.08 mmol) to give the product as light yellow crystals (Crystals suitable for single crystal X-ray structure determination were grown by slow evaporation of the compound in ethyl acetate). Yield (27.89 g, 77 %). m.p: 88-90 °C; $[\alpha]_D^{20} = -125.3$ (c 0.25, MeOH), ^1H NMR (400 MHz, CDCl_3) δ : 11.42 (1H, s, NH), 8.55 (1H, dd, $^3J_{\text{HH}} = 8.4$, $^4J_{\text{HH}} = 0.8$ Hz, ArH), 7.79-7.72 (2H, m, ArH), 7.64-7.56 (1H, m, ArH), 7.56-7.41 (5H, m, ArH), 7.16-7.04 (2H, m, ArH), 6.92 (1H, ddd, $^3J_{\text{HH}} = 7.6$, $^3J_{\text{HH}} = 7.5$, $^4J_{\text{HH}} = 1.1$ Hz, ArH), 6.83-6.74 (1H, m, ArH), 3.90 (1H, d, $^2J_{\text{HH}} = 13.2$ Hz, Ar-CHH-N), 3.73 (1H, d, $^2J_{\text{HH}} = 13.2$ Hz, Ar-CHH-N), 3.35 (1H, dd, $^3J_{\text{HH}} = 10.1$, $^4J_{\text{HH}} = 4.5$ Hz, $\alpha(\text{Pro})\text{-CH}$), 3.22 (1H, ddd, $^2J_{\text{HH}} = 8.8$, $^3J_{\text{HH}} = 6.5$, $^4J_{\text{HH}} = 2.2$ Hz, $\beta(\text{Pro})\text{-CHH}$), 2.48-2.42 (1H, m, $\beta(\text{Pro})\text{-CHH}$), 2.28-2.18 (1H, m, $\delta(\text{Pro})\text{-CHH}$), 1.98-1.91 (1H, m, $\delta(\text{Pro})\text{-CHH}$), 1.86-1.71 (2H, m, $\gamma(\text{Pro})\text{-CH}_2$); ^{13}C NMR (100 MHz, CDCl_3) δ 197.8 (C=O), 174.4 (C=O), 161.0 (d, $^1J_{\text{CF}} = 246.1$ Hz, CF), 139.0 (Ar-C), 138.6 (Ar-C), 133.3 (Ar-CH), 132.5 (Ar-CH), 132.4 (Ar-CH), 131.7 (d, $^3J_{\text{CF}} = 3.2$ Hz, Ar-CH), 130.1 (Ar-2CH), 128.7 (d, $^3J_{\text{CF}} = 8.0$, Ar-CH), 128.3 (Ar-2CH), 125.6 (Ar-C), 124.9 (d, $^2J_{\text{CF}} = 14.4$ Hz, Ar-C), 123.9 (d, $^4J_{\text{CF}} = 3.2$ Hz, Ar-CH), 122.3 (Ar-CH), 121.5 (Ar-CH), 115.1 (d, $^2J_{\text{CF}} = 22.4$ Hz, Ar-CH), 1145.0 (Ar-CH), 68.0 ($\alpha(\text{Pro})\text{-CH}$), 53.8 ($\delta(\text{Pro})\text{-CH}_2$), 52.0 (Ar-CH₂-N), 31.1 ($\beta(\text{Pro})\text{-CH}_2$), 24.3 ($\gamma(\text{Pro})\text{-CH}_2$); ^{19}F NMR (376 MHz, CDCl_3) δ -117.5 (s); HRMS-ESI (calcd for $\text{C}_{25}\text{H}_{24}\text{N}_2\text{O}_2\text{F}$) 403.1822, found 403.1822 ($\Delta = 0.0$ ppm); HPLC (OD-H column, hexane (5 %)/iPrOH isocratic): 13.06 min.

6.4.5 Synthesis of (*S*)-({2-[1-(2-fluorobenzyl)benzyl]pyrrolidine-2-carboxamide}-phenyl}phenylmethylene)-alaninato-*N,N',N'',O*} nickel(II) **56**



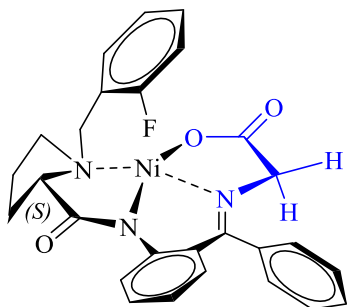
The general procedure (C) was followed using (*S*)-*N*-(2-benzoylphenyl)-1-(2-fluorobenzyl)pyrrolidine-2-carboxamide **95** (10 g, 24.85 mmol), Ni(NO₃)₂·6H₂O (14.45 g, 49.70 mmol), alanine (4.43 g, 49.70 mmol) and potassium hydroxide (9.76 g, 173.93 mmol) to give the product as a red powder (Crystals suitable for single crystal X-ray structure determination were grown by slow evaporation of the compound in ethyl acetate). Yield (12.71 g, 99 %), 99:1 d.r; m.p.: 282-284 °C (283–285 °C);⁴⁸ (hexane/EtOAc); [α]_D²⁰ = 3685.876 (*c* 0.01 in CHCl₃). ¹H NMR (400 MHz, CDCl₃) δ 8.25 (1H, td, ³*J*_{HH} = 7.4, ⁴*J*_{HH} = 1.9 Hz, ArH), 8.06 (1H, dd, ³*J*_{HH} = 8.6, ⁴*J*_{HH} = 0.8 Hz, ArH), 7.48-7.40 (2H, m, ArH), 7.38 (1H, m, ArH), 7.22-7.16 (2H, m, ArH), 7.15-7.07 (2H, m, ArH), 6.99 (1H, ddd, ³*J*_{HH} = 9.8, ³*J*_{HH} = 8.2 Hz, ArH), 6.89 (1H, m, ArH), 6.71-6.56 (2H, m, ArH), 4.33 (1H, dd, ²*J*_{HH} = 12.9, 0.8 Hz, Ar-CHH-N), 3.83 (1H, q, ³*J*_{HH} = 7.1 Hz, α -CH-Me), 3.73 (1H, dd, ²*J*_{HH} = 12.9, 0.7 Hz, Ar-CHH-N), 3.74-3.65 (1H, m, β (Pro)-CHH), 3.54-3.47 (2H, m, α (Pro)-CH, γ (Pro)-CHH), 2.87-2.78 (1H, m, δ (Pro)-CHH), 2.64-2.49 (1H, m, δ (Pro)-CHH), 2.26-2.17 (1H, m, γ (Pro)-CHH), 2.12-2.00 (1H, m, β (Pro)-CHH), 1.51 (3H, d, ²*J*_{HH} = 7.0 Hz, CH₃); ¹³C NMR (100 MHz, CDCl₃) δ 180.4 (C=O), 180.1 (C=O), 170.4 (C=N), 161.6 (d, ¹*J*_{CF} = 247.7 Hz, CF), 142.1 (Ar-C), 134.2 (d, ⁴*J*_{CF} = 2.4 Hz, Ar-CH), 133.5 (Ar-C), 133.2 (Ar-CH), 131.3 (Ar-CH), 131.2 (Ar-CH), 129.7 (Ar-CH), 129.7 (Ar-CH), 128.9 (d, ³*J*_{CF} = 3.6 Hz, Ar-CH), 127.4 (d, ²*J*_{CF} = 22.7 Hz, Ar-CH), 126.6 (Ar-C), 124.6 (d, ³*J*_{CF} = 3.6 Hz, Ar-CH), 120.8 (Ar-CH), 120.4 (d, ²*J*_{CF} = 14.4 Hz, Ar-C), 124.4 (Ar-CH), 116.2 (Ar-CH), 115.9 (Ar-CH), 70.4 (α -CH), 66.6 (α (Pro)-CH), 57.1 (δ (Pro)-CH₂), 55.6 (Ar-CH₂-N), 30.7 (β (Pro)-CH₂), 24.2 (γ (Pro)-CH₂), 21.9 (CH₃); ¹⁹F NMR (376 MHz, CDCl₃) δ -113.9 (s); IR (ν_{max} /cm⁻¹, neat) 1678, 1621, 1592, 1449, 1446, 1440, 1359, 1330, 1307, 1263, 1232, 1166, 1132, 1111, 1063, 1017, 966, 912, 850, 804, 761, 747, 710, 681, 656; ¹⁹F NMR (376 MHz, CDCl₃) δ -113.9 (s); HRMS-ESI (calcd for C₂₈H₂₇N₃O₃F⁵⁸Ni [M+H]⁺) 530.1390, found 530.1393 (Δ = 0.6 ppm), (calcd for C₂₈H₂₇N₃O₃F⁶⁰Ni [M+H]⁺) 532.1344, found 532.1363 (Δ = 3.6 ppm). HPLC (OD-H column, hexane (5 %)/iPrOH isocratic): 18.36 min.

6.4.6 Synthesis of (*R*)-({2-[1-(2-fluorobenzyl)benzyl]pyrrolidine-2-carboxamide]-phenyl}phenylmethylene)-*R*-alaninato-*N,N',N'',O*} nickel^{II} **98**



The general procedure (C) was followed using (*R*)-*N*-(2-benzoylphenyl)-1-(2-fluorobenzyl)pyrrolidine-2-carboxamide **96** (11.5 g, 28.57 mmol), Ni(NO₃)₂·6H₂O (16.6 g, 57.14 mmol), alanine (6.7 g, 57.14 mmol) and potassium hydroxide (11.2 g, 200.01 mmol) to give the product as a red powder (Crystals suitable for single crystal X-ray structure determination were grown by slow evaporation of the compound in ethyl acetate. These confirmed the (*R, R*) stereochemistry of the product complex). Yield (15.73 g, 99 %), (99:1 dr); (m.p: 175-177 °C) (hexane/EtOAc); [α]_D²⁰ -135.454 (*c* 0.05 in CHCl₃). ¹H NMR (400 MHz, CDCl₃) δ ppm 8.32 (1H, d, ³*J*_{HH} = 6.8 Hz, ArH), 8.11 (1H, d, ³*J*_{HH} = 8.6 Hz, ArH), 7.41-7.54 (3H, m, ArH), 7.10-7.26 (4H, m, ArH), 7.05 (1H, d, ³*J*_{HH} = 8.8 Hz, ArH), 6.96 (1H, d, ³*J*_{HH} = 7.0 Hz, ArH), 6.60-6.72 (2H, m, ArH), 4.39 (1H, d, ²*J*_{HH} = 12.9 Hz, Ar-CHH-N), 3.92 (1H, q, ³*J*_{HH} = 6.8 Hz, α -CH), 3.81 (1H, d, ²*J*_{HH} = 12.9 Hz, Ar-CHH-N), 3.74-3.78 (1H, m, β -CHH), 3.45-3.55 (2H, m, α (Pro)-CH, γ -CHH), 2.74-2.88 (1 H, m, δ (Pro)-CHH), 2.49-2.64 (1H, m, δ (Pro)-CHH), 2.19-2.25 (1H, m, γ (Pro)-CHH), 2.01-2.14 (1H, m, β (Pro)-CHH), 1.59 (3H, d, ³*J*_{HH} = 6.8 Hz, CH₃); ¹³C NMR (101 MHz, DCCl₃) δ ppm 180.61 (C=O), 180.2 (C=O), 170.3 (C=N), 161.6 (d, ¹*J*_{CF} = 249.3 Hz, CF), 142.0 (Ar-C), 134.2 (d, ⁴*J*_{CF} = 3.2 Hz, Ar-CH), 133.4 (Ar-CH), 133.2 (Ar-C), 132.1 (Ar-CH), 131.2 (d, ³*J*_{CF} = 9.6 Hz, Ar-CH), 129.7 (Ar-CH), 128.9 (Ar-CH), 128.8 (Ar-2CH), 127.5 (Ar-CH), 127.2 (Ar-CH), 126.6 (Ar-C), 124.6 (d, ³*J*_{CF} = 3.2 Hz, Ar-CH), 123.9 (Ar-CH), 120.8 (Ar-CH), 120.5 (d, ²*J*_{CF} = 14.4 Hz, Ar-C), 116.1 (d, ²*J*_{CF} = 22.4 Hz, Ar-CH), 70.4 (C α -H), 66.9 (α (Pro)-CH), 57.1 (δ -CH₂), 55.6 (Ar-CH₂-N), 30.7 (β -CH₂), 24.2 (γ -CH₂), 21.8 (CH₃); ¹⁹F NMR (376 MHz, CDCl₃) δ -113.9 (s); HRMS-ESI (calcd for C₂₈H₂₆N₃O₃FNa⁵⁸Ni [M+Na]⁺) 552.1209, found 552.1206 (Δ = -0.5 ppm), (calcd for C₂₈H₂₆N₃O₃FNa⁶⁰Ni [M+Na]⁺) 554.1164, found 554.1174 (Δ = 1.8 ppm). HPLC (OD-H column, hexane (5 %)/*i*PrOH isocratic): 15.07 min.

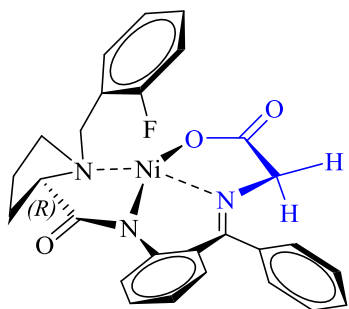
6.4.7 Synthesis of (*S*)-({2-[1-(2-fluorobenzyl)benzyl]pyrrolidine-2-carboxamide]-phenyl}phenylmethylene)-glycinato-*N,N',N'',O*} nickel^{II} **55**



The general procedure (C) was followed using (*S*)-*N*-(2-benzoylphenyl)-1-(2-fluorobenzyl)pyrrolidine-2-carboxamide **95** (19.5 g, 48.45 mmol), Ni(NO₃)₂·6H₂O (28.18 g, 290.8 mmol), glycine (7.27 g, 96.90 mmol) and potassium hydroxide (19.03 g, 56.11 mmol) to give the product as a red powder. Yield (22.619 g, 91 %), (98:2 ee); m.p.: 125–127 °C (124–126 °C),⁹⁵

(hexane/EtOAc); $[\alpha]_D^{20} = 2387.736$ (*c* 0.01 in CHCl₃). ¹H NMR (400 MHz, CDCl₃) δ ppm 8.33 (1H, td, ³*J*_{HH} = 7.5, ⁴*J*_{HH} = 1.9 Hz, ArH), 8.28 (1H, dd, ³*J*_{HH} = 8.8, ⁴*J*_{HH} = 1.0 Hz, ArH), 7.47–7.57 (3H, m, ArH), 7.29–7.36 (1H, m, ArH), 7.19–7.28 (2H, m, ArH), 7.08–7.16 (2H, m, ArH), 6.99 (1H, s, ArH), 6.82 (1H, dd, ³*J*_{HH} = 8.2, ⁴*J*_{HH} = 1.76 Hz, ArH), 6.72 (1H, ddd, ³*J*_{HH} = 8.2, ³*J*_{HH} = 7.0, ⁴*J*_{HH} = 1.2 Hz, ArH), 4.48 (1H, d, ²*J*_{HH} = 12.9 Hz, Ar-CHH-N), 3.94 (1H, d, ²*J*_{HH} = 13.5 Hz, Ar-CHH-N), 3.72 (2H, AB quartet, ²*J*_{HH} = 20.4 Hz, α-CH₂), 3.59–3.65 (1H, m, β(Pro)-CHH), 3.46 (1H, dd, ²*J*_{HH} = 10.8, ³*J*_{HH} = 5.7 Hz, α(Pro)-CH), 3.31–3.42 (1H, m, γ(Pro)-CHH), 2.60–2.72 (1H, m, δ(Pro)-CHH), 2.41–2.55 (1 H, m, δ(Pro)-CHH), 2.04–2.18 (2H, m, β(Pro)-CHH, γ(Pro)-CHH); ¹³C NMR (100 MHz, CDCl₃) δ ppm 181.0 (C=O), 177.3 (C=O), 171.7 (C=N), 161.8 (d, ¹*J*_{CF} = 249.3, CF), 142.4 (Ar-C), 134.6 (Ar-C), 134.2 (d, ³*J*_{CF} = 3.2 Hz, Ar-CH), 133.3 (Ar-C), 132.3 (Ar-CH), 131.4 (³*J*_{CF} = 9.6 Hz, Ar-CH), 129.7 (²*J*_{CF} = 17.6 Hz, Ar-CH), 129.4 (Ar-CH), 126.3 (Ar-C), 125.7 (Ar-CH), 125.3 (Ar-CH), 124.6 (d, ⁴*J*_{CF} = 3.2 Hz, Ar-CH), 124.4 (Ar-CH), 121.0 (Ar-CH), 120.4 (d, ²*J*_{CF} = 14.4 Hz, C), 116.3 (Ar-CH), 116.1 (Ar-CH), 70.0 (α(Pro)-CH), 61.3 (α-CH₂), 57.2 (δ(Pro)-CH₂), 55.7 (Ar-CH₂-N), 30.6 (β(Pro)-CH₂), 23.8 (γ(Pro)-CH₂); ¹⁹F NMR (376 MHz; CDCl₃) −113.7 (s); IR (ν_{max}/cm^{−1}, neat): 3057, 2975, 1678, 1633, 1588, 1546, 1489, 1470, 1439, 1365, 1332, 1302, 1256, 1228, 1172, 1160, 1128, 1115, 1091, 1061, 1024, 965, 929, 920, 862, 812, 787, 768, 757, 726, 703, 688; ¹⁹F NMR (376 MHz, CDCl₃) δ -113.7 (s); HRMS-ESI (calcd for C₂₇H₂₅N₃O₃F⁵⁸Ni [M+H]⁺) 516.1233, found 516.1244 (Δ = 2.1 ppm), (calcd for C₂₇H₂₅N₃O₃F⁶⁰Ni [M+H]⁺) 516.1188, found 516.1187 (Δ = -0.2 ppm). HPLC (OD-H column, hexane (5 %)/iPrOH isocratic): 12.86 min.

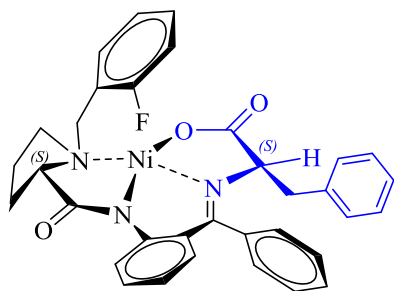
6.4.8 Synthesis of (*R*)-({2-[1-(2-fluorobenzyl)benzyl]pyrrolidine-2-carboxamide]-phenyl}phenylmethylene)-glycinato-*N,N',N'',O* nickel^{II} **97**



The general procedure (C) was followed using (*R*)-*N*-(2-benzoylphenyl)-1-(2-fluorobenzyl)pyrrolidine-2-carboxamide **96** (5 g, 12.42 mmol), Ni(NO₃)₂·6H₂O (7.23 g, 24.85 mmol) and glycine (1.865 g, 24.85 mmol) and potassium hydroxide (4.879 g, 86.96 mmol) to give the product as a red powder. Yield (5.91 g, 92 %), (98:2 ee); m.p.: 112–114 °C (hexane/EtOAc); ¹H NMR (400 MHz,

CDCl₃) δ ppm 8.33 (1H, td, ³J_{HH} = 7.4, ⁴J_{HH} = 1.6 Hz, ArH), 8.11 (1H, dd, ³J_{HH} = 8.3, ⁴J_{HH} = 0.9 Hz, ArH), 7.47–7.57 (3H, m, ArH), 7.08–7.30 (4H, m, ArH), 6.97–6.99 (1H, m, ArH), 6.82 (1H, dd, ³J_{HH} = 8.2, ⁴J_{HH} = 1.6 Hz, ArH), 6.71 (1H, td, ³J_{HH} = 7.6, ³J_{HH} = 7.6, ⁴J_{HH} = 1.1 Hz, ArH), 4.45 (1H, d, ²J_{HH} = 12.9 Hz, Ar-CHH-N), 3.91 (1H, d, ²J_{HH} = 12.9 Hz, Ar-CHH-N), 3.73 (1H, AB quartet, ³J_{HH} = 20.2 Hz, α-CH), 3.56–3.64 (1H, m, β(Pro)-CHH), 3.48 (1H, dd, ³J_{HH} = 10.9, ³J_{HH} = 5.8 Hz, α(Pro)-CH), 3.31–3.42 (1H, m, γ(Pro)-CHH), 2.61–2.68 (1 H, m, δ(Pro)-CHH), 2.41–2.52 (1H, m, δ(Pro)-CHH), 2.03–2.15 (2H, m, γ(Pro)-CHH, β(Pro)-CHH); ¹³C NMR (100 MHz, CDCl₃) δ ppm 180.9 (C=O), 177.3 (C=O), 171.6 (C=N), 161.7 (d, ¹J_{CF} = 249.3 Hz, CF), 142.4 (Ar-C), 134.5 (Ar-CH), 134.2 (d, ³J_{CF} = 3.2 Hz, Ar-CH), 133.2 (Ar-C), 132.2 (Ar-CH), 131.4 (d, ³J_{CF} = 8.0 Hz, Ar-CH), 129.8 (Ar-CH), 129.6 (Ar-CH), 129.3 (Ar-2CH), 126.3 (Ar-C), 125.6 (Ar-CH), 125.3 (Ar-CH), 124.6 (d, ³J_{CF} = 3.2 Hz, Ar-CH), 124.3 (Ar-CH), 120.9 (Ar-CH), 120.5 (d, ²J_{CF} = 14.4 Hz, C), 116.1 (d, ²J_{CF} = 20.8 Hz, Ar-CH), 70.0 (α-CH₂), 61.3 (α (Pro)-CH), 57.3 (δ(Pro)-CH₂), 55.8 (Ar-CH₂-N), 30.6 (β(Pro)-CH₂), 23.7 (γ(Pro)-CH₂); ¹⁹F NMR (376 MHz; CDCl₃) −113.6 (s); ¹⁹F NMR (376 MHz, CDCl₃) δ −113.9 (s); HRMS-ESI (calcd for C₂₇H₂₅N₃O₃F⁵⁸Ni [M+H]⁺) 516.1233, found 516.1213 (Δ = −3.9 ppm), (calcd for C₂₇H₂₅N₃O₃F⁶⁰Ni [M+H]⁺) 516.1188, found 516.1186 (Δ = −0.4 ppm). HPLC (OD-H column, hexane (5 %)/iPrOH isocratic): 19.27 min.

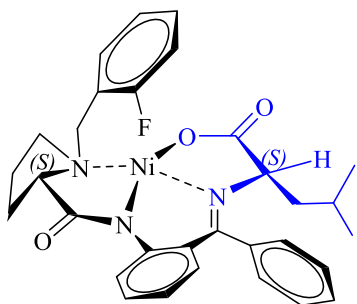
6.4.9 Synthesis of (*S*)-({2-[1-(2-fluorobenzyl)benzyl]pyrrolidine-2-carboxamide]-phenyl}phenylmethylene)-phenylalaninato-*N,N',N'',O*} nickel^{III} **99**



The general procedure (C) was followed using (*S*)-*N*-(2-benzoylphenyl)-1-(2-fluorobenzyl)pyrrolidine-2-carboxamide **95** (2 g, 4.97 mmol), Ni(NO₃)₂·6H₂O (2.89 g, 9.94 mmol) and phenylalanine (1.31 g, 7.95 mmol) potassium hydroxide (1.95 g, 34.79 mmol) to give the product as a red powder (Crystals suitable for single

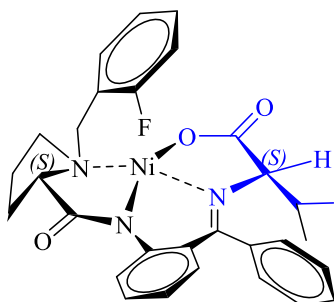
crystal X-ray structure determination were grown by slow evaporation of the compound in ethylacetate. These confirmed the (*S, S*) stereochemistry of the product complex). Yield (2.985 g, 99 %), 99:1 d.r.; m.p: 205-206 °C (hexane/EtOAc); ¹H NMR (400 MHz, CDCl₃) δ ppm 8.35 (1H, br t, ³J_{HH} = 6.9 Hz, ArH), 8.11 (1H, br d, ³J_{HH} = 8.6 Hz, ArH), 7.42-7.55 (3H, m, ArH), 7.12-7.26 (4H, m, ArH), 7.04 (1H, br t, ³J_{HH} = 8.9 Hz, ArH), 6.94 (1H, br d, ³J_{HH} = 7.0 Hz, ArH), 6.60-6.71 (2H, m, ArH), 4.24-4.30 (2H, m, Ar-CHH-N, Ar-CHH), 3.71 (1H, br d, ²J_{HH} = 13.3 Hz, Ar-CHH-N), 3.31-3.27 (1H, m, α-CH), 3.60-3.73 (2H, m, α(Pro)-CH, β(Pro)-CHH), 2.83 (1H, d, ²J_{HH} = 13.7 Hz, Ar-CHH), 2.40-2.29 (3H, m, γ (Pro)-CHH, δ (Pro)-CH₂), 1.94-1.85 (1H, m, γ(Pro)-CHH), 1.73-1.62 (1H, m, β(Pro)-CHH); ¹³C NMR (100 MHz, CDCl₃) δ ppm 180.0 (C=O), 178.5 (C=O), 171.2 (C=N), 161.7 (d, ¹J_{CF} = 247.7 Hz, CF), 142.9 (Ar-C), 135.9 (Ar-C), 134.2 (Ar-C), 134.1 (d, ³J_{CF} = 8.0 Hz, Ar-CH), 133.6 (Ar-CH), 132.4 (Ar-CH), 131.1 (d, ³J_{CF} = 8.0 Hz, Ar-CH), 130.6 (Ar-CH), 129.8 (Ar-CH), 128.8 (Ar-2CH), 127.9 (Ar-CH), 127.4 (Ar-CH), 127.2 (Ar-CH), 126.2 (Ar-C), 124.4 (d, ⁴J_{CF} = 3.2 Hz, Ar-CH), 123.3 (Ar-CH), 120.6 (Ar-CH), 120.4 (d, ²J_{CF} = 14.4 Hz, Ar-C), 116.0 (d, ²J_{CF} = 22.37 Hz, Ar-CH), 71.6 (α(Pro)-CH), 70.4 (α-CH), 56.9 (Ar-CH₂-N), 55.8 (δ(Pro)-CH₂), 39.7 (Ar-CH₂), 30.6 (β(Pro)-CH₂), 23.1 (γ(Pro)-CH₂); ¹⁹F NMR (376 MHz, CDCl₃) δ -113.9 (s); HRMS-ESI (calcd for C₃₄H₃₁N₃O₃F⁵⁸Ni [M+H]⁺) 606.1703, found 6.6.1703 (Δ = 0.0 ppm), (calcd for C₃₄H₃₁N₃O₃F⁶⁰Ni [M+H]⁺) 608.1657, found 608.1677 (Δ = 3.3 ppm).

6.4.10 Synthesis of (S)-({2-[1-(2-fluorobenzyl)benzyl]pyrrolidine-2-carboxamide}-phenyl)phenylmethylene)-(S)-leucinato-*N,N',N'',O* nickel^{II} **100**



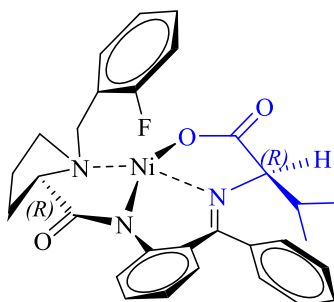
The general procedure (C) was followed using (S)-*N*-(2-benzoylphenyl)-1-(2-fluorobenzyl)pyrrolidine-2-carboxamide **95** (6 g, 14.91 mmol), Ni(NO₃)₂·6H₂O (8.67g, 29.82 mmol), leucine (5.87g, 44.73 mmol) and potassium hydroxide (5.86 g, 104.36 mmol) to give the product as a red powder (Crystals suitable for single crystal X-ray structure determination were grown by slow evaporation of the compound in ethyl acetate. These confirmed the (*S,S*) stereochemistry of the product complex). Yield (6.34 g, 98 %), (99:1 d.r); m.p: 187-189 °C; ¹H NMR (500 MHz, CDCl₃) δ ppm 8.35 (1H, br t, ³*J*_{HH} = 6.9 Hz, ArH), 8.11 (1H, br d, ³*J*_{HH} = 8.61 Hz, ArH), 7.42-7.55 (3H, m, ArH), 7.11-7.29 (4H, m, ArH), 7.04 (1H, br t, ³*J*_{HH} = 8.90 Hz, ArH), 6.94 (1H, br d, ³*J*_{HH} = 7.04 Hz, ArH), 6.60-6.71 (2H, m, ArH), 4.47 (1H, br d, ²*J*_{HH} = 12.9 Hz, Ar-CHH-N), 3.87 (1H, dd, ³*J*_{HH} = 10.6, ³*J*_{HH} 3.3 Hz, α-CH), 3.82 (1H, br d, ²*J*_{HH} = 12.9 Hz, Ar-CHH-N), 3.61-3.73 (1H, m, β(Pro)-CHH), 3.46-3.52 (2H, m, α(Pro)-CH, γ(Pro)-CHH), 2.84-2.95 (1H, m, δ(Pro)-CHH), 2.43-2.63 (2H, m, δ(Pro)-CHH, γ(Pro)-CHH), 2.22-2.18 (1H, m, CH₂), 2.04-2.11 (1H, m, β(Pro)-CHH), 1.90-1.95 (1H, m, δ(Pro)-CHH), 1.74-1.85 (1H, m, CH), 0.87 (3H, br d, *J*_{HH} = 6.7 Hz, CH₃), 0.75 (3H, br d, ³*J*_{HH} = 6.8 Hz, CH₃); ¹³C NMR (100 MHz, CDCl₃) δ ppm δ 180.0 (C=O), 179.2 (C=O), 169.7 (C=N), 161.6 (d, ¹*J*_{CF} = 247.7 Hz, CF), 142.1 (Ar-C), 134.2 (d, ³*J*_{CF} = 3.2 Hz, Ar-CH), 133.6 (Ar-C), 133.2 (Ar-CH), 132.0 (Ar-CH), 131.1 (d, ³*J*_{CF} = 8.0 Hz, Ar-CH), 129.7 (Ar-CH), 128.9 (Ar-2CH), 127.8 (Ar-CH), 127.6 (Ar-CH), 126.7 (Ar-C), 124.5 (d, ⁴*J*_{CF} = 3.2 Hz, Ar-CH), 123.8 (Ar-CH), 120.7 (Ar-CH), 120.5 (d, ²*J*_{CF} = 14.4 Hz, Ar-C), 116.1 (d, ²*J*_{CF} = 22.37 Hz, Ar-CH), 70.3 (α(Pro)-CH), 69.1 (α-CH), 57.0 (δ-CH₂), 55.5 (Ar-CH₂-N), 46.1 (CH₂ leucine), 30.7 (β-CH₂), 24.3 (CH₃), 24.0 (γ-CH₂), 23.8 (CH₃), 20.6 (CH(CH₃)₂); ¹⁹F NMR (376 MHz, CDCl₃) δ -113.94 (s); HRMS-ESI (calcd for C₃₁H₃₃N₃O₃F⁵⁸Ni [M+H]⁺) 572.1859, found 572.1847 (Δ = -2.1 ppm), (calcd for C₂₈H₂₇N₃O₃F⁶⁰Ni [M+Na]⁺) 594.1679, found 594.1664 (Δ = -2.5 ppm).

6.4.11 Synthesis of (*S*)-({2-[1-(2-fluorobenzyl)benzyl]pyrrolidine-2-carboxamide}-phenyl)phenylmethylene)-*S*-valinato-*N,N',N'',O*} nickel^{II} **101**



The general procedure (C) was followed using (*S*)-*N*-(2-benzoylphenyl)-1-(2-fluorobenzyl)pyrrolidine-2-carboxamide **95** (11.5 g, 28.5741 mmol), Ni(NO₃)₂·6H₂O (16.618 g, 57.147 mmol) and valine (6.695 g, 57.147 mmol) and potassium hydroxide (11.223 g, 200.015 mmol) to give the product as a red powder (Crystals suitable for single crystal X-ray structure determination were grown by slow evaporation of the compound in ethylacetate. These confirmed the (*S,S*) stereochemistry of the product complex). Yield (15.730 g, 99 %), (99:1 d.r); m.p: 187-189 °C; ¹H NMR (500 MHz, CDCl₃) δ ppm 8.25-8.32 (2H, m, ArH), 7.44-7.52 (3H, m, ArH), 7.12-7.28 (4H, m, ArH), 6.98-7.03 (1H, m, ArH), 6.92 (1H, d, ³J_{HH} = 7.1 Hz, ArH), 6.63-6.68 (2H, m, ArH), 4.45 (1H, br d, ²J_{HH} = 13.1 Hz, Ar-CHH-N), 3.85 (1H, d, ²J_{HH} = 13.1 Hz, Ar-CHH-N), 3.82 (1H, br d, ³J_{HH} = 3.5 Hz, α-CH), 3.45-3.49 (2H, m, α(Pro)-CH, β(Pro)-CHH), 3.28-3.40 (1H, m, γ(Pro)-CHH), 2.85-2.93 (1H, m, δ(Pro)-CHH), 2.50-2.62 (1H, m, δ(Pro)-CHH), 2.03-2.11 (2H, m, γ(Pro)-CHH, β(Pro)-CHH), 1.92 (3H, br d, ³J_{HH} = 6.7 Hz, CH₃), 1.74-1.85 (1H, m, CH), 0.75 (3H, br d, ³J_{HH} = 6.8 Hz, CH₃); ¹³C NMR (100 MHz, CDCl₃) δ ppm δ 179.9 (C=O), 177.7 (C=O), 170.8 (C=N), 161.6 (d, ¹J_{CF} = 249.3 Hz, CF), 142.4 (Ar-C), 134.2 (Ar-CH), 134.1 (Ar-CH), 133.5 (Ar-C), 132.3 (Ar-CH), 131.1 (d, ³J_{CF} = 9.6 Hz, Ar-CH), 129.6 (Ar-CH), 128.9 (Ar-2CH), 128.7 (Ar-CH), 128.0 (Ar-CH), 127.2 (Ar-CH), 126.5 (Ar-C), 124.4 (d, ³J_{CF} = 3.2 Hz, Ar-CH), 123.3 (Ar-CH), 120.6 (Ar-CH), 120.4 (d, ²J_{CF} = 14.4 Hz, Ar-C), 116.1 (d, ²J_{CF} = 22.4 Hz, Ar-CH), 75.4 (α-CH), 70.5 (α(Pro)-CH), 56.5 (δ(Pro)-CH₂), 55.8 (Ar-CH₂-N), 34.2 (CH), 30.7 (β(Pro)-CH₂), 23.1 (γ(Pro)-CH₂), 19.7 (CH₃), 18.1 (CH₃); ¹⁹F NMR (376 MHz, CDCl₃) δ -113.9 (s); HRMS-ESI (calcd for C₃₀H₃₀N₃O₃F⁵⁸NiNa [M+Na]⁺) 580.1522, found 580.1520 (Δ = -0.2 ppm), (calcd for C₃₀H₃₀N₃O₃F⁶⁰NiNa [M+Na]⁺) 582.1477, found 582.1496 (Δ = -3.3 ppm).

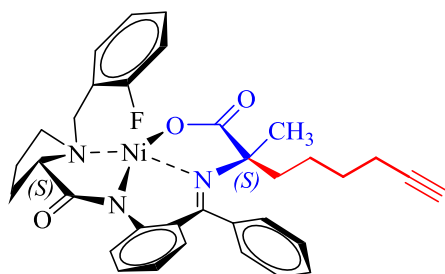
6.4.12 Synthesis of (*R*)-({2-[1-(2-fluorobenzyl)benzyl]pyrrolidine-2-carboxamide]-phenyl}phenylmethylene)-*R*-valinato-*N,N',N'',O*} nickel^{II} **102**



The general procedure (**C**) was followed using (*S*)-*N*-(2-benzoylphenyl)-1-(2-fluorobenzyl)pyrrolidine-2-carboxamide **96** (0.5 g, 1.242 mmol), Ni(NO₃)₂·6H₂O (0.720 g, 2.485 mmol), valine (0.291 g, 2.485 mmol) in methanol and potassium hydroxide (0.488 g, 8.698 mmol) to give the product as a red powder (Crystals suitable for single crystal X-ray structure determination were grown by slow evaporation of the compound in ethyl acetate. These confirmed the (*R*, *R*) stereochemistry of the product complex). Yield (0.647 g, 93 %), (98:2 d.r); m.p: 175-177 °C; ¹H NMR (400 MHz, CDCl₃) δ ppm 8.24-8.32 (2H, m, ArH), 7.42-7.55 (3H, m, ArH), 7.10-7.27 (4H, m, ArH), 6.98-7.04 (1H, m, ArH), 6.92 (1H, d, ³J_{HH} = 7.0 Hz, ArH), 6.90-6.94 (1H, m, ArH), 6.67 (2H, d, ³J_{HH} = 3.9 Hz, ArH), 4.47 (1H, br d, ²J_{HH} = 13.3 Hz, Ar-CHH-N), 3.87 (1H, d, ²J_{HH} = 13.3 Hz, Ar-CHH-N), 3.82 (1H, br d, ³J_{HH} = 12.9 Hz, α-CH), 3.43-3.50 (2H, m, α(Pro)-CH, β-CHH), 3.38-3.29 (1H, m, γ-CHH), 2.84-2.95 (1H, m, δ-CHH), 2.50-2.63 (1H, m, δ-CHH), 2.02-2.13 (2H, m, γ-CHH, β-CHH), 1.92 (3H, br d, ³J_{HH} = 6.7 Hz,), 1.74-1.85 (1H, m, CH), 0.75 (3H, br d, ¹J_{HH} = 6.8 Hz,); ¹⁹F NMR (376 MHz, CDCl₃) δ -113.8 (s); HRMS-ESI (calcd for C₃₀H₃₀N₃O₃F⁵⁸NiNa [M+Na]⁺) 580.1522, found 580.1525 (Δ = 0.1 ppm), (calcd for C₃₀H₃₀N₃O₃F⁶⁰NiNa [M+Na]⁺) 582.1477, found 582.1493 (Δ = -2.7 ppm).

6.5 Experimental for Chapter 3

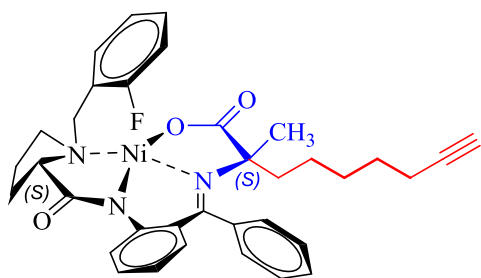
6.5.1 Synthesis of (*S*)-({2-[1-(2-fluorobenzyl)benzyl]pyrrolidine-2-carboxamide]-phenyl}phenylmethylene)-(*S*)-hexynylalaninato-*N,N',N'',O*}nickel(II) **134**



The general procedure (**D**) was followed using potassium tert-butoxide (3.555 g, 31.684 mmol), (*S*)-({2-[1-(2-fluorobenzyl)pyrrolidine-2-carboxamide] phenyl}phenylmethylene)-alaninato-*N,N',N'',O*} nickel(II) (**56**) (4.200 g, 7.921 mmol) in DMF and a solution of 6-iodohex-1-yne (3.130 g, 23.763 mmol) in DMF, to give the product as a red powder (Crystals suitable for single crystal X-ray structure determination were grown by slow evaporation of the compound in ethylacetate. These confirmed the (*S*, *S*) stereochemistry of the product complex).

(Yield 3.412 g, 70 %); (99 % dr) m.p: 212-214 °C; $[\alpha]_D^{20} = 2302.952$ (c 0.01 in CHCl_3). $^1\text{H-NMR}$ (400 MHz, CDCl_3) δ 8.30 (1H, td, $^3J_{\text{HH}} = 7.4$, $^4J_{\text{HH}} = 1.4$ Hz, ArH), 8.03 (1H, br d, $^3J_{\text{HH}} = 8.6$ Hz, ArH), 7.44-7.52 (2H, m, ArH), 7.36-7.43 (1H, m, ArH), 7.21 (2 H, td, $^3J_{\text{HH}} = 7.4$, $^4J_{\text{HH}} = 1.4$ Hz), 7.21 (1H, m, ArH), 7.06-7.18 (2H, m, ArH), 7.01 (1H, d, $^3J_{\text{HH}} = 8.6$, Hz, ArH), 6.61-6.69 (2H, m, ArH), 6.67-6.61 (2H, m, ArH), 4.51 (1H, d, $^2J_{\text{HH}} = 13.5$ Hz, Ar-CHH-N), 3.95 (1H, d, $^2J_{\text{HH}} = 13.3$ Hz, Ar-CHH-N), 3.56-3.67 (1H, dd, $^3J_{\text{HH}} = 7.4$, $^4J_{\text{HH}} = 1.4$ Hz, $\alpha(\text{Pro})$ -CH), 3.41 (1H, (1H, m, $\beta(\text{Pro})$ -CHH), 3.22-3.36 (1H, m, $\gamma(\text{Pro})$ -CHH), 2.74-2.82 (1H, m, $\delta(\text{Pro})$ -CHH), 2.46-2.60 (2H, m, $\delta(\text{Pro})$ -CHH, $\gamma(\text{Pro})$ -CHH), 2.30 (2H, td, $^3J_{\text{HH}} = 7.4$, $^4J_{\text{HH}} = 1.4$ Hz, CH_2), 2.17-2.00 (3H, m, $\beta(\text{Pro})$ -CHH, CH_2), 1.98 (1H, t, $^4J_{\text{HH}} = 2.5$ Hz, $\text{C}\equiv\text{CH}$), 1.69 (1H, dt, m, CHH), 1.42-1.64 (3H, m, CHH, CH_2), 1.26 (3H, s, CH_3); $^{13}\text{C NMR}$ (100 MHz, CDCl_3) 182.4 (C=O), 180.2 (C=O), 172.6 (C=N), 161.8 (d, $^1J_{\text{CF}} = 248.5$, CF), 141.6 (Ar-C), 136.6 (Ar-C), 134.2 (d, $^3J_{\text{CF}} = 3.20$, Ar-CH), 133.4 (Ar-CH), 131.6 (Ar-CH), 131.3 (d, $^3J_{\text{CF}} = 9.59$, Ar-CH), 130.3 (Ar-CH), 129.4 (Ar-CH), 128.8 (Ar-CH), 128.0 (Ar-CH), 127.3 (Ar-CH), 126.9 (Ar-C), 124.5 (d, $^4J_{\text{CF}} = 3.20$, Ar-CH), 124.0 (Ar-CH), 120.8 (Ar-CH), 120.5 (d, $^2J_{\text{CF}} = 14.38$, C), 116.1 (d, $^2J_{\text{CF}} = 22.37$, Ar-CH), 83.9 ($\text{HC}\equiv\text{C}$), 78.0 ($\text{C}\equiv\text{C}$), 70.2 ($\alpha(\text{Pro})$ -CH), 69.1 (Ar- CH_2 -N), 56.8 (α -C), 55.9 ($\delta(\text{Pro})$ - CH_2), 39.5 ($\beta(\text{Pro})$ - CH_2), 30.6 ($\text{HC}\equiv\text{C}$ - CH_2), 29.8 (CH_3), 28.3 ($\text{HC}\equiv\text{C}$ -(CH_2)₃- CH_2), 24.9 (CH_2), 23.3 ($\gamma(\text{Pro})$ - CH_2), 18.4 (CH_2). IR ($\nu_{\text{max}}/\text{cm}^{-1}$, neat): 3257, 2933, 2159, 1665, 1632, 1575, 1534, 1491, 1470, 1459, 1437, 1354, 1328, 1308, 1279, 1250, 1159, 1111, 1079, 1062, 1011, 972, 930, 888, 837, 753, 717, 672; $^{19}\text{F NMR}$ (376 MHz, CDCl_3) δ -113.7 (s); HRMS-ESI (calcd for $\text{C}_{34}\text{H}_{35}\text{N}_3\text{O}_3\text{F}^{58}\text{Ni}$ $[\text{M}+\text{H}]^+$) 610.2016, found 610.2011 ($\Delta = -0.8$ ppm), (calcd for $\text{C}_{34}\text{H}_{35}\text{N}_3\text{O}_3\text{F}^{60}\text{Ni}$ $[\text{M}+\text{H}]^+$) 612.1970, found 612.1998 ($\Delta = 4.6$ ppm).

6.5.2 Synthesis of (S)-({2-[1-(2-fluorobenzyl)benzyl]pyrrolidine-2-carboxamide}phenyl)methylene)-(S)-heptynylalaninato-*N,N',N'',O*}nickel^{II} **135**

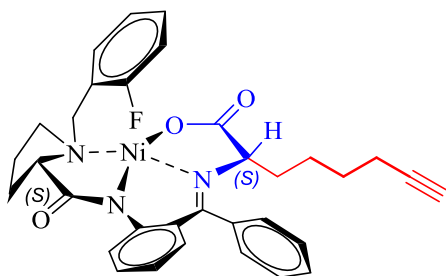


The general procedure (**D**) was followed using potassium tert-butoxide (2.963 g, 26.404 mmol), (S)-({2-[1-(2-fluorobenzyl)pyrrolidine-2-carboxamide]phenyl)methylene)-alaninato-*N,N',N'',O*} nickel(II) (**56**) (3.500 g, 6.60 mmol) and a solution of 7-iodohept-1-yne

(**3**) (4.398 g, 19.80 mmol) in DMF, to give the product as a red-orange solid. (Yield 3.029 g, 74 %), (98 % dr), m.p: 184-186 °C; $[\alpha]_D^{20} = 2707.993$ (c 0.01 in CHCl_3). $^1\text{H-NMR}$ (400

MHz, CDCl₃) δ 8.30 (1H, td, $^3J_{\text{HH}} = 7.4$, $^4J_{\text{HH}} = 1.8$ Hz, ArH), 8.03 (1H, br d, $^3J_{\text{HH}} = 8.2$ Hz, ArH), 7.45-7.51 (2H, m, ArH), 7.36-7.42 (H, m, ArH), 7.27-7.35 (2H, m, ArH), 7.18-7.23 (H, m, ArH), 7.23 (H, td, $^3J_{\text{HH}} = 7.4$, $^4J_{\text{HH}} = 1.5$ Hz, ArH), 7.15 (1H, ddd, $^3J_{\text{HH}} = 8.6$, $^3J_{\text{HH}} = 6.0$, $^4J_{\text{HH}} = 2.6$ Hz, ArH), 7.06-7.12 (H, m, ArH), 6.96 (1H, d, $^3J_{\text{HH}} = 7.6$, Hz, ArH), 6.61-6.66 (2H, m, ArH), 4.51 (1H, d, $^2J_{\text{HH}} = 12.9$ Hz, Ar-CHH-N), 3.95 (1H, d, $^2J_{\text{HH}} = 12.7$ Hz, Ar-CHH-N), 3.61 (1H, dd, $^3J_{\text{HH}} = 10.0$, $^3J_{\text{HH}} = 6.5$ Hz, $\alpha(\text{Pro})$ -CH), 3.20-3.32 (1H, m, $\beta(\text{Pro})$ -CHH), 2.80-2.73 (1H, m, $\gamma(\text{Pro})$ -CHH), 2.48-2.58 (1H, m, $\delta(\text{Pro})$ -CHH), 2.28-2.36 (1H, m, $\delta(\text{Pro})$ -CHH), 2.30 (2H, td, $^3J_{\text{HH}} = 7.0$, $^4J_{\text{HH}} = 2.6$ Hz, $\gamma(\text{Pro})$ -CHH, $\beta(\text{Pro})$ -CHH), 2.13-1.92 (4H, m, CH₂-CH₂), 1.98-1.75 (4H, m, CH₂-CH₂), 1.37-1.49 (2H, m, CH₂), 1.24 (3H, s, CH₃); ¹³C NMR (100 MHz, CDCl₃) 182.4 (C=O), 180.1 (C=O), 172.4 (C=N), 161.7 (d, $^1J_{\text{CF}} = 249.3$ Hz, CF), 141.5 (Ar-C), 136.6 (Ar-C), 134.2 (d, $^3J_{\text{CF}} = 3.20$, Ar-CH), 133.4 (Ar-CH), 131.6 (Ar-CH), 131.3 (d, $^3J_{\text{CF}} = 8.0$ Hz, Ar-CH), 130.2 (Ar-CH), 129.4 (Ar-CH), 128.8 (Ar-CH), 127.9 (Ar-CH), 127.2 (Ar-CH), 126.9 (Ar-CH), 124.5 (d, $^4J_{\text{CF}} = 3.20$, Ar-CH), 123.9 (Ar-CH), 120.8 (Ar-CH), 120.5 (d, $^2J_{\text{CF}} = 16.0$ Hz, C), 116.1 (d, $^2J_{\text{CF}} = 22.4$ Hz, Ar-CH), 84.2 (HC \equiv C), 78.1 (C \equiv C), 70.2 ($\alpha(\text{Pro})$ -CH), 68.6 (Ar-CH₂-N), 56.8 (α -C), 55.9 ($\delta(\text{Pro})$ -CH₂), 39.9 ($\beta(\text{Pro})$ -CH₂), 30.6 (HC \equiv C-CH₂), 29.7 (CH₃), 28.7 (CH₂), 28.3 (HC \equiv C-(CH₂)₃-CH₂), 25.4 (CH₂), 23.3 ($\gamma(\text{Pro})$ -CH₂), 18.4 (CH₂). ¹⁹F NMR (376 MHz, CDCl₃) δ -113.7 (s); ¹⁹F NMR (376 MHz, CDCl₃) δ -113.68 (s); IR (vmax/cm⁻¹, neat): 3301, 2934, 2860, 2160, 1977, 1738, 1666, 1635, 1588, 1543, 1491, 1470, 1457, 1439, 1355, 1334, 1254, 1231, 1164, 1110, 1060, 970, 911, 752, 726, 708; HRMS-ESI (calcd for C₃₅H₃₆N₃O₃F⁵⁸Ni [M+H]⁺) 623.2116, found 623.2011 ($\Delta = -0.8$ ppm), (calcd for C₃₅H₃₆N₃O₃F⁶⁰Ni [M+H]⁺) 625.2013, found 625.1999 ($\Delta = 4.6$ ppm).

6.5.3 Synthesis of (S)-({2-[1-(2-fluorobenzyl)benzyl]pyrrolidine-2-carboxamide}phenyl)methylphenylmethylen-(S)-hexynylglycinato-*N,N',N'',O*nickel^{II} **136**

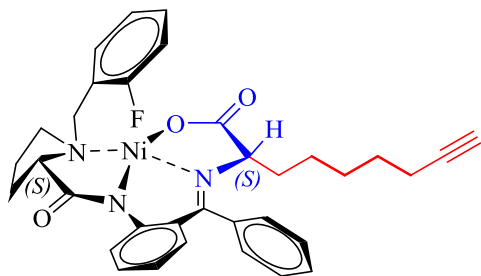


The general procedure (**E**) was followed using potassium tert-butoxide (1.087 g, 9.685 mmol) in THF, (S)-({2-[1-(2-fluorobenzyl)pyrrolidine-2-carboxamide]phenyl} phenylmethylen)-glycinato-*N,N',N'',O*nickel^{II} (**55**) (5.00 g, 9.685 mmol) and a solution of 6-iodohex-1-yne (1.276

mL, 9.685 mmol) in THF, to give the product as a reddish-orange solid (Crystals suitable for single crystal X-ray structure determination were grown by slow evaporation of the

compound in ethyl acetate. These confirmed the (*S*, *S*) stereochemistry of the product complex). (Yield 3.702 g, 64 %); (98: 2 dr); m.p: 233-235 °C. ¹H-NMR (400 MHz, CDCl₃) δ 8.30 (1H, td, ³*J*_{HH} = 7.4, ⁴*J*_{HH} = 1.8 Hz, ArH), 8.03 (1H, br d, ³*J*_{HH} = 8.7 Hz, ArH), 7.43-7.55 (3H, m, ArH), 7.14-7.28 (4H, m, ArH), 7.04 (1H, ddd, ³*J*_{HH} = 9.8, ³*J*_{HH} = 8.3, ⁴*J*_{HH} = 1.3 Hz, ArH), 6.93-6.95 (1H, m, ArH), 6.64-6.70 (2H, m, ArH), 4.43 (1H, d, ²*J*_{HH} = 13.0 Hz, Ar-CHH-N), 3.92-3.94 (1H, d, ²*J*_{HH} = 13.3 Hz, Ar-CHH-N), 3.56-3.67 (1H, dd, ³*J*_{HH} = 7.4, ⁴*J*_{HH} = 1.4 Hz, α(Pro)-CH), 3.41 (1H, (1H, m, β(Pro)-CHH), 3.22-3.36 (1H, m, γ(Pro)-CHH), 2.74-2.82 (1H, m, δ(Pro)-CHH), 2.46-2.60 (2H, m, δ(Pro)-CHH, γ(Pro)-CHH), 2.30 (2H, td, ³*J*_{HH} = 7.4, ⁴*J*_{HH} = 1.4 Hz, CH₂), 2.17-2.00 (3H, m, β(Pro)-CHH, CH₂), 1.98 (1H, t, ⁴*J*_{HH} = 2.5 Hz, C≡CH), 1.69 (1H, dt, ³*J*_{HH} = 13.3, ⁴*J*_{HH} = 4.7 Hz, CHH), 1.42-1.64(3H, m, CHH, CH₂), 1.26 (3H, s, CH₃); ¹³C NMR (100 MHz, CDCl₃) 182.4 (C=O), 180.1 (C=O), 172.6 (C=N), 161.8 (d, ¹*J*_{CF} = 248.5 Hz, CF), 141.6 (Ar-C), 136.6 (Ar-C), 134.2 (d, ³*J*_{CF} = 3.2 Hz, Ar-CH), 133.4 (Ar-CH), 131.6 (Ar-CH), 131.2 (d, ³*J*_{CF} = 9.6 Hz, Ar-CH), 130.2 (Ar-CH), 129.4 (Ar-CH), 128.8 (Ar-C), 128.0 (Ar-CH), 127.3 (Ar-CH), 126.9 (Ar-CH), 124.5 (d, ⁴*J*_{CF} = 3.20, Ar-CH), 124.0 (Ar-CH), 120.8 (Ar-CH), 120.5 (d, ²*J*_{CF} = 14.4 Hz, C), 116.1 (d, ²*J*_{CF} = 22.37 Hz, Ar-CH), 83.9 (HC≡C), 78.0 (C≡C), 70.2 (α(Pro)-CH), 69.1 (Ar-CH₂-N), 56.8 (α-C), 55.9 (δ(Pro)-CH₂), 39.5 (β(Pro)-CH₂), 30.6 (HC≡C-C-CH₂), 29.8 (CH₃) 28.7 (CH₂), 28.3 (HC≡C-(CH₂)₃-CH₂), 24.9 (γ-CH₂), 23.3 (CH₂), 18.4 (CH₂). ¹⁹F NMR (376 MHz, CDCl₃) δ -113.9 (s); HRMS-ESI (calcd for C₃₃H₃₃N₃O₃F⁵⁸Ni [M+H]⁺) 596.1859, found 596.1843 (Δ = -2.7 ppm), (calcd for C₃₃H₃₃N₃O₃F⁶⁰Ni [M+H]⁺) 598.1814, found 598.1810(Δ = -0.7 ppm).

6.5.4 Synthesis of (*S*)-({2-[1-(2-fluorobenzyl)benzyl]pyrrolidine-2-carboxamide]-phenyl}phenyl methylene)-(*S*)-heptynylglycinato-*N,N',N'',O*}nickel(II) **137**

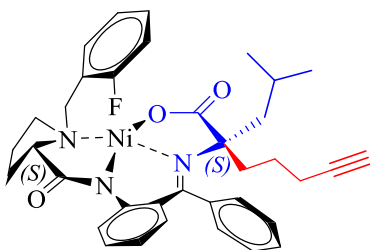


The general procedure (E) was followed using potassium tert-butoxide (1.087 g, 9.685 mmol) in THF (30.00 mL), (*S*)-({2-[1-(2-fluorobenzyl)pyrrolidine-2-carboxamide]phenyl}phenylmethylene)-glycinato-*N,N',N'',O*}nickel(II) (**55**) (5.00 g, 9.685 mmol)

and a solution of 7-iodohept-1-yne (**3**) (1.936 g, 9.685 mmol) in THF, to give the product as a reddish-orange solid. (Crystals suitable for single crystal X-ray structure determination were grown by slow evaporation of the compound in ethyl acetate. These confirmed the (*S*, *S*) stereochemistry of the product complex). (Yield 4.050 g, 76 %); (99

: 1 dr); m.p.: 241-243 °C; $[\alpha]_D^{20} = 3063.881$ (c 0.01 in CHCl_3). $^1\text{H-NMR}$ (400 MHz, CDCl_3) δ 8.31 (1H, td, $^3J_{\text{HH}} = 7.4$, $^4J_{\text{HH}} = 1.8$ Hz, ArH), 8.17 (1H, br d, $^3J_{\text{HH}} = 8.4$ Hz, ArH), 7.44-7.54 (3H, m, ArH), 7.21-7.29 (2H, m, ArH), 7.04 (1H, ddd, $^3J_{\text{HH}} = 9.8$, $^3J_{\text{HH}} = 8.3$, $^4J_{\text{HH}} = 1.2$ Hz, ArH), 6.93 (1H, d, $^3J_{\text{HH}} = 7.1$ Hz, ArH), 6.63-6.70 (2H, m, ArH), 4.43 (1H, d, $^2J_{\text{HH}} = 12.9$ Hz, Ar-CHH-N), 3.91 (1H, dd, $^3J_{\text{HH}} = 8.2$, $^4J_{\text{HH}} = 3.3$ Hz, $\alpha(\text{Pro})\text{-CH}$), 3.84 (1H, d, $^2J_{\text{HH}} = 12.9$ Hz, Ar-CHH-N), 3.45-3.62 (3H, m, $\alpha\text{-CH}$, $\beta(\text{Pro})\text{-CHH}$, $\gamma(\text{Pro})\text{-CHH}$), 2.80-2.88 δ (1H, m, $\delta(\text{Pro})\text{-CHH}$), 2.52-2.62 (1H, m, $\delta(\text{Pro})\text{-CHH}$), 2.01-1.95 (5H, m, CH_2 , CH_2 , $\gamma(\text{Pro})\text{-CHH}$), 1.95-2.02 (1H, m, $\beta(\text{Pro})\text{-CHH}$), 1.93 (1H, t, $^4J_{\text{HH}} = 2.5$ Hz, $\text{HC}\equiv\text{C}$), 1.55-1.68 (2H, m, CH_2), 1.41-1.52 (2H, m, CH_2), 1.19-1.37 (2H, m, CH_2), $^{13}\text{C NMR}$ (100 MHz, CDCl_3) 180.0 (C=O), 179.3 (C=O), 170.4 (C=N), 161.6 (d, $^1J_{\text{CF}} = 247.7$ Hz, CF), 142.3 (Ar-C), 134.2 (Ar-CH), 133.8 (Ar-C), 133.3 (Ar-CH), 132.2 (Ar-CH), 131.2 (d, $^3J_{\text{CF}} = 9.6$ Hz, Ar-CH), 129.8 (Ar-CH), 128.9 (Ar-CH), 128.9 (Ar-CH), 127.6 (Ar-CH), 127.2 (Ar-CH), 126.6 (Ar-CH), 124.5 (d, $^3J_{\text{CF}} = 3.2$ Hz, Ar-CH), 123.7 (Ar-CH), 120.8 (Ar-CH), 120.4 (d, $^2J_{\text{CF}} = 14.4$ Hz, C), 116.1 (d, $^2J_{\text{CF}} = 22.4$ Hz, Ar-CH), 84.3 ($\text{HC}\equiv\text{C}$), 70.4 ($\text{HC}\equiv\text{C}$), 70.3 ($\alpha(\text{Pro})\text{-CH}$), 68.4 (Ar- $\text{CH}_2\text{-N}$), 56.8 ($\alpha\text{-CH}$), 55.6 ($\delta(\text{Pro})\text{-CH}_2$), 35.3 ($\beta(\text{Pro})\text{-CH}_2$), 30.7 ($\text{HC}\equiv\text{C-CH}_2$), 28.4 ($\gamma(\text{Pro})\text{-CH}_2$), 28.1 (CH_2), 24.9 ($\text{HC}\equiv\text{C-(CH}_2)_3\text{-CH}_2$), 23.7 (CH_2), 18.3 (CH_2); $^{19}\text{F NMR}$ (376 MHz, CDCl_3) δ -113.9 (s); HRMS-ESI (calcd for $\text{C}_{34}\text{H}_{35}\text{N}_3\text{O}_3\text{F}^{58}\text{Ni}$ $[\text{M}+\text{H}]^+$) 610.2016, found 610.2016 ($\Delta = 0.0$ ppm), (calcd for $\text{C}_{34}\text{H}_{35}\text{N}_3\text{O}_3\text{F}^{60}\text{Ni}$ $[\text{M}+\text{H}]^+$) 612.1970, found 612.1995 ($\Delta = 4.1$ ppm).

6.5.5 Synthesis of (S)-({2-[1-(2-fluorobenzyl)benzyl]pyrrolidine-2-carboxamide}phenyl)methylene)-(S)-leucinato-N,N',N'',O}nickel^{II} **138**

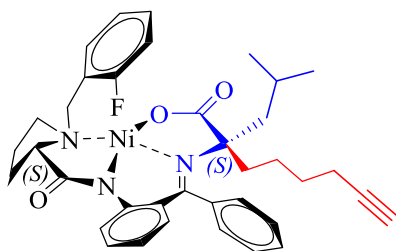


The general procedure (**D**) was followed using potassium tert-butoxide (0.423 g, 7.54 mmol), in dry DMF (5.00 mL).

(S)-({2-[1-(2-fluorobenzyl)pyrrolidine-2-carboxamide]phenyl}phenylmethylene)-(S)-leucinato-N,N',N'',O}nickel^{II} **100** (1.00 g, 1.89 mmol) and 5-iodopent-1-yne (1.070 g, 5.66 mmol) in DMF, to give the product compound as a reddish-orange solid. The product produced epimeric mixture (*S*: *R*) few milligrams were isolated and analysed (62:38 mixture) (Purification could not be achieved by column chromatography). (Yield 0.792 g, 66 %); 218-219 °C. $^1\text{H NMR}$ (400 MHz, CDCl_3) δ 8.49 (1H, m, ArH), 8.08 (1H, br dd, $^3J_{\text{HH}} = 8.5$, $^4J_{\text{HH}} = 1.1$ Hz, ArH), 7.26-7.53 (3H, m, ArH),

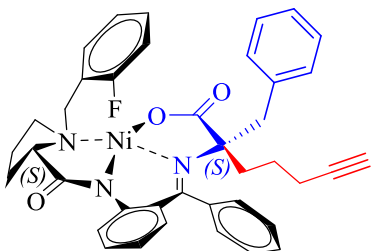
7.38 (1H, t, $^3J_{\text{HH}} = 7.4$ Hz, ArH), 7.32-7.62 (2H, m, ArH), 7.05-7.22 (2H, m, ArH), 7.01 (1H, d, $^3J_{\text{HH}} = 7.8$ Hz, ArH), 6.62 (1H, ddd, $^3J_{\text{HH}} = 8.3$, $^3J_{\text{HH}} = 7.0$, $^4J_{\text{HH}} = 1.3$ Hz, ArH), 6.53 (1H, dd, $^3J_{\text{HH}} = 8.4$, $^4J_{\text{HH}} = 1.6$ Hz, ArH), 4.18 (1H, d, $^2J_{\text{HH}} = 12.7$ Hz, Ar-CHH-N), 3.95 (1H, d, $^2J_{\text{HH}} = 12.7$ Hz, Ar-CHH-N), 3.58-3.66 (1H, t, $^3J_{\text{HH}} = 8.3$ Hz, $\alpha(\text{Pro})$ -CH), 3.47 (1H, dd, $^3J_{\text{HH}} = 10.4$, $^4J_{\text{HH}} = 6.7$ Hz, $\beta(\text{Pro})$ -CHH), 3.02-3.18 (1H, m, $\gamma(\text{Pro})$ -CHH), 2.77-2.90 (1H, m, $\delta(\text{Pro})$ -CHH), 2.49-2.67 (1H, m, $\delta(\text{Pro})$ -CHH), 2.19-2.35 (2H, m, HC \equiv C-CH₂), 1.99-2.17 (4H, m, HC \equiv C-(CH₂)₂-CH₂, HC \equiv C, γ -CHH), 1.72-1.83 (1H, m, CH leucine), 1.47-1.66 (3H, m, (CH₂ leucine, $\beta(\text{Pro})$ -CHH), 1.44 (3H, d, $^3J_{\text{HH}} = 6.5$ Hz, CH₂), 1.23-1.28 (2H, m, HC \equiv C-C-CH₂), 1.06 (3H, d, $^3J_{\text{HH}} = 6.7$ Hz, CH₃); ¹³C NMR (100 MHz, CDCl₃) 182.6 (O-C=O), 180.0 (C=O), 172.7 (C=N), 161.7 (d, $^1J_{\text{CF}} = 247.7$ Hz, CF), 141.7 (Ar-C), 136.6 (Ar-C), 134.1 (Ar-2CH), 133.6 (Ar-CH), 131.7 (Ar-CH), 131.2 (d, $^3J_{\text{CF}} = 8.0$, Ar-CH), 129.6 (Ar-CH), 128.6 (Ar-C), 128.3 (Ar-CH), 127.9 (d, $^3J_{\text{CF}} = 9.6$ Hz, Ar-CH), 127.1 (Ar-CH), 120.7 (Ar-CH), 124.7 (d, $^4J_{\text{CF}} = 3.2$ Hz, Ar-CH), 123.9 (Ar-CH), 120.8 (Ar-CH), 121.5 (d, $^2J_{\text{CF}} = 14.4$ Hz, Ar-C), 116.2 (d, $^2J_{\text{CF}} = 20.8$, Ar-CH), 84.0 (HC \equiv C), 80.9 (C-COO), 71.6 (HC \equiv C), 68.9 ($\alpha(\text{Pro})$ -CH), 57.4 (Ar-CH₂-N), 57.4 ($\delta(\text{Pro})$ -CH₂), 46.1 (CH₂ leucine), 41.9 (HC \equiv C-(CH₂)₂-CH₂), 30.6 ($\beta(\text{Pro})$ -CH₂), 25.2 (CH leucine), 24.2 (CH₃ leucine), 23.3 ($\gamma(\text{Pro})$ -CH₂), 23.1 (HC \equiv C-CH₂-CH₂), 22.8 (CH₃ leucine), 18.3 (HC \equiv C-CH₂), ¹⁹F NMR (376 MHz, CDCl₃) δ -113.7 (s); HRMS-ESI (calcd for C₃₉H₃₆N₃O₃F⁵⁸NiNa [M+Na]⁺) 694.1992, found 694.1990 ($\Delta = -0.3$ ppm), (calcd for C₃₉H₃₆N₃O₃F⁶⁰NiNa [M+Na]⁺) 696.1946, found 696.1980 ($\Delta = 4.9$ ppm).

6.5.6 Synthesis of (S)-({2-[1-(2-fluorobenzyl)benzyl]pyrrolidine-2-carboxamide}phenyl}phenylmethylene)-(S)-1-hexyl-leucinato-*N,N',N'',O*}nickel^{II} **139**



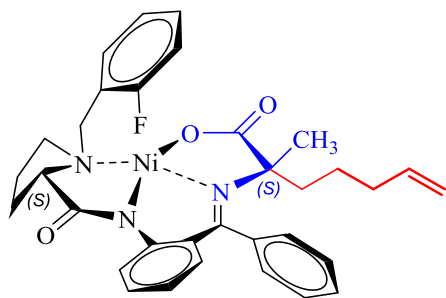
The general procedure (**D**) was followed using potassium tert-butoxide (0.801 g, 7.139 mmol) in dry DMF (10.00 mL), (S)-({2-[1-(2-fluorobenzyl)pyrrolidine-2-carboxamide]phenyl}phenylmethylene)-(S)-leucinato-*N,N',N'',O*}nickel^{II} **100** (1.00 g, 1.785 mmol) and 6-iodohex-1-yne (1.039 g, 5.354 mmol) in DMF, at -30 °C to give the products as a reddish-orange solid. (The product showed distereoisomers mixture (*S*: *R*). 3:1 which could not be separated) (Yield 0.792 g, 66 %); m.p.: 233-236 °C. ¹⁹F NMR (376 MHz, CDCl₃) δ -113.7, -113.8 (s); HRMS-ESI (calcd for C₃₇H₄₀N₃O₃F⁵⁸NiNa [M+Na]⁺) 674.2305, found 674.2321 ($\Delta = 2.4$ ppm), (calcd for C₇₄H₈₀N₆O₆F₂⁶⁰NiNa [2M+Na]⁺) 1327.4702, found 1327.4763 ($\Delta = 4.9$ ppm).

6.5.7 Synthesis of (S)-({2-[1-(2-fluorobenzyl)benzyl]pyrrolidine-2-carboxamide}phenyl)methylene)-(S)-1-pentyl-phenylalaninato-*N,N',N'',O*}nickel^{II} **140**



The general procedure (**D**) was followed using potassium tert-butoxide (0.740 g, 6.60 mmol) in dry DMF (10.00 mL), (S)-({2-[1-(2-fluorobenzyl)pyrrolidine-2-carboxamide]phenyl)methylene)-(S)phenylalaninato-*N,N',N'',O*}nickel^{II} **99** (1.00 g, 1.65 mmol) and a solution of 5-iodopent-1-yne (0.96 g, 4.95 mmol) in DMF, to give the product compound as a reddish-orange solid (Crystals suitable for single crystal X-ray structure determination were grown by slow evaporation of the compound in ethyl acetate. These confirmed the (*S*, *S*) stereochemistry of the product complex). (Yield 0.756 g, 68 %); m.p.: 203-205 °C. ¹H NMR (400 MHz, CDCl₃) δ 8.32 (1H, t, ³J_{HH} = 6.8 Hz, ArH), 7.74 (1H, br dd, ³J_{HH} = 8.5, ⁴J_{HH} = 0.9 Hz, ArH), 7.37-7.47 (4H, m, ArH), 7.28-7.35 (2H, m, ArH), 7.20-7.26 (3H, m, ArH), 7.05-7.15 (4H, m, ArH), 6.58-6.73 (1H, m, ArH), 4.22 (1H, d, ²J_{HH} = 12.9 Hz, Ar-CHH-N), 3.70 (1H, dd, ³J_{HH} = 8.8, ⁴J_{HH} = 6.7 Hz, β-CHH), 3.61 (1H, d, ²J_{HH} = 12.7 Hz, Ar-CHH-N), 3.40 (1H, dd, ³J_{HH} = 10.8, ³J_{HH} = 5.7 Hz, α(Pro)-CH), 2.18-3.30 (1H, m, γ(Pro)-CHH), 3.03 (2H, AB quartet, ²J_{HH} = 19.8 Hz, Ar-CH₂), 2.52-2.69 (2H, m, δ(Pro)-CHH, (Pro)-CHH), 2.23-2.48 (1H, m, HC≡C-CHH), 2.19-2.35 (2H, m, HC≡C-CHH, HC≡C), 1.99-2.20 (4H, m, HC≡C-C-CH₂-CH₂), 1.84 (1H, td, ³J_{HH} = 13.4, ³J_{HH} = 13.4, ⁴J_{HH} = 4.2 Hz, γ(Pro)-CHH), 1.84 (1H, td, ³J_{HH} = 13.3, ³J_{HH} = 13.3, ⁴J_{HH} = 4.2 Hz, β(Pro)-CHH), ¹³C NMR (100 MHz, CDCl₃) 180.9 (O-C=O), 180.7 (C=O), 173.0 (C=N), 161.5 (d, ¹J_{CF} = 248.0 Hz, CF), 141.4 (Ar-C), 136.7 (Ar-C), 136.5 (Ar-C), 134.5 (d, ⁴J_{CF} = 2.0, Ar-CH), 133.0 (Ar-CH), 131.5 (Ar-CH), 131.0 (d, ³J_{CF} = 9.0, Ar-CH), 129.7 (Ar-4CH), 129.2 (Ar-C), 128.5 (Ar-2CH), 128.3 (Ar-CH), 128.3 (Ar-CH), 127.3 (d, ⁴J_{CF} = 7.0 Hz, Ar-CH), 126.7 (Ar-CH), 124.7 (Ar-CH), 124.3 (Ar-CH), 120.9 (d, ²J_{CF} = 11.1 Hz, Ar-C), 120.8 (Ar-CH), 116.0 (d, ²J_{CF} = 22.1 Hz, Ar-CH), 83.5 (α-C), 81.4 (HC≡C), 69.9 (α(Pro)-CH), 69.2 (Ar-CH₂-N), 58.1 (HC≡C), 57.4 (δ(Pro)-CH₂), 56.1 (Ar-CH₂), 46.2 (HC≡C-CH₂-CH₂), 38.1 (β(Pro)-CH₂), 24.7 (γ(Pro)-CH₂), 23.5 (HC≡C-(CH₂)₂-CH₂), 18.4 (HC≡C-CH₂); ¹⁹F NMR (376 MHz, CDCl₃) δ -113.6 (s); HRMS-ESI (calcd for C₃₉H₃₇N₃O₃F⁵⁸Ni [M+H]⁺) 672.2172, found 672.2180 (Δ = 1.8 ppm), (calcd for C₃₉H₃₇N₃O₃F⁶⁰Ni [M+H]⁺) 674.2127, found 674.2155 (Δ = 4.2 ppm).

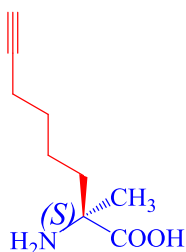
6.5.8 Synthesis of (S)-({2-[1-(2-fluorobenzyl)benzyl]pyrrolidine-2-carboxamide}phenyl)methyl-ene)-(S)-pentenylalaninato-*N,N',N'',O*}nickel^{II} **142**



The general procedure (**F**) was followed using potassium tert-butoxide (169.3 mg, 1.51 mmol.) in dry DMF (10ml) (S)-({2-[1-(2-fluorobenzyl)pyrrolidine-2-carboxamide]phenyl}phenylmethyl-ene) alaninato-*N,N',N'',O*}nickel^{II} **56** (200 mg, 0.38 mmol) and 1-bromo-4-pentene

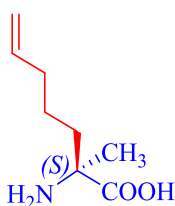
(0.134 mL, 1.13 mmol) to give the title compound as a blood red solid. (161 mg, 71 %); m.p = 189–191 °C. ¹H NMR (400 MHz, CDCl₃) δ 8.29 (1H, td, ³J_{HH} = 7.4, ⁴J_{HH} = 1.0 Hz, ArH), 8.03 (1H, td, ³J_{HH} = 8.3, ⁴J_{HH} = 3.2 Hz, ArH), 7.50–7.44 (2H, m, ArH), 7.38 (1H, m, ArH), 7.32 (1H, m, ArH), 7.28 (1H, t, ²J_{HH} = 7.4 Hz, ArH), 7.15 (1H, ddd, ²J_{HH} = 8.5, ³J_{HH} = 6.1, ⁴J_{HH} = 2.5 Hz, ArH), 7.09 (1H, t, ³J_{HH} = 9.1 Hz, ArH), 6.99 (1H, d, ³J_{HH} = 7.7 Hz, ArH), 6.67–6.61 (2H, m, ArH), 5.86 (1H, ddt, ²J_{HH} = 16.8, ³J_{HH} = 10.3, ⁴J_{HH} = 6.5 Hz, CH=CHH), 5.08 (1H, dd, ³J_{HH} = 17.0, 1.5 Hz, CH=CHH(*cis*)), 5.02 (1H, d, ³J_{HH} = 10.2 Hz, CHCHH(*trans*)), 4.52 (1H, d, ²J_{HH} = 13.1 Hz, Ar-CHH-N), 3.95 (1H, d, ²J_{HH} = 13.5 Hz, Ar-CHH-N), 3.61 (1H, dd, ³J_{HH} = 10.3, ³J_{HH} = 6.5 Hz, α(Pro)-CH), 3.41 (1H, dd, ³J_{HH} = 10.7, ³J_{HH} = 6.4 Hz, β(Pro)-CHH), 3.24 (1H, m, γ(Pro)-CHH), 2.78 (1H, m, δ(Pro)-CHH), 2.52 (1H, m, δ(Pro)-CHH), 2.40 (1H, m, γ(Pro)-CHH), 2.16–1.99 (5H, m, CH₂, CH₂, β(Pro)-CHH), 1.76–1.62 (2H, m, CH₂), 1.23 (3H, s, CH₃); ¹³C NMR (100 MHz, CDCl₃) 182.3 (C=O), 180.1 (C=O), 172.4 (C=N), 161.8 (d, ¹J_{CF} = 246.9, CF), 141.5 (Ar-C), 137.8 (Ar-CH), 136.6 (Ar-C), 134.2 (d, ³J_{CF} = 4.2, Ar-CH), 133.4 (Ar-CH), 131.6 (Ar-CH), 131.2 (d, ³J_{CF} = 8.1, Ar-CH), 130.3 (Ar-CH), 129.4 (Ar-CH), 128.8 (Ar-CH), 128.0 (Ar-C), 127.3 (Ar-CH), 126.9 (Ar-CH), 124.6 (d, ⁴J_{CF} = 2.7, Ar-CH), 124.0 (Ar-CH), 120.7 (Ar-CH), 120.4 (d, ²J_{CF} = 14.5, Ar-C), 116.2 (d, ²J_{CF} = 22.4, Ar-CH), 115.4 (CH=CH₂), 78.1 (CH=CH₂), 70.1 (α-C), 56.7 (α(Pro)-CH), 55.9 (δ(Pro)-CH), 39.8 (β(Pro)CH₂), 33.7 (CH₂), 30.6 (γ(Pro)-CH₂), 29.6 (CH₃), 25.3 (CH₂), 23.3 (CH₂). [α]_D²⁰+2730 (c 0.05, CHCl₃); ¹⁹F NMR (376 MHz, CDCl₃) δ −113.7 (s); HRMS-ESI (calcd for C₃₃H₃₅N₃O₃F⁵⁸Ni [M+H]⁺) 598.2016, found 598.2014 (Δ = −0.2 ppm), (calcd for C₃₃H₃₅N₃O₃F⁶⁰Ni [M+H]⁺) 600.1970, found 600.1982 (Δ = 0.3 ppm).

6.5.9 (S)-2-amino-2-methyloct-7-ynoic acid 143



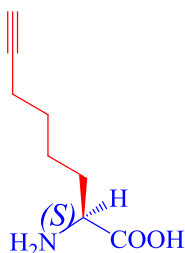
The general procedure (G) was followed using (S)-({2-[1-(2-fluorobenzyl)benzyl]pyrrolidine-2-carboxamide]-phenyl}phenylmethylene)-(S)-hexynylalaninato-*N,N'*,*N''*,*O*}nickel^(II) **134** (3.300 g, 0.541 mmol) in methanol, and hydrochloric acid (3 M) (75 mL) at 50 °C to give the product (S)-2-amino- hept-6-enoic acid as viscous yellowish oily. (Yield 767 mg, 81 %). ¹H-NMR (400 MHz, D₂O) δ 2.29-2.32 (1H, m, C≡CH), 2.14-2.23 (2H, m, ε-CH₂), 1.66-1.87 (2H, m, β-CH₂), 1.13-1.52 (3H, m, δ-CH₂, γ-CHH) 1.43 (3H, s, CH₃); 1.25-1.35 (1H, m, γ-CHH); ¹³C NMR (100 MHz, D₂O) δ ppm 176.9 (O-C=O), 85.8 (HC≡C), 69.4 (HC≡C), 61.6 (α-CH), 36.6 (β-CH₂), 27.5 (CH₃), 22.4 (δ-CH₂), 22.4 (γ-CH₂), 17.2 (ε-CH₂); HRMS-ESI (calcd for C₉H₁₆NO₂ [M+H]⁺) 170.1181, found 170.1173 (Δ = -4.7 ppm).

6.5.10 Synthesis of (S)-2-amino-2-methylhept-6-enoic acid 144



The general procedure (G) was followed using (S)-({2-[1-(2-fluorobenzyl)pyrrolidine-2-carboxamide]phenyl}phenylmethylene)-(S)pentenylglycinato-*N,N',N'',O*}nickel^(II) **142** (0.200 g, 0.34 mmol) in methanol (20.00 mL) and hydrochloric acid (3M) (2.4 mL) at 70 °C to give the product as a white powder (52.8 mg, 63 %); m.p: 251-253 °C, ¹H NMR (400 MHz, D₂O) δ 5.80 (1H, ddt, ³J_{HH} = 17.0, 10.2, 6.5 Hz, CHvCH₂), 5.06-4.97 (2H, m, CHvCHH), 2.07 (2H, q, ³J_{HH} = 7.0 Hz, δ-CH₂), 1.87-1.77 (1H, m, β-CHH), 1.74-1.66 (1H, m, β-CHH), 1.50-1.39 (4H, m, CH₃, γ-CHH), 1.35-1.23 (m, 1H, γ-CHH); ¹³C NMR (100 MHz, D₂O) δ 177.2 (C=O), 138.7 (CH₂=CH), 115.1 (CH₂=CH), 61.6 (α-C), 36.7 (β-CH₂), 32.8 (δ-CH₂), 22.5 (CH₃), 22.5 (γ-C); HRMS-ESI (calcd for C₈H₁₆NO₂ [M+H]⁺) 158.1165, found 158.1181 (Δ = -10.1 ppm).

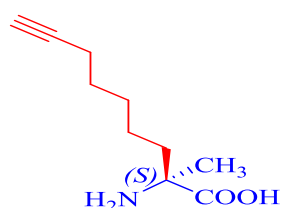
6.5.11 Synthesis of (S)-2-amino-2-methyloct-7-ynoic acid 145



The general procedure (H) was followed using (S)-({2-[1-(2-fluorobenzyl)benzyl]pyrrolidine-2-carboxamide]-phenyl}phenylmethylene)-(S)-hexynylglycinato-*N,N'*,*N''*,*O*}nickel^(II) **136** (3.500 g, 6.708 mmol) and 8-hydroxyquinoline (2.747 g, 18.924 mmol) in mixture of the solvents (water: acetonitrile 1:4) (150mL) to give the product as a white powder. (Yield 767 mg, 84 %); m.p.: 152-154 °C. ¹H-NMR

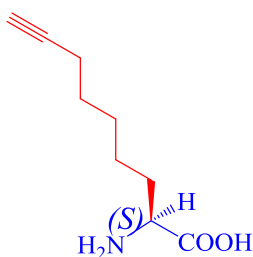
(400 MHz, D₂O) δ 3.69 (1H, t, $^3J_{\text{HH}} = 6.1$ Hz, α -CH), 2.30 (1H, t, $^4J_{\text{HH}} = 2.5$ Hz, C \equiv CH), 2.17 (2H, td, $^3J_{\text{HH}} = 6.9$, $^4J_{\text{HH}} = 2.5$ Hz, ε -CH₂), 1.76-1.91 (2H, m, β -CH₂), 1.36-1.57 (4H, m, δ -CH₂, γ -CH₂); ¹³C NMR (100 MHz, D₂O) 174.85 (O-C=O), 85.82 (HC \equiv C), 69.40 (HC \equiv C), 54.84 (α -C), 29.91 (β -C), 27.24 (δ -C), 23.52 (γ -C), 17.23 (ε -C); IR ($\nu_{\text{max}}/\text{cm}^{-1}$, neat): 3290, 3065, 2946, 1740, 1521, 1478, 1449, 1414, 1337, 1229, 1148, 1103, 1076, 1007, 938, 872, 758, 732; HRMS-ESI (calcd for C₈H₁₄NO₂ [M+H]⁺) 156.1025, found 156.1018 ($\Delta = -4.7$ ppm).

6.5.12 Synthesis of (S)-2-amino-2-methylnon-8-ynoic acid 146



The general procedure (**H**) was followed using (S)-({2-[1-(2-fluorobenzyl)benzyl]pyrrolidine-2-carboxamide]-phenyl} phenylmethylene)-(S)-heptynylalaninato-*N,N'*,*N''*,*O*}nickel^{II} **135** (5.850 g, 9.369 mmol) and 8-hydroxyquinoline (4.080 g, 28.108 mmol) in mixture of the solvents (water: acetonitrile 1:4) (150mL) to give the product as a white powder. (Yield 1.260 g, 73 %.); ¹H-NMR (400 MHz, D₂O) δ 2.30 (1H, t, $^4J_{\text{HH}} = 2.4$ Hz, C \equiv CH), 2.16 (2H, td, $^3J_{\text{HH}} = 6.9$, $^4J_{\text{HH}} = 2.5$ Hz, ζ -CH₂), 1.65-1.86 (2H, m, γ -CH₂), 1.13-1.52 (9H, m, ε -CH₂, β -CH₂, δ -CH₂, CH₃); IR ($\nu_{\text{max}}/\text{cm}^{-1}$, neat): 3298, 2939, 2518, 1705, 1504, 1478, 1449, 1340, 1248, 1180, 1085, 952, 875, 758, 737; HRMS-ESI (calcd for C₁₀H₁₇NO₂ [M+H]⁺) 183.1338, found 184.1339 ($\Delta = -0.5$ ppm).

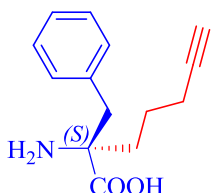
6.5.13 Synthesis of (S)-2-aminonon-8-ynoic acid 147



The general procedure (**H**) was followed using (S)-({2-[1-(2-fluorobenzyl)benzyl]pyrrolidine-2-carboxamide]-phenyl} phenylmethylene)-(S)-heptynylglucinato-*N,N'*,*N''*,*O*}nickel^{III} **137** (3.850 g, 6.708 mmol) and 8-hydroxyquinoline (2.747 g, 18.924 mmol) in mixture of the solvents (water: acetonitrile 1:4) (150mL) to give the product as a colourless oily. (Yield 796 mg, 75 %); m.p.: 152-154 °C. ¹H-NMR (400 MHz, D₂O) δ 3.68 (1H, t, $^3J_{\text{HH}} = 6.1$ Hz, α -CH), 2.30 (1H, t, $^4J_{\text{HH}} = 2.5$ Hz, C \equiv CH), 2.17 (2H, td, $^3J_{\text{HH}} = 6.9$, $^4J_{\text{HH}} = 2.5$ Hz, ζ -CH₂), 1.74-1.89 (2H, m, β -CH₂), 1.26-1.52 (6H, m, γ -CH₂, δ -CH₂, ε -CH₂); ¹³C NMR (100 MHz, D₂O) 192.1 (O-C=O), 86.3 (HC \equiv C), 69.1 (HC \equiv C), 54.8 (α -CH), 30.3 (β -CH₂), 27.5 (ε -CH₂), 27.3 (δ -CH₂), 23.8 (γ -CH₂), 17.4 (ζ -CH₂); IR ($\nu_{\text{max}}/\text{cm}^{-1}$, neat): 3373, 3284, 2936, 2860, 2159, 2023, 1750, 1736, 1708, 1673, 1558, 1476, 1451, 1387, 1318, 1267, 1236,

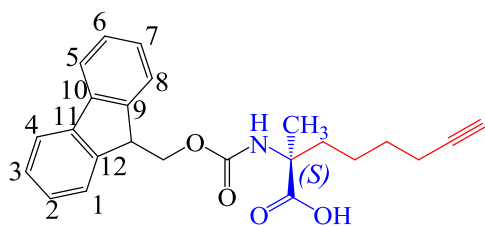
1194, 1163, 1140, 1101, 1088, 1059, 1035, 994, 973, 864, 819, 777, 757; HRMS-ESI (calcd for $C_9H_{15}NO_2$ $[M+H]^+$) 170.1181, found 170.1178 ($\Delta = -1.8$ ppm).

6.5.14 Synthesis of (*S*)-2-amino-2-benzylhept-6-ynoic acid **148**



The general procedure (**H**) was followed using (*S*)-({2-[1-(2-fluorobenzyl)benzyl]pyrrolidine-2-carboxamide}phenyl}phenyl methylene)-(*S*)-1-pentyl-leucinato-*N,N',N'',O*}nickel^(III) **140** (250 mg, 371.78 mmol) and 8-hydroxyquinoline (0.161 g, 1.115 mmol) were dissolved in mixture of the solvents (water: acetonitrile 1:4) (25 mL) to give the product as a white powder. (Yield 69 mg, 80 %); m.p.: 132-133 °C: 1H -NMR (400 MHz, DMSO- d_6) δ 7.19-7.31 (5H, m, ArH), 3.13 (1H, d, $^2J_{HH} = 13.4$ Hz, Ar-CHH), 3.07 (1H, d, $^2J_{HH} = 13.4$ Hz, Ar-CHH), 2.79 (1H, t, $^4J_{HH} = 2.4$ Hz, C \equiv CH), 2.02-2.14 (2H, m, δ -CH $_2$), 1.71-1.84 (1H, m, β -CHH), 1.71-1.84 (3H, m, β -CHH, γ -CH $_2$); ^{13}C NMR (100 MHz, DMSO- d_6) δ ppm 178.5 (O-C=O), 136.0 (Ar-C), 130.6 (Ar-2CH), 128.0 (Ar-2CH), 126.5 (Ar-CH), 92.9 (C \equiv C), 84.2 (C \equiv CH), 71.4 (α -C), 63.2 (Ar-CH $_2$), 42.1 (β -CH $_2$), 26.5 22.7 (γ -CH $_2$), 18.0 (δ -CH $_2$); HRMS-ESI (calcd for $C_{14}H_{18}NO_2$ $[M+H]^+$) 232.1338, found 232.1342 ($\Delta = 1.7$ ppm).

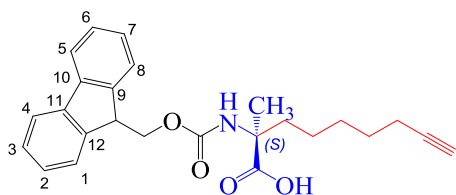
6.5.15 Synthesis of (*S*)-2-(((9H-fluoren-9-yl)methoxy)carbonyl)amino)-2-methyloct-7-ynoic acid **149**



The general procedure (**I**) was followed using (*S*)-2-amino-2-methylnon-8-ynoic acid **143** (0.722 g, 4.267 mmol), sodium carbonate (1.179 g, 8.533 mmol) and 9-fluorenyl-methyl-*N*-succinimidyl carbonate (2.158 g, 6.400 mmol) to give (*S*)-2-(((9H-fluoren-9-yl)methoxy)carbonyl) amino)-2-methylnon-8-ynoic acid as a white powder. (Yield 0.837 g, 50 %); $[\alpha]_D^{20} = 6.4832$ (c 0.01 in $CHCl_3$). 1H NMR (400 MHz, CD_3OD): δ 7.68 (2H, br d, $^3J_{HH} = 7.4$ Hz, fluorenyl 1-H and 8-H), 7.55 (2H, pseudo d, fluorenyl 4-H and 5-H), 7.32 (2H, pseudo t, fluorenyl 2-H and 7-H), 7.28 (2H, pseudo t, fluorenyl 2-H and 7-H), 4.21 (2H, d, $^3J_{HH} = 6.5$ Hz CH $_2$ -O), 4.09 (1H, d, $^3J_{HH} = 8.2$ Hz, CH-CH $_2$ -O), 2.05 (2H, m, HC \equiv C, β -CHH), 1.77 (2H, t, $^3J_{HH} = 7.9$ Hz, ϵ -CH $_2$), 0.70-1.55 (8H, m, β -CHH, γ -CH $_2$, δ -CH $_2$, CH $_3$). ^{13}C NMR (100 MHz, CD_3OD): δ 177.78 (COOH), 157.15 (CONH), 145.33 (fluorenyl (Ar-2Cq), 142.60 (fluorenyl (Ar-2Cq), 128.79 (Ar-2CH), 128.18 (Ar-2CH), 126.28 (Ar-2CH), 120.94 (Ar-2CH), 84.78 (C \equiv CH), 69.71

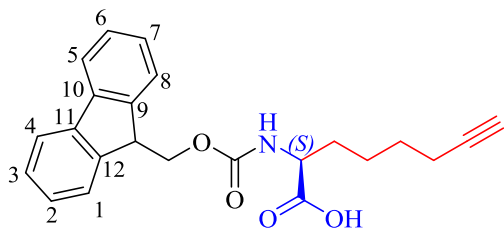
(CH₂-O), 67.47 (HC≡C), 60.29 (α-C), 48.46 (fluorenyl C), 37.36 (β-CH₂), 29.75 (δ-CH₂), 24.05 (CH₃), 23.31 (γ-CH₂), 18.94 (ε-CH₂); HRMS-ESI (calcd for C₂₄H₂₆NO₄ [M+H]⁺) 392.1862, found 392.1872 (Δ = 2.5 ppm). HPLC (OD-H column, hexane (50 %)-iPrOH isocratic +0.1 % AcOH): 5.55 min.

6.5.16 Synthesis of (S)-2-((((9H-fluoren-9-yl)methoxy)carbonyl)amino)-2-methylnon-8-ynoic acid 150



The general procedure (I) was followed using (S)-2-amino-2-methylnon-8-ynoic acid **146** (0.350 g, 1.910 mmol), sodium carbonate (0.527 g, 3.820 mmol) and 9-fluorenyl-methyl-*N*-succinimidyl carbonate (0.966 g, 2.865 mmol) to give (S)-2-((((9H-fluoren-9-yl)methoxy)carbonyl)amino)-2-methylnon-8-ynoic acid as a white powder. (Yield 543 mg, 61 %); $[\alpha]_D^{20} = 10.6015$ (*c* 0.01 in CHCl₃). ¹H NMR (400 MHz, CDCl₃): δ 10.93 (1H, br s, COOH), 7.74 (2H, br d, ³J_{HH} = 7.6 Hz, fluorenyl 1-H and 8-H), 7.57 (2H, pseudo d, fluorenyl 4-H and 5-H), 7.38 (2H, pseudo t, fluorenyl 2-H and 7-H), 7.30 (2H, pseudo t, fluorenyl 2-H and 7-H), 5.54 (1H, bro s, NH), 4.39 (2H, pseudo d, CH₂-O), 4.19 (1H, t, ³J_{HH} = 5.87 Hz, CH-CH₂-O), 2.05 (3H, br s, CH₃), 1.92 (1H, t, ⁴J_{HH} = 2.3 Hz, HC≡C), 0.88-1.68 (10H, m, β-CHH, ε-CHH, δ-CHH, γ-CHH, ζ-CHH). ¹³C NMR (100 MHz, CDCl₃): δ 178.77 (COOH), 154.36 (CONH), 143.36 (fluorenyl (Ar-2C)), 140.96 (fluorenyl (Ar-2C)), 127.30 (Ar-2CH), 126.67 (Ar-2CH), 124.54 (Ar-2CH), 119.59 (Ar-2CH), 83.98 (C≡CH), 67.93 (CH₂-O), 66.18 (HC≡C), 59.38 (α-C), 46.79 (fluorenyl CH), 36.15 (β-CH₂), 28.07 (ε-CH₂), 27.70 (δ-CH₂), 23.03 (CH₃), 22.84 (γ-CH₂), 17.87 (ζ-CH₂); HRMS-ESI (calcd for C₂₅H₂₇NO₄ [M+H]⁺) 406.2018, found 406.2024 (Δ = -1.5 ppm). HPLC (OD-H column, hexane (50 %)-iPrOH isocratic +0.1 % AcOH): 5.58 min.

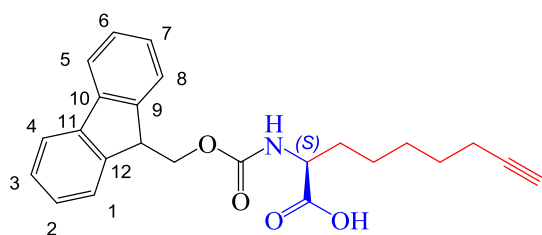
6.5.17 Synthesis of (S)-2-((((9H-fluoren-9-yl)methoxy)carbonyl)amino)oct-7-ynoic acid. 151



The general procedure (I) was followed using (S)-2-amino-oct-7-ynoic acid **145** (0.66 g, 4.252 mmol) and sodium carbonate (0.676 g, 6.3789 mmol) and of 9-fluorenyl-methyl-*N*-succinimidyl carbonate (2.869 g, 8.505 mmol) to give (S)-2-((((9H-fluoren-9-yl)methoxy)carbonyl)amino)oct-7-ynoic acid as a white

powder. (Yield 1.130 g, 70 %); $[\alpha]_D^{20} = 2.9678$ (c 0.01 in CHCl_3). ^1H NMR (400 MHz, CDCl_3): δ 9.79 (br. s, COOH), 7.65 (2H, br d, $^3J_{\text{HH}} = 7.4$ Hz, fluorenyl 1-H and 8-H), 7.51 (2H, pseudo d, fluorenyl 4-H and 5-H), 7.29 (2H, pseudo t, fluorenyl 2-H and 7-H), 7.20 (2H, pseudo t, fluorenyl 2-H and 7-H), 5.38 (1H, d, $^3J_{\text{HH}} = 8.0$ Hz, NH), 4.26-4.36 (2H, m, $\text{CH}_2\text{-O}$), 4.12 (1H, t, $^3J_{\text{HH}} = 6.7$ Hz, $\alpha\text{-CH}$) 2.49-2.63 (2 H, m, $\text{CH-CH}_2\text{-O}$, $\zeta\text{-CHH}$), 2.08 (2H, m, $\beta\text{-CH}_2$), 1.99 (1H, s, $\text{HC}\equiv\text{C}$), 1.77-1.88 (1H, m, $\zeta\text{-CHH}$), 1.30-1.67 (4H, m, $\varepsilon\text{-CH}_2$, $\gamma\text{-CH}_2$, $\delta\text{-CH}_2$). ^{13}C NMR (100 MHz, CDCl_3): δ 177.4 (COOH), 156.2 (CONH), 143.8 (fluorenyl (Ar-C), 143.7 (fluorenyl (Ar-C), 143.6 (Ar-2CH), 127.7 (Ar-2CH), 127.1 (Ar-2CH), 125.1 (Ar-2C), 120.0 (Ar-2CH), 84.0 ($\text{C}\equiv\text{CH}$), 68.8 ($\text{CH}_2\text{-O}$), 67.1 ($\text{HC}\equiv\text{C}$), 53.5 ($\alpha\text{-CH}$), 47.2 (fluorenyl CH), 31.7 ($\beta\text{-CH}_2$), 27.8 ($\delta\text{-CH}_2$), 24.3 ($\gamma\text{-CH}_2$), 18.2 ($\varepsilon\text{-CH}_2$); HRMS-ESI (calcd for $\text{C}_{23}\text{H}_{23}\text{NO}_4\text{Na}$ $[\text{M}+\text{Na}]^+$) 400.1525, found 400.1544 ($\Delta = 4.7$ ppm). HPLC (OD-H column, hexane (50 %)-iPrOH isocratic +0.1 % AcOH): 6.43 min.

6.5.18 Synthesis of (S)-2-((((9H-fluoren-9-yl)methoxy)carbonyl)amino)non-8-ynoic acid.152



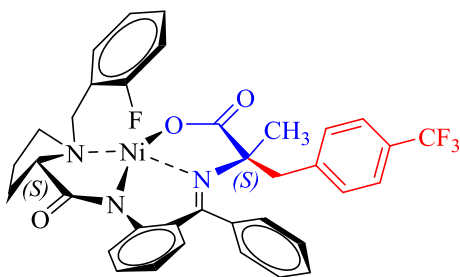
The general procedure (**I**) was followed using (S)-2-aminonon-8-ynoic acid **147** (0.690 g, 4.078 mmol), potassium carbonate (1.127 g, 8.155 mmol) and 9-fluorenylmethyl-*N*-succinimidyl carbonate (2.063 g,

6.116 mmol) to give the product as a viscous colourless oil (Yield 1.401 g, 87 %); $[\alpha]_D^{20} = 6.7199$ (c 0.01 in CHCl_3). ^1H NMR (400 MHz, CDCl_3): δ 8.66 (1H, br. s, COOH), 7.76 (2H, br d, $^3J_{\text{HH}} = 7.4$ Hz, fluorenyl 1-H and 8-H), 7.59 (2H, pseudo d, fluorenyl 4-H and 5-H), 7.39 (2H, pseudo t, fluorenyl 2-H and 7-H), 7.31 (2H, pseudo t, fluorenyl 2-H and 7-H), 5.33 (1H, d, $^3J_{\text{HH}} = 8.2$ Hz, NH), 4.36-4.48 (2H, m, $\text{CH}_2\text{-O}$), 4.22 (1 H, t, $^3J_{\text{HH}} = 6.8$ Hz, $\alpha\text{-CH}$) 3.65-3.71 (1H, m, $\text{CH-CH}_2\text{-O}$), 2.70 (1 H, s, $\text{HC}\equiv\text{C}$), 2.52-2.69 (1H, m, $\zeta\text{-CHH}$), 2.13-2.20 (2H, m, $\beta\text{-CH}_2$), 1.92-1.95 (1H, m, $\zeta\text{-CHH}$), 1.65-1.78 (1H, m, $\varepsilon\text{-CHH}$), 1.52-1.57 (2H, m, $\varepsilon\text{-CHH}$, $\delta\text{-CHH}$), 1.35-1.46 (3H, m, $\delta\text{-CHH}$, $\beta\text{-CH}_2$). ^{13}C NMR (100 MHz, CDCl_3): δ 176.8 (COOH), 156.2 (CONH), 143.8 (fluorenyl (Ar-C), 143.7 (fluorenyl (Ar-C), 141.3 (Ar-2CH), 127.7 (Ar-2CH), 127.1 (Ar-2CH), 125.1 (Ar-2C), 120.0 (Ar-2CH), 84.4 ($\text{C}\equiv\text{CH}$), 68.4 ($\text{CH}_2\text{-O}$), 67.1 ($\text{HC}\equiv\text{C}$), 53.7 (C- α), 47.2 (fluorenyl CH), 32.2 ($\beta\text{-CH}_2$), 28.1 ($\varepsilon\text{-CH}_2$), 25.4 ($\delta\text{-CH}_2$), 24.7 ($\gamma\text{-CH}_2$), 18.3 ($\zeta\text{-CH}_2$); HRMS-ESI

(calcd for $C_{24}H_{26}NO_4$ $[M+H]^+$) 392.1862, found 392.1870 ($\Delta = 2.0$ ppm). HPLC (OD-H column, hexane (50 %)-iPrOH isocratic +0.1 % AcOH): 6.27 min.

6.6 Experimental for Chapter 4

6.6.1 Synthesis of (S)-({2-[1-(2-fluorobenzyl)benzyl]pyrrolidine-2-carboxamide]phenyl}phenylmethylene)-(S)-4-(trifluoromethyl)benzenyl-alaninato-*N,N',N'',O*}nickel^{II}. **186**

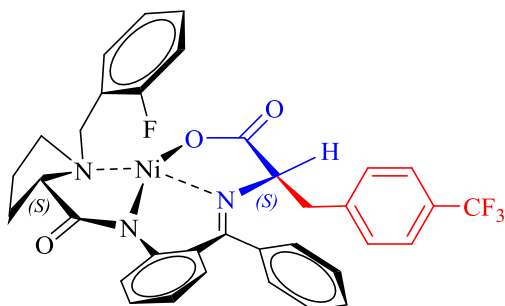


The general procedure (**F**) was followed using 10 equivalents of potassium tert-butoxide (1.058 g, 18.86 mmol) in DMF (10.00 mL)mL), (S)-({2-[1-(2-fluorobenzyl)pyrrolidine-2-carboxamide]phenyl}phenylmethylene)-(S)-alaninato-*N,N',N'',O*}nickel^{II} **56** (1.00 g, (1.89

mmol) and 1-(bromomethyl)-4-trifluoromethylbenzene (1.352 g, 5.66 mmol) to give the product as a reddish-orange solid. (Yield 0.96 g, 77 %); (98 % dr); m.p.: 231-233 °C. ¹H NMR (400 MHz, CDCl₃) δ 8.13-8.20 (2H, m, ArH), 7.73 (2H, d, ³J_{HH} = 7.9 Hz, ArH), 7.49-7.57 (4H, m, ArH), 7.37-7.47 (2H, m, ArH), 7.08-7.24 (4H, m, ArH), 7.00 (1H, t, ³J_{HH} = 9.0 Hz, ArH), 6.63 (2H, d, ³J_{HH} = 4.0 Hz, ArH), 4.28 (1H, d, ²J_{HH} = 13.1, Ar-CHH-N), 3.78 (1H, d, ²J_{HH} = 13.1, Ar-CHH-N), 3.14-3.31 (2H, m, α (Pro)-CH, Ar-CHH), 3.01-3.07 (2H, m, Ar-CHH, β (Pro)-CHH), 2.12-2.35 (2H, m, γ (Pro)-CHH, δ (Pro)-CHH), 1.72-1.91 (2H, m, δ (Pro)-CHH, γ (Pro)-CHH), 1.53-1.62 (1H, m, β (Pro)-CHH), 1.23 (3H, s, CH₃); ¹³C NMR (100 MHz, CDCl₃) δ 180.6 (C=O), 179.9 (C=O), 172.7 (C=N), 161.6 (d, ¹J_{CF} = 248.0 Hz, CF), 142.3 (Ar-C), 141.0 (Ar-C), 136.7 (Ar-C), 134.0 (Ar-CH), 133.9 (d, ⁴J_{CF} = 3.0 Hz, Ar-CH), 132.1 (Ar-CH), 131.2 (s, Ar-3CH), 131.1 (d, ³J_{CF} = 6.0 Hz, Ar-CH), 129.7 (q, ²J_{CF3} = 32.12 Hz, Ar-CF₃), 129.6 (Ar-CH), 128.2 (Ar-CH), 127.7 (Ar-C), 127.3 (Ar-CH), 127.2 (Ar-CH), 125.6 (d, ³J_{CF} = 4.0 Hz, Ar-CH), 124.4 (d, ⁴J_{CF} = 3.0 Hz, Ar-CH), 124.3 (q, ¹J_{CF3} = 272.05 Hz, Ar-CF₃), 123.4 (Ar-CH), 120.6 (d, ²J_{CF} = 14.1 Hz, Ar-C), 120.6 (Ar-CH), 115.9 (d, ²J_{CF} = 22.1 Hz, Ar-CH), 78.5 (α -C), 70.0 (α (Pro)-CH), 56.6 (Ar-CH₂-N), 56.2 (Ar-CH₂), 45.7 (β (Pro)-CH₂), 30.2 (δ (Pro)-CH₂), 29.9 (CH₃), 22.6 (γ (Pro)-CH₂); ¹⁹F NMR (376 MHz, CDCl₃) δ -113.8 (s), -62.3 (s), HRMS-ESI (calcd for $C_{36}H_{32}N_3O_3F_4^{58}Ni$ $[M+H]^+$) 688.1733, found 688.1754 ($\Delta = 3.1$ ppm), (calcd for $C_{36}H_{32}N_3O_3F_4^{60}Ni$ $[M+H]^+$) 690.1688, found 690.1722 ($\Delta = 4.9$ ppm).

6.6.2 Synthesis of (S)-({2-[1-(2-fluorobenzyl)benzyl]pyrrolidine-2-carboxamide} phenyl)phenylmethylene)-(S and R)-4-(trifluoromethyl)benzenyl-glycinato-*N,N',N'',O*}nickel^{II} (187 and 188)

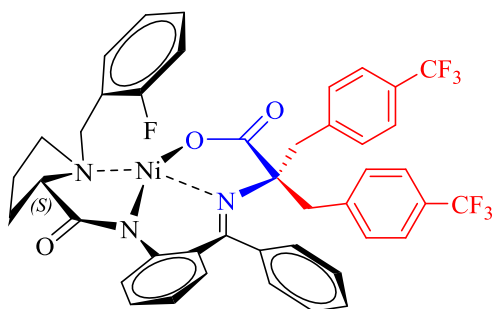
The general procedure (F) was followed using four equivalents of potassium tert-butoxide (0.423 g, 7.54 mmol) in dry DMF (5.0 mL), (S)-({2-[1-(2-fluorobenzyl)benzyl]pyrrolidine-2-carboxamide} phenyl)phenylmethylene)-(S)alaninnato-*N,N',N'',O*}nickel^{II} **55** (1.00 g, 1.89 mmol) and 1-(bromomethyl)-4-(trifluoromethyl)benzene (495 g, 2.08 mmol, 1.1 eq.) gave the product as a mixture of mono- and di-substituted (87:13). product as a reddish-orange solid. Purification was achieved via Biotage instrument (50:50 ethylacetate: DCM or 5:95 MeOH: DCM) to give the products as red powders.



The major product was isolated mono-substituted as a reddish-orange solid. (Yield 0.859 g, 66 %); (99 % dr); m.p.: 218-219 °C. ¹H NMR (400 MHz, CDCl₃) δ 8.28 (1H, d, ³J_{HH} = 8.8 Hz, ArH), 8.21 (1H, td, ³J_{HH} = 7.3, ⁴J_{HH} = 1.6 Hz, ArH), 7.67 (2H, d, ³J_{HH} =

8.2 Hz, ArH), 7.45-7.62 (3H, m, ArH), 7.26-7.35 (3H, m, ArH), 7.09-7.20 (3H, m, ArH), 6.93-7.01 (2H, m, ArH), 6.66-6.75 (2H, m, ArH), 4.32 (1H, t, ³J_{HH} = 5.0 Hz, α(Pro)-CH), 4.25 (1H, d, ²J_{HH} = 12.9 Hz, Ar-CHH-N), 3.70 (1H, d, ²J_{HH} = 12.9 Hz, Ar-CHH-N), 3.30 (1H, dd, ²J_{HH} = 13.7, ³J_{HH} = 9.8 Hz, α-CH), 3.04-3.09 (2H, m, CHH-Ar-CF₃, β(Pro)-CHH), 2.84-2.89 (1H, dd, ²J_{HH} = 13.7, ³J_{HH} = 9.8 Hz, CHH-Ar-CF₃), 1.82-1.91 (3H, m, γ(Pro)-CHH, δ(Pro)-CH₂), 1.91-1.85 (1H, m, β(Pro)-CHH) 1.68-1.74 (1H, m, γ(Pro)-CHH), ¹³C NMR (125 MHz, CDCl₃) δ 180.0 (C=O), 177.9 (C=O), 171.6 (C=N), 161.5 (d, ¹J_{CF} = 247.7 Hz, CF), 142.9 (Ar-C), 140.1 (Ar-C), 134.1 (Ar-C), 133.9 (d, ⁴J_{CF} = 3.2 Hz, Ar-CH), 133.6 (Ar-CH), 132.6 (Ar-CH), 131.1 (d, ³J_{CF} = 8.0 Hz, Ar-CH), 130.9 (Ar-2CH), 129.9 (Ar-CH), 129.6 (q, ²J_{CF3} = 32.1 Hz, Ar-C-CF₃), 129.3 (Ar-CH), 129.0 (Ar-CH), 127.7 (Ar-CH), 127.1 (Ar-CH), 126.0 (Ar-C), 125.7 (d, ³J_{CF} = 3.2 Hz, Ar-CH), 125.6 (Ar-CH), 124.4 (Ar-CH), 123.5 (q, ¹J_{CF3} = 271.6 Hz, Ar-CF₃), 123.3 (Ar-CH), 120.7 (Ar-CH), 120.51 (d, ²J_{CF} = 14.4 Hz, Ar-C), 116.0 (d, ²J_{CF} = 22.4 Hz, Ar-CH), 71.0 (α(Pro)-CH), 70.3 (α-CH), 56.9 (N-CHHAr), 56.0 (CHHAr), 39.2 (β(Pro)-CH₂), 30.5 (δ(Pro)-CH₂), 22.9 (γ(Pro)-CH₂); ¹⁹F NMR (376 MHz, CDCl₃) δ -113.7 (s), -62.4 (s), HRMS-ESI (calcd for C₃₅H₂₉N₃O₃F₄Na⁵⁸Ni [M+Na]⁺) 696.1396, found 696.1406 (Δ =

1.4 ppm), (calcd for $C_{35}H_{29}N_3O_3F_4Na^{60}Ni [M+Na]^+$) 698.1351, found 698.1382 ($\Delta = 4.4$ ppm).



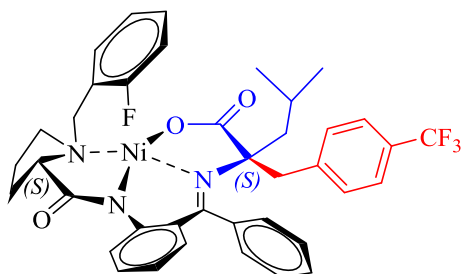
The minor product was isolated di-substituted as a reddish-orange solid (Yield 0.107 g, 8 %); m.p.: 218-219°C. 1H NMR (400 MHz, $CDCl_3$) δ 8.07 (1H, td, $^3J_{HH} = 7.4$ Hz, $^4J_{HH} = 1.4$ Hz ArH), 7.86 (1H, dd, $^3J_{HH} = 8.6$, $^4J_{HH} = 0.8$ Hz, ArH), 7.79 (2H, d, $^3J_{HH} = 8.0$ Hz, ArH), 7.8

(2H, d, $^3J_{HH} = 8.2$, ArH), 7.7 (2H, d, $^3J_{HH} = 8.0$, ArH), 7.42-7.56 (4H, m, ArH), 7.32 (1H, t, $^3J_{HH} = 7.2$ Hz, ArH), 7.17-7.25 (2H, m, ArH), 6.99-7.15 (3H, m, ArH), 6.84 (1H, d, $^3J_{HH} = 7.8$ Hz, ArH), 6.50-6.62 (2H, m, ArH), 4.38 (1H, d, $^2J_{HH} = 13.1$ Hz, Ar-CHH-N), 3.50 (1H, d, $^2J_{HH} = 12.9$ Hz, Ar-CHH-N), 3.40 (1H, d, $^2J_{HH} = 17.4$ Hz, Ar-CHH-N), 3.25-3.35 (2H, m, α (Pro)-CH, Ar-CHH), 3.00-3.15 (2H, m, Ar-CHH, β (Pro)-CHH), 2.74 (1H, d, $^2J_{HH} = 17.4$ Hz, Ar-CHH), 2.22-2.34 (1H, m, γ (Pro)-CHH), 2.00-2.16 (1H, m, δ (Pro)-CHH), 1.74-1.92 (2H, m, δ (Pro)-CHH, γ (Pro)-CHH), 1.51-1.63 (1H, m, β (Pro)-CHH), ^{13}C NMR (125 MHz, $CDCl_3$) δ 180.2 (C=O), 179.1 (C=O), 172.9 (C=N), 161.6 (d, $^1J_{CF} = 247.7$ Hz, CF), 142.4 (Ar-C), 141.1 (Ar-C), 140.5 (Ar-C), 136.4 (Ar-CH), 133.7 (Ar-CH), 133.6 (d, $^3J_{CF} = 3.2$ Hz, Ar-CH), 132.1 (Ar-CH), 131.5 (Ar-3CH), 131.3 (d, $^3J_{CF} = 8.0$ Hz, Ar-CH), 130.1 (Ar-CH), 130.0 (d, $^2J_{CF3} = 32.1$ Hz, Ar-C-CF₃), 129.4 (Ar-3CH), 128.8 (Ar-CH), 128.3 (d, $^2J_{CF3} = 32.5$ Hz, Ar-C-CF₃), 128.2 (Ar-C), 127.7 (Ar-2C), 127.4 (Ar-CH), 127.2 (Ar-CH), 125.9 (Ar-CH), 125.8 (Ar-CH), 125.5 (Ar-CH), 125.4 (Ar-CH), 124.1 (q, $^1J_{CF3} = 271.6$ Hz, Ar-2C-CF₃), 123.9 (Ar-CH), 120.7 (Ar-CH), 120.6 (d, $^2J_{CF} = 14.4$ Hz, Ar-C), 116.1 (d, $^2J_{CF} = 22.4$ Hz, Ar-CH), 80.3 (α (Pro)-CH), 69.8 (α -C), 57.9 (Ar-CH₂-N), 56.6 (Ar-CH₂), 45.8 (Ar-CH₂), 45.4 (β -C), 30.4 (δ (Pro)-CH₂), 22.7 (γ (Pro)-CH₂); ^{19}F NMR (376 MHz, $CDCl_3$) δ -113.3 (s), -62.4 (s), -62.3 (s), HRMS-ESI (calcd for $C_{43}H_{34}N_3O_3F_7Na^{58}Ni [M+Na]^+$) 854.1740, found 854.1750 ($\Delta = 1.2$ ppm), (calcd for $C_{43}H_{34}N_3O_3F_7Na^{60}Ni [M+Na]^+$) 856.1694, found 856.1732 ($\Delta = 4.4$ ppm).

6.6.3 Synthesis of (S)-({2-[1-(2-fluorobenzyl)benzyl]pyrrolidine-2-carboxamide}phenyl)phenylmethylene)-(S and R)-4-(trifluoromethyl)benzenyl-leucinato-N,N',N'',O}nickel(II) (190 and 191)

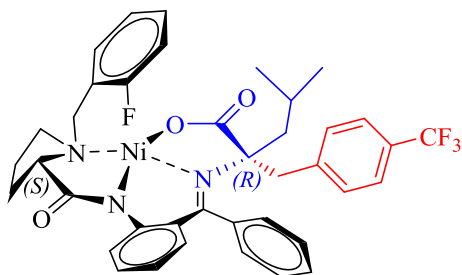
The general procedure (F) was followed using 4 equivalents of potassium tert-butoxide (0.423 g, 7.54 mmol) in dry DMF (5.0 mL/mL), (S)-({2-[1-(2-fluorobenzyl)pyrrolidine-2-carboxamide]phenyl}phenylmethylene)-(S)-valaninato-N,N',N'',O}nickel^{II} **100** (1.00

g, 1.89 mmol) and 1-(bromomethyl)-2-fluorobenzene (1.070 g, 5.66 mmol) to give the products as a diastereoisomers *S* and *R* (3:1). Purification was achieved via Biotage instrument (50:50 ethylacetate: DCM or 5:95 MeOH: DCM) to give the products as red powders.



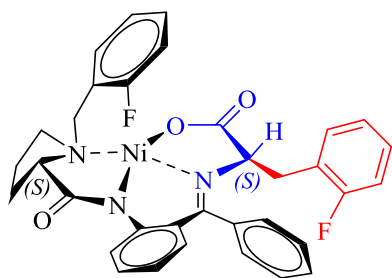
The major product was isolated as (*S,S*) diastereoisomer as a reddish-orange solid (Crystals suitable for single crystal X-ray structure determination were grown by slow evaporation of the compound in ethylacetate.

These confirmed the (*S,S*) stereochemistry of the product complex). (Yield 0.859 g, 66 %); m.p.: 228-229 °C. ^1H NMR (400 MHz, CDCl_3) δ 8.21 (1H, t, $^3J_{\text{HH}} = 7.1$ Hz, ArH), 7.80 (1H, d, $^3J_{\text{HH}} = 8.3$ Hz, ArH), 7.76 (2H, d, $^3J_{\text{HH}} = 8.0$ Hz, ArH), 7.67 (2H, d, $^3J_{\text{HH}} = 7.9$ Hz, ArH), 7.49-7.61 (3H, m, ArH), 7.41-7.48 (1H, m, ArH), 7.21-7.24 (2H, m, ArH), 7.15 (2H, br t, $^3J_{\text{HH}} = 7.3$ Hz, ArH), 7.04 (1H, t, $^3J_{\text{HH}} = 8.9$ Hz, ArH), 6.67 (2H, d, $^3J_{\text{HH}} = 3.6$ Hz, ArH), 4.32 (1H, br d, $^2J_{\text{HH}} = 12.9$ Hz, Ar-CHH-N), 3.73 (1H, d, $^2J_{\text{HH}} = 12.9$ Hz, Ar-CHH-N), 3.22 (1H, dd, $^2J_{\text{HH}} = 10.1$, $^3J_{\text{HH}} = 7.2$ Hz, CHH-leucine), 3.08 (1H, d, $^2J_{\text{HH}} = 13.9$ Hz, Ar-CHH), 2.99-3.02 (1H, m, $\alpha(\text{Pro})$ -CH), 2.74 (1H, d, $^2J_{\text{HH}} = 14.1$ Hz, Ar-CHH), 2.16-2.32 (2H, m, $\beta(\text{Pro})$ -CHH, $\gamma(\text{Pro})$ -CHH), 1.83-1.85 (1H, m, $\delta(\text{Pro})$ -CHH), 1.71-1.79 (2H, m, $\delta(\text{Pro})$ -CHH, CH-leucine), 1.50-1.67 (3H, m, CHH-leucine, $\gamma(\text{Pro})$ -CHH, $\beta(\text{Pro})$ -CHH), 1.13 (3H, d, $^3J_{\text{HH}} = 6.4$ Hz, CH_3), 1.12 (3H, d, $^3J_{\text{HH}} = 6.6$ Hz, CH_3); ^{13}C NMR (125 MHz, CDCl_3) δ 180.8 (C=O), 180.1 (C=O), 173.0 (C=N), 160.9 (d, $^1J_{\text{CF}} = 248.0$ Hz, CF), 142.1 (Ar-C), 141.1 (Ar-C), 136.8 (Ar-C), 134.0 (d, $^4J_{\text{CF}} = 3.0$ Hz, Ar-CH), 133.6 (Ar-CH), 131.8 (Ar-CH), 131.3 (Ar-4CH), 131.2 (d, $^2J_{\text{CF}} = 8.0$ Hz, Ar-CH), 128.8 (Ar-2CH), 129.7 (Ar-C), 129.2 (q, $^2J_{\text{CF}_3} = 32.1$ Hz, Ar-C-CF₃), 128.1 (d, $^3J_{\text{CF}} = 6.0$ Hz, Ar-CH), 127.5 (Ar-CH), 125.6 (d, $^4J_{\text{CF}} = 3.0$ Hz, Ar-CH), 124.5 (d, $^3J_{\text{CF}} = 3.0$ Hz, Ar-CH), 124.2 (Ar-CH), 124.2 (q, $^1J_{\text{CF}_3} = 272.1$ Hz, Ar-CF₃), 120.9 (Ar-CH), 120.6 (d, $^2J_{\text{CF}} = 14.1$ Hz, Ar-C), 116.2 (d, $^2J_{\text{CF}} = 22.1$ Hz, Ar-CH), 81.3 (Ar-CH₂-N), 70.2 ($\alpha(\text{Pro})$ -C), 57.1 ($\delta(\text{Pro})$ -CH₂), 56.5 (α -C), 48.4 (Ar-CH₂), 43.7 ($\beta(\text{Pro})$ -C), 30.4 (CH₂-leucine), 24.8 (CH-leucine), 23.9 (CH₃), 22.4 ($\gamma(\text{Pro})$ -CH₂), 21.4 (CH₃); ^{19}F NMR (376 MHz, CDCl_3) δ -114.1 (s), -62.4 (s), HRMS-ESI (calcd for $\text{C}_{39}\text{H}_{37}\text{N}_3\text{O}_3\text{F}_4\text{Na}^{58}\text{Ni}$ [$\text{M}+\text{Na}$] $^+$) 752.2022, found 752.2025 ($\Delta = 0.4$ ppm), (calcd for $\text{C}_{39}\text{H}_{37}\text{N}_3\text{O}_3\text{F}_4\text{Na}^{60}\text{Ni}$ [$\text{M}+\text{H}$] $^+$) 754.1977, found 754.2008 ($\Delta = 4.1$ ppm).



The minor of product isolated as the (*R*) diastereoisomer as a reddish-orange solid (Yield 0.226 g, 17 %); m.p.: 215-217 °C. ¹H NMR (400 MHz, CDCl₃) δ 8.11 (1H, t, ³J_{HH} = 7.1 Hz, ArH), 7.79 (1H, d, ³J_{HH} = 8.3 Hz, ArH), 7.66 (2H, d, ³J_{HH} = 8.0 Hz, ArH), 7.49-7.55 (1H, d, m, ArH), 7.39-7.45 (4H, m, ArH), 7.23-7.29 (2H, m, ArH), 7.04-7.10 (4H, m, ArH), 6.26 (2H, d, ³J_{HH} = 3.8 Hz, ArH), 4.35 (1H, br d, ²J_{HH} = 12.7 Hz, Ar-CHH-N), 3.66 (1H, t, 3.61 Hz, α(Pro)-CH) 3.60 (1H, d, ²J_{HH} = 12.9 Hz, Ar-CHH-N), 3.22 (1H, dd, ³J_{HH} = 10.3, ³J_{HH} = 6.2 Hz, δ(Pro)-CH), 3.16-3.25 (1H, m, β(Pro)-CHH), 3.05 (2H, s, Ar-CH₂) 2.60-2.65 (1H, m, γ(Pro)-CHH), 2.42-2.50 (1H, m, δ(Pro)-CHH), 2.03-2.09 (2H, m, γ(Pro)-CHH, β(Pro)-CHH), 1.70 (1H, dd, ²J_{HH} = 14.3, ³J_{HH} = 8.5 Hz, CHH-leucine), 1.51 (1H, dd, ²J_{HH} = 14.5, ³J_{HH} = 3.8 Hz, CHH-leucine), 1.37 (3H, d, ³J_{HH} = 6.4 Hz, CH₃), 1.13 (3H, d, ³J_{HH} = 6.6 Hz, CH₃); ¹³C NMR (125 MHz, CDCl₃) δ 180.9 (C=O), 180.6 (C=O), 173.0 (C=N), 1601.5 (d, ¹J_{CF} = 248.0 Hz, CF), 141.6 (Ar-C), 140.9 (Ar-C), 136.7 (Ar-C), 134.0 (d, ⁴J_{CF} = 3.0 Hz, Ar-CH), 133.2 (Ar-CH), 131.6 (Ar-CH), 131.2 (Ar-CH), 131.1 (Ar-CH), 130.1 (Ar-3CH), 129.7 (Ar-CH), 129.2 (q, ²J_{CF3} = 32.1 Hz, Ar-C-CF₃), 128.9 (Ar-C), 128.1 (Ar-CH), 127.2 (Ar-CH), 125.3 (d, ³J_{CF} = 3.0 Hz, Ar-CH), 124.5 (d, ³J_{CF} = 3.0 Hz, Ar-CH), 124.2 (Ar-CH), 124.1 (q, ¹J_{CF3} = 272.1 Hz, Ar-CF₃), 120.9 (Ar-CH), 120.5 (d, ²J_{CF} = 14.1 Hz, Ar-C), 116.2 (d, ²J_{CF} = 22.1 Hz, Ar-CH), 80.1 (Ar-CH₂-N), 69.8 (α(Pro)-CH), 57.8 (δ(Pro)-CH₂), 56.2 (α-C), 46.9 (Ar-CH₂), 46.8 (β(Pro)-CH₂), 30.7 (CH₂-leucine), 25.1 (CH-leucine), 24.5 (CH₃), 23.4 (γ(Pro)-CH₂), 22.3 (CH₃); ¹⁹F NMR (376 MHz, CDCl₃) δ -113.5 (s), -62.5 (s), HRMS-ESI (calcd for C₃₉H₃₇N₃O₃F₄Na⁵⁸Ni [M+Na]⁺) 752.2022, found 752.2047 (Δ = 3.3 ppm), (calcd for C₃₉H₃₇N₃O₃F₄Na⁶⁰Ni [M+H]⁺) 754.1977, found 754.2019 (Δ = 5.6 ppm).

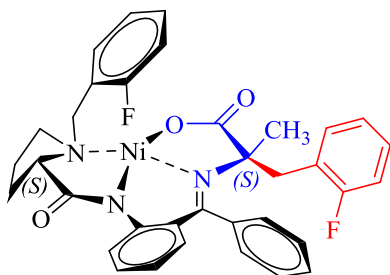
6.6.4 Synthesis of (S)-({2-[1-(2-fluorobenzyl)benzyl]pyrrolidine-2-carboxamide}phenyl)phenylmethylene)-(S)-2-fluorobenzenyl-glycinato-*N,N',N'',O*}nickel^{II} **191**



The general procedure (**F**) was followed using 4 equivalents of potassium tert-butoxide (0.423 g, 7.54 mmol) in dry DMF (5.00 mL), (S)-({2-[1-(2-fluorobenzyl)pyrrolidine-2-carboxamide]phenyl}phenylmethylene)-(S)-alaninato-*N,N',N'',O*}nickel^{II} **55** (1.00 g, 1.89 mmol) and 1-(bromomethyl)-2-

fluorobenzene (1.070 g, 5.66 mmol) to give the product as a reddish-orange solid. (Yield 0.792 g, 66 %); (96 : 4 dr), m.p.: 218-219 °C. ¹H NMR (500 MHz, CDCl₃) δ 8.31 (1H, d, ³J_{HH} = 8.6 Hz ArH), 8.22-8.27 (1H, td, ³J_{HH} = 7.4, ⁴J_{HH} = 1.3 Hz ArH), 7.35-7.57 (5H, m, ArH), 7.09-7.30 (8H, m, ArH), 6.95-7.02 (2H, m, ArH), 6.64-6.72 (2H, m, ArH), 4.28 (2H, d of AB multiplets, ³J_{HH} = 9.5 Hz, Ar-CH₂-N), 3.74 (1H, d, ²J_{HH} = 13.1 Hz, Ar-CHH-N), 3.45 (1H, d, ³J_{HH} = 8.3 Hz, α-C), 3.06-3.21 (2H, m, β(Pro)-CHH, Ar-CHH-N), 2.94 (1H, dd, ³J_{HH} = 14.0, ⁴J_{HH} = 4.4 Hz, α(Pro)-CH), 2.28-2.46 (3H, m, δ-CH₂, γ-CHH), 1.94-1.88 (1H, m, γ-CHH), 1.66-1.78 (1H, m, β-CHH); ¹³C NMR (125 MHz, CDCl₃) δ 179.9 (C=O), 178.4 (C=O), 172.1 (C=N), 162.0 (d, ¹J_{CF} = 246.1 Hz, CF), 161.6 (d, ¹J_{CF} = 247.7 Hz, CF), 142.9 (Ar-C), 134.1 (Ar-CH), 134.0 (Ar-C), 133.6 (Ar-CH), 132.9 (d, ³J_{CF} = 4.8 Hz, Ar-CH), 132.4 (Ar-CH), 131.1 (d, ³J_{CF} = 8.0 Hz, Ar-CH), 130.8 (Ar-CH), 129.7 (Ar-CH), 129.3 (d, ³J_{CF} = 9.6 Hz, Ar-CH), 128.9 (Ar-CH), 128.2 (d, ⁴J_{CF} = 3.2 Hz, Ar-CH), 127.2 (Ar-CH), 126.3 (Ar-C), 124.7 (d, ³J_{CF} = 3.2 Hz, Ar-CH), 124.4 (d, ²J_{CF} = 3.2 Hz, Ar-CH), 123.2 (Ar-CH), 123.1 (d, ²J_{CF} = 16.0 Hz, Ar-C), 120.5 (Ar-CH), 120.4 (d, ²J_{CF} = 14.4 Hz, Ar-C), 116.0 (d, ²J_{CF} = 22.4 Hz, Ar-CH), 115.6 (d, ²J_{CF} = 22.4 Hz, Ar-CH), 70.8 (α-C), 70.5 (α(Pro)-C), 56.8 (CHHAr), 55.8 (CHHAr), 33.2 (β-C), 30.7 (δ-C), 23.1 (γ-C); ¹⁹F NMR (376 MHz, CDCl₃) δ -113.6 (s), -62.3 (s), HRMS-ESI (calcd for C₃₄H₃₀N₃O₃F₂⁵⁸Ni [M+H]⁺) 624.1609, found 624.1617 (Δ = 1.3 ppm), (calcd for C₃₄H₃₀N₃O₃F₂⁶⁰Ni [M+H]⁺) 626.1563, 626.1579 (Δ = 2.6 ppm).

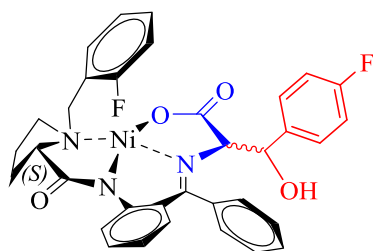
6.6.5 Synthesis of (S)-({2-[1-(2-fluorobenzyl)benzyl]pyrrolidine-2-carboxamide]phenyl}phenylmethylene)-(S)-2-fluorobenzenyl-alaninato-*N,N',N'',O*}nickel^{II} **192**



The general procedure (**F**) was followed using 4 equivalents of potassium tert-butoxide (0.423 g, 7.54 mmol), (S)-({2-[1-(2-fluorobenzyl)pyrrolidine-2-carboxamide]phenyl}phenylmethylene)-(S)-alaninato-*N,N',N'',O*}nickel^{II} **56** (1.00 g, 1.89 mmol) and a solution of 1-(bromomethyl)-2-fluorobenzene (1.070 g,

5.66 mmol) to give the product as a reddish-orange solid. (Crystals suitable for single crystal X-ray structure determination were grown by slow evaporation of the compound in ethylacetate. These confirmed the (*S,S*) stereochemistry of the product complex). (Yield 0.832 g 69 %); (98 : 2 dr); m.p.: 218-219 °C. ¹H NMR (500 MHz, CDCl₃) δ 8.19-8.27 (2H, m, ArH), 7.38-7.52 (5H, m, ArH), 7.30 (1H, d, ³J_{HH} = 7.2 Hz, ArH), 7.10-7.27 (6H, m, ArH), 7.01 (1H, t, ³J_{HH} = 8.8 Hz, ArH), 6.60-6.64 (2H, d, m, ArH), 4.31 (1H, d, ²J_{HH} = 13.1, Ar-CHH-N), 3.83 (1H, d, ²J_{HH} = 12.9 Hz, Ar-CHH-N), 3.45 (1H, d, ²J_{HH} = 13.9 Hz, Ar-CHH), 3.26 (1H, t, ³J_{HH} = 8.6 Hz, α(Pro)-CH), 3.07-3.13 (1H, m, β(Pro)-CHH), 2.98 (1H, d, ²J_{HH} = 13.9, Ar-CHH), 2.23-2.32 (2H, m, γ(Pro)-CHH, δ(Pro)-CHH), 2.05-2.16 (1H, m, δ(Pro)-CHH), 1.82-1.88 (1H, m, γ(Pro)-CHH), 1.58-1.67 (1H, m, β(Pro)-CHH), 1.09 (3H, s, CH₃); ¹³C NMR (125 MHz, CDCl₃) δ 180.7 (C=O), 179.8 (C=O), 173.2 (C=N), 162.3 (d, ¹J_{CF} = 245.9 Hz, CF), 161.6 (d, ¹J_{CF} = 248.0 Hz, CF), 142.3 (Ar-C), 137.0 (Ar-C), 134.0 (s, Ar-2CH), 133.4 (d, ³J_{CF} = 4.0 Hz, Ar-CH), 131.9 (Ar-2CH), 131.1 (Ar-CH), 130.8 (Ar-CH), 129.4 (d, ³J_{CF} = 8.0 Hz, CH), 129.3 (Ar-CH), 128.4 (Ar-CH), 127.9 (Ar-C), 127.4 (d, ³J_{CF} = 7.0 Hz, Ar-CH), 127.0 (Ar-CH), 124.8 (d, ³J_{CF} = 3.0 Hz, Ar-CH), 124.4 (d, ³J_{CF} = 3.0 Hz, Ar-CH), 123.8 (d, ²J_{CF} = 16.1 Hz, Ar-C), 123.0 (Ar-CH), 120.5 (d, ²J_{CF} = 14.1 Hz, Ar-C), 120.3 (Ar-CH), 116.1 (d, ²J_{CF} = 23.1 Hz, Ar-CH), 115.9 (d, ²J_{CF} = 23.1 Hz, Ar-CH), 78.8 (α-C), 70.2 (α(Pro)-CH), 56.6 (Ar-CH₂-N), 56.1 (Ar-CH₂), 40.9 (δ(Pro)-CH₂), 30.3 (β(Pro)-CH₂), 29.4 (CH₃), 22.8 (γ(Pro)-CH₂); ¹⁹F NMR (376 MHz, CDCl₃) δ -113.6 (s), -62.3 (s); HRMS-ESI (calcd for C₃₅H₃₂N₃O₃F₂⁵⁸Ni [M+H]⁺) 638.1765, found 638.1777 (Δ = 1.9 ppm), (calcd for C₃₅H₃₂N₃O₃F₂⁶⁰Ni [M+H]⁺) 640.1720, found 640.1752 (Δ = 5.0 ppm).

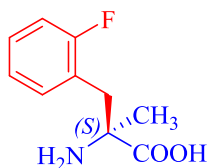
6.6.6 Synthesis of (S)-({2-[1-(2-fluorobenzyl)benzyl]pyrrolidine-2-carboxamide}phenyl)methyl-phenylmethylene)-(S)-2-hydroxy-4-fluorobenzenyl-glycinato-*N,N',N'',O*}nickel^{II} **198**



A fresh solution of sodium methoxide (3 ml, 2.2 M) was added to ({2-[1-(2-fluorobenzyl)pyrrolidine-2-carboxamide]phenyl}phenylmethylene)-(amino acid)ato-*N,N',N'',O*} nickel^{II} **55** (1 g, 1.937 mmol, 1 eq.) under an atmosphere of nitrogen. The reaction mixture was stirred for 20 min, with the colour of the mixture darkening over this time. The reaction was cooled to (-10 to -15 °C) using a chiller instrument and 4-fluorobenzaldehyde (0.4 ml, 3.874 mmol, 2 eq.) was added dropwise to the reaction mixture. The reaction mixture was stirred for 24 hours. The chiller instrument was removed, and the reaction mixture then stirred for 1 h at room temperature. The progress of the reaction was monitored via TLC (methanol: dichloromethane 5:95) and ¹⁹F NMR spectroscopy. Water (20-25 ml) was added to the mixture to quench the reaction; the mixture was concentrated *in vacuo* and extracted with dichloromethane (3 x 100 ml). The combined organic extracts were washed with brine solution (3 x 20 ml), dried with anhydrous MgSO₄ and concentrated *in vacuo*. Purifications via the Biotage instrument gave the product as a reddish-orange solid diastereoisomer. (Crystals suitable for single crystal X-ray structure determination were grown by slow evaporation of the compound in ethylacetate. These confirmed the (*S*) stereochemistry of the product complex). (Yield 0.756 g, 61 %); (1 : 1 dr); m.p.: 213-214 °C; ¹H NMR (500 MHz, CDCl₃) δ 8.49 (1H, d, ³J_{HH} = 8.7 Mz, ArH), 7.53-7.61 (3 H, m, ArH), 7.25-7.45 (8H, m, ArH), 7.07-7.18 (3H, m, ArH), 6.85 (1H, d, ³J_{HH} = 7.9 Hz, ArH), 6.78 (1H, d, ³J_{HH} = 7.6 Hz, ArH), 4.92 (1H, br s, C-OH), 4.70 (1H, d, ³J_{HH} = 5.5 Hz, Ar-CH-O), 4.38 (1H, d, ³J_{HH} = 5.3 Hz, α-CH), 3.98 (1H, d, ²J_{HH} = 14 Hz, Ar-CHH-N), 3.68-3.75 (1H, m, β(Pro)-CHH), 3.63 (1H, d, ²J_{HH} = 15.1 Hz, Ar-CH-N), 3.24 (1H, d, ³J_{HH} = 9.4 Hz, α(Pro)-CHH), 2.35-2.39 (1H, m, γ(Pro)-CHH), 2.14-2.2.34 (1H, m, δ(Pro)-CHH), 1.94-1.85 (1H, m, δ(Pro)-CHH), 1.38-1.45 (2H, m, β(Pro)-CHH, γ(Pro)-CHH), ¹³C NMR (125 MHz, CDCl₃) δ 181.6 (C=O), 178.0 (C=O), 173.1 (C=N), 163.2 (d, ¹J_{CF} = 247.0 Hz, CF), 161.6 (d, ¹J_{CF} = 249.0 Hz, CF), 142.3 (Ar-C), 134.8 (d, ²J_{CF} = 3.2 Hz, Ar-CH), 133.2 (d, ³J_{CF} = 2.0 Hz, Ar-C), 133.0 (Ar-CH), 132.8 (Ar-C), 132.2 (Ar-CH), 130.4 (d, ³J_{CF} = 8.0 Hz, Ar-CH), 129.3 (Ar-CH), 128.5 (Ar-2CH), 128.4 (Ar-CH), 128.2 (Ar-CH), 127.1 (Ar-CH), 125.8 (Ar-CH), 124.9 (Ar-C), 123.6 (d, ³J_{CF} = 3.0 Hz, Ar-CH), 123.8 (Ar-2CH), 120.0 (Ar-CH), 117.7 (d, ²J_{CF}

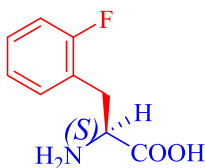
= 15.1 Hz, Ar-C), 115.2 (d, $^2J_{CF}$ = 23.1 Hz, Ar-C), 114.6 (d, $^2J_{CF}$ = 21.1 Hz, Ar-2CH), 72.8 (Ar-C-OH), 71.8 (α -CH), 67.6 (α (Pro)-CH) 54.6 (Ar-CH₂-N), 52.0 (γ (Pro)-CH₂), 30.2 (β (Pro)-CH₂), 22.6 (δ (Pro)-CH₂); ^{19}F NMR (376 MHz, CDCl₃) δ -113.3 (d), -113.0 (d); HRMS-ESI (calcd for C₃₄H₃₀N₃O₄F₂⁵⁸Ni [M+H]⁺) 640.1558, found 640.1552 (Δ = -0.6 ppm), (calcd for C₃₄H₃₀N₃O₄F₂⁶⁰Ni [M+H]⁺) 642.1512, found 642.1528 (Δ = 2.5 ppm).

6.6.7 Synthesis of (S)-2-amino-3-(2-fluorophenyl)-2-methylpropanoic acid 202



The general procedure (**H**) was followed using (S)-({2-[1-(2-fluorobenzyl)benzyl]pyrrolidine-2-carboxamide}phenyl)phenyl methylene)-(S)-2-fluorobenzyl-alaninato-*N,N'*,*N''*,*O*}nickel(III) **192** (450 mg, 0.705 mmol) and 8-hydroxyquinoline (307 mg, 2.115 mmol) to give the product as a white viscous colourless oil. (Yield 119 mg, 86 %); ^1H NMR (400 MHz, D₂O) δ 7.44 (1H, br t, $^3J_{\text{HH}}$ = 7.4 Hz, ArH), 7.23-7.31 (1H, m, ArH), 3.13 (1H, d, $^4J_{\text{HH}}$ = 13.7 Hz, ArH), 3.01 (1H, d, $^4J_{\text{HH}}$ = 13.7 Hz, ArH), 1.25 (3H, s, CH₃); ^{13}C NMR (100 MHz, D₂O) δ ppm 175.4 (O-C=O), 161.0 (d, $^1J_{CF}$ = 244.5 Hz, Ar-C), 133.1 (Ar-CH), 128.8 (d, $^3J_{CF}$ = 8.0 Hz, Ar-CH), 124.1 (Ar-CH), 122.7 (d, $^2J_{CF}$ = 14.4 Hz, Ar-C), 115.0 (d, $^2J_{CF}$ = 22.4 Hz, Ar-C), 60.1 (α -C), 35.4 (CH₂), 22.1 (CH₃); ^{19}F NMR (376 MHz, D₂O) δ -73.7 (s), HRMS-ESI (calcd for C₁₀H₁₃NO₂F [M+H]⁺) 198.0930, found 198.0931 (Δ = 0.5 ppm).

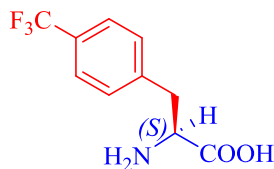
6.6.8 Synthesis of (S)-2-amino-3-(2-fluorophenyl)propanoic acid 203



The general procedure (**H**) was followed using (S)-({2-[1-(2-fluorobenzyl)benzyl]pyrrolidine-2-carboxamide}phenyl)phenyl methylene)-(S)-2-fluorobenzyl-glycinato-*N,N'*,*N''*,*O*}nickel(III) **188** (600 mg, 961 mmol) and 8-hydroxyquinoline (419 mg, 2.883 mmol) to give the product as a white powder. (Yield 119 mg, 68 %); m.p.: 147-149 °C; ^1H NMR (400 MHz, DMSO-*d*₆) δ 7.42 (1H, br t, $^3J_{\text{HH}}$ = 7.0 Hz, ArH), 7.21 (1H, t, $^3J_{\text{HH}}$ = 13.1 Hz, ArH), 1.76 (2H, t, $^3J_{\text{HH}}$ = 8.2 Hz, ArH), 3.39-3.47 (2H, m, α -CH, CHH), 2.86 (1H, t, $^3J_{\text{HH}}$ = 8.2 Hz, CHH); ^{13}C NMR (100 MHz, DMSO) δ ppm 178.8 (O-C=O), 160.4 (d, $^1J_{CF}$ = 247.2 Hz, Ar-C), 131.6 (d, $^3J_{CF}$ = 3.2 Hz, Ar-CH), 131.4 (Ar-CH), 128.2 (d, $^2J_{CF}$ = 7.9 Hz, Ar-CH), 124.1 (d, $^3J_{CF}$ = 2.4 Hz, Ar-CH), 114.9 (d, $^2J_{CF}$ = 21.5 Hz, Ar-C),

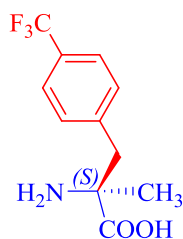
53.7 (α -C), 31.5 (CH_2); ^{19}F NMR (376 MHz, $CDCl_3$) δ -62.37 (s), HRMS-ESI (calcd for $C_9H_{11}NO_2F$ $[M+H]^+$) 184.0774, found 184.0775 (Δ = 0.5 ppm).

6.6.9 Synthesis of (S)-2-amino-3-(4-(trifluoromethyl)phenyl)propanoic acid 204



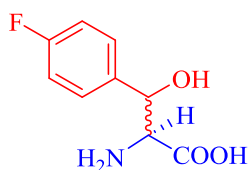
The general procedure (**H**) was followed using (S)-({2-[1-(2-fluorobenzyl)benzyl]pyrrolidine-2-carboxamide} phenyl}phenylmethylene)(S)-4-(trifluoromethyl)benzenyl-glycinato-*N,N'*,*N''*,*O*}nickel^(II) **187** (730 mg, 1.082 mmol) and 8-hydroxyquinoline (417 mg, 3.248 mmol) to give the product as a white powder. (Yield 235 mg, 93 %); m.p.: 111-112 °C; 1H -NMR (500 MHz, D_2O and drops of $DMSO-d_6$) δ 7.7 (2H, d, $^3J_{HH}$ = 5.77 Hz, ArH), 7.40 (1H, d, $^3J_{HH}$ = 5.77 Hz, ArH), 3.89 (2H, br t, $^3J_{HH}$ = 5.7 Hz, α -CH), 3.10 (1H, dd, $^2J_{HH}$ = 14.0, $^3J_{HH}$ = 4.7 Hz, CH), 2.65 (1H, dd, $^2J_{HH}$ = 14.2, $^3J_{HH}$ = 7.7 Hz, CH); ^{13}C NMR (100 MHz, D_2O and drops of $DMSO-d_6$) δ ppm 174.8 (O=C=O), 140.0 (Ar-CH), 129.8 (Ar-2CH), 128.8 (q, $^2J_{CF}$ = 33.1 Hz, Ar-C- CF_3), 125.8 (Ar-C), 125.7 (Ar-CH), 124.1 (q, $^1J_{CF}$ = 276.3 Hz, CF_3), 55.9 (α -C), 36.8 (CH_2); ^{19}F NMR (376 MHz, D_2O and drops of $DMSO-d_6$) δ -60.7 (s), HRMS-ESI (calcd for $C_{10}H_{11}NO_2F_3$ $[2M+H]^+$) 234.0742, found 234.0754 (Δ = 4.5 ppm).

6.6.10 Synthesis of (S)-2-amino-2-methyl-3-(4-(trifluoromethyl)phenyl)propanoic acid 205



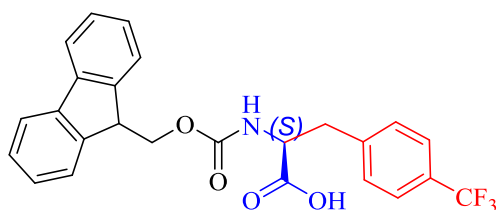
The general procedure (**H**) was followed using (S)-({2-[1-(2-fluorobenzyl)benzyl]pyrrolidine-2-carboxamide}phenyl}phenylmethylene)-(S)-4-(trifluoromethyl)benzenyl-alaninato-*N,N'*,*N''*,*O*}nickel^(II) **186** (0.400 g, 0.582 mmol) and 8-hydroxyquinoline (253 g, 1.746 mmol) to give the product as a white powder. (Yield 99 mg, 69 %); m.p.: 117-119 °C; 1H -NMR (500 MHz, D_2O) δ 7.64 (2H, d, $^3J_{HH}$ = 7.5 Hz, ArH), 7.36 (2H, d, $^3J_{HH}$ = 7.4 Hz, ArH), 3.27 (1H, d, $^2J_{HH}$ = 7.4 Hz, CHH -ArH), 3.00 (1H, d, $^2J_{HH}$ = 13.7 Hz, CHH -ArH), 1.48 (3H, s, CH_3); ^{13}C NMR (100 MHz, D_2O) δ ppm 176.3 (O=C=O), 138.8 (Ar-C), 130.5 (Ar-2CH), 130.2 (q, $^2J_{CF}$ = 32.6 Hz, Ar-C- CF_3), 125.6 (Ar-2CH), 123.9 (q, $^1J_{CF}$ = 272.2 Hz, CF_3), 61.8 (α -C), 42.7 (Ar- CH_2), 22.6 (CH_3); ^{19}F NMR (376 MHz, $DMSO-d_6$) δ -62.4 (s), HRMS-ESI (calcd for $C_{11}H_{11}NF_3$ $[M-COOH]^+$) 202.0844, found 202.0837 (Δ = 0.4 ppm), (calcd for $C_{11}H_{13}NO_2F_3$ $[M+H]^+$) 248.0898, found 248.0900 (Δ = 0.8 ppm).

6.6.11 Synthesis of 2-amino-3-(4-fluorophenyl)-3-hydroxypropanoic acid **206**



The general procedure (**H**) was followed using (*S*)-({2-[1-(2-fluorobenzyl)benzyl]pyrrolidine-2-carboxamide}phenyl)phenyl methylene)-(*S*)-4-fluorobenzenyl-glycinato-*N,N'*,*N''*,*O*}nickel^(III) **198** (500 mg, 0.781 mmol) and 8-hydroxyquinoline (466 mg, 2.343 mmol) to give the product as a white powder. (Yield 107 mg, 69 %); m.p.: 132-134 °C; ¹H NMR (400 MHz, DMSO-*d*₆) δ 8.15-8.56 (2H, br s, NH₂), 7.45 (1H, dd, ³*J*_{HH} = 8.1, ⁴*J*_{HH} = 5.8 Hz, ArH), 7.22 (2H, t, ³*J*_{HH} = 8.8 Hz, ArH), 6.00 (1H, s, C-OH), 3.98 (1H, d, ³*J*_{HH} = 4.5 Hz, CH), 2.04 (1H, d, ³*J*_{HH} = 4.7 Hz, α-CH); ¹³C NMR (100 MHz, DMSO-*d*₆) δ ppm 168.4 (O-C=O), 161.7 (d, ¹*J*_{CF} = 242.9 Hz, Ar-C), 136.1 (Ar-C), 128.6 (d, ³*J*_{CF} = 8.0 Hz, Ar-2CH), 114.9 (d, ²*J*_{CF} = 22.4 Hz, Ar-2CH), 70.1 (CH), 58.6 (α-C); ¹⁹F NMR (376 MHz, CDCl₃) δ -114.9 (s), HRMS-ESI (calcd for C₉H₁₁NO₃F [M+H]⁺) 200.0723, found 200.0732 (Δ = 4.5 ppm).

6.6.12 Synthesis of (*S*)-2-(((9H-fluoren-9-yl)methoxy)carbonyl)amino)-3-(4-(trifluoromethyl)phenyl) propanoic acid **207**



The general procedure (**I**) was followed using (*S*)-2-amino-3-(4-(trifluoromethyl)phenyl)propanoic acid **204** (0.255 g, 1.094 mmol) and sodium carbonate (0.302 g, 2.187 mmol) and 9-fluorenyl-methyl-*N*-succinimidyl carbonate (0.553 g, 1.640 mmol). To give the product as a white powder. (Yield 0.232 g, 46 %). ¹H NMR (400 MHz, CDCl₃): δ 7.83-7.91 (2H, m, ArH), 7.60-7.69 (2H, m, ArH), 7.24-7.49 (8H, m, ArH), 4.15-4.29 (3H, m, CH₂-O, α-CH), 43.18-3.22 (1H, m, CH-CH₂-O), 2.05 (2H, m, CH₂). ¹³C NMR (100 MHz, METHANOL-*d*₄): δ 172.7 (COOH), 156.0 (CONH), 145.8 (fluorenyl (Ar-Cq), 143.8 (Ar-C), 140.7 (fluorenyl (Ar-Cq), 129.9 (Ar-C), 127.6 (Ar-2C), 127.0 (Ar-C), 125.1 (Ar-C), 124.9 (Ar-C), 120.0 (Ar-2C), 65.3 (CH₂-O), 54.5 (α-CH), 46.7 (CH-CH₂-O), 36.44 (CH₂), ¹⁹F NMR (376 MHz, 62.22 DMSO-*d*₆) δ -60.8 (s), HRMS-ESI (calcd for C₂₄H₂₆NO₄ [M+H]⁺) 392.1862, found 392.1872 (Δ = 2.5 ppm).

6.7 Experimental for Chapter 5

6.7.1 Peptide syntheses

The peptides were synthesized using a solid-phase peptide synthesizer on an automated, microwave-assisted Biotage synthesizer. Rink Amide MBHA resin (substitution: 0.1 mmol/g) was used for all peptide syntheses. The Biotage synthesizer, manual mechanical shaking at RT and a microwave were used to synthesise the peptides.

6.7.2 General procedure

The general procedures for peptide synthesis can be divided into two types:

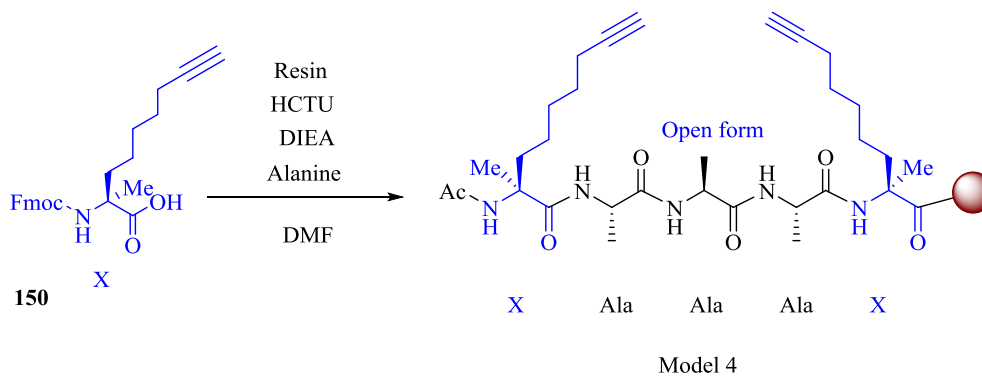
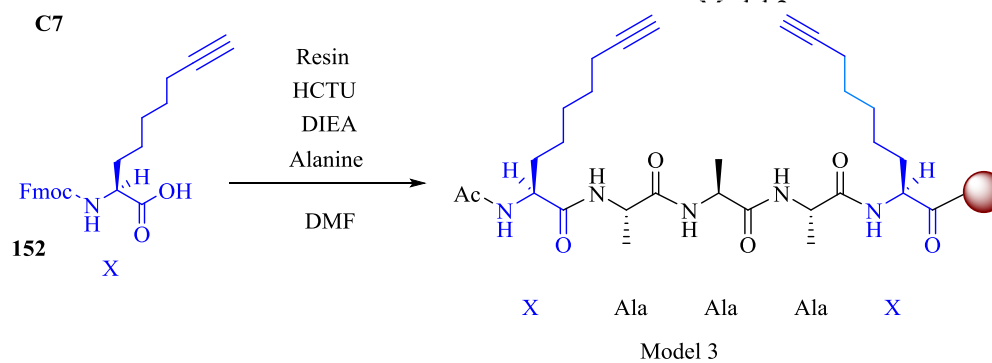
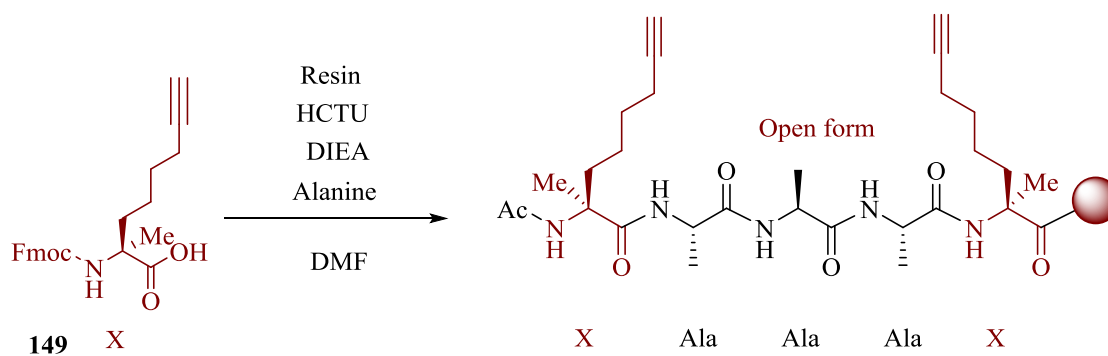
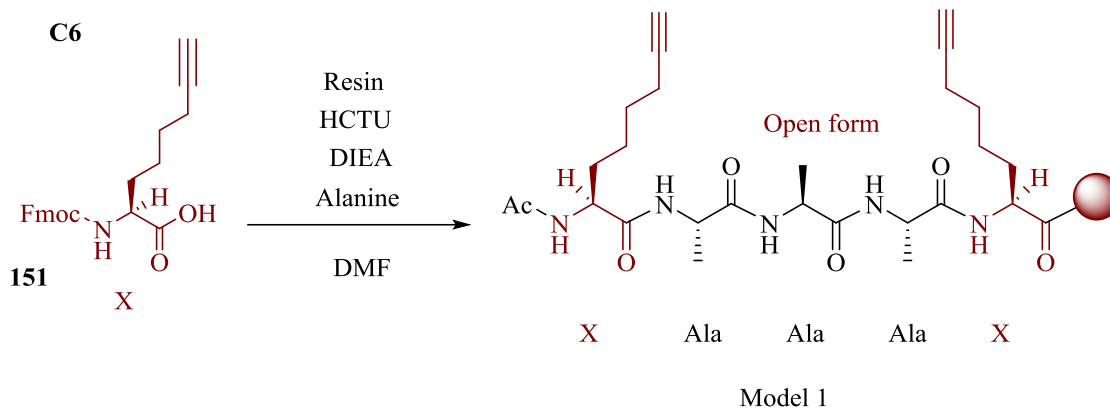
6.7.2.1 Automated peptide synthesis:

Four equivalents of Fmoc-amino acids dissolved in DMF (dry) to make a solution (0.2 M) related to the resin equivalent (Rink Amide MBHA resin). The amino acids and all the chemicals required were measured relative to a 0.1 mmol scale of the resin. Four equivalents of HCTU 0.5 M in DMF was used as an amino acid activator. In addition, eight equivalents of the activator base solution were made up to 2 M (DIPEA in NMP). The protected amino acid starting materials were also made up to four equivalents in DMF. The second step, after each coupling reaction, was the decoupling. A solution of piperidine was made up by dissolving the piperidine in DMF (dry) (20 % v/v) with Oxyma Pure (0.1M). Double coupling of Fmoc-Arg(Pbf)-OH was carried out using double the amount at the same concentration.

All the coupling reaction programmes were performed at 75 °C for 5 min, followed by the deprotection step at 75 °C for 3 min. Acetic anhydride (5 M) was made up in DMF to protect the last amine group in the last amino acid after preparing all the solutions in a 10 mL vessel. All relevant parameters were programmed into the Biotage; for instance, the sequences, concentration and the kind of resin used to synthesize the peptide. The peptides were analysed via LC-MS and HPLC, and purified via HPLC semi-prep.

6.7.2.2 General procedure for manual method in peptides synthesis

Peptide synthesis



6.7.2.3 Amino acid coupling:

6.7.2.3.1 Using shaker instrument:

Three equivalents of Fmoc-protected amino acid were dissolved in DMF (dry) to make a solution (0.2 M). Three equivalents of HCTU were dissolved in DMF (dry) (0.2 M), and double equivalents of DIPEA in NMP (0.4 M) were added to the solution. The solution was lifted to activate with gentle shaking for 5-10 min. The resin was prepared by lifting in DCM for 30 min then dried gently with a stream of nitrogen. The solution was poured into the prepared resin. The mixture was gently shaken for 15 min for each normal amino acid and 1 h for the unnatural amino acids. The resin was then dried under a stream of nitrogen and washed sequentially with DMF, MeOH and DCM (3 x 3 ml of each). The resin was gently dried under nitrogen. The resin was tested (negative) to the Kaiser Test to see the same unchanged yellow colour for a protected NH_2 group of the peptide-resin. The peptides previously analysed with LCMC were subjected to the cleavage test using 5 mg of the peptide-resin dissolved in acetonitrile: water (1:1) (1-2 mL) to verify the conversion ratio of the product.

6.7.2.3.2 Under Microwave conditions:

The resin was transferred to the microwave tube. Three equivalents of natural Fmoc-protected amino acid or two equivalents of unnatural Fmoc-protected amino acid were made up to 0.2 M in DMF (dry). Two equivalents of HCTU were dissolved in DMF (dry) (0.2 M), and four equivalents of DIPEA dissolved in NMP were added to the solution. The solution was lifted to activate for 5-10 min. The resin was added to the reaction mixture. In the microwave, all the Fmoc-protected amino acids were coupled at 70 °C for 5 min. also, the same conditions used in the Fmoc-deprotection by used piperidine in dry DMF (20 % v/v) after each coupling step. After each protection and deprotection, the Kaiser Test was performed as an indicator of free NH_2 groups.

6.7.2.3.3 Fmoc-deprotection:

A solution of piperidine in dry DMF (20 % v/v) was added to the resin, then shaken for 15-20 min, followed by sequential washing with DMF, MeOH and DCM (3 x 3 mL of each). The resin was gently dried under nitrogen. The resin was tested using the Kaiser Test, where a blue colour (positive) for deprotected NH_2 group on the peptide-resin was observed.

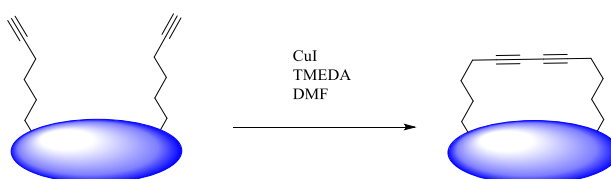
6.7.2.3.4 Protect NH₂ group of the peptide-resin (acetyl capping).

The last amino acid in the peptide resin was protected (-NH₂) with three equivalents of acetic anhydride in the peptide-resin, then shaken for 30-60 min, followed by sequential washing with DMF, MeOH and DCM (3 x 3 mL of each). The resin was gently dried under nitrogen and stored in a vacuum desiccator. The resin was tested using the Kaiser Test, with the same unchanged yellow colour (negative) for protected NH₂ groups on the peptide-resin.

6.7.2.3.5 Cleavage test:

The final step in the peptide synthesis was the cleavage test. Dry peptide resin (5-10 mg) was placed in small peptide synthesis vial. 2-3 mL TFA/TES/water (95:2.5:2.5) were added and the mixture shaken for 1-1.5 h, or 3 h if the peptide contained Arg. The filtrate was gently dried under nitrogen to mechanically remove the TFA. The dried sample was diluted with 1-1.5 ml acetonitrile:water (1:1) and sonicated for 10-15 min in order to fully dissolve the solid and allow analysis via LC-MS in order to find the conversion ratio and purity of the product. The same procedure was performed on a larger scale (Peptide Cleavage from resin) by increasing the amount of TFA in the solution. The peptide was washed with cold diethyl ether and precipitated by centrifugation. This washing method was repeated in triplicate. The peptide was dried in a freeze dryer for 24 h and then stored in the freezer.

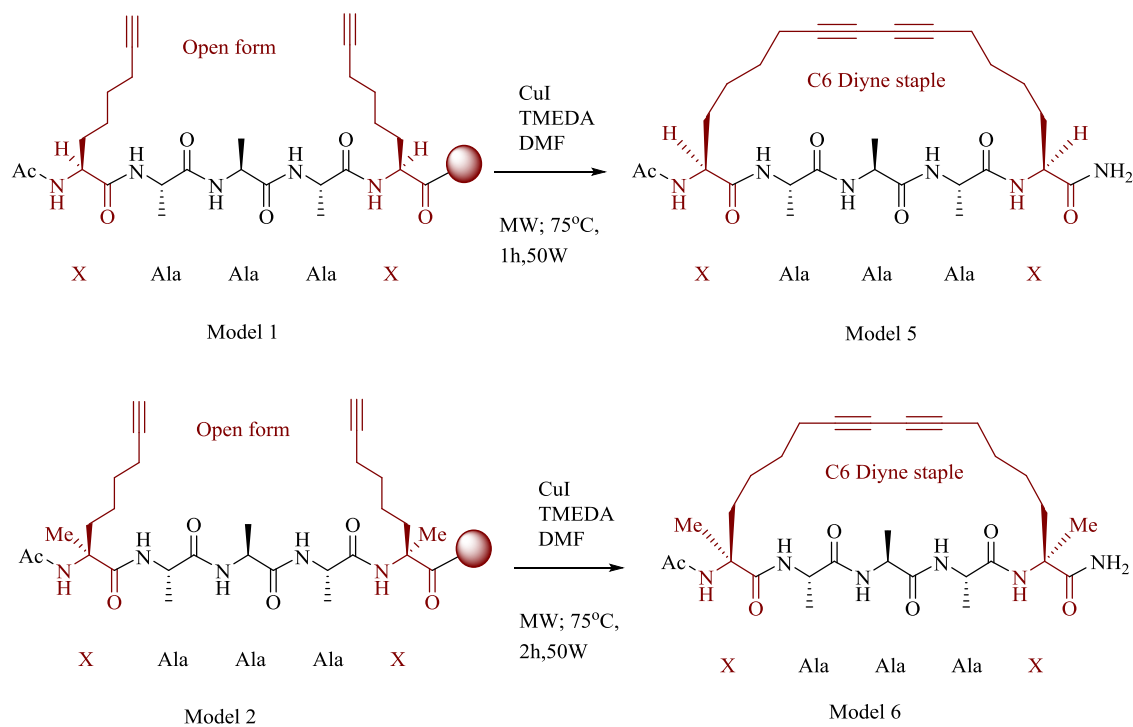
6.7.3 Glaser-Hay Coupling ring closing metathesis:



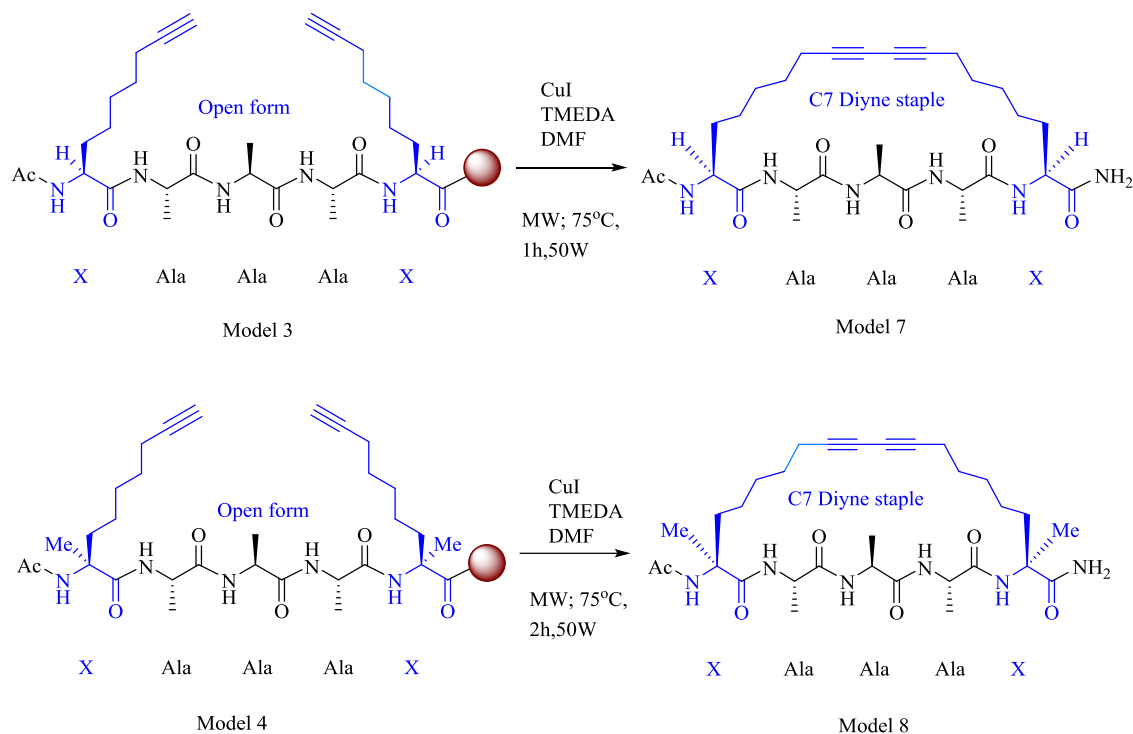
One equivalent of the dry peptide-resin was placed in DMF (dry) for 20-30 min to swell, followed by sequential washing in DMF, MeOH and DCM (3 x 3 ml of each). The peptide-resin was then gently dried under nitrogen. Copper iodide (20 eq.) and TMEDA (42 eq.) were added, followed by 4-5 ml DMF (dry) and the mixture shaken for 5 min. It was heated via microwave for 1 h for the glycine-derivative-peptide and 2 h for the alanine-derivative-peptide at 75 °C and power 50 W. The ring closure was monitored via

LC-MS until complete conversion was observed. The reaction mixture was transferred to a peptide synthesis vial, followed by sequential washing with DMF, MeOH and DCM (3 x 3 mL of each). The resin was gently dried under nitrogen and stored in a desiccator at low pressure.

C6 ring closing



C7 ring closing

**6.7.4 Peptide purification:**

HPLC (reverse-phase) was used to purify the crude peptides. Both analytical results (HPLC analytical and LC-MS) were compared to find the best ratio for use in the semi-prep HPLC. The sample was dissolved in a mixture of less than 2 ml of water:acetonitrile (1:1). The solution was sonicated until it became clear. The solvents used in the purification were water (1 % TFA) and acetonitrile (1 % TFA). LC-MS was used to analyse the fractions, including the pure peptide, which were then combined and dried in the freeze dryer for 24-48 h. The purity was analysed via LC-MS and analytical HPLC. The mass was measured relative to the UV extinction coefficient for the samples with UV active groups (aromatic). The pure product was stored in the fridge.

6.7.5 Circular Dichroism

Circular dichroism was used to study the geometric structure of the secondary peptides and protein folding. Spectra were recorded using a Chirascan TM-plus circular dichroism spectrometer (Applied Photophysics) with a 10 mm path length. The concentration of the peptide was 50 μ M at 20 °C. The sample was dissolved in a solution (1 mL) of deionised water and TFE (9:1 v/v) to get the best confirmation. Three spectra were recorded for each peptide was measured triple from 185-260 nm and the time per point was 0.25 s.

The peptides spectra show a geometrical shape at 222 nm for the alpha-helical. The four type of peptides were compared to select the best of the peptides modules related to the CD results.

6.8 Synthesis of peptides modules (1-8)

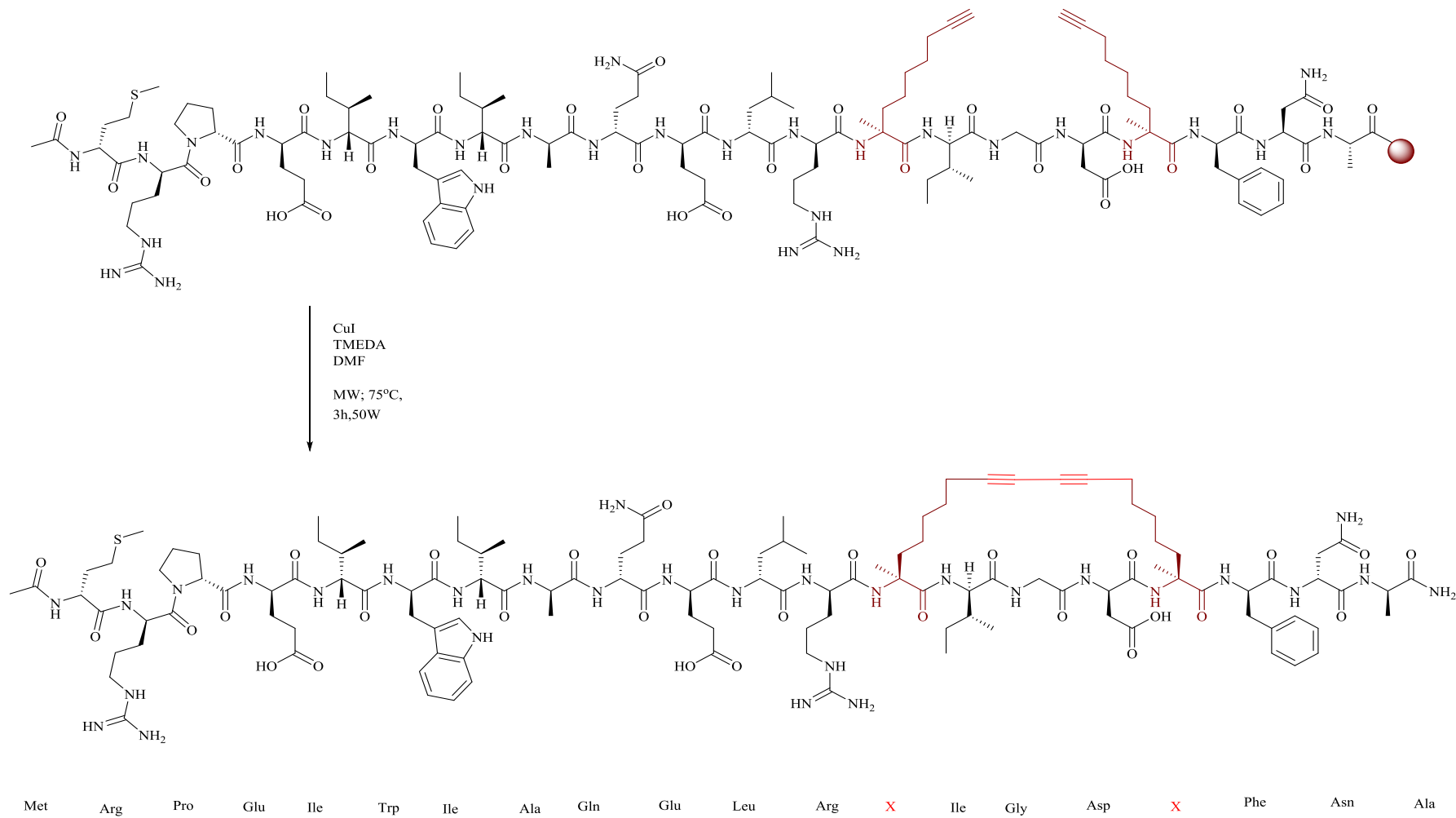
The peptide was synthesised on Rink amide MBHA resin (0.49 mmol/ g) using SPPS manual and microwave–assistance on 0.1 mmol scales. Manual microwaving was used to ensure ring closure (2 h for glycine derivatives and 3 h for alanine derivatives). The peptide ring closure was monitored via LC-MS for the converted product. All peptides were purified with semi-prep HPLC and analysed via analytical HPLC (UV 214 nm) and LC-MS. See the table below for peptide module characterisatio

Table1: peptides Characterization and Purification. Purified with semi-prep HPLC after analyse with HPLC analytical and LC-MS, using the flowing gradient: ^a5-100 % MeCN/H₂O with (0.1 % TFA), 30 min gradient, ^a5-60 % MeCN/H₂O with (0.1 % TFA), 30 min gradient,

Peptide		Formula weight	Calculated MW (Da)	Found MW (Da)	Δ MW (ppm)	t _R (min)	Purity (%)	Yield (%)
Model 1 C6(H) 151	Ring open	C ₂₇ H ₄₃ N ₆ O ₆	547.3244	547.3257	2.4	18.837	99	15
Model 2 C6(Me) 149		C ₂₉ H ₄₆ N ₆ O ₆ Na	597.3377	597.3392	2.5	20.883	99	23
Model 3 C7(H) 152		C ₂₉ H ₄₇ N ₆ O ₆	575.3557	575.3567	1.7	20.810 ^a	98	12
Model 4 C7(Me) 150		C ₃₁ H ₅₀ N ₆ O ₆ Na	625.3690	625.3724	5.4	22.953 ^a	96	9
Model 5 C6(H)	Diyne staple	C ₂₇ H ₄₀ N ₆ O ₆	567.2907	567.2922	2.6	64.134 ^b	99	21
Model 6 C6(Me)		C ₂₉ H ₄₅ N ₆ O ₆	573.3401	573.3409	1.4	20.883 ^a	99	27
Model 7 C7(H)		C ₂₉ H ₄₅ N ₆ O ₆	573.3401	573.3403	0.3	36.210 ^a	98	22
Model 8 C7(Me)		C ₃₁ H ₄₈ N ₆ O ₆ Na	623.3533	623.3552	3.0	21.063 ^a	99	13

Synthesis a modification of BIM peptide and purification.

BIM peptide



6.8.1 Synthesis a modification of BIM peptide and purification.

The peptide was synthesis on Rink amide MBHA resin (1.05 mmol/g, molecular weight: 2488.1 g/mol) using SPPS method and using biotage microwave synthesis (automatic system). The solution of amino acids were peppered with 4 equivalent to make a solutions with (0.2) in DMF. Also, a solution of DIEA (8 eq.) (2M) in NMP, 0.5 equivalents of HCTU in DMF, Acetic anhydride (5M) in DMF and 20 % of piperidine in DMF. One third of the peptide was cleaved from the rink resin using a mixture of TFA/TES/H₂O solution by shacked it hardly for 3h. The TFA was removed with stem of nitrogen to give 42 % as a crud peptide. The crude peptide was analyzed with analytical HPLC and the LC-MS. The peptide was purified with semi-prip HPLC (UV 214 nm) using the flowing gradient: 45-65 % MeCN:H₂O with (0.1 % TFA), 60 min gradient to give the open ring BIM peptide derivative as a white solid (fluffy). HRMS-ESI (calcd for C₁₁₉H₁₈₄N₃₀O₂₉S [M+2H]⁺) 1266.1876, found 1266.1808 (Δ = 5.3 ppm), (calcd [M+3H]⁺) 844.4610, found 844.4542 (Δ = 8.0 ppm); Rt (26.562 min).

6.8.2 BIM stapled helix pepide

BIM peptide-resin (299.0 mg, 54.862 μ mol, 1 eq.) was reacted was transferred to microwave vessel. Cupper iodide (208 mg, 1097.2 μ mol, 20 eq.) and TMEDA (344.82 μ L, 2304.22 μ mol, (42 eq.) in DMF (3mL). The reaction mixture was reacted in microwave for 3h at 75 °C. The reaction was monitored with LC-MS. The peptide was cleaved from the rink resin using a mixture of TFA/TES/H₂O solution by shacked it hardly for 3h. The crude peptide was analyzed with analytical HPLC and the LC-MS. The peptide was purified with semi-prip HPLC (UV 214 nm) using the flowing gradient: 50-80 % MeCN: H₂O with (0.1 % TFA), 60 min gradient to give stapled helix pepide BIM peptide derivative as a white solid (fluffy),the TFA was removed by dissolve the peptide with HCl (10 %) and dried it in freeze dryer. This step was repeat for three times. HRMS-ESI (calcd for C₁₁₉H₁₈₄N₃₀O₂₉S [M+2H]⁺) 1265.1798, found 1265.1677 (Δ = 9.5 ppm), (calcd [M+H]⁺) 2529.3518, found 2529.3538 (Δ = -7.9 ppm); MALDI found 2528.4924; Rt (16.190 min). The real mass was calculated using the UV-Vis related to the extinction coefficient to the tryptophan amino acid in the BIM peptide.

BIM-104 RC						UV		
Wavelength (nm)	Absorbance	Extinction coeff	[Sample]	Bim stapled	MW	Moles in sample	moles in stock	Mass (g)
280	0.25156	5560	4.52446E-05	0.00135734	2529.01	2.71468E-08	1.35734E-06	0.003432722
280	0.25082	5560	4.51115E-05	0.00135335	2529.01	2.70669E-08	1.35335E-06	0.003422624
280	0.26042	5560	4.68381E-05	0.00140514	2529.01	2.81029E-08	1.40514E-06	0.003553623
	0.25426667	5560	4.57314E-05	0.00137194	2529.01	2.74388E-08	1.37194E-06	0.003469656
								0.003469656
				(C2*30*2529.01)/5560				

BIM_104_RO_1						UV		
Wavelength (nm)	Absorbance	Extinction coeff	[Sample]	Bim non-stapled	MW	Moles in sample	moles in stock	Mass (g)
280	0.15283	5560	2.74874E-05	0.00082462	2531.02	1.64924E-08	8.24622E-07	0.002087136
280	0.1535	5560	2.76079E-05	0.00082824	2531.02	1.65647E-08	8.28237E-07	0.002096285
280	0.15232	5560	2.73957E-05	0.00082187	2531.02	1.64374E-08	8.21871E-07	0.002080171
	0.15288333	5560	2.7497E-05	0.00082491	2531.02	1.64982E-08	8.2491E-07	0.002087864
								0.002087864
				(C2*30*2531.02)/5560				

Dissolve in 1
mL

take 20 µL + 580 µL (1:1 water: acetonitrile) = 600 µL

1:1 water: acetonitrile

References

1. C. J. Braun and M. T. Hemann, *Expert Review of Anticancer Therapy*, 2016, **16**, 977-987.
2. T. Sato, K. Izawa, J. L. Aceña, H. Liu and V. A. Soloshonok, *Eur. J. Org. Chem.*, 2016, 2757-2774.
3. V. A. Soloshonok, C. Cai and V. J. Hruby, *Tetrahedron: Asymmetry*, 1999, **10**, 4265-4269.
4. J. E. McMurry, *Organic Chemistry; Seventh Edition*, Cengage Learning, 2007.
5. N. Errington and A. J. Doig, *Biochemistry*, 2005, **44**, 7553-7558.
6. V. Azzarito, K. Long, N. S. Murphy and A. J. Wilson, *Nat. Chem.*, 2013, **5**, 161- 173.
7. H. D. Herce, W. Deng, J. Helma, H. Leonhardt and M. C. Cardoso, *Nat. Commun.*, 2013, **4**.
8. L. Su and W. Xu, *Science in China Series B: Chemistry*, 2009, **52**, 535-548.
9. M. D. Boersma, H. S. Haase, K. J. Peterson-Kaufman, E. F. Lee, O. B. Clarke, P. M. Colman, B. J. Smith, W. S. Horne, W. D. Fairlie and S. H. Gellman, *J. Am. Chem. Soc.*, 2012, **134**, 315-323.
10. A. Patgiri, A. L. Jochim and P. S. Arora, *Acc. Chem. Res.*, 2008, **41**, 1289-1300.
11. M. E. Karpen, P. L. De Haseth and K. E. Neet, *Protein Sci.*, 1992, **1**, 1333-1342.
12. D. J. Barlow and J. M. Thornton, *J. Mol. Biol.*, 1988, **201**, 601-619.
13. S. Y. Shim, Y.-W. Kim and G. L. Verdine, *Chem. Biol. Drug Des.*, 2013, **82**, 635-642.
14. C. A. Rohl and A. J. Doig, *Protein Sci.*, 1996, **5**, 1687-1696.
15. A. L. Jochim and P. S. Arora, *ACS Chem. Biol.*, 2010, **5**, 919-923.
16. A. G. Jamieson, N. Boutard, D. Sabatino and W. D. Lubell, *Chem. Biol. Drug Des.*, 2013, **81**, 148-165.
17. J. M. Scholtz, H. Qian, V. H. Robbins and R. L. Baldwin, *Biochem.*, 1993, **32**, 9668-9676.
18. J. S. Albert and A. D. Hamilton, *Biochem.*, 1995, **34**, 984-990.
19. R. N. Chapman, G. Dimartino and P. S. Arora, *J. Am. Chem. Soc.*, 2004, **126**, 12252-12253.
20. J. C. Phelan, N. J. Skelton, A. C. Braisted and R. S. McDowell, *J. Am. Chem. Soc.*, 1997, **119**, 455-460.

21. S. Kneissl, E. J. Loveridge, C. Williams, M. P. Crump and R. K. Allemann, *Chem. BioChem.*, 2008, **9**, 3046-3054.
22. D. Y. Jackson, D. S. King, J. Chmielewski, S. Singh and P. G. Schultz, *J. Am. Chem. Soc.*, 1991, **113**, 9391-9392.
23. F. Ruan, Y. Chen and P. B. Hopkins, *J. Am. Chem. Soc.*, 1990, **112**, 9403-9404.
24. M. R. Ghadiri and A. K. Fernholz, *J. Am. Chem. Soc.*, 1990, **112**, 9633-9635.
25. J. P. Schneider, J. D. Lear and W. F. DeGrado, *J. Am. Chem. Soc.*, 1997, **119**, 5742-5743.
26. R. P. Cheng, S. H. Gellman and W. F. DeGrado, *Chem. Rev.* 2001, **101**, 3219-3232.
27. A. D. Bautista, C. J. Craig, E. A. Harker and A. Schepartz, *Curr. Opin. Chem. Biol.*, 2007, **11**, 685-692.
28. J. Garner and M. M. Harding, *Org. Biomol. Chem.*, 2007, **5**, 3577-3585.
29. C. M. Goodman, S. Choi, S. Shandler and W. F. DeGrado, *Nat. Chem. Biol.*, 2007, **3**.
30. D. Wang, K. Chen, J. L. Kulp and P. S. Arora, *J. Am. Chem. Soc.*, 2006, **128**, 9248-9256.
31. D. Wang, K. Chen, G. Dimartino and P. S. Arora, *Org. Biomol. Chem.* 2006, **4**, 4074-4081.
32. J. Yang, K. Zhao, Y. Gong, A. Vologodskii and N. R. Kallenbach, *J. Am. Chem. Soc.*, 1998, **120**, 10646-10652.
33. M. Siedlecka, G. Goch, A. Ejchart, H. Sticht and A. Bierzyński, *Proc. Natl. Acad. Sci. U. S. A.*, 1999, **96**, 903-908.
34. L. Serrano, M. Bycroft and A. R. Fersht, *J. Mol. Biol.*, 1991, **218**, 465-475.
35. C. A. Hunter, J. Singh and J. M. Thornton, *J. Mol. Biol.*, 1991, **218**, 837-846.
36. V. M. K. Anjana R. , Sherlin D., Kumar S. P., Naveen K., Kanth P. S. and Sekar K., *Bioinformation*, 2012, **8**, 1220-1224.
37. C. D. Tatko and M. L. Waters, *J. Am. Chem. Soc.*, 2004, **126**, 2028-2034.
38. S. Kumar and R. Nussinov, *ChemBioChem*, 2002, **3**, 604-617.
39. S. Marqusee and R. L. Baldwin, *Proc. Natl. Acad. Sci.*, 1987, **84**, 8898-8902.
40. L. Adamian and J. Liang, *J. Mol. Biol.*, 2001, **311**, 891-907.
41. T. H. Walther and A. S. Ulrich, *Curr. Opin. Struct. Biol.*, 2014, **27**, 63-68.
42. B. Ibarra-Molero, J. A. Zitzewitz and C. R. Matthews, *J. Mol. Biol.*, 2004, **336**, 989-996.
43. D. S. Horne, *Curr. Opin. Colloid Interface Sci.*, 2017, **28**, 74-86.
44. H. H. Kuo, C. Chan, L. L. Burrows and C. M. Deber, *Chem. Biol. Drug Des.*, 2007, **69**, 405-412.
45. S. Marqusee and R. L. Baldwin, *Proc. Natl. Acad. Sci.*, 1987, **84**, 8898-8902.
46. T. Lalonde, T. G. Shepherd, S. Dhanvantari and L. G. Luyt, *Peptide Science*, 24055.

47. Y. Zhu, J. Han, J. Wang, N. Shibata, M. Sodeoka, V. A. Soloshonok, J. A. S. Coelho and F. D. Toste, *Chem. Rev.*, 2018, **118**, 3887-3964.
48. B. Aillard, N. S. Robertson, A. R. Baldwin, S. Robins and A. G. Jamieson, *Org. Biomol. Chem.*, 2014, **12**, 8775-8782.
49. T. N. Grossmann, J. T.-H. Yeh, B. R. Bowman, Q. Chu, R. E. Moellering and G. L. Verdine, *Proc. Natl. Acad. Sci.*, 2012, **109**, 17942-17947.
50. Y. N. Belokon, A. G. Bulychev, S. V. Vitt, Y. T. Struchkov, A. S. Batsanov, T. V. Timofeeva, V. A. Tsiryapkin, M. G. Ryzhov and L. A. Lysova, *J. Am. Chem. Soc.*, 1985, **107**, 4252-4259.
51. L. D. Walensky, A. L. Kung, I. Escher, T. J. Malia, S. Barbutto, R. D. Wright, G. Wagner, G. L. Verdine and S. J. Korsmeyer, *Science*, 2004, **305**, 1466-1470.
52. F. Bernal, A. F. Tyler, S. J. Korsmeyer, L. D. Walensky and G. L. Verdine, *J. Am. Chem. Soc.*, 2007, **129**, 2456-2457.
53. Y.-W. Kim, P. S. Kutchukian and G. L. Verdine, *Org. Lett.*, 2010, **12**, 3046-3049.
54. G. L. Verdine and G. J. Hilinski, *Drug Discovery Today: Technologies*, 2012, **9**, e41-e47.
55. S. J. Miller and R. H. Grubbs, *J. Am. Chem. Soc.*, 1995, **117**, 5855-5856.
56. C. W. Lee and R. H. Grubbs, *Org. Lett.*, 2000, **2**, 2145-2147.
57. J. L. LaBelle, S. G. Katz, G. H. Bird, E. Gavathiotis, M. L. Stewart, C. Lawrence, J. K. Fisher, M. Godes, K. Pitter, A. L. Kung and L. D. Walensky, *J. Clin. Invest.*, 2012, **122**, 2018-2031.
58. Ø. Jacobsen, J. Klaveness and P. Rongved, *Molecules*, 2010, **15**, 6638-6677.
59. T. Okamoto, K. Zobel, A. Fedorova, C. Quan, H. Yang, W. J. Fairbrother, D. C. S. Huang, B. J. Smith, K. Deshayes and P. E. Czabotar, *ACS Chem. Biol.*, 2013, **8**, 297-302.
60. F. Barragán, V. Moreno and V. Marchán, *Chem. Commun.*, 2009, 4705-4707.
61. Y. E. Bergman, M. P. Del Borgo, R. D. Gopalan, S. Jalal, S. E. Unabia, M. Ciampini, D. J. Clayton, J. M. Fletcher, R. J. Mulder and J. A. Wilce, *Org. Lett.*, 2009, **11**, 4438-4440.
62. R. N. Chapman and P. S. Arora, *Org. Lett.*, 2006, **8**, 5825-5828.
63. C. E. Schafmeister, J. Po and G. L. Verdine, *J. Am. Chem. Soc.* 2000, **122**, 5891-5892.
64. E. N. G. Marsh, in *Methods Enzymol.*, ed. L. P. Vincent, Academic Press, Second Edition, 2016, vol. Volume 580, pp. 251-278.
65. P. Shah and A. D. Westwell, *J. Enzyme Inhib. Med. Chem.*, 2007, **22**, 527-540.
66. H. J. Son, W. Wang, T. Xu, Y. Liang, Y. Wu, G. Li and L. Yu, *J. Am. Chem. Soc.*, 2011, **133**, 1885-1894.

67. A. C. Stuart, J. R. Tumbleston, H. Zhou, W. Li, S. Liu, H. Ade and W. You, *J. Am. Chem. Soc.*, 2013, **135**, 1806-1815.
68. R. Smits, C. D. Cadicamo, K. Burger and B. Kokschi, *Chem. Soc. Rev.*, 2008, **37**, 1727-1739.
69. X. L. Qiu and F. L. Qing, *Eur. J. Org. Chem.*, 2011, 3261-3278.
70. K. Mikami, S. Fustero, M. Sánchez-Roselló, J. L. Aceña, V. Soloshonok and A. Sorochinsky, *Synthesis*, 2011, 3045-3079.
71. J. L. Aceña, A. E. Sorochinsky and V. A. Soloshonok, *Synthesis*, 2012, **44**, 1591-1602.
72. M. Salwiczek, E. K. Nyakatura, U. I. Gerling, S. Ye and B. Kokschi, *Chem. Soc. Rev.*, 2012, **41**, 2135-2171.
73. E. N. G. Marsh, *Acc. Chem. Res.*, 2014, **47**, 2878-2886.
74. C. Jäckel and B. Kokschi, *Eur. J. Org. Chem.*, 2005, **2005**, 4483-4503.
75. N. C. Yoder and K. Kumar, *Chem. Soc. Rev.*, 2002, **31**, 335-341.
76. Y. Zhou, J. Wang, Z. Gu, S. Wang, W. Zhu, J. L. Aceña, V. A. Soloshonok, K. Izawa and H. Liu, *Chem. Rev.*, 2016, **116**, 422-518.
77. I. Ojima, *Fluorine in Medicinal Chemistry and Chemical Biology*, John Wiley & Sons, 2009.
78. Y. Suzuki, B. C. Buer, H. M. Al-Hashimi and E. N. G. Marsh, *Biochemistry*, 2011, **50**, 5979-5987.
79. A. Sutherland and C. L. Willis, *Nat. Prod. Rep.*, 2000, **17**, 621-631.
80. X.-L. Qiu, W.-D. Meng and F.-L. Qing, *Tetrahedron Lett.*, 2004, **60**, 6711-6745.
81. R. FILLER and H. NOVAR, *J. Org. Chem.* 1960, **25**, 733-736.
82. M. A. Danielson and J. J. Falke, *Annu. Rev. Biophys. Biomol. Struct.*, 1996, **25**, 163-195.
83. J. Xiao, B. Weisblum and P. Wipf, *J. Am. Chem. Soc.*, 2005, **127**, 5742-5743.
84. T. Tsushima, K. Kawada, S. Ishihara, N. Uchida, O. Shiratori, J. Higaki and M. Hirata, *Tetrahedron Lett.*, 1988, **44**, 5375-5387.
85. M. Raasch, *J. Org. Chem.*, 1958, **23**, 1567-1568.
86. R. Dannley and R. Taborsky, *J. Org. Chem.*, 1957, **22**, 1275-1276.
87. N. Muller, *J. fluorine Chem.*, 1987, **36**, 163-170.
88. G. Kreil, *Ann. Rev. Biochem.*, 1997, **66**, 337-345.
89. T. K. Ellis, H. Ueki, T. Yamada, Y. Ohfuné and V. A. Soloshonok, *J. Org. Chem.*, 2006, **71**, 8572-8578.
90. A. E. Sorochinsky, H. Ueki, J. L. Aceña, T. K. Ellis, H. Moriwaki, T. Sato and V. A. Soloshonok, *Org. Biomol. Chem.*, 2013, **11**, 4503-4507.

91. R. E. Gawley, *J. Org. Chem.*, 2006, **71**, 2411-2416.
92. A. E. Sorochinsky, J. L. Aceña, H. Moriwaki, T. Sato and V. A. Soloshonok, *Amino Acids*, 2013, **45**, 691-718.
93. A. E. Sorochinsky, J. L. Aceña, H. Moriwaki, T. Sato and V. Soloshonok, *Amino Acids*, 2013, **45**, 1017-1033.
94. A. S. Saghiyan, S. A. Dadayan, S. G. Petrosyan, L. L. Manasyan, A. V. Geolchanyan, S. M. Djamgaryan, S. A. Andreasyan, V. I. Maleev and V. N. Khrustalev, *Tetrahedron: Asymmetry*, 2006, **17**, 455-467.
95. A. S. Saghiyan, A. S. Dadayan, S. A. Dadayan, A. F. Mkrtchyan, A. V. Geolchanyan, L. L. Manasyan, H. R. Ajvazyan, V. N. Khrustalev, H. H. Hambardzumyan and V. I. Maleev, *Tetrahedron: Asymmetry*, 2010, **21**, 2956-2965.
96. A. Le Chevalier Isaad, F. Barbetti, P. Rovero, A. M. D'Ursi, M. Chelli, M. Chorev and A. M. Papini, *Eur. J. Org. Chem.*, 2008, 5308-5314.
97. Y. N. Belokon, N. B. Bespalova, T. D. Churkina, I. Císařová, M. G. Ezernitskaya, S. R. Harutyunyan, R. Hrdina, H. B. Kagan, P. Kočovský, K. A. Kochetkov, O. V. Larionov, K. A. Lyssenko, M. North, M. Polášek, A. S. Peregudov, V. V. Prisyazhnyuk and Š. Vyskočil, *J. Am. Chem. Soc.*, 2003, **125**, 12860-12871.
98. V. A. Soloshonok and T. Ono, *J. Fluorine Chem.*, 2009, **130**, 547-549.
99. D. E. Patterson, S. Xie, L. A. Jones, M. H. Osterhout, C. G. Henry and T. D. Roper, *Org. Process Res. Dev.*, 2007, **11**, 624-627.
100. J. Li, S. Zhou, J. Wang, A. Kawashima, H. Moriwaki, V. A. Soloshonok and H. Liu, *Eur. J. Org. Chem.*, 2016, 999-1006.
101. F. Zhang, H. Sun, Z. Song, S. Zhou, X. Wen, Q.-L. Xu and H. Sun, *J. Org. Chem.*, 2015, **80**, 4459-4464.
102. A. Lauria, R. Delisi, F. Mingoia, A. Terenzi, A. Martorana, G. Barone and A. M. Almerico, *Eur. J. Org. Chem.*, 2014, 3289-3306.
103. S. B. Ferreira, A. C. Sodero, M. F. Cardoso, E. S. Lima, C. R. Kaiser, F. P. Silva Jr and V. F. Ferreira, *J. Med. Chem.*, 2010, **53**, 2364-2375.
104. B. Worrell, J. Malik and V. V. Fokin, *Science*, 2013, 1229506.
105. S. Mario, L. C. I. Alexandra, R. Paolo, P. A. Maria, C. Michael and D. U. A. Maria, *Eur. J. Org. Chem.*, 2010, 446-457.
106. C. Glaser, *Ann. Chem.*, 1870, **137**, 154.
107. C. Glaser, *Ber. Dtsch. Chem. Ges.*, 1869, **2**, 422-424.
108. K. Fujimoto, M. Kajino and M. Inouye, *Eur. J. Org. Chem.*, 2008, **14**, 857-863.

109. M. C. N. Brauer, R. A. W. Neves Filho, B. Westermann, R. Heinke and L. A. Wessjohann, *J. Org. Chem.*, 2015, **11**, 25-30.
110. S. Verlinden, N. Geudens, J. C. Martins, D. Tourwe, S. Ballet and G. Verniest, *Org. Biomol. Chem.*, 2015, **13**, 9398-9404.
111. N. Auburger, M. D. Pisa, M. Larregola, G. Chassaing, E. Peroni, S. Lavielle, A.-M. Papini, O. Lequin and J.-M. Mallet, *Bio. Med. Chem.*, 2014, **22**, 6924-6932.
112. R. B. Merrifield, *J. Am. Chem. Soc.*, 1963, **85**, 2149-2154.
113. G. L. Patrick, *An introduction to medicinal chemistry*, Oxford university press, 2013.
114. F. S. P. P. Synthesis, *An introduction to medicinal chemistry*, Oxford University Press Inc., New York, 2000.
115. S.-S. Wang, *J. Am. Chem. Soc.*, 1973, **95**, 1328-1333.
116. K. Barlos, D. Gatos, J. Kallitsis, G. Papaphotiu, P. Sotiriu, Y. Wenqing and W. Schäfer, *Tetrahedron Lett.*, 1989, **30**, 3943-3946.
117. K. Barlos, D. Gatos, S. Kapos, G. Papaphotiu, W. Schäfer and Y. Wenqing, *Tetrahedron Lett.*, 1989, **30**, 3947-3950.
118. J. M. Collins, M. J. Collins and a. R. C. Steorts, Novel method for enhanced solid phase peptide synthesis using microwave energy, 2003.
119. M. Larhed and K. Olofsson, *Microwave methods in organic synthesis*, Springer, 2006.
120. S. A. Kawamoto, A. Coleska, X. Ran, H. Yi, C. Yang and S. Wang, *J. Med. Chem.*, 2012, **55**, 1137-1146.
121. A. J. Wilson, *Chem. Soc. Rev.*, 2009, **38**, 3289-3300.
122. U. Schollkopf, *Tetrahedron Lett.*, 1983, **39**, 2085-2091.
123. K. Undheim, *Amino Acids*, 2008, **34**, 357-402.
124. Y. N. Belokon, I. Zel'tser, V. Bakhmutov, M. Saporovskaya, M. Ryzhov, A. Yanovskii, Y. T. Struchkov and V. Belikov, *J. Am. Chem. Soc.*, 1983, **105**, 2010-2017.
125. Y. N. Belokon, *Pure Appl. Chem.*, 1992, **64**, 1917-1924.
126. V. A. Soloshonok, C. Cai, T. Yamada, H. Ueki, Y. Ohfune and V. J. Hruby, *J. Am. Chem. Soc.*, 2005, **127**, 15296-15303.
127. V. A. Soloshonok, D. V. Avilov and V. P. Kukhar, *Tetrahedron: Asymmetry*, 1996, **7**, 1547-1550.
128. V. A. Soloshonok, D. V. Avilov, V. P. Kukhar, L. Van Meervelt and N. Mischenko, *Tetrahedron Lett.*, 1997, **38**, 4671-4674.
129. A. Popkov, V. Langer, P. A. Manorik and T. Weidlich, *Transition Met. chem.*, 2003, **28**, 475-481.

130. Y. N. Belokon, V. I. Tararov, V. I. Maleev, T. F. Savel'eva and M. G. Ryzhov, *Tetrahedron: Asymmetry*, 1998, **9**, 4249-4252.
131. H. Ueki, T. K. Ellis, C. H. Martin, T. U. Boettiger, S. B. Bolene and V. A. Soloshonok, *J. Org. Chem.*, 2003, **68**, 7104-7107.
132. B. B. De and N. R. Thomas, *Tetrahedron: Asymmetry*, 1997, **8**, 2687-2691.
133. A. Popkov, A. Gee, M. Nádvorník and A. Lyčka, *Transition Met. chem.*, 2002, **27**, 884-887.
134. Y. N. Belokon, V. I. Bakmutov, N. I. Chernoglazova, K. A. Kochetkov, S. V. Vitt, N. S. Garbalinskaya and V. M. Belikov, *J. Chem. Soc. Perkin Transactions 1*, 1988, 305-312.
135. G. Clayden and N. Greeves, *Organic Chemistry*, 2012, 542-543.
136. R. Chinchilla and C. Nájera, *Chem. Rev.*, 2007, **107**, 874-922.
137. S. Parpart, A. Petrosyan, S. J. Ali Shah, R. A. Adewale, P. Ehlers, T. Grigoryan, A. F. Mkrtchyan, Z. Z. Mardiyan, A. J. Karapetyan, A. H. Tsaturyan, A. S. Saghyian, J. Iqbal and P. Langer, *RSC Advances*, 2015, **5**, 107400-107412.
138. G. Sun, M. Wei, Z. Luo, Y. Liu, Z. Chen and Z. Wang, *Org. Process Res. Dev.*, 2016, **20**, 2074-2079.
139. J. Henrik and P. D. Sejer, *Eur. J. Org. Chem.*, 2012, 4267-4281.
140. H. T. ten Brink, D. T. S. Rijkers and R. M. J. Liskamp, *J. Org. Chem.*, 2006, **71**, 1817-1824.
141. Ø. Jacobsen, H. Maekawa, N.-H. Ge, C. H. Görbitz, P. Rongved, O. P. Ottersen, M. Amiry-Moghaddam and J. Klaveness, *J. Org. Chem.*, 2011, **76**, 1228-1238.
142. M. Lo Conte, S. Pacifico, A. Chambery, A. Marra and A. Dondoni, *J. Org. Chem.*, 2010, **75**, 4644-4647.
143. G. Chouhan and K. James, *Org. Lett.*, 2011, **13**, 2754-2757.
144. W. Larissa B., S. Theo, T. Kim C. M. F., K. Bernard, B. Quirinus B., S. Hans E. and R. Floris P. J. T., *Adv. Synth. Cat.*, 2001, **343**, 662-674.
145. J. van der Louw, J. L. van der Baan, C. M. D. Komen, A. Knol, F. J. J. de Kanter, F. Bickelhaupt and G. W. Klumpp, *Tetrahedron: Lett.*, 1992, **48**, 6105-6122.
146. K. A. Choquette, D. V. Sadasivam and R. A. Flowers, *J. Am. Chem. Soc.*, 2010, **132**, 17396-17398.
147. G. Xu, X. Li and H. Sun, *J. Organomet. Chem.*, 2011, **696**, 3011-3014.
148. J. Clayden, N. Greeves and S. G. Warren, *Organic Chemistry*, Oxford University Press, Oxford; New York, 2012.

149. L. Peng, J. DeSousa, Z. Su, B. M. Novak, A. A. Nevzorov, E. R. Garland and C. Melander, *Chem. Commun.*, 2011, **47**, 4896-4898.
150. C. A. Brown and A. Yamashita, *J. Am. Chem. Soc.*, 1975, **97**, 891-892.
151. Y. H. Lau, P. de Andrade, N. Skold, G. J. McKenzie, A. R. Venkitaraman, C. Verma, D. P. Lane and D. R. Spring, *Org. Biomol. Chem.*, 2014, **12**, 4074-4077.
152. Y. H. Lau, P. de Andrade, S.-T. Quah, M. Rossmann, L. Laraia, N. Sköld, T. J. Sum, P. J. Rowling, T. L. Joseph and C. Verma, *Chem. Sci.*, 2014, **5**, 1804-1809.
153. K. Yin, C. Li, J. Li and X. Jia, *Green Chemistry*, 2011, **13**, 591-593.
154. D. Westphal, G. Dewson, P. E. Czabotar and R. M. Kluck, *Biochimica et Biophysica Acta (BBA) - Molecular Cell Research*, 2011, **1813**, 521-531.
155. D. V. Vorobyeva, A. K. Mailyan, A. S. Peregudov, N. M. Karimova, T. P. Vasilyeva, I. S. Bushmarinov, C. Bruneau, P. H. Dixneuf and S. N. Osipov, *Tetrahedron Lett.*, 2011, **67**, 3524-3532.
156. G. Song, M. Jin, Z. Li and P. Ouyang, *Org. Biomol. Chem.*, 2011, **9**, 7144-7150.
157. A. S. Saghiyan, S. G. Petrosyan, L. L. Manasyan, S. A. Dadayan, A. V. Geolchanyan, H. A. Panosyan, V. I. Maleev and V. N. Khrustalev, *Synth. Commun.*, 2011, **41**, 493-506.
158. M. A. Maestro, F. Avecilla, A. E. Sorochniky, T. K. Ellis, J. L. Aceña and V. A. Soloshonok, *Eur. J. Org. Chem.*, 2014, 4309-4314.
159. C. M. Starks, *J. Am. Chem. Soc.*, 1971, **93**, 195-199.
160. K. Maruoka, John Wiley & Sons, *Asymmetric phase transfer catalysis*, 2008.
161. V. A. Soloshonok, T. Yamada, H. Ueki, A. M. Moore, T. K. Cook, K. L. Arbogast, A. V. Soloshonok, C. H. Martin and Y. Ohfuné, *Tetrahedron Lett.*, 2006, **62**, 6412-6419.
162. A. Kawashima, C. Xie, H. Mei, R. Takeda, A. Kawamura, T. Sato, H. Moriwaki, K. Izawa, J. Han, J. L. Acena and V. A. Soloshonok, *RSC Advances*, 2015, **5**, 1051-1058.
163. A. Muppidi, H. Zhang, F. Curreli, N. Li, A. K. Debnath and Q. Lin, *Bioorg. Med. Chem. Lett.*, 2014, **24**, 1748-1751.
164. Y. Wang, X. Song, J. Wang, H. Moriwaki, V. A. Soloshonok and H. Liu, *Amino Acids*, 2017, **49**, 1487-1520.
165. Y. Nian, J. Wang, S. Zhou, W. Dai, S. Wang, H. Moriwaki, A. Kawashima, V. A. Soloshonok and H. Liu, *J. Org. Chem.*, 2016, **81**, 3501-3508.
166. K. L. G. Yuan, and L. Yingchun, *Patent China*, 2013.
167. V. Prachayasittikul, S. Prachayasittikul, S. Ruchirawat and V. Prachayasittikul, *Drug design, development and therapy*, 2013, **7**, 1157.
168. C. Isanbor and D. O'Hagan, *J. Fluorine Chem.*, 2006, **127**, 303-319.

169. K. L. Kirk, *J. Fluorine Chem.*, 2006, **127**, 1013-1029.
170. H. J. Böhm, D. Banner, S. Bendels, M. Kansy, B. Kuhn, K. Müller, U. Obst-Sander and M. Stahl, *ChemBioChem*, 2004, **5**, 637-643.
171. J. Fried and E. F. Sabo, *J. Am. Chem. Soc.*, 1954, **76**, 1455-1456.
172. E. N. G. Marsh, in *Methods in Enzymology*, ed. V. L. Pecoraro, Academic Press, Second Edition, 2016, vol. 580, 251-278.
173. C. J. Pace and J. Gao, *Acc. Chem. Res.*, 2013, **46**, 907-915.
174. R.-Y. Zhu, K. Tanaka, G.-C. Li, J. He, H.-Y. Fu, S.-H. Li and J.-Q. Yu, *J. Am. Chem. Soc.*, 2015, **137**, 7067-7070.
175. W. E. Klunk, Y. Wang, G.-f. Huang, M. L. Debnath, D. P. Holt and C. A. Mathis, *Life Sci.*, 2001, **69**, 1471-1484.
176. E. P. Gillis, K. J. Eastman, M. D. Hill, D. J. Donnelly and N. A. Meanwell, *J. Med. Chem.*, 2015, **58**, 8315-8359.
177. J. M. Edwards, J. P. Derrick, C. F. van der Walle and A. P. Golovanov, *Mol. Pharmacol.*, 2018.
178. F. Evanics, J. L. Kitevski, I. Bezsonova, J. Forman-Kay and R. S. Prosser, *Biochimica et Biophysica Acta (BBA) - General Subjects*, 2007, **1770**, 221-230.
179. E. N. G. Marsh and Y. Suzuki, *ACS Chem. Biol.*, 2014, **9**, 1242-1250.
180. J. Gerig, *Biophysics Textbook Online*, 2001, 1-35.
181. P. P. Rodionov and G. G. Furin, *J. Fluorine Chem.*, 1990, **47**, 361-434.
182. J. Rivera-Chávez, H. A. Raja, T. N. Graf, J. E. Burdette, C. J. Pearce and N. H. Oberlies, *J. Nat. Prod.*, 2017, **80**, 1883-1892.
183. S. K. Holmgren, K. M. Taylor, L. E. Bretscher and R. T. Raines, *Nature*, 1998, **392**, 666.
184. C. J. Pace and J. Gao, *Accounts of chemical research*, 2012, **46**, 907-915.
185. J. A. Olsen, D. W. Banner, P. Seiler, B. Wagner, T. Tschopp, U. Obst-Sander, M. Kansy, K. Müller and F. Diederich, *ChemBioChem*, 2004, **5**, 666-675.
186. A. V. Samet, D. J. Coughlin, A. C. Buchanan and A. A. Gakh, *Synth. Commun.*, 2002, **32**, 941-946.
187. R. N. Patel, *Stereoselective biocatalysis*, CRC Press, 2000.
188. F. Parmeggiani, S. L. Lovelock, N. J. Weise, S. T. Ahmed and N. J. Turner, *Angew. Chem. International Edition*, 2015, **54**, 4608-4611.
189. S. Murthy and S. Nathan, *Organic chemistry: made simple*, Elsevier, 2013.

190. V. A. Soloshonok, V. P. Kukhar, S. V. Galushko, N. Y. Svistunova, D. V. Avilov, N. A. Kuz'mina, N. I. Raevski, Y. T. Struchkov, A. P. Pysarevsky and Y. N. Belokon, *J. Chem. Soc., Perkin Trans. 1*, 1993, 3143-3155.
191. V. A. Soloshonok, D. V. Avilov, V. P. Kukhar, V. I. Tararov, T. F. Savel'eva, T. D. Churkina, N. S. Ikonnikov, K. A. Kochetkov, S. A. Orlova and A. P. Pysarevsky, *Tetrahedron: Asymmetry*, 1995, **6**, 1741-1756.
192. D. Migoń, D. Neubauer and W. Kamysz, *The Protein Journal*, 2018, **37**, 2-12.
193. J. Zhang, K. Huang, K. O'Neill, X. Pang and X. Luo, *Cell death & disease*, 2016, **7**, e2266.
194. R. Rezaei Araghi, J. A. Ryan, A. Letai and A. E. Keating, *ACS Chemical Biology*, 2016.
195. R. N. Zhao, S. Fan, J. G. Han and G. Liu, *J. Biomol. Struct. Dyn.*, 2015, **33**, 1067-1081.
196. G. H. Bird, E. Gavathiotis, J. L. LaBelle, S. G. Katz and L. D. Walensky, *ACS Chem. biol.*, 2014, **9**, 831-837.
197. G. L. Verdine and C. E. Schafmeister, Google Patents, Second Edition, 2007.
198. P. S. Kutchukian, J. S. Yang, G. L. Verdine and E. I. Shakhnovich, *J. Am. Chem. Soc.*, 2009, **131**, 4622-4627.
199. K. Sakagami, T. Masuda, K. Kawano and S. Futaki, *Mol. Pharmacol.*, 2018, **15**, 1332-1340.
200. H. Chapuis, J. Slaninová, L. Bednářová, L. Monincová, M. Buděšínský and V. Čerovský, *Amino Acids*, 2012, **43**, 2047-2058.
201. P. M. Cromm, S. Schaubach, J. Spiegel, A. Fürstner, T. N. Grossmann and H. Waldmann, *Nat. Commun.*, 2016, **7**, 11300.
202. C. Glaser, *Berichte der deutschen chemischen Gesellschaft*, 1869, **2**, 422-424.
203. Y.-N. Li, J.-L. Wang and L.-N. He, *Tetrahedron Lett.*, 2011, **52**, 3485-3488.
204. N. J. Greenfield, *TrAC Trends in Anal. Chem.*, 1999, **18**, 236-244.
205. S. M. Kelly, T. J. Jess and N. C. Price, *Biochimica et Biophysica Acta (BBA)-Proteins and Proteomics*, 2005, **1751**, 119-139.
206. S. T. Campbell, K. J. Carlson, C. J. Buchholz, M. R. Helmers and I. Ghosh, *Biochemistry*, 2015, **54**, 2632-2643.
207. P. E. Czabotar, P. M. Colman and D. C. S. Huang, *Cell Death Differ.*, 2009, **16**, 1187-1191.
208. W. C. Chan and P. D. White, *Fmoc Solid Phase Peptide Synthesis*, Oxford University Press, 2000.

209. J. Jover, P. Spuhler, L. Zhao, C. McArdle and F. Maseras, *Catal. Sci. Tech.*, 2014, **4**, 4200-4209.
210. A. Krasinski, Z. Radić, R. Manetsch, J. Raushel, P. Taylor, K. B. Sharpless and H. C. Kolb, *J. Am. Chem. Soc.*, 2005, **127**, 6686-6692.
211. A. A. Yeagley, Z. Su, K. D. McCullough, R. J. Worthington and C. Melander, *Org. Biomol. Chem.*, 2013, **11**, 130-137.

Appendix

Conferences

Conferences Attended

RSC, Chemistry Biology and Bio-organic Chemistry Symposium, University of Bristol, 19th May 2015.

Posters presentations:

- A) Poster presentation: “Synthesis of Fmoc-Protected Novel Amino Acids for Application in Solid Phase Peptide Synthesis” Emad KH. Zangana, Eric G. Hope and Andrew G. Jamieson, RSC, Organic Division Midlands Meeting in 7/04/2017 in the department of chemistry - University of Leicester
- B) Poster presentation: “Synthesis of Fmoc-Protected Novel Amino Acids for Application in Solid Phase Peptide Synthesis” Emad KH. Zangana, Eric G. Hope and Andrew G. Jamieson, Departmental Research Day in 4/07/2017 in the department of chemistry - University of Leicester
- C) Poster presentation: “Synthesis of Fmoc-Protected Novel Amino Acids for Application in Solid Phase Peptide Synthesis” Emad KH. Zangana, Eric G. Hope and Andrew G. Jamieson, 17th Annual RSC Fluorine Subject Group Postgraduate Meeting /Tilton and Swithland Suite, John Foster Hall/ Leicester in 18-19th September 2017.

Crystal data and structure refinements

Table 1: Crystal Data and Structure Refinement for **2.3**, **2.4** and **2.5**

	2.3	2.4	2.5
Identification code	14104	16018	17029
Empirical formula	C ₂₅ H ₂₃ F N ₂ O ₂	C ₂₅ H ₂₃ F N ₂ O ₂	C ₃₁ H ₃₃ F N ₃ Ni O ₃
Formula weight	402.45	402.45	573.31
Temperature	150(2) K	150(2) K	150(2) K
Wavelength	0.71073 Å	0.71073 Å	0.71073 Å
Crystal system	Orthorhombic	Orthorhombic	Orthorhombic

Space group	P2(1)2(1)2(1)	P2(1)2(1)2(1)	P2(1)2(1)2(1)
Unit cell dimensions	a = 8.3079(15) Å b = 11.2851(19) Å c = 21.194(4) Å $\alpha = 90^\circ$ $\beta = 90^\circ$ $\gamma = 90^\circ$	a = 8.3079(15) Å b = 11.2851(19) Å c = 21.194(4) Å $\alpha = 90^\circ$ $\beta = 90^\circ$ $\gamma = 90^\circ$	a = 9.069(16) Å b = 14.82(3) Å c = 23.13(4) Å $\alpha = 90^\circ$ $\beta = 90^\circ$ $\gamma = 90^\circ$
Volume	1987.0(6) Å ³	1992.6(6) Å ³	3108(9) Å ³
Z	4	4	4
Density (calculated)	1.345 Mg/m ³	1.342 Mg/m ³	1.225 Mg/m ³
Absorption coefficient	0.092 mm ⁻¹	0.092 mm ⁻¹	0.663 mm ⁻¹
F(000)	848	848	1204
Crystal size	0.44 x 0.33 x 0.10 mm ³	0.31 x 0.23 x 0.10 mm ³	0.37 x 0.18 x 0.15 mm ³
Theta range for data collection	1.92 to 26.00°	1.92 to 25.99°	1.76 to 25.99°
Index ranges	-10 ≤ h ≤ 10, -13 ≤ k ≤ 13, -25 ≤ l ≤ 26	-10 ≤ h ≤ 10, -13 ≤ k ≤ 13, -26 ≤ l ≤ 25	-11 ≤ h ≤ 11, -18 ≤ k ≤ 18, -28 ≤ l ≤ 27
Reflections collected	15629	15915	24461
Independent reflections	2243 [R(int) = 0.0876]	2247 [R(int) = 0.1594]	6107 [R(int) = 0.2365]
Completeness to theta = 26.00°	100.0 %	99.8 %	99.9 %
Absorption correction	Empirical	Empirical	Empirical
Max. and min. transmission	0.928 and 0.715	0.962 and 0.691	0.862 and 0.131
Refinement method	Full-matrix least-squares on F ²	Full-matrix least-squares on F ²	Full-matrix least-squares on F ²
Data / restraints / parameters	2243 / 0 / 271	2247 / 0 / 272	6107 / 32 / 382

Goodness-of-fit on F^2	0.969	0.847	0.906
Final R indices [$I > 2\sigma(I)$]	R1 = 0.0414, wR2 = 0.0796	R1 = 0.0534, wR2 = 0.0907	R1 = 0.0838, wR2 = 0.1787
R indices (all data)	R1 = 0.0552, wR2 = 0.0839	R1 = 0.1035, wR2 = 0.1059	R1 = 0.1427, wR2 = 0.2033
Absolute structure parameter	?	?	-0.01(3)
Largest diff. peak and hole	0.166 and -0.185 $\text{e.}\text{\AA}^{-3}$	0.229 and -0.235 $\text{e.}\text{\AA}^{-3}$	0.741 and -0.853 $\text{e.}\text{\AA}^{-3}$

Table 2: Crystal Data and Structure Refinement for **2.6**, **2.9** and **2.10**

	2.6	2.9	2.10
Identification code	17058	17086	17043
Empirical formula	C ₂₈ H ₂₆ F N ₃ Ni O ₃	C ₃₄ H ₃₀ F N ₃ Ni O ₃	C ₃₁ H ₃₂ F N ₃ Ni O ₃
Formula weight	530.23	606.32	572.31
Temperature	150(2) K	150(2) K	150(2) K
Wavelength	0.71073 Å	0.71073 Å	0.71073 Å
Crystal system	Orthorhombic	Triclinic	Orthorhombic
Space group	P2(1)2(1)2(1)	P-1	P2(1)2(1)2(1)
Unit cell dimensions	a = 9.5733(19) Å b = 9.954(2) Å c = 25.533(5) Å $\alpha = 90^\circ$ $\beta = 90^\circ$ $\gamma = 90^\circ$	a = 10.329(5) Å b = 12.030(5) Å c = 12.160(5) Å $\alpha = 90^\circ$ $\beta = 90^\circ$ $\gamma = 90^\circ$	a = 15.337(3) Å b = 16.841(4) Å c = 21.766(5) Å $\alpha = 90^\circ$ $\beta = 90^\circ$ $\gamma = 90^\circ$
Volume	2433.2(8) Å ³	1403.2(10) Å ³	5622(2) Å ³
Z	4	2	8
Density (calculated)	1.447 Mg/m ³	1.435 Mg/m ³	1.352 Mg/m ³

Absorption coefficient	0.841 mm ⁻¹	0.739 mm ⁻¹	0.733 mm ⁻¹
F(000)	1104	632	2400
Crystal size	0.27 x 0.24 x 0.20 mm ³	0.45 x 0.21 x 0.16 mm ³	0.48 x 0.11 x 0.09 mm ³
Theta range for data collection	1.60 to 26.00°	1.71 to 26.00°	1.53 to 26.00°
Index ranges	-11 ≤ h ≤ 11, -12 ≤ k ≤ 12, -31 ≤ l ≤ 31	-12 ≤ h ≤ 12, -14 ≤ k ≤ 14, -14 ≤ l ≤ 14	-18 ≤ h ≤ 18, -20 ≤ k ≤ 20, -26 ≤ l ≤ 26
Reflections collected	18932	10763	44535
Independent reflections	4774 [R(int) = 0.0764]	5416 [R(int) = 0.0554]	11034 [R(int) = 0.1583]
Completeness to theta = 26.00°	100.0 %	98.4 %	100.0 %
Absorption correction	Empirical	Empirical	Empirical
Max. and min. transmission	0.862 and 0.649	0.862 and 0.588	0.862 and 0.649
Refinement method	Full-matrix least-squares on F ²	Full-matrix least-squares on F ²	Full-matrix least-squares on F ²
Data / restraints / parameters	4774 / 67 / 314	5416 / 0 / 379	11034 / 24 / 725
Goodness-of-fit on F²	1.039	0.996	0.825
Final R indices [I > 2σ(I)]	R1 = 0.0786, wR2 = 0.2116	R1 = 0.0550, wR2 = 0.1157	R1 = 0.0610, wR2 = 0.0869
R indices (all data)	R1 = 0.0930, wR2 = 0.2221	R1 = 0.0747, wR2 = 0.1226	R1 = 0.1165, wR2 = 0.1021

Absolute structure parameter	0.06(3)		0.063(14)
Largest diff. peak and hole	1.670 and -0.808 e.Å ⁻³	0.917 and -0.394 e.Å ⁻³	0.381 and -0.479 e.Å ⁻³

Table 3: Crystal Data and Structure Refinement for **2.11**, **3.1** and **2.3**

	2.11	3.1	3.3
Identification code	17004	15058	16051
Empirical formula	C132 H144 F4 N12 Ni4 O18	C68 H70 F2 N6 Ni2 O7	C132 H134 F4 N12 Ni4 O15
Formula weight	2497.43	1238.72	2439.35
Temperature	150(2) K	150(2) K	150(2) K
Wavelength	0.71073 Å	0.71073 Å	0.71073 Å
Crystal system	Orthorhombic	Monoclinic	Orthorhombic
Space group	P2(1)2(1)2(1)	P2(1)	P2(1)2(1)2(1)
Unit cell dimensions	a = 9.285(3) Å b = 14.674(5) Å c = 23.560(8) Å α = 90° β = 90° γ = 90°	a = 11.5353(18) Å b = 11.9177(18) Å c = 22.402(3) Å α = 90° β = 90° γ = 90°	a = 9.129(2) Å b = 11.991(3) Å c = 26.711(7) Å α = 90° β = 90° γ = 90°
Volume	3210.1(18) Å ³	3024.3(8) Å ³	2923.8(13) Å ³
Z	1	2	1
Density (calculated)	1.292 Mg/m ³	1.360 Mg/m ³	1.385 Mg/m ³
Absorption coefficient	0.652 mm ⁻¹	0.689 mm ⁻¹	0.712 mm ⁻¹
F(000)	1312	1300	1278
Crystal size	0.22 x 0.14 x 0.10 mm ³	0.21 x 0.07 x 0.03	0.30 x 0.21 x 0.05

		mm ³	mm ³
Theta range for data collection	1.63 to 26.00°	1.80 to 26.00°.	1.52 to 25.99°.
Index ranges	-11≤h≤11, -17≤k≤18, -26≤l≤29	-14≤h≤14, -14≤k≤14, -27≤l≤27	-11≤h≤11, -14≤k≤14, -32≤l≤32
Reflections collected	20688	23942	23077
Independent reflections	6293 [R(int) = 0.1295]	6253 [R(int) = 0.1743]	5745 [R(int) = 0.2026]
Completeness to theta = 26.00°	99.7 %	99.9 %	99.8 %
Absorption correction	Empirical	Empirical	Empirical
Max. and min. transmission	0.862 and 0.498	0.862 and 0.659	0.862 and 0.479
Refinement method	Full-matrix least-squares on F ²	Full-matrix least-squares on F ²	Full-matrix least-squares on F ²
Data / restraints / parameters	6293 / 34 / 400	6253 / 776 / 768	5745 / 387 / 379
Goodness-of-fit on F²	0.966	0.801	0.825
Final R indices [I>2sigma(I)]	R1 = 0.0697, wR2 = 0.1573	R1 = 0.0608, wR2 = 0.0787	R1 = 0.0645, wR2 = 0.1098
R indices (all data)	R1 = 0.0988, wR2 = 0.1699	R1 = 0.1304, wR2 = 0.0943	R1 = 0.1438, wR2 = 0.1280
Absolute structure parameter	-0.02(2)	?	0.02(2)
Largest diff. peak and hole	0.851 and -0.392 e.Å ⁻³	0.418 and -0.489 e.Å ⁻³	0.501 and -0.386 e.Å ⁻³

Table 4: Crystal Data and Structure Refinement for **3.4**, **3.7** and **3.7a**

	3.4	3.7	3.7 a
Identification code	15128	17077	17102
Empirical formula	C136 H138 F4 N12 Ni4 O13	C40 H38 Cl2 F N3 Ni O3	C40 H40 F N3 Ni O4
Formula weight	2459.42	757.34	704.46
Temperature	150(2) K	150(2) K	150(2) K
Wavelength	0.71073 Å	0.71073 Å	0.71073 Å
Crystal system	Orthorhombic	Orthorhombic	Monoclinic
Space group	P2(1)2(1)2(1)	P2(1)2(1)2(1)	P2(1)
Unit cell dimensions	a = 9.1958(17) Å b = 12.380(2) Å c = 25.938(5) Å $\alpha = 90^\circ$ $\beta = 90^\circ$ $\gamma = 90^\circ$	a = 11.497(2) Å b = 12.555(2) Å c = 24.489(4) Å $\alpha = 90^\circ$ $\beta = 90^\circ$ $\gamma = 90^\circ$	a = 10.140(3) Å b = 11.958(3) Å c = 13.625(4) Å $\alpha = 90^\circ$ $\beta = 90^\circ$ $\gamma = 90^\circ$
Volume	2953.0(10) Å ³	3534.8(11) Å ³	1651.8(8) Å ³
Z	1	4	2
Density (calculated)	1.383 Mg/m ³	1.423 Mg/m ³	1.416 Mg/m ³
Absorption coefficient	0.704 mm ⁻¹	0.749 mm ⁻¹	0.641 mm ⁻¹
F(000)	1290	1576	740
Crystal size	0.35 x 0.15 x 0.06 mm ³	0.24 x 0.13 x 0.05 mm ³	0.34 x 0.23 x 0.13 mm ³
Theta range for data collection	1.57 to 26.00°	1.66 to 26.00°	1.49 to 26.00°
Index ranges	-11 ≤ h ≤ 11, -15 ≤ k ≤ 14, -31 ≤ l ≤ 31	-14 ≤ h ≤ 14, -15 ≤ k ≤ 15, -30 ≤ l ≤ 30	-12 ≤ h ≤ 12, -14 ≤ k ≤ 14, -16 ≤ l ≤ 16
Reflections collected	23110	27935	12820
Independent reflections	5802 [R(int) = 0.0646]	6932 [R(int) = 0.1888]	6235 [R(int) = 0.0571]

Completeness to theta = 26.00°	100.0 %	99.9 %	99.7 %
Absorption correction	Empirical	Empirical	Empirical
Max. and min. transmission	0.894 and 0.746	0.862 and 0.583	0.862 and 0.434
Refinement method	Full-matrix least-squares on F ²	Full-matrix least-squares on F ²	Full-matrix least-squares on F ²
Data / restraints / parameters	5802 / 26 / 388	6932 / 0 / 451	6235 / 2 / 444
Goodness-of-fit on F²	1.014	0.818	0.990
Final R indices [I>2sigma(I)]	R1 = 0.0537, wR2 = 0.1370	R1 = 0.0679, wR2 = 0.1111	R1 = 0.0483, wR2 = 0.1024
R indices (all data)	R1 = 0.0606, wR2 = 0.1407	R1 = 0.1492, wR2 = 0.1352	R1 = 0.0580, wR2 = 0.1059
Absolute structure parameter	0.02(2)	0.01(3)	0.032(14)
Largest diff. peak and hole	1.371 and -0.833 e.Å ⁻³	0.447 and -0.726 e.Å ⁻³	0.525 and -0.419 e.Å ⁻³

Table 5: Crystal Data and Structure Refinement for **4.5**, **4.7** and **4.8**

	4.5	4.7	4.8
Identification code	17111	16161	16133
Empirical formula	C ₃₉ H ₃₇ F ₄ N ₃ Ni O ₃	C ₇₂ H ₇₁ F ₄ N ₆ Ni ₂ O _{8.50}	C ₃₈ H ₃₇ F ₂ N ₃ Ni O ₆
Formula weight	730.43	1349.77	728.42
Temperature	150(2) K	150(2) K	150(2) K
Wavelength	0.71073 Å	0.71073 Å	0.71073 Å
Crystal system	Orthorhombic	Monoclinic	Monoclinic
Space group	P2(1)2(1)2(1)	P2(1)	P2(1)

Unit cell dimensions	a = 11.7699(17) Å b = 12.2952(17) Å c = 46.543(7) Å $\alpha = 90^\circ$ $\beta = 90^\circ$ $\gamma = 90^\circ$	a = 10.396(2) Å b = 10.790(3) Å c = 14.173(3) Å $\alpha = 90^\circ$ $\beta = 90^\circ$ $\gamma = 90^\circ$	a = 12.276(8) Å b = 10.906(7) Å c = 13.165(8) Å $\alpha = 90^\circ$ $\beta = 90^\circ$ $\gamma = 90^\circ$
Volume	6735.4(16) Å ³	1565.8(6) Å ³	1667.5(18) Å ³
Z	8	1	2
Density (calculated)	1.441 Mg/m ³	1.431 Mg/m ³	1.451 Mg/m ³
Absorption coefficient	0.642 mm ⁻¹	0.678 mm ⁻¹	0.646 mm ⁻¹
F(000)	3040	705	760
Crystal size	0.38 x 0.21 x 0.18 mm ³	0.35 x 0.16 x 0.06 mm ³	0.13 x 0.12 x 0.03 mm ³
Theta range for data collection	0.87 to 26.00°	1.46 to 26.00°	1.64 to 26.00°
Index ranges	-14 ≤ h ≤ 14, -15 ≤ k ≤ 15, -56 ≤ l ≤ 57	-12 ≤ h ≤ 12, -13 ≤ k ≤ 13, -17 ≤ l ≤ 17	-15 ≤ h ≤ 15, -13 ≤ k ≤ 13, -16 ≤ l ≤ 16
Reflections collected	53022	12237	13099
Independent reflections	13238 [R(int) = 0.1069]	6099 [R(int) = 0.0846]	3454 [R(int) = 0.2609]
Completeness to theta = 26.00°	100.0 %	99.8 %	99.8 %
Absorption correction	Empirical	Empirical	Empirical
Max. and min. transmission	0.862 and 0.379	0.862 and 0.219	0.862 and 0.358
Refinement method	Full-matrix least-squares on F ²	Full-matrix least-squares on F ²	Full-matrix least-squares on F ²
Data / restraints / parameters	13238 / 16 / 915	6099 / 11 / 436	3454 / 81 / 462

Goodness-of-fit on F^2	0.900	0.947	0.833
Final R indices [$I > 2\sigma(I)$]	R1 = 0.0525, wR2 = 0.0652	R1 = 0.0628, wR2 = 0.1198	R1 = 0.0790, wR2 = 0.1443
R indices (all data)	R1 = 0.0822, wR2 = 0.0719	R1 = 0.0845, wR2 = 0.1273	R1 = 0.1827, wR2 = 0.1753
Absolute structure parameter	0.035(10)	0.032(18)	?
Largest diff. peak and hole	0.586 and -0.505 $\text{e.}\text{\AA}^{-3}$	0.666 and -0.479 $\text{e.}\text{\AA}^{-3}$	0.640 and -0.731 $\text{e.}\text{\AA}^{-3}$

Table 6: Crystal Data and Structure Refinement for Side product

	Side product
Identification code	18056
Empirical formula	C30 H29.75 Cl F N3 Ni O3.38
Formula weight	599.48
Temperature	150(2) K
Wavelength	0.71073 \AA
Crystal system	Triclinic
Space group	P1
Unit cell dimensions	a = 10.7481(18) \AA b = 11.609(2) \AA c = 12.511(2) \AA $\alpha = 90^\circ$ $\beta = 90^\circ$ $\gamma = 90^\circ$
Volume	1356.4(4) \AA^3
Z	2
Density (calculated)	1.468 Mg/m^3
Absorption coefficient	0.860 mm^{-1}
F(000)	624

Crystal size	0.27 x 0.24 x 0.20 mm ³
Theta range for data collection	1.76 to 26.00°
Index ranges	-13 ≤ h ≤ 13, -14 ≤ k ≤ 14, -15 ≤ l ≤ 15
Reflections collected	10640
Independent reflections	9408 [R(int) = 0.0415]
Completeness to theta = 26.00°	98.7 %
Absorption correction	Empirical
Max. and min. transmission	0.856 and 0.717
Refinement method	Full-matrix least-squares on F ²
Data / restraints / parameters	9408 / 19 / 712
Goodness-of-fit on F²	0.982
Final R indices [I > 2σ(I)]	R1 = 0.0535, wR2 = 0.1214
R indices (all data)	R1 = 0.0630, wR2 = 0.1266
Absolute structure parameter	0.042(14)
Largest diff. peak and hole	1.479 and -0.532 e.Å ⁻³